ISSN 0704-3716

Canadian Translation of Fisheries and Aquatic Sciences

No. 5079

Biology of a microsporidian: Glugea atherini n.sp., parasite of the atherine Atherina boyeri Risso, 1810, (Pisces - Teleost) occurring in coastal lagoons

P. Berrebi

Original title: Biologie d'une microsporidie: Glugea atherini n.sp. Parasite de l'atherine: Atherina boyeri Risso, 1810, (Poisson - Teleosteen) des etangs cotiers

In: Thèse pour obtenir le grade de Docteur de 3ème cycle, Université des Sciences et Techniques du Languedoc, (France), 1978

Original language: French

Available from:

Canada Institute for Scientific and Technical Information
National Research Council
Ottawa, Ontario, Canada K1A 0S2

1984

238 typescript pages

Academy of Montpellier

CTFAS 5079

Languedoc University of Science and Technology

THESIS

presented at the Languedoc University of Science and Technology

for the Doctorate

Parasitology, Pathology, Ecophysiological Relationships

Contribution to the Biological Study of Brackish Areas of the French Mediterranean Coast.

BIOLOGY OF A MICROSPORIDIAN: *Glugea atherini* n. sp. PARASITE OF THE ATHERINE *Atherina boyeri* Risso, 1810, (PISCES - TELEOST) OCCURRING IN COASTAL LAGOONS.

by Patrick Berrebi

Defended in June 1978 before the Examining Board

Mr. L. Euzet, Chairman

Mr. C. Vago, Member of the Institute

Mr. G. Bouix — Assessors

Mr. J.P. Trilles

FORWARD

I take this opportunity to thank Professor G. Bouix, my thesis director, who devoted a great deal of his time to supervising my research and the subsequent writing of this thesis. I greatly appreciated the atmosphere of directness and informality in which our discussions were held and am very grateful that through Professor Bouix's open-minded attitude, I was able to adopt a biochemical approach that is seldom used in the Laboratory to carry out my research.

I should also like to thank:

Professor L. Euzet, Chairman of the Board, who always welcomed me cordially in his department where Mr. Gabrion and Mr. Maillard helped me in the field of helminthology.

Professor C. Vago, a member of the Institute, who accepted to judge this work.

Professor J.P. Trilles, who, through our discussions, helped me considerably in the complex field of physiology.

It is not possible to mention all the other investigators who provided invaluable assistance. I thank them all, in particular:

Professor A. Raibaut and Professor J.P. Quignard in the field of parasitic copepods, ichthyology and lagoonal environments.

Mr. Loubès who aided me a great deal in the electron microscopic and histochemical study of microsporidians.

Janice, my devoted friend; Mrs. Nicole Pasteur as well as Professor Thaler's entire laboratory team for their practical and theoretical assistance in the field of enzyme electrophoresis.

All the laboratory staff, in particular, Mr. J. Barral, Mrs. S. Oustau and Mrs. J. Boyer who displayed considerable patience in typing this text.

The many fishermen, who are vital props in this kind of work, especially Mr. Scopel, who was always ready to help and be of service, Mr. Laplace and the fishermen of the Rhône Mort.

Last but certainly not least, my parents and Ghislaine, to them I wish to express my affection.

TABLE OF CONTENTS

CHAPTER ONE

INTRODUCTION

I - INTRODUCTION

A/ Microsporidia: Historical Background and General Comments

For a long time, these organisms were considered pluricellular and classified as a subphylum of Cnidosporida. It was only with the development of electron microscopy that they were found to be unicellular with highly specific characteristics, warranting re-classification among the MICROSPORA (Sprague, 1977).

Arthropods are the most common hosts of microsporidians which attack both larval and adult forms of insects and crustaceans alike, producing cysts and resulting in diffuse invasion of the tissues and even total invasion of the host.

Nosemia bombycis Naegeli, 1857, was one of the first species described because of its economic significance. This particular parasite attacks silkworms in many parts of the world, i.e., France, Italy, Germany, Australia, Hungary, Japan, India, etc.... It has a rapid cycle, weakening the larva which becomes less active, loses its appetite and finally dies. Spots cover the larva in a disease called "pébrine" which causes particular ravages in breeding farms because it can be transmitted via the ovary.

Fish seem to be the most common victims among vertebrates although other groups are also subject to microsporidian infestation:

a) Batrachians: Pleistophora myotrophica Canning, Elkan and Trigg, 1964, attacks muscle fibers in the toad, Bufo bufo. The result is a number of white, thread-like lesions which gradually destroy the motor muscles (Canning et al., 1964). Death eventually ensues. One species of microsporidians is also found in newt larvae where it forms white cysts.

b) Reptiles are not spared. Pleistophora danilewskyi (Pfeiffer, 1895) produces parallel, elongate lesions of the muscles in various species.

c) Birds are attacked by only one species, i.e., Encephalitozoon sp. Kemps and Kluge, 1975. The spores develop in the kidneys, gall bladder, liver and intestines. Infection is fatal in some lovebirds.

d) Mammals are even more subject to infection. Thelohania apodemi Doby et al., 1963, among many other species, has been found in field mice where it causes hypertrophy of the spleen. Encephalitozoon cuniculi Levaditi, Nicolau and Schoen, 1923, has been studied in mice and has also been found to be pathogenic in rabbits and foxes.

Infection with Encephalitozoon sp. Siebold and Fussel, 1973 has been described in the monkey, Callicebus moloch.

Lastly, infection with Nosema connori Sprague, 1974, was reported in a child (Margileth et al., 1973) and with Encephalitozoon matsubayashii Sprague, 1977, in adults.

Some microsporidians, such as Encephalitozoon cuniculi, produce ascites and hypertrophy of the liver and spleen in mice (Morris et al., 1956; Nelson, 1962; Lainson et al., 1964). There is evidence of a relationship between this particular microsporidian and cancer in mammals. Petri and Schmidt, 1966, showed that the parasite inhibited cancer in rats with malignant cells and to some extent immunized the animals against "transmissible" malignant tumours.

Lastly, Arison et al, 1966, demonstrated that the microsporidians causing ascites in mice had an inhibiting effect on some mice tumours.

The spore is the key stage in identifying microsporidians. It is during this final stage of parasitic development that microsporidiosis can be macroscopically detected. In the case of arthropods, the tissues acquire a characteristically white colour only when a very large number of spores have accumulated in the hemolymph or muscles. In fish, cysts of varying sizes usually develop but they are not detected until great numbers of spores have formed. Spore-formation is the only stage that can be seen with the naked eye, if only because of the vast number of spores produced. It is for this reason that early studies focussed on this particular stage. Furthermore, it is the only stage in which the microsporidian assumes a definite shape and there exists an internal structure made up of characteristic components.

The typical spore consists of the following:

- a very solid protective envelope containing an endospore and an exospore. Neither dessication, osmotic shock or mechanic action such as crushing, or ultrasonic vibrations seem to be able to break it (personal observations). Only some stains are capable of crossing the barrier and impregnating the contents.

- sporoplasm which is reduced and limited by a cytoplasmic

membrane on the inner side of the envelope. The nucleus is not always visible. There are no mitochondria, but occasionally a number of ribosomes may be seen in alignment.

- a posterior vacuole, which is occasionally visible although it can not always be seen with the electron microscope.

- the polar filament, which constitutes one of the basic elements of the spore. The posterior portion of the filament is generally coiled. A cross section reveals up to twelve concentric layers. According to the most generally accepted theories, the filament consists of a hollow tube which is extruded by eversion. The anterior portion is essentially straight. It thickens into a complex of structures representing over half of the spore. The polar cap undoubtedly serves to attach the filament.

- the polaroplast. Regardless of whether it is lamellar or vacuolar, it is thought to swell as a result of special osmotic properties and to increase the internal pressure of the spore. The filament then pierces the weaker anterior portion of the envelope and is violently expelled.

This structural system provides the parasite with a free-living phase (in the water, in the case of fish-infesting microsporidians). Dissemination, like penetration of the new host's digestive tract, is an easy and entirely passive process. In the living environment, there is an as yet unexplained stimulus which

induces sudden extrusion of the filament which may be up to 25 times as long as the spore. The sporoplasm (or at least the nucleus, according to some authors, i.e., Sprague and Vernick, 1968) is thought to be carried along and injected into the host. Microsporidians are exclusively intracellular. Depending on the species, extremely rapid reproduction of the parasite results in cyst formation or diffuse invasion of infected tissue. The process is essentially the same in its development, regardless of the final outcome.

The initial stage is merogony with activation of the cell. Vegetative plasmodia divide in the cytoplasm of host cells, thereby very rapidly increasing the number of parasites. The many resulting meronts begin the second phase of development, i.e., sporulation. This phase ends with the production of spores after further division. The parasite generally becomes isolated with or without destruction of the host component. The sporonts yield a characteristic number of sporoblasts that give rise to spores with the formation of capsules, filaments and other spore-related organelles (sporogenesis). The final phase leads to the production of a sac full of spores. In arthropods, in the absence of cysts, a large number of spores may be found in the dead host. In fish, the cyst envelope usually acts as a sac.

B/ The Microsporidia of Fish

After Gluge's observations in fish (1838), the first microsporidian species to be described was Glugea anomala (Moniez, 1887) Gurley, 1893, in sticklebacks. Then came Thelohan's studies in 1892-95 (Glugea destruens, G. ovoidea, G. cordis, G. depressa) and Gurley's observations in 1893 (Glugea anomala, Plesitophora typicalis). The list has grown until now dozens of species have been described and assigned to various genera, i.e., Glugea Thelohan, 1891, Pleistophora Gurley, 1893, Nosema Naegeli, 1857, Ichthyospordium Caullery and Mesnil, 1905, Thelohania Henneguy, 1892, Mrazekia Léger and Hesse, 1922, Spraguea Weissenberg, 1976 and Heterosporis Schubert, 1969.

This rapid expansion of research in thefield is due to various factors. First of all, the parasite has a distinctive behavioural pattern. Infection generally results in the development of cysts or xenomas which are remarkable for their size or profusion. The parasite-host relationship in these xenomas has incited some authors to speak of symbiosis. Under the electron microscope, the organelles of the host seem to be in the service of the parasite. This is the case with the mitochondria and the endoplasmic reticulum which closely fit around various microsporidian stages.

In addition, these parasites have aroused special interest because of the severe damage they cause in fish in breeding farms or

in the natural environment. In nature, the Microsporidia are capable of parasitizing a significant portion of fish populations.

Pleistophora cepedianae (Putz, Hoffman and Dunbar, 1965) infests Dorosoma cepedianum alevins, inducing cyst formation in the general cavity. There may be up to 90% parasitism in young-of-the-year specimens and the mortality rate is high.

Glugea hertwigii Weiseenberg, 1911, has become an increasingly greater threat in North American smelts (Osmerus eperlanus). In the Canadian Great Lakes, parasitism reached 93% in 1967. It is thought that the parasite, while not solely responsible, has contributed to the death of thousands of tons of smelts.

Glugea weissenbergi Sprague and Vernick, 1968, infests 50% of the Apeltes quadracus population at all times of the year.

In breeding farms, epidemics can decimate the stock. Pleistophora ovariae Summerfelt 1964, prevents Notemigonus crysoleucas, a very popular species in the United States, from reproducing by attacking the ovary.

In British Columbia, Pleistophora salmonae has caused the death of up to 75% of the salmonids in breeding farms (Putz et al., 1965).

In order to study the atherine-infesting microsporidian, we selected some examples for reference purposes. We researched the literature for two types of material, i.e., statistical information with epidemiological and experimental data, and observations describing the infestation process and the parasite's life cycle. Histochemical and ultrastructural optical techniques were employed.

1 - Statistical Research

. Glugea anomala (Moniez, 1887) infests the connective tissue (intestinal wall and other organs) of Gasterosteus aculeatus and Pungitius pungitius. This species served as a model in the outstanding contributions made by Weissenberg (1968) on the parasite-host relationship. This parasite forms large xenomas (vegetative stages at the edge and spores in the middle of the cyst) which can deform the body of the host and result in a high mortality rate. The subcutaneous cysts may break and release spores into the water. By using intermediate hosts (copepods?), Weissenberg succeeded in inducing experimental infestation, but failed to provide any details on the technique he employed. His work was based essentially on optical microscopy which makes it difficult to compare his results with current ultrastructural findings (Weissenberg, 1968).

. Pleistophora ovariae Summerfelt, 1964, parasitizes Notemigomus crysoleucas in virtually all the fish breeding farms in the United States where it constitutes a major threat. The parasite

attacks only females and the resulting rate of parasitic involvement reaches almost 50%. It makes its way to the ovaries and consequently destroys large numbers of eggs and developing embryos, thereby considerably reducing female fertility without killing the adults. The authors suggest that there are two types of transmission, i.e., peroral and transovarian if the infested ovule has been fertilized. The parasite becomes established in the ovule, giving it a white appearance. There is no cystic wall formation (Summerfelt and Warner, 1970).

. Glugea stephani Hagenmüller, 1899, attacks many pleuronectid fishes, e.g., Pleuronectes flesus, P. platessa, P. limanda, P. americanus, Parophrys vetulus, ... Recent studies have been conducted on this microsporidian (Stunkard and Lux, 1965; Wellings et al., 1969; Olson and Pratt, 1973; Olson, 1976). The infected fish is blind with dilated eyes and protruding (1 cm) anus. The cysts are always found in the connective tissue. The most serious involvement occurs in the digestive tract which is always the first organ to be infested (the intestinal wall may be entirely replaced with cysts which become hard and chalky). Then, it is the turn of the pyloric ceca, the bile ducts, liver, mesenteric lymph nodes and occasionally, the ovary. In the case of plaice (Pseudopleuronectes), the most severely infested specimens are the young fry of under 6 cm. The cyst is surrounded by a layer of lymphocyte-infiltrated connective tissue from the host. Under this wall, there is a syncytial layer of cytoplasm

with large vesicular nuclei and young parasitic stages. Mature spores are found in the middle of the cyst. Stundard and Lux (1965) never succeeded in infesting Pseudopleuronectes americanus even after 8 months. They fed bits of infested intestine or mollusks previously injected with spores to healthy plaice. Since the youngest infested fish only feed on small invertebrates, it was hypothesized that there might be an intermediate host. Olson (1976) on the other hand, succeeded in infesting Parophrys vetulus. Infestation occurred only at temperatures above 15°C both in a natural environment and in breeding farms. The most successful results were achieved at 18°C when the fish were fed various small crustaceans that had previously been placed in a spore suspension. Peroral infestation by means of spores in suspension proved feasible but less effective. The cysts appeared after 30 to 60 days. All other attempts to infest other species of fish failed.

. Glugea hertwigii Weissenberg, 1911, parasitizes Osmerus eperlanus and O. mordax in the large drainage basins of Canada and in many lakes. A number of studies have been devoted to this parasite, i.e., Delisle, 1969; Delisle and Veilleux, 1969; Chen and Powel, 1972; Nepszy and Dechtiar, 1972; Delisle, 1972. Microsporidiosis is confined to three of the four drainage basins with the largest smelt populations but only 11 out of 128 stretches of water contain microsporidians. Out of the three races of smelts, only the dwarf

smelt is infested. Infection peaks with maximum gonad activity. In 1967, from June to September, the infestation rate soared from 7% to 93%, whereas from 1965 to 1966, the rate remained stable at 5.5%. The number of cysts per individual rose from 0.1 in June to 0.2 in July, 10 in August and 40 in September. The author interprets these findings as representing an interhost invasion from May to August and an intrahost invasion from August to September. The microsporidian has a predilection for young-of-the-year fish and the rate of infestation drops progressively until the age of 5. In 1969, 89% of 0+ fish (under 1 year) were parasitized. In the following year, 90% of the 1+ animals (between 1 and 2 years) suffered the same fate. Massive mortality was recorded in 2+ fish (between 2 and 3 years of age) after the reproduction period. The disease is consequently not fatal in the young fish. In the male, the first and main organ to be parasitized is the digestive tract. The liver and skin are rarely infected and the testicles hardly ever show any involvement. In the female, 70% of infections occur in the ovary which is penetrated by and replaced with the parasite. The chief sites of infection are as follows: the anterior intestine (an average of 6.6 cysts), middle intestine (4.7 cysts), posterior intestine (3.8 cysts), pyloric ceca (2.7 cysts), stomach (2.1 cysts). Secondary sites are the peritoneum (1.2 cysts), gonads (1), liver (0.9), anal region (0.7), swim bladder (0.4), oesophagus (0.4), adipose tissue (0.3), skin (0.2), heart (0.15) and kidneys (0.1). In 4- or 5-year

old adults, the cysts harden, become pasty and yellowish (tissue resistance). Pathogenic action may be expressed by a mechanical effect in which the organs are compressed, making swimming difficult or by reduction in the female's egg-laying capacity through destruction of the ovules and compression. When this action is associated with the stress attending reproduction, it seems to be fatal.

2 - Research on the Parasitic Cycle

. Pleistophora hypessobryconis Shaperclaus, 1941, infests the flank muscles of several species of aquarium fish, e.g., Hyphessobrycon sp. Merogony begins with the formation of small (4 x 2 µm) oval stages with one or two nuclei. These stages are surrounded by host cytoplasm released from injured cells, by ergastoplasm and ribosomes. This particular arrangement undoubtedly helps to spread the disease in the host. The increase in nuclear size and number results in meront formation. The wall, pierced with pores, is now 0.3 µm thick. There are no Golgi bodies, mitochondria or fibrils, but ribosomes and ergastoplasm are observed. The pansporoblast stage begins once the proper number of nuclei has been reached, and the ergastoplasmic vesicles occur in parallel alignment. The cytoplasm divides around the nuclei. Sporogenesis is accompanied by a thickening of the wall. Vesicles surround the yellow filament, forming the double membrane of the latter which acquires its customary structure. The polaroplasm, consisting of parallel lamellae, may arise from the er-

gastoplasm. The cap is made up of roughly 15 layers. Its dense substance penetrates the thicker anterior portion of the filament (Lom and Corliss, 1967).

Experimental attempts to achieve infestation perorally succeeded in H. inessa, but proved difficult. They were easier in Carassus auratus. Intramuscular injections of crushed host tissue readily resulted in infestation of Carassus auratus, Cyprinus carpio and Tinca tinca (Lom, 1969).

. Glugea weissenbergi Sprague and Vernick, 1968, invades 50% of Apeltes quadracus, a species from the Solomon Islands in which it forms subperitoneal cysts 1 to 6 mm in size. The mature xenoma consists of a vascularized wall and a layer of cytoplasm from the host with a number of nuclei. Spores are found in the center of the xenoma. Under the electron microscope, Sprague and Vernick (1968) observed annulate lamellae which they interpreted as being prolongations of host nuclei. The gemmules comprise the first, very small parasitic stages. They are thought to arise from nuclear prolongations. Then the nuclei of the sporongic cylinders divide and the future sporogony vacuole develops. The mature plasmodium forms a distinct entity within the sporogony vacuole and produces sporonts. The latter divide into sporoblasts (3 μm in diameter), each with an off-center nucleus, and ergastoplasmic vacuoles that are parallel to the nuclear membrane. The sporoblasts elongate and the spores mature.

The spore nucleus, however, is never clearly defined. The posterior vacuole is not visible. During merogony, components from the host and parasite are intimately connected. In this article, several hypotheses have been proposed:

- Some images have been interpreted as representing diplokaryons prefiguring sexual autogamy.

- The gemmules are thought to arise from prolongations of degenerate host nuclei. The genetic material of the microsporidian is consequently included in the DNA of the host cell.

- It is suggested that the polar filament is produced by the last nuclear division of the sporont. During this division, the nuclear membrane stretches without breaking. Microtubules contained in the stretched intermediary portion develop into filaments. Each half nucleus is assumed to be the only element introduced into the host cell by the spore. It constitutes genetic material with some nucleoplasm.

. Nosema fennica Lom and Weiser, 1969, forms ovoid cysts, 2.5 mm in diameter, on the fins of catfish (Silurus glanis)found in Finnish waterways. The cyst wall is 30 µm thick and often less. There is a characteristic superficial layer with degenerate host nuclei, then a plasma layer with vegetative parasitic stages. Mature spores are found in the center of the cyst.

Under the electron microscope, the first meronts are plasmodia that are roughly round in shape, 11 µm in diameter and contain 9 nuclei. The second meronts consist of strips, 3 x 13 µm, with 5 nuclei. The latter divide into coffee-bean-shaped diplokaryon stages. Sporogony produces uninucleate spores which are never paired and which contain single posterior vacuoles. These xenomas can penetrate the fish, but the released spores are phagocytized (Lom and Weiser, 1969)

. Ichthyosporidium sp. Schwartz, 1963, produces giant subcutaneous tumours of up to 5 cm in length in Leiostomus xanthurus. The initial stage is 15 to 20 µm in diameter. It is surrounded by numerous migratory cells. The following stages encapsulate and form a number of subdivided cysts that develop asynchronously and infiltrate the parasitized tissues. The cyst wall becomes vascularized. Within the wall, there is karyokinetic division of the nucleus. Later, the invaded migratory cells divide by simple cytokinesis. Hypertrophy of the cyst corresponds to sporogony with the formation of typical sporoblasts and spores. The final tumour consists of a mass of spores threaded with the remainder of cytoplasmic membranes. Since the cyst walls are destroyed, the spores are able to escape into surrounding tissue, but they are phagocytized. Symbiosis does not occur in this case. The giant cell is not stimulated by the parasite. Instead, it is a defensive response by the fish organism (Sprague, 1969).

C/ The Microsporidian Infesting Atherines

The eight microsporidian species which we have briefly described from findings in the literature generally parasitize only a single organ, such as the digestive tract or the gonads. When the infection is more serious, the parasite may spread to other organs. In other words, it may be said to have found a "single entrance door" from which it has access to other organs. The "exit door" corresponds either to the burst cyst which releases its spores into the water (Glugea anomala) or to the death and decomposition of the host, which also results in the release of mature spores.

In the case of atherinids, there is a "double entrance door" since cysts can become independently implanted either in the digestive tract (in which case, they are small) or in the general cavity or swim bladder (in which case, they may become very large)

This distinctive characteristic plus a number of other features constitute a very interesting subject for study.

CHAPTER TWO

THE MICROSPORIDIAN: *Glugea atherini* n. sp. AND ITS HOST: *Atherina boyeri* Risso 1810

PLANCHE I

PLATE I

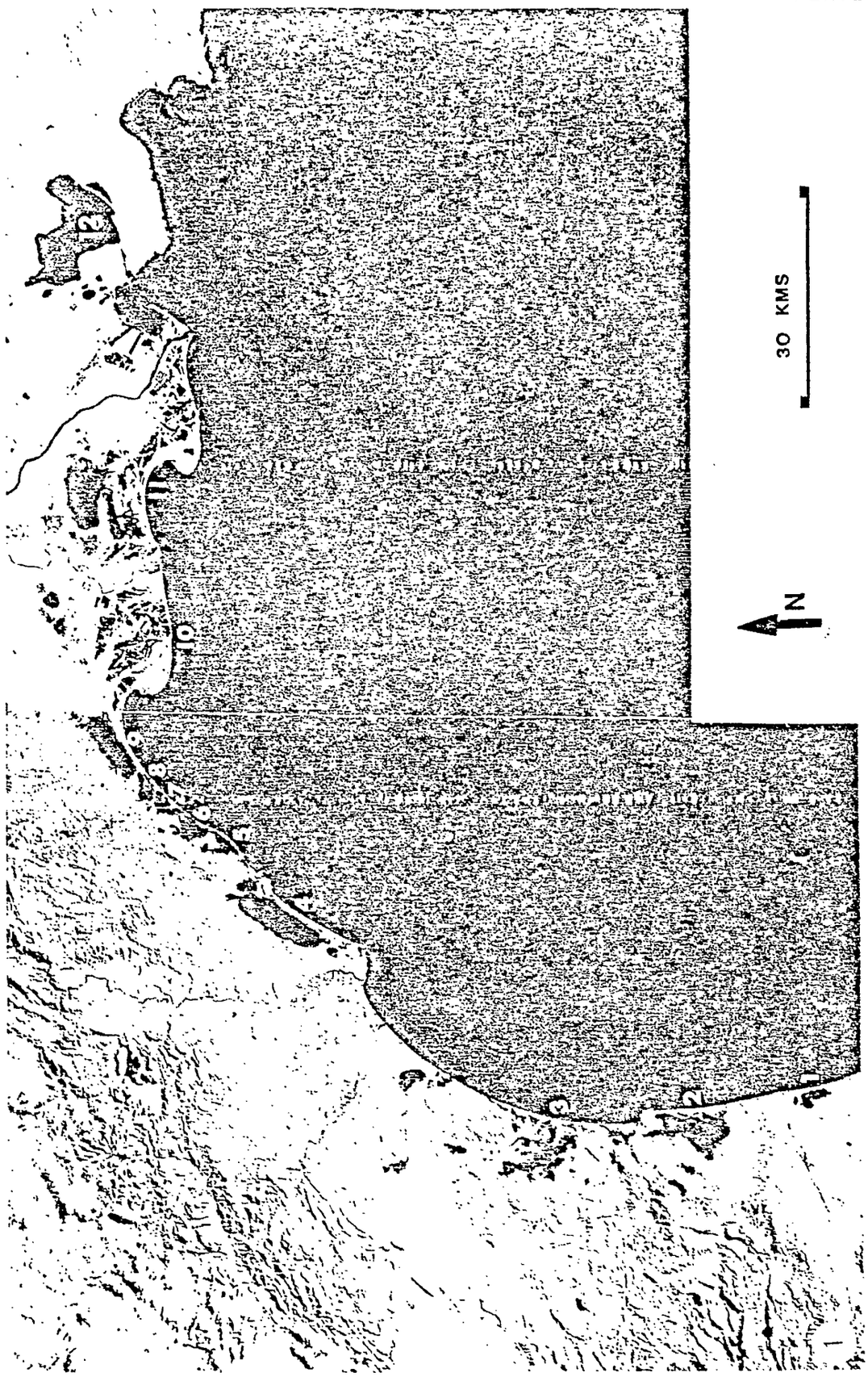

II - THE MICROSPORIDIAN AND ITS HOST

A - Environment

1/ Conditions and Approach

Most of the lagoons along the French Mediterranean coast were explored, some more frequently than others. In January 1975, the atherine-infesting microsporidian was discovered in the Grande Roubine. Since then, most of the lagoons west of the Etang de Mauguio and as far as the Spanish boarder have been examined. East of the Etang de Mauguio, specimens were taken from the abovementioned Grande Roubine as well as the Rhône Mort (or Rhône de Saint-Roman) in the Petite Camargue area. Specimens were collected from the northern portion of the Etang du Vaccarès in the Camargue, and in the Marseilles region, from the Etang de Berre and the Etang de l'Olivier (see Plate 1, photo 1). In addition, batches of fish were caught in the Mediterranean proper near Port Vendres, in the Pyrénées Orientales region, in Corsica (Etang d'Urbino) and in Tunisia (Etang de Tunis). Along the Atlantic coast, only the Arcachon basin was explored. Fig. 30 gives the position of the various lagoons and their interconnections.

Plate 1

1 - Infrared photo by satellite of the Golfe du Lion and the lagoons of the Roussillon-Languedoc-Provence coast. Scale: 1/962500. (from 1 to 12: see Fig. 30).

pH, chlorine ion and dissolved oxygen levels in the water and temperature were recorded at the time specimens were collected. For the sake of clarity, salt concentrations will always be given in grammes of chlorine ions (or rather, halogen ions, i.e., fluorine, bromine, iodine) per liter of water. Values were obtained by the More Knudsen method. Knudsen's tables will be used for conversion into total saline levels although they are not entirely reliable when levels are very high or, conversely, very low. Table 1 shows the range of variation for the months when specimens were obtained.

2/ Description of the Environment

A virtually unbroken string of lagoons, each with its own characteristics, hugs the French Mediterranean coast from one end to the other.

With the exception of the Thau basin, all the lagoons west of the mouth of the Rhône, i.e., most of them, were formed when the bodies of water were isolated from the Mediterranean by the build-up of a generally very narrow strip of land of alluvial origin. A marine current carries sediment from the Rhône and deposits it in the curve of the Golfe du Lion. Bays or gulfs resulting from the Flandrian uplift when the sea level rose from -25 m to 0 m, were isolated from the sea by sandbars. This was the case for the following lagoons: Canet, Leucate-Salses, Bages-Sigean, Ingril,

Geographic area GROUPE GEOGRAPHIQUE	Lagoons ETANGS	Cl^- (g/l)	pH	Dissolved O_2 O_2 dissout mg/l	Température	Number of Nombre de pêches	catch time Mois de pêche (months)
Roussillon	Canet	10.8	7.5	/	7°	2	10 & 11
Aude	Bages	0	8.3	9	7°	1	11
Thau	Thau	13.9 à 15	7.7 à 7.9	11	4 à 13°	5	1,2,10, 11,12
	Canal du Rhône à Sète	3.7 à 19	7.5 à 8	6 à 9	5 à 21°	6	1,2,9, 10,11, 12
From De Palavas	Vic - Moures	7.9	7.8	/	9 à 10°	4	1 et 10
à to	Pérols	/	/	9	14°	1	4
Carnon	Grec	5.2	7.5	10	10°	3	10
Mauguio	Mauguio	1.8 à 13.3	7.05 à 9.4	5 à 11	4 à 19°	33	1,2,3,4, 6,9,10, 11,12
	Grande Roubine	0.6 à 3	/	/	7 à 22°	2	8 & 11
Petite Camargue	Rhône Mat	11 à 12.6	7.4 à 8	8 à 10	4 à 8°	6	1-11,12
Camargue	Vaccarès	3,3	/	/	/	2	1
Berre	Olivier	0,1	/	/	/	1	5

Table No. 1. Range in Variations in Some Parameters during Specimen Collection in Most of the Lagoons Studied

Vic-Moures-Pierre Blanche, Arnel-Prévost, Méjean-Pérols-Grec, Mauguio, as well as for the lagoons of the Petite Camargue area, e.g., Rhône Mort, and the Camargue, e.g., Vaccarès.

The origins of the Etang de Thau are completely different. This basin was formed by a local geological rift which explains why it is so deep (up to 10 m deep) and consequently why it has a considerable volume of water and why its saline levels are stable. They are, in fact, slightly lower than those found in the sea. Exchanges with the Mediterranean are facilitated by large capacity canals which cross the town of Sète.

The Etang de Berre is the largest in France. It is a syncline which was invaded by the sea during the Flandrian uplift. Salt levels are high.

The string of lagoons along the Languedoc coast are crossed by the Canal du Rhône à Sète. At times, the canal runs along the lagoons and at others, it runs between them (see Plate II). This is the case with the Etang d'Ingril in which both halves have retained the same name. Further east, the Etang de Vic-Moures to the north and the Etang de Pierre-Blanche to the south originally formed only one lagoon. The same also applied to the lagoon pair made up of the Etang de l'Arnel to the north and the Etang du Prévost to the

south and to the pair consisting of the Etang du Méjean and the Etang de Pérols to the north and the Etang du Grec to the south (Plate II, photos 3 and 4). The Etang de Mauguio, the last of the lagoons under consideration, was not cleaved in two. Instead, the canal runs along the southern shore with four main access points (Plate II, photo 2). There is little direct communication between the lagoons which are sometimes indirectly joined via the canal or, depending on the season, via the sea.

The canal, however, hardly qualifies as a typical waterway. It is fed by a number of sources and, as a result, varies considerably in saline content. Each lagoon supplies it with a certain amount of water in which the salt content differs because of various phenomena:

Plate II

2 - Communication between the Etang de Mauguio and the Canal du Rhône à Sète via a channel at Carnon.

3 - The Canal du Rhône à Sète artificially separates lagoons that originally formed a single body of water. In the photo, the canal between Carnon and Palavas separating the Etang du Grec from the Etang de Pérols.

4 - Lagoons that have been separated (in the photo, the Etang du Méjean and the Etang du Grec) may communicate via the canal.

PLANCHE II

PLATE II

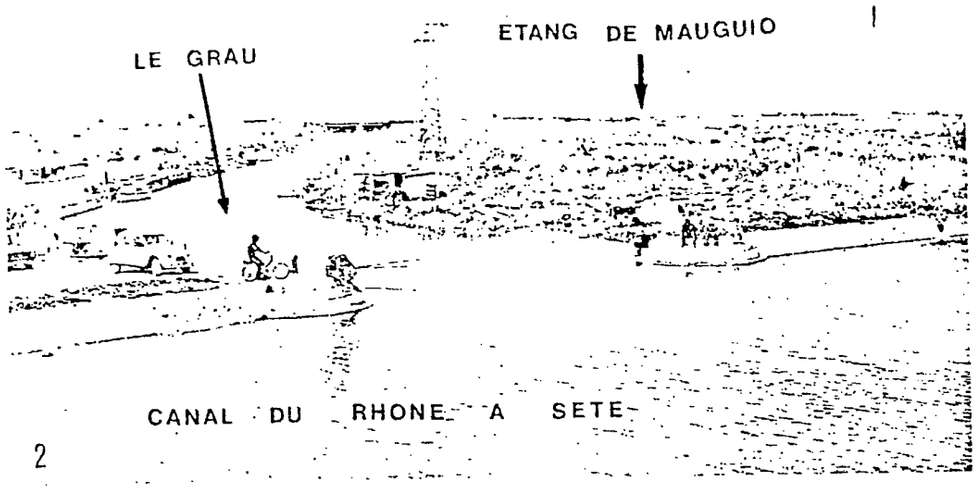

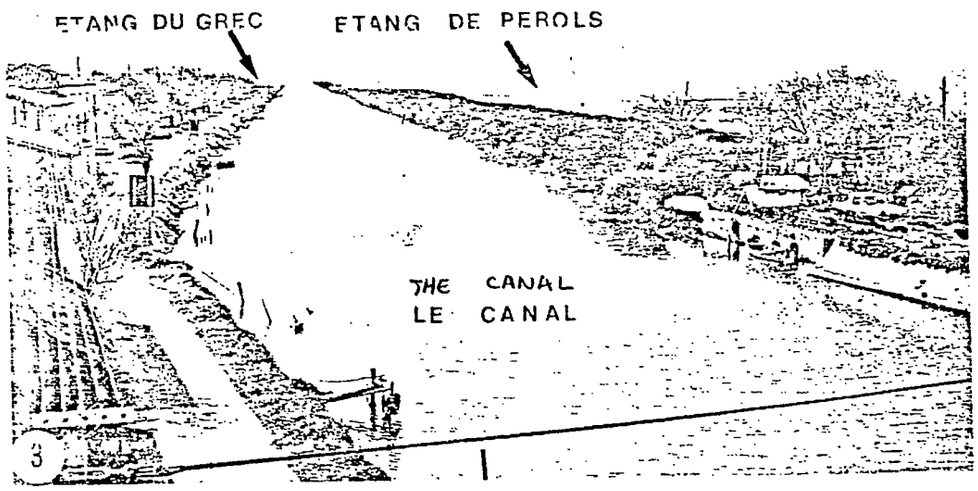

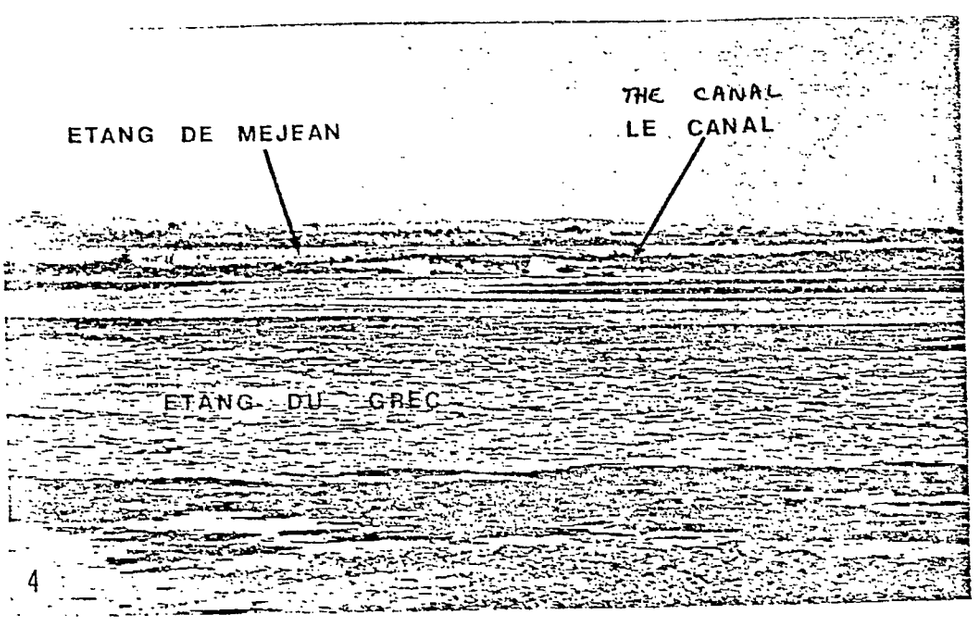

Certain winds and tides sweep the sea toward the canal.

Conditions in the canal are made even more complex by its connections with the Etang de Thau at one end and the Rhône River at the other. The currents vary a great deal and may be reversed several times in the same day. At the very same moment, they may flow in opposite directions at different points as a result of wind action, tidal influences and the inflow of fresh water.

The Canal du Rhône à Sète therefore does not constitute a continuous path of migration from one end of its course to the other because the stimuli to which fish respond, such as salt levels, currents, temperature and food supply, are not constant.

The lagoons are generally fairly shallow. The Etang de l'Arnel, for instance, has an average depth of 35 cm. Alluvium-laden water continually flows into the lagoons leaving deposits which further reduce their depth. Other deposits are borne by the winds, especially after ploughing, and by the waves that wash over the sandbars.

These lagoons are subject to very specific weather conditions. Winds frequently displace the water to such an extent that at times when the Mistral blows hard, the northernportion of the lagoons is swept dry. There is a high degree of evaporation due to the combined action of the sun and the wind. Irregular and sometimes

torrential rainfall supplies large amounts of fresh water, especially in the spring and fall, but also at other times of the year after a major rainstorm. Then there are the Mediterranean tides (several decimeters at certain times) and the marine winds which dump large amounts of salt water into the lagoons. In this phenomenon, the channels joining the lagoons with the sea play a key role since they permit the water to flow freely in both directions, thereby providing a balance in the chemistry of the water and in the fish population.

It should be pointed out that human intervention has also played a significant role. Work on the Etang de Berre increased the saline content of the lagoon, whereas work on the sandbar separating the Etang de Canet from the sea resulted in a decrease in salt levels in the lagoon.

All these elements introduce a very high degree of variability in saline levels and temperature in these buffer zones between limnic and salt water.

Mercier (1973) studied the Etang de Bages for three years and recorded four distinct stages which generally apply to shallow lagoons:

. from December to March, the saline levels range from 8 to 12‰. There is a limnic influence.

. April to June constitutes a transition period marked by a progressive increase in saline levels (spring winds).

. from July to September, saline levels peak. There is a marine influence.

. from October to November, there is a progressive decrease in salt levels. This is a transition period marked by autumn rains.

A number of authors have classified brackish water, labelling each type. Petit, for instance, established a scale corresponding to the saline content (1943):

limnic environment.....from 0 to 3‰ total saline content

prelimnic environment.....from 3 to 5‰ total saline content

brackish environment.....from5 to 9‰ total saline content

prebrackish environment....from 9 to 15‰ total saline content

submarine environment.....from 15 to 36‰ total saline content

marine environment.....over 36‰ total saline content.

Redeke-Valikangas established another system of classification, also based on saline levels, which was adopted by the 1958 Venise Symposium:

hyperhaline water.....over 40‰ total saline content

euhaline water.....30 to 40‰ total saline content

mixolaline water.....0.5 to 30‰ total saline content

mixo-euhaline.....over 30‰ but under sea salt levels

mixo-polyhaline....18 to 30‰ total saline content

mixo-mesohaline....5 to 18‰ total saline content

mixo-oligohaline... 0.5 to 5‰ total saline content

limnetic water.....under 0.5‰ total saline content

One last example of special interest is provided by Aguesse (1957) who classified the waters of the Camargue taking variations into account:

oligobrackish water ...0.5 to 5 g/l average annual saline content

brackish water.....5 to 16 g/l average annual saline content

polybrackish water.....16 to 40 g/l average annual saline content

salt water.....over 40 g/l average annual saline content.

Aguesse added another set of terms to this classification which were related to the degree of variation in saline levels.

While these classifications may prove extremely useful in a stable environment, they do not add anything new to a description of lagoonal environments which exhibit such extremes in saline levels that the water may fall into several different categories in a single year. By way of example, determinations of saline levels carried out during this study using Petit's scale showed that the Etang de Mauguio shifted from a prelimnic to a submarine environment in the course of the year; in other words, the lagoon embraced four different categories in succession. According to Redeke and Valikungas's scale, it could be classified under the four subdivisions comprising a mixohaline environment and with Aguesse's scale as a reference, it fell into two or three categories in succession.

Since these conventional systems of classification seem to complicate the issue rather than simplify it, it seems preferable to describe the water in terms of the species inhabiting it instead of taking the opposite approach (Raibaut, 1967). In this paper, water samples will be characterized by chlorine ion concentrations and total saline levels obtained by means of Knudsen's tables.

In summer, the temperature is generally higher in the lagoons than in the sea and may reach 36°C. In winter, the reverse is true. All of this greatly affects the seasonal migration of fish.

pH has little influence on the overall biotope. It is, in fact, the result and not the cause of the various phenomena described above. pH can, however, have an influence on certain micro-organisms. Aleem (1952) showed that when the pH dropped to roughly 6.6 in the Etang de Canet, some peridinian populations (Amphidinium rhynchocephalus) disappeared while others (Oxyratis maxima) increased in massive numbers.

One of the phenomena that takes on a great deal of importance in fish migration is pollution due to the proliferation of certain organisms. Guelorget and Michel (1976) defined three types of pollution, which they referred to as the red, the white and the black tides. The colour of the water may vary, but the process is basically the same. There is a series of characteristic phenomena which generally occur in summer and which are still poorly understood. The pH drops by almost a point, phytoplankton and macrophytes rapidly proliferate, then decompose, creating a black slimy layer containing sulfate-reducing anaerobic bacteria that produce toxic hydrogen sulfide (H_2S) with a characteristic nauseating odour. Hydrogen sulfide combined with the action of sulfur-oxidizing aerobic

bacteria releasing metalloid sulfur and the action of cellulolytic organisms (Senz, 1951) result in a considerable drop in oxygen levels and in the destruction of any microfauna unable to escape. Guelorget and Michel (1976) claim that temperature (which may reach 28°C) is a contributing factor in the emergence of the tides. Another factor is mineral salt-laden waste water from large cities. While aerobic heterotrophic bacteria are not a predominant feature, they remain an important adjuvant in a phenomenon whose real causes are still poorly understood. A simple drop in temperature or a shift in the water due to the wind eliminates the problem.

Like all biotopes with highly variable conditions, few species are represented, but those that are have large populations. In addition to species adapted to brackish water, there are freshwater and saltwater fish that are able to tolerate the unstable conditions of the lagoon for a time. This is the case with the stickleback which invades the Etang de Mauguio after a heavy downpour. It is also the case with the sea pike, which ventures into the lagoons during warm periods when evaporation and dry conditions increase saline levels.

Floral and faunal microorganisms are well represented in these environments. In addition to highly specific bacteria, there are large populations of diatoms and peridinians. Protozoans (ciliates and amoebae) are also well represented. Aquatic flora includes the genera: Ulva, Enteromorpha, Codium, Gracilaria, Potamogon, Ruppia, Ectocarpus, Zoostera, etc... Plant beds provide shelter for the preys of a number of fish, including atherines. The preys include some polychaetes and a number of crustaceans, such as the genera Corophium, Orchestia, Talitrus, Gammarus, Idothea,

Sphaeroma, Crangon, etc.... To this list can be added planktonic copepods and from time to time dipterans of the family Cucilidae which fall into the water during their summer flight.

All of these organisms are connected by food chains as well as by a number of parasites, such as trematodes, in particular, which can be found in mollusks, e.g., the genera Gibbula, Hydrobia, Cardium, Tapes, Abra, and fish, e.g., the genera Dicentrarchus, Gobius, Diplodus, Atherina, as well as in pipefish, blennies, mullet, sole and eel and occasionally in sea birds that help themselves to their share of fish, especially smelt, a choice meal for black-headed and herring gulls.

B - Study of the Host

1/ The Different Species of Atherines Collected

Atherines are teleost fish belonging to the order Mugiliformes.

The fish in this order are characterized by:

- cycloid or ctenoid scales on the body and head
- a dentate edge, arising from the premaxillae, along the upper jaw only
- two dorsal fins with spines on the anterior fin
- pelvic fins with 1 to 5 rays
- a ventral thoracic fin
- a forked caudal fin.

The order includes three main families, i.e., the Atherinidae, Sphyraenidae (e.g., Barracuda), Mugilidae. The Atherinidae are more closely related to the Mugilidae than to the Sphyraenidae.

The Atherinidae are characterized by:

- a spiny anterior dorsal fin with over 4 rays
- an anal fin with 1 to 3 spines
- 31 to 60 vertebrae
- small size, with a silvery stripe along the lateral line
- a dentate pharyngeal bone; oblique opening of the mouth.

Throughout the world, there are 57 known genera but only two are present in the Mediterranean, i.e., the genera Atherina and Pranesus. The genus Atherina is distinguished by a well-developed upward slanting mandible.

A large number of atherine species have been described in Europe and definite confusion reigns within the genus. Kiener and Spillman (1969) studied the species found along the French coasts and reduced the 18-odd species described to 3. In addition, the genera Hepsetia Bonaparte and Atherina Linnaeus, 1758, were combined into one, i.e., Atherina Linnaeus, 1758, which was, however, subdivided into two subgenera, i.e., Atherina and Hepsetia.

a) Atherina (Atherina) hepsetus Linnaeus, 1758, (See Plate III, photos 5 and 7) is without a synonym since its classification has been virtually uncontested. This species lives in the sea near the coast or in lagoons with a predominantly marine influence. It is found throughout the Mediterranean basin, in the Black Sea, Caspian Sea and near Madeira in the Atlantic where a few rare populations have been reported (Kiener and Spillman, 1969; Ladiges and Vogt, 1965) (See Fig. 1).

The species is distinguished by the absence of teeth on the ectopterygoids, ascending median processes of the premaxillae that project between the orbits. These processes are much longer than the horizontal portions bearing the teeth (Plate III, photo 6). There is one very characteristic feature: this species has over 58 scales on the lateral line between the gill and the tail and 53 to 57 vertebrae. As a result, it is the most slender of the various atherine species, attaining up to 20 cm in length.

Plate III

5 - Atherina boyeri (A.B.), Atherina hepsetus (A.H.) and Atherina presbyter (A.P.), the 3 atherine species studied (X 0.95).

6 - Comparison of the premaxillae of the 3 species studied. A = ascending median process; B = dentate horizontal portion (X 4.5).

7 - Detail of the head (X 2)

8 - Atherina boyeri specimen (X 2.1)

PLANCHE III

PLATE III

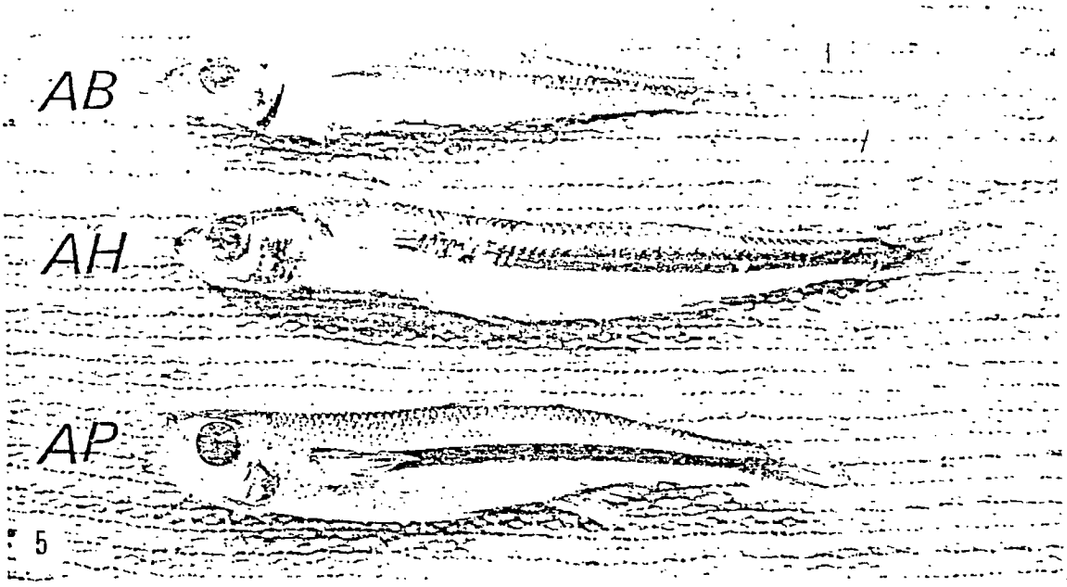

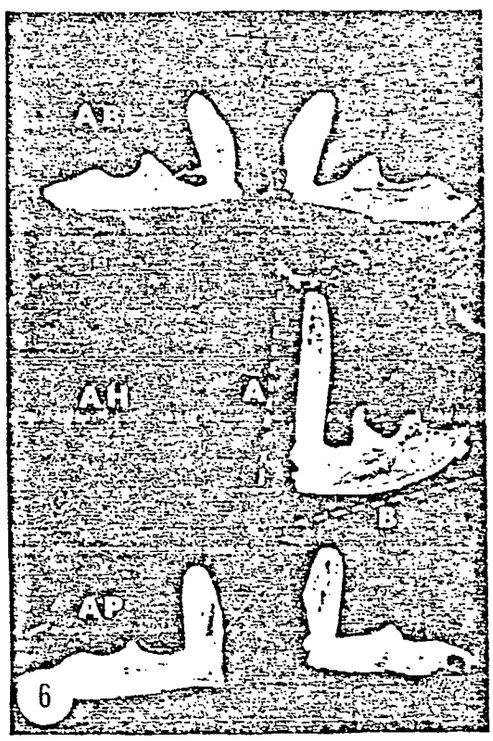

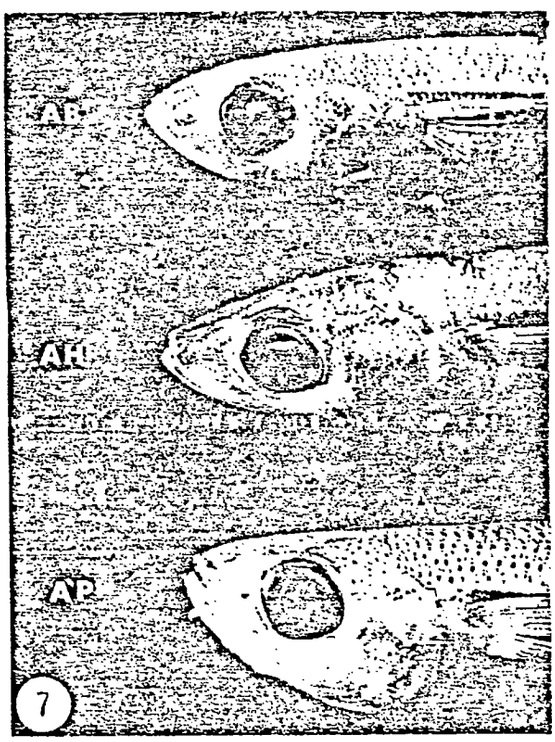

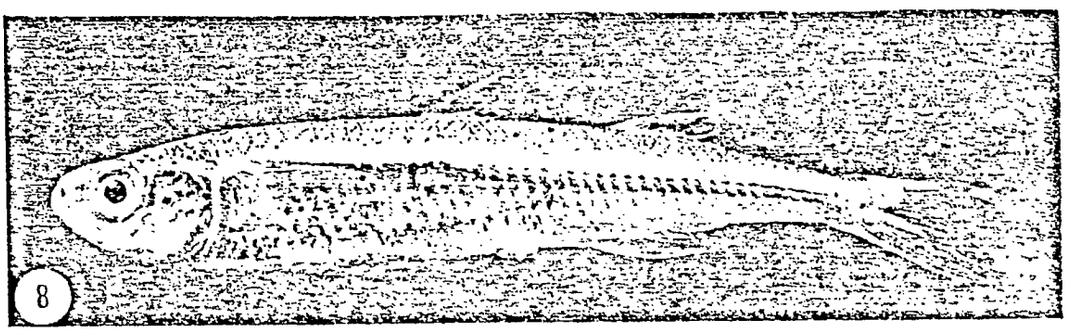

In the course of this study, we examined specimens from the Etang de Thau and the Etang d'Urbino in Corsica. Both of these bodies of water are deep and predominantly marine in influence (See Fig. 1). The species does not appear to harbour any microsporidians.

b) Atherina (Hepsetia) presbyter Cuvier, 1829. The nomenclature has not changed since 1829. There are no serious synonyms. The species is found in large numbers along the Atlantic coast from Morocco to as far away as the Scandinavian peninsula. Rare lots have been reported along the Mediterranean coast as far as Marseilles on the northern coast and Tunis, on the southern (Ladiges and Vogt, 1965) (See Figure 2).

This species also lacks teeth on the ectopterigoids. The ascending median processes of the premaxillae are short and generally smaller than the dentate horizontal portions (see Plate III, photo 6). There are 52 to 57 scales on the lateral line and 46 to 52 vertebrae. While the species is as long as Atherina (Atherina) hepsetus, i.e., 20 cm, maximum, it is more compact and is consequently the heaviest of the atherinids.

We dissected specimens from the Arcachon basin as well as two lots caught near Port Vendres (Roussillon), where the species seems to exist in vaster numbers than is normally reported and where it is referred to as the "sea smelt" (See Fig. 2). It does not seem to harbour any microsporidians.

c) Atherina (Hepsetia) boyeri Risso, 1810, (See Plate III, photos 5, 7 and 8). It is very commonly found in brackish water. It is an euryhaline species par excellence, since it occurs in

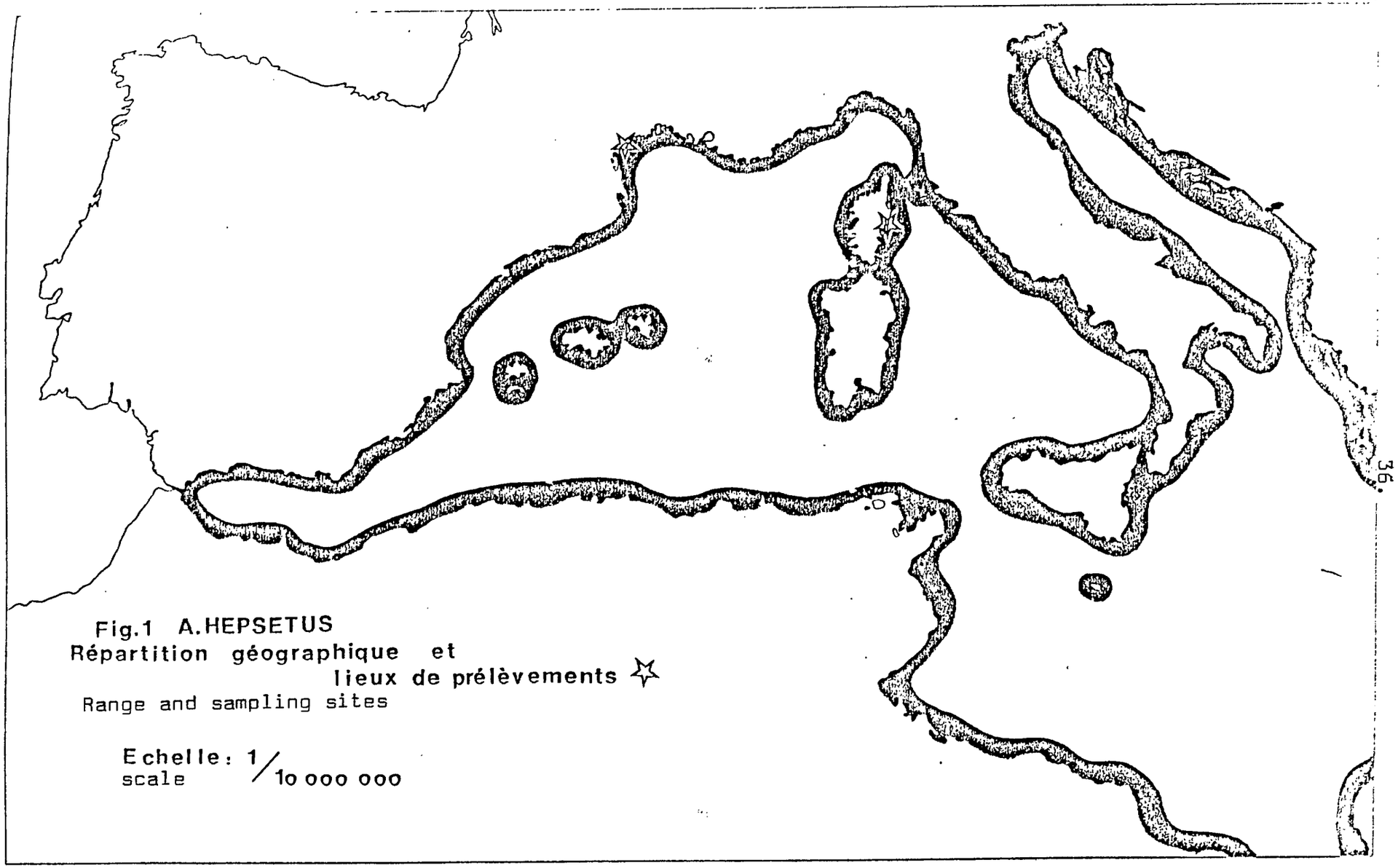

Fig.1 A.HEPSETUS
Répartition géographique et
lieux de prélèvements ☆
Range and sampling sites

Echelle : 1/10 000 000
scale

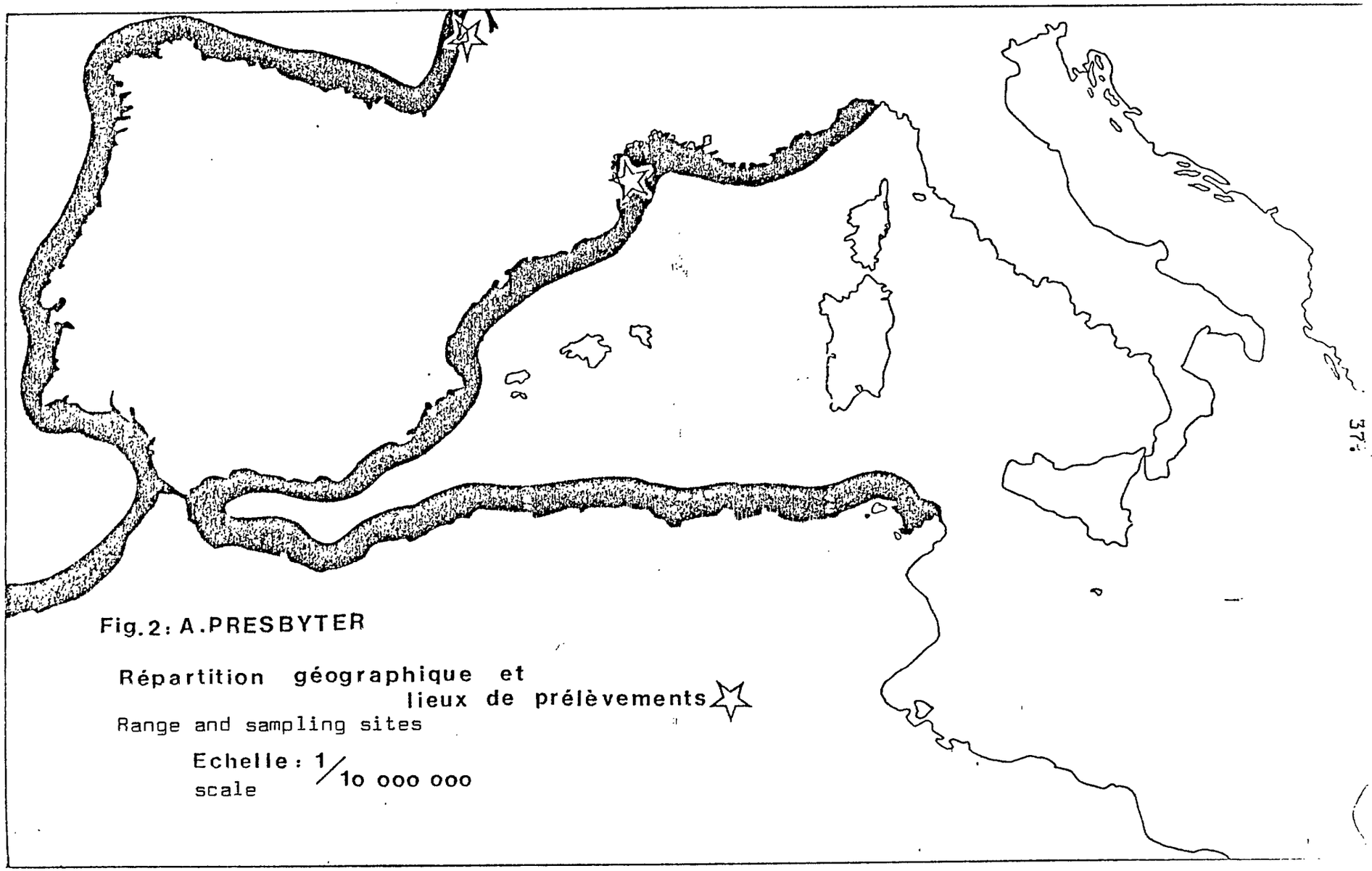

Fig.2: A.PRESBYTER

Répartition géographique et lieux de prélèvements ☆

Range and sampling sites

Echelle : 1/10 000 000
scale

water ranging from virtually fresh to hypersaline (lagoons of Israel with 70‰ salt content and the salinas of Corsica with 77‰ salt). During this investigation, atherinids were kept under conditions of 64‰ saline content without any untoward effects. This species lives in the sea as well as in lagoons (where conditions are extremely variable) and even in streams. Some species have been caught in a stream that flows into the Petit Rhône where saline levels are below 0.1‰. The diet varies with the environment. It may consist primarily of zooplankton (phytoplankton cannot be digested) in the sea and deep marine lagoons but be essentially benthic (large numbers of crustaceans) in shallow brackish lagoons. Variations of this range in the living conditions of different populations of the same species combined with genetic isolation have resulted in a high degree of polymorphism. There are consequently a number of variable characteristics which should be used with caution in any system of classification. This is true, for instance, of the number of vertebrae, the shape of the hemal arches, gill rakers, body proportions, etc. This polymorphism undoubtedly accounts for the number of synonyms assigned to the species: Atherina (Hepsetia) boyeri Risso, 1810 (= A. mochon Cuvier, 1829; A. pontica Eichwald, 1831; A. caspia Eichwald, 1831; A. mochon pontica Eichwald, 1831; A risso Cuvier, Valenciennes, 1835; A. sarda Cuvier, Valenciennes, 1835; A. mochon rissoi Cuvier, Valenciennes, 1835; A. sardinella Fowler, 1834; A. lacustris Bonaparte, 1836; A. boieri Depéret, 1883; A. hyalosoma Facciola, 1885; A. riqueti Roule, 1902; A. bonapartii Boulenger, 1907; A. mochon var. aegyptica Boulenger, 1907).

A. boyeri lives along the coasts, in the lagoons and occasionally the waterways of the entire Mediterranean, Black Sea and Caspian Sea. A few rare populations have been caught near Madeira in the

Atlantic and off the coasts of Great Britain and the Scandinavian peninsula. The last two locations are totally exceptional and no explanation can be provided (See Fig. 3).

This species is distinguished by very small teeth on the ectopterigoids, ascending median processes of the premaxillae, that are smaller than the dentate horizonatal portion and by 40 to 47 vertebrae. It is the smallest of the three species since it attains a maximum length of 13 cm and the 3-year-old specimens we dissected rarely exceeded 9 cm. It is a compact fish, resembling Atherina presbyter in shape.

The lots we studied came from various sources (see Fig. 4), i.e.,

- coastal waterways: Petit Rhône, Grande Roubine, Canal du Rhône à Sète;
- deep, marine-type or submarine-type lagoons (Audoin, 1962) along the French coast: Bassin de Thau, Etang de Berre;
- shallow, brackish lagoons: Etang de Canet, Etang de Bages-Sigean, Etang d'Ingril, Etangs de Vic-Moures-Pierre Blanche, Etangs de Prévost-Arnel, Etangs de Méjean-Pérols-Grec, Etang de Mauguio, Etang du Rhône in Petite Camargue, Etang du Vaccarès in Camargue and the Etang de l'Olivier in Provence.
- distant sites: Etang d'Urbino in Corsica
  Etang de Tunis in Tunisia.

Atherina boyeri provides the local fishermen in the Roussillon-Languedoc-Provence region with one of their means of subsistance. This is particularly true of the Etang de Mauguio where it consti-

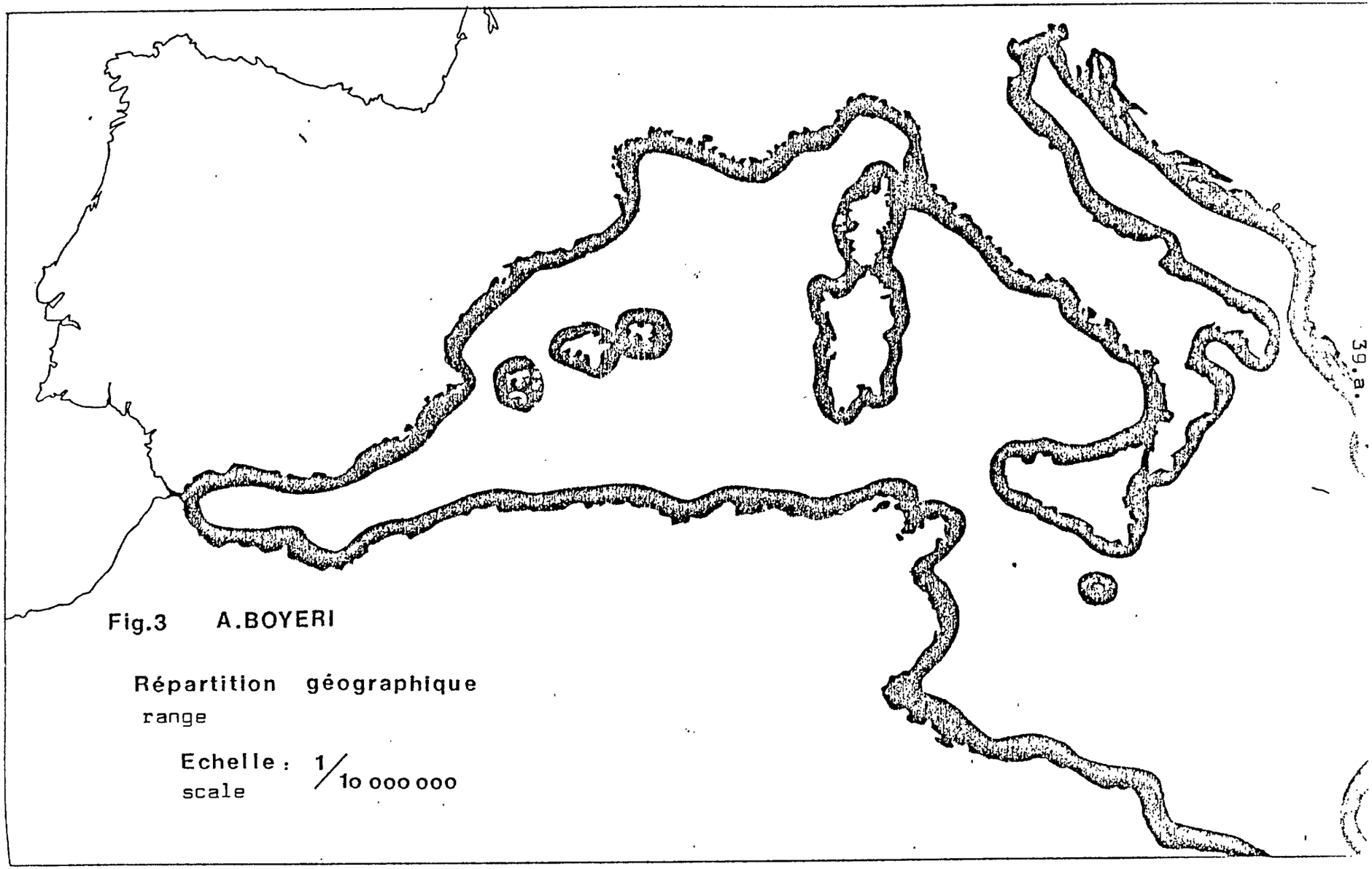

Fig.3 A.BOYERI

Répartition géographique
range

Echelle : 1/10 000 000
scale

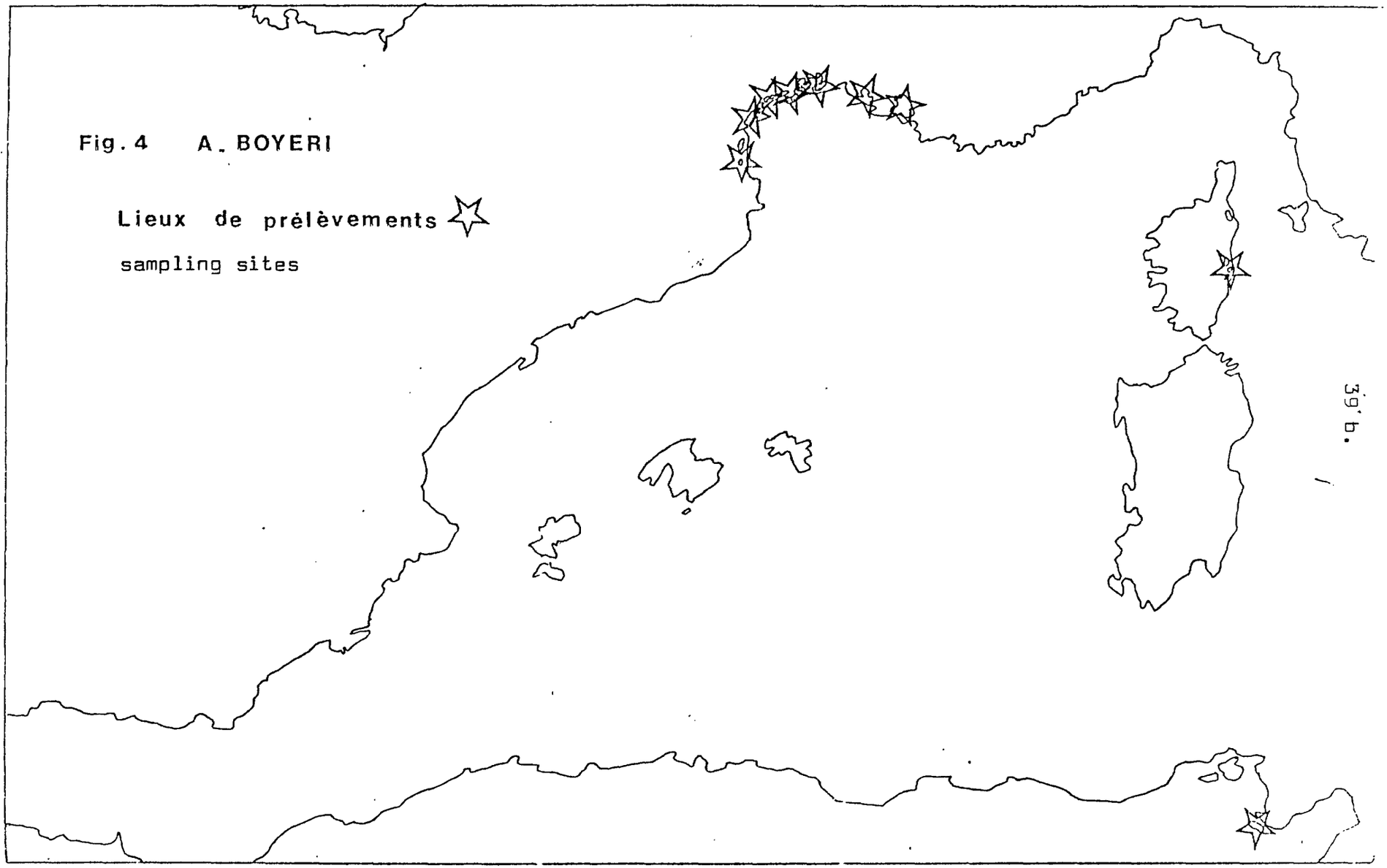
Fig. 4 A. BOYERI
Lieux de prélèvements
sampling sites
39°b.

tutes part of the daily take along with sea perch, mullet and eels. The catch has considerably dropped over the last twenty years, as with most other species, on account of pollution due to an uncontrolled increase in the number of summer vacationers. Atherina boyeri is apparently the only host of the microsporidian species studied here. In Fig. 30, we have shown the geographic range of infested populations.

2/ Key to Determining Species, after Kiener and Spillman, 1969.

The following key is still valid for lots from the sources we have just mentioned. Caution is recommended in applying it to atherinids from areas that have not been studied.

** The ascending median process of the premaxilla is longer than the horizontal dentate portion.

A single species, i.e., Atherina (Atherina) hepsetus Linnaeus, 1758 (over 58 scales on the lateral line and over 53 vertebrae).

** The ascending median process of the premaxilla is equal to or shorter than the horizontal dentate portion.

* fewer than 50 scales on the lateral line

Atherina (Hepsetia) boyeri Risso, 1810

(under 13 cm long, teeth on the ectopterigoid)

* 52 to 57 scales on the lateral line

Atherina (Hepsetia) presbyter Cuvier, 1829

(up to 20 cm long, no teeth on the ectopterigoid).

SPECIES	A. (H.) boyeri	A. (H.) presbyter	A. (A.) hepsetia
teeth on the ectopterigoids	yes	no	no
appearance of the premaxilla	ascending median process smaller than horizontal dentate portion	ascending median process smaller than horizontal dentate portion	ascending median process longer than horizontal dentate portion
number of scales on lateral line	under 50	52 to 57	over 58
number of vertebrae	40 to 47	46 to 52	53 to 57
general characteristics	size: 13 cm max.	20 cm max.	20 cm max.
	appearance: blocky	blocky	slender
	geographic range:		
	Mediterranean, coast and lagoons, Black Sea Caspian Sea rare populations near Madeira	Atlantic, coast and marine lagoons, from Morocco to Scandinavia, Med. coast to Marseilles and Tunis	Med., coast and marine lagoons, Black Sea rare populations near Madeira

3/ Observations in Atherina boyeri in Lagoonal Areas

We have gained insight into the biology of this fish through the study of the microsporidiosis to which it falls prey. In the course of our observations, we recorded the following: fish length, gender, sexual maturity, parasitic fauna.

a) Size, Sex, and Age. Examination of the scales revealed that only a very thorough study would make it possible to deduce the age of the fish. The winter growth rings seem to be lost in a multitude of supernumerary rings. Environmental changes combined

with climatic variations probably interfere with normal growth ring formation and make it difficult to read them correctly. As a result, it was not possible to establish a linear growth curve for this atherinid. According to Hervé (1978) who studied the fish in the Etang de Canet and the Etang de Salses, yearlings are approximately 45 mm in length, 2-year-old specimens attain 65 mm in length, whereas the 3-year-old fish are close to 80 mm. During this investigation, other means were used to try to evaluate growth in terms of age. Fig. 5 summarizes the various operations. A double histogram of frequency of size class was established for males and for females (a) from a lot of 100 individuals fished in the Etang de Mauguio. Each of these histograms yielded a trimodal curve for each sex. Assuming that this trimodality corresponds to three distinct generations, the lot was divided into three groups, taking the inflexion points of the cumulative curve (b) into account. Once the average length of individuals from each generation was calculated, it was possible to determine the average length in relation to sex at 9, 21 and 33 months. (The average hatching date was taken to be the end of May). Extrapolation of these findings yielded the linear growth curve as a function of the sex of the fish (c).

Fig. 5 - 5A
5A Histograms of frequency of fish sizes in males and in females. Figures with a circle represent average size for each generation.
5B Cumulative curves with inflection points (A_1, A_2, B_1 and B_2).
5C Linear growth curve as a function of age with the average size in males (▷) and females (▬), taking into account the interruption of growth in winter (h).

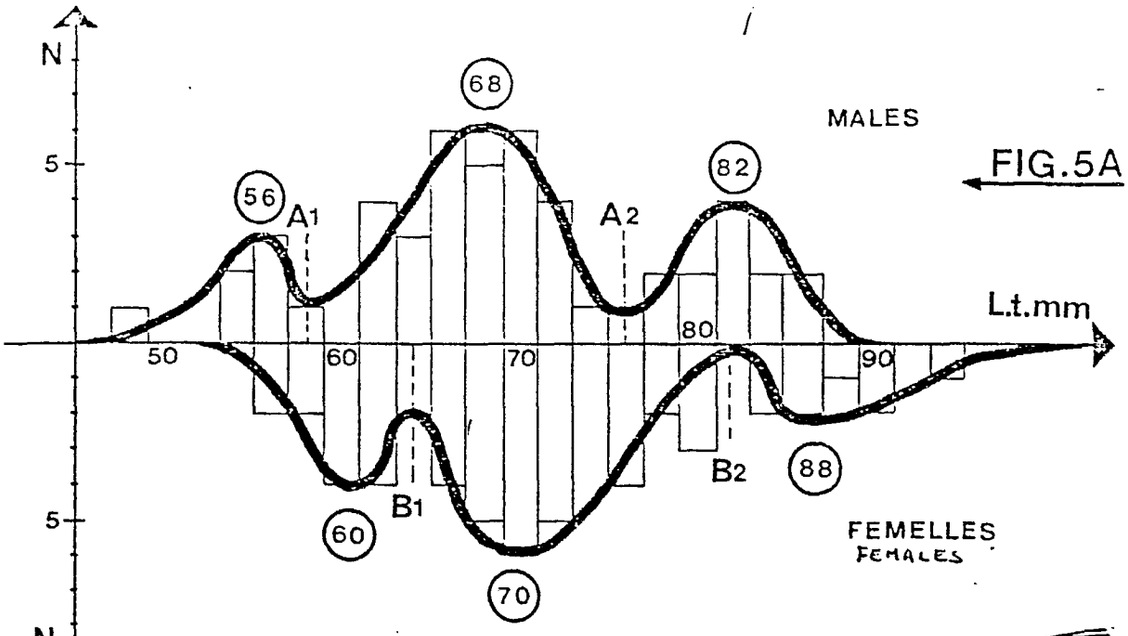

FIG.5A

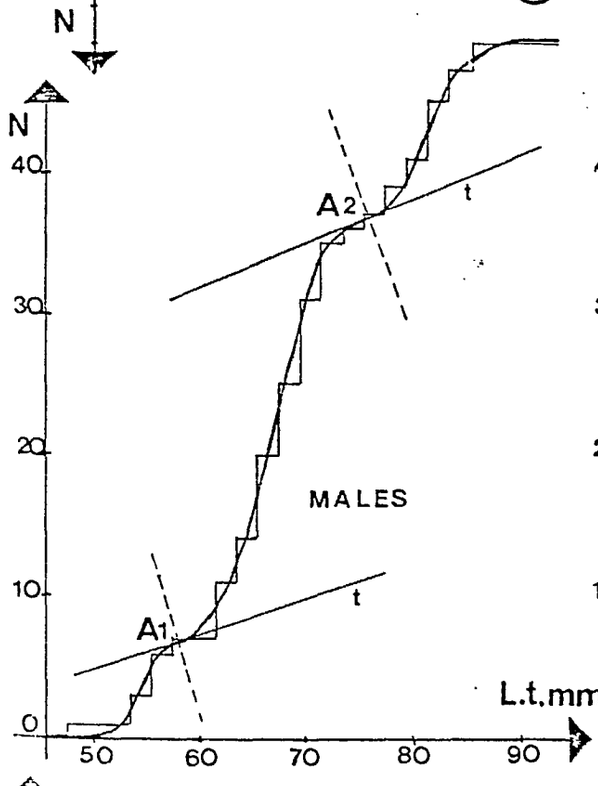

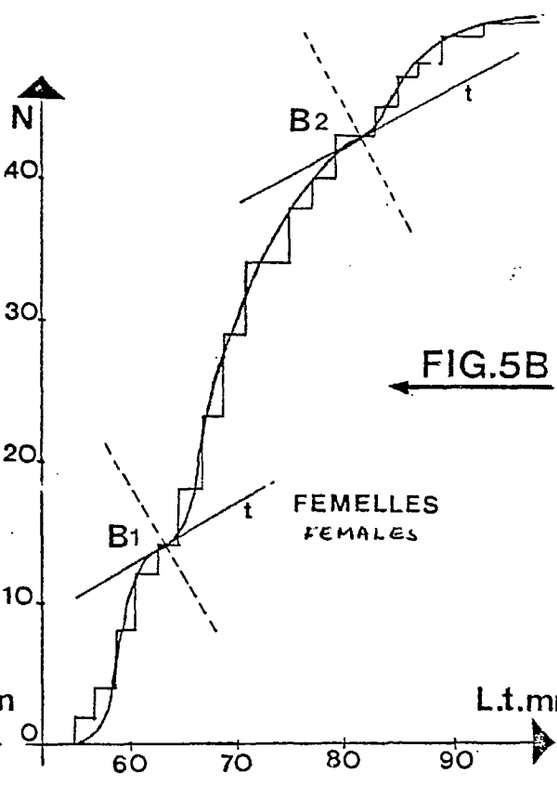

FIG.5B

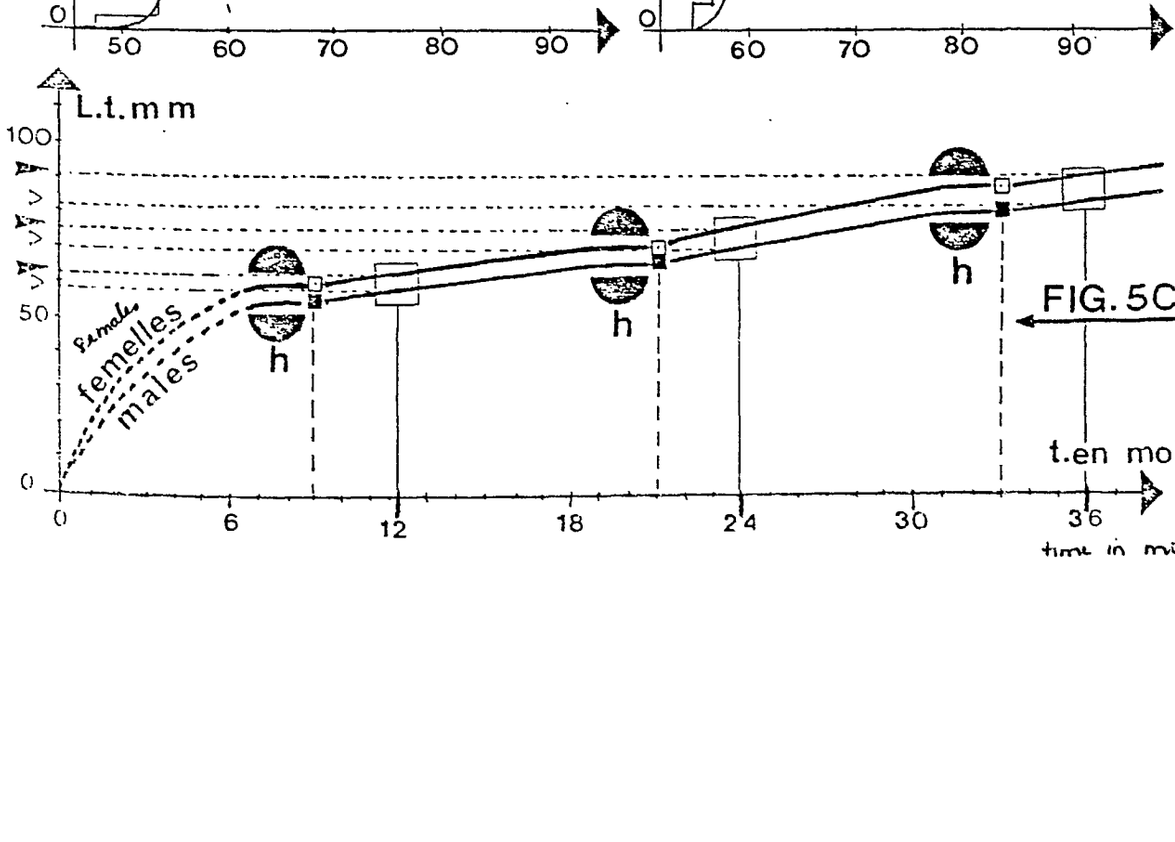

FIG.5C

Average length of a male yearling = 60 mm
Average length of a female yearling = 60 mm
Average length of a 2-year-old male = 70 mm
Average length of a 2-year-old female = 75 mm
Average length of a 3-year-old male = 80 mm
Average length of a 3-year-old female = 90 mm.

As these results are only approximate, they should be considered with caution. They will be used, however, as a basis for research on microsporidiosis.

The sex ratio was also calculated for each catch. It was expressed in terms of the male-to-female ratio. Details are included in Table 2.

As may be seen, there was considerable variability in the sex ratio since no regular changes were observed as a result of geographic location or the seasons. These findings were based on 4,148 dissected fish. Kohler (1976) reported a sex ratio of 1.1 for roughly 1,000 fish caught in the Etang du Prévost.

b) Reproduction. Over close to a 2-year period, we examined the gonads from fish that came from various sources. A maturity scale was established for Atherina boyeri:

0 = totally quiescent gonads or, in females, dilated but empty gonads (recent egg-laying)
1 = ovules, visible to the naked eye - white testicles
2 = gonads extending as far as the liver
3 = gonads of maximum size, clearly compressing the liver.

Lagoon Etangs	date	sex-ratio	number of specimens n
Canet	10-76	0,85	100
Bages	9-76	1	90
Thau	10-76	0,92	47
	10-76	0,85	100
Vic-Moures	12-76	0,69	100
	1-77	0,74	54
	3-77	0,67	50
Prévost	12-76	0,75	79
Grec	3-77	1,5	43
Mauguio	10-76	0,81	100
	10-76	0,72	38
	11-76	1,35	80
	12-76	0,96	80
	1-77	0,85	95
	2-77	0,96	100
	3-77	0,66	82
	4-77	1,24	100
	6-77	0,49	81
	8-77	0,96	100
	8-77	2,03	100
	9-77	1,27	100
	9-77	0,96	100
	10-77	0,96	100
	10-77	0,96	100
	11-77	0,96	100
	12-77	0,73	90
	1-78	1,32	100
	2-78	0,96	100
Rhône Mort	11-76	0,89	100
	11-76	0,64	100
	1-77	0,75	100
Vaccarès	1-77	0,85	50
Berre	5-77	0,89	100
Olivier	5-77	1,7	100

Table No. 2. Sex Ratios

In order to characterize the state of maturity of a given population (young-of-the-year smelts were excluded), the figures were added and the sum was divided by the number of fish, yielding a result that could range from 0 to 3.

On the basis of findings in over 1,700 fish caught in the Etang de Mauguio, the reference number was equal to 0 from September to January, 0.7 in February, 1 in March, 2.05 in April and 1.95 in June. The figure dipped to 0.02 in August and dropped further to 0 in September. As a result, it may be concluded that the egg-laying period in the Etang de Mauguio extends from the middle of April to the end of July (See Fig. 6).

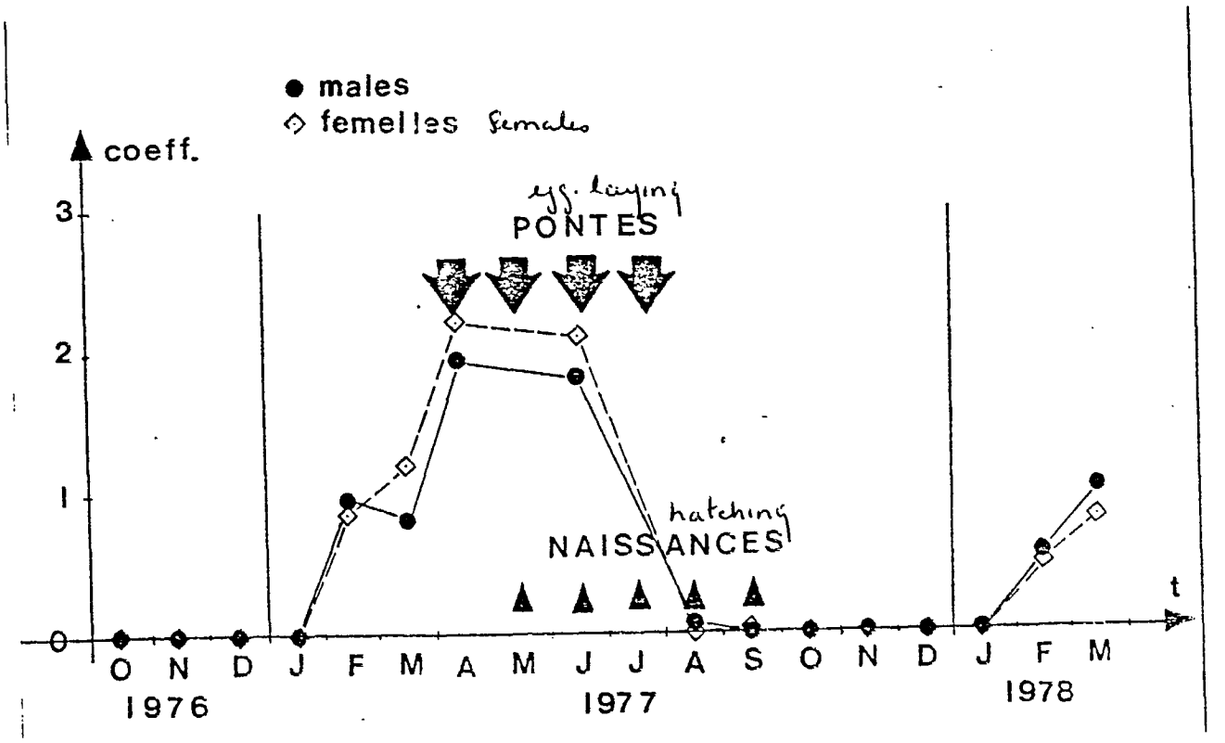

Fig. 6. Changes in the Sexual Maturity Coefficient over the Year

These findings correspond roughly to the results given by Kohler (1976) for the Etang du Prévost and by Hervé (1978) for the Etang de Canet and the Etang de Salses.

c) Parasitic Fauna. During the course of this investigation, we enumerated 16 different parasites (See Fig. 7). They included:

PROTOZOANS

CILIATES. Urceolariidae: not determined, on the gills.

Ophryoglenidae: Ichthyophtirius multifiliis on the gills, subcutaneous

COCCIDIA.

Eimeriidae: Eimeria sp., in the digestive tube (Fig. 8)

MICROSPORIDIANS.

Glugeidae: Glugea atherini sp. n., the subject of this investigation

MYXOSPORIDIANS

Ceratomyxidae: Ceratomyxa sp., in the gall bladder (Fig. 9)

Protozoans and myxosporidians are parasites that generally require long period of observation. Consequently, there was no systematic attempt to identify them during dissection operations nor to establish their frequency of occurrence. Often, they were observed only once or twice. A member of the family Urceolariidae, for instance, was observed only once, in a fish caught in the Etang de Mauguio. The species Ichthyophtirius multifiliis was detected only after breeding when it was found in large numbers in a lot of atherines caught in the Canal du Rhône à Sète in the region of Frontignan-La Peyrade. Coccidia were observed twice or three times in fish from the same source. Myxosporidians were found only once, in the gall bladder of a fish caught at the same site.

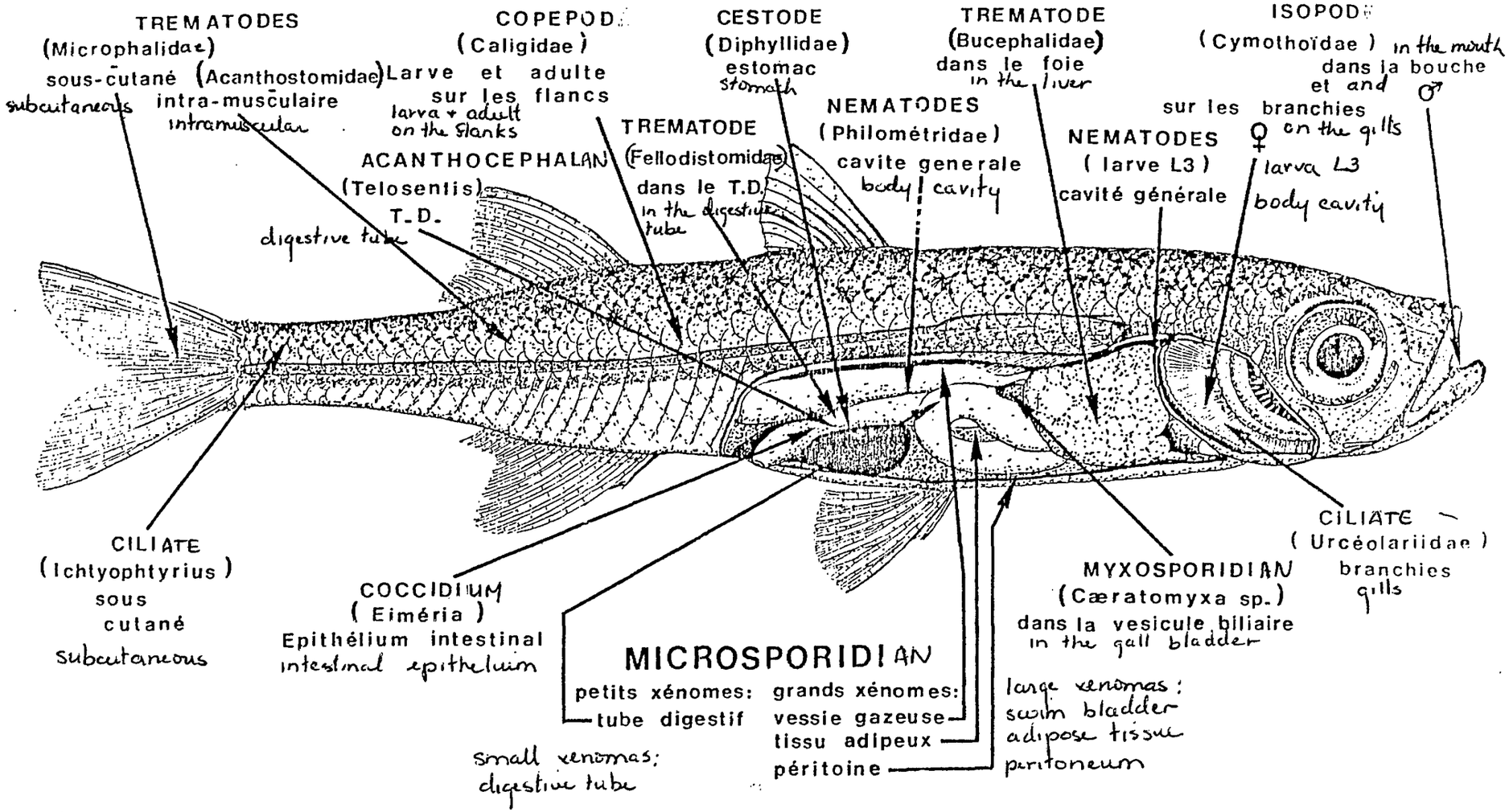

FIG_7 ► PARASITIC FAUNA OF ATHERINA BOYERI
PARASITOFAUNE DE ATHERINA BOYERI (x4)

METAZOANS

PLATYHELMINTHES. Cestodes

Diphyllidae: Bothriocephalus sp., in the stomach (Fig. 10)

One point regarding the genus Bothriocephalus sp. warrants closer scrutiny. The usual cycle is as follows: the adults invade the intestines of selachians and occasionally teleosts. Once the eggs have been laid, they produce free-living coracidium larvae which are ingested by copepods. The larvae develop into procercoids and subsequently into plerocercoids which, as a result of the food chain, usually infest the body cavity of teleost fish. The latter are in turn eaten by the definitive hosts where the plerocercoids attain maturity.

We recorded one instance in which an atherine was infested with 5 cestodes. A thorough study of the parasites revealed that the genital system was well-developed but that the testicles were not involved in vitellogenesis. This could only mean that these were plerocercoids with a precocious genital system or else, very young adults that had not yet attained sexual maturity. If these were in fact plerocercoids, their location in the digestive tract can only be considered an aberration. If, on the other hand, they were adults, it is not clear how this individual could have devoured another teleost, acting as the intermediate host for the plerocercoids. The only answer to this riddle resides in another cestode, i.e., Bothriocephalus cuspidatus. The cycle of this species, which infests a member of the Percidae family, was described by Essex in 1928. The plerocercoid is found in the intestine of the host and the adult in the cecum of the same individual. It is not known whether the parasite spends its last two stages in the same host. It can be assumed that the Bothriocephalus specimens infesting the atherine remained in the same individual for the plerocercoid and

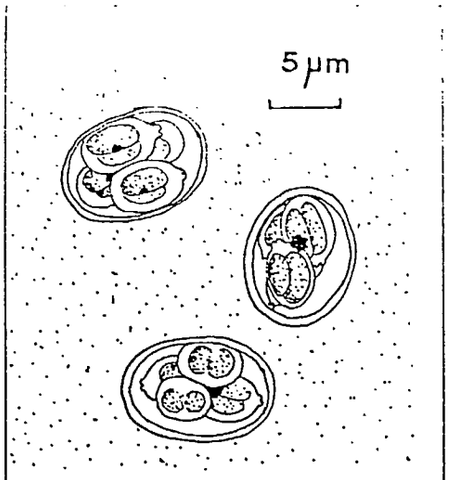

Fig.8 Eimeria sp.

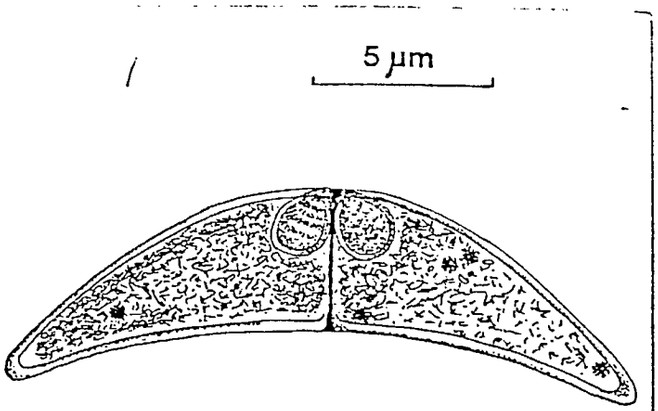

Fig.9 Ceratomyxa sp.

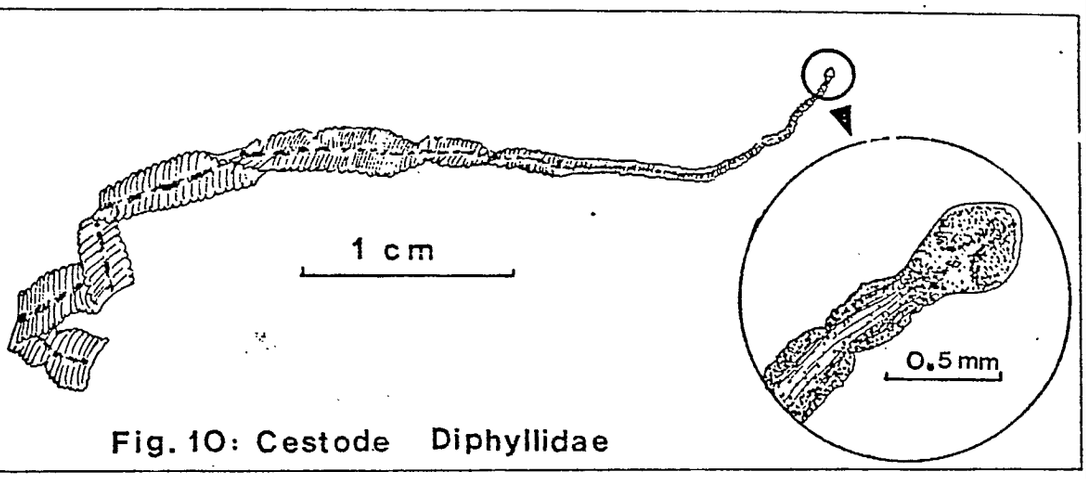

Fig. 10: Cestode Diphyllidae

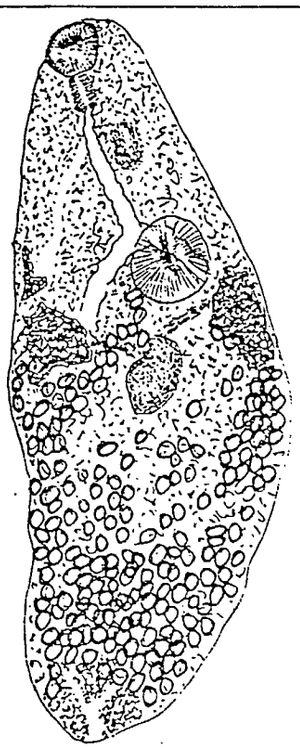

Fig.12: Bacciger bacciger

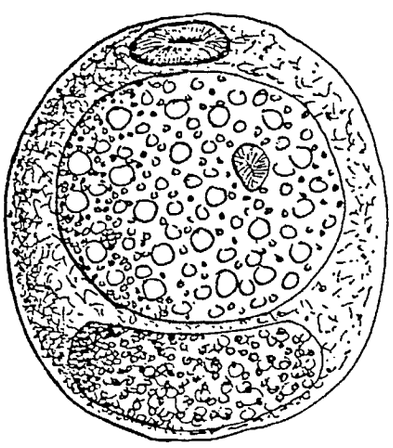

Fig.11: Labratrema minimus

adult stages. It may also be that the atherine we examined was an accidental host since this type of parasitism is extremely rare. In fact, this was the only case recorded in the 1,783 fish collected in the Etang de Mauguio.

Trematodes.

Microphalidae (subject to revision: not determined, encysted metacercariae under the skin (Plate IV, photo 9)

Acanthostomidae: Acanthostomum imbutiforme (Molin, 1859) Gohar, 1934 and Timoniella praeteritum (Loos, 1910) Maillard, 1974, encysted metcercariae in the muscles

Bucephalidae: Labratrema minimus Stossich, 1887, encysted metacercariae in the liver and body cavity (Fig. 11)

Fellodistomidae: Bacciger bacciger (Rud, 1819) Nicoll, 1914, adult in the digestive tract (Fig. 12 and Plate IV, photo 10)

Acanthocephalans:

Illiosentidae: Telosentis molini van Cleave, 1923, in the digestive tract (Fig. 13).

Plate IV

9 - Atherina boyeri caught in the Rhône de Saint Roman. K = metacercarial cysts of Microphalidae (x 2.8)

10 -Optical microphotograph of a semi-fine section of Bacciger bacciger fixed, then stained with toluidine blue. EH = intestinal epithelium of the host; PM = muscular pharynx; VB = mouth sucker; VV = ventral sucker (x 550)

11 - Caligus pageti attached to the left side of an atherine. FF = frontal filament; ZL = area injured by the copepod's mouth parts (x 4.8)

12 - Blood smear stained with May-Grunwald-Giemsa stain; the sample was taken from a living fish with generalized scepticemia. HD = degenerate red blood cells; N = nucleus from a damaged red blood cell (x 1,600).

PLANCHE IV

PLATE IV

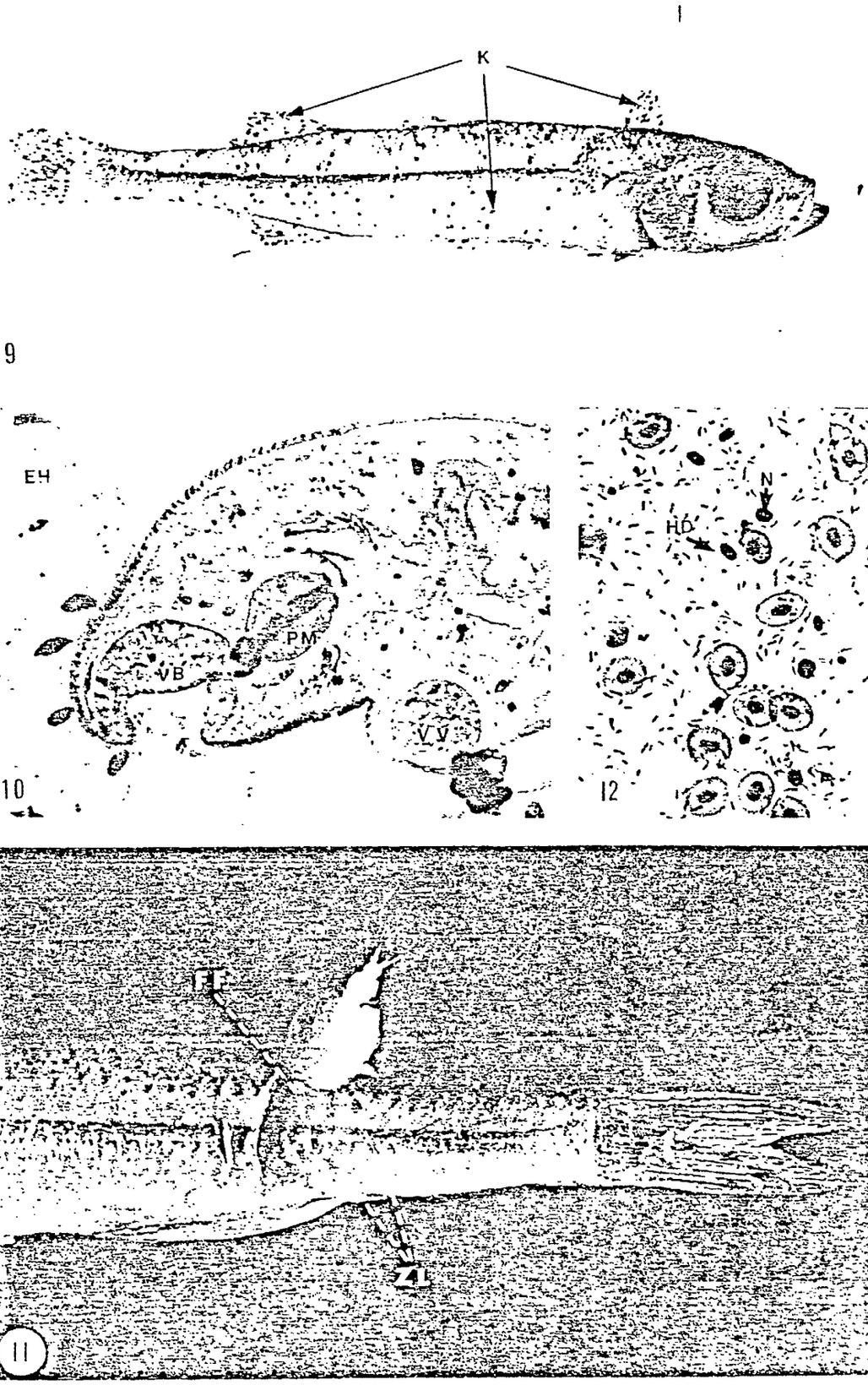

NEMATHELMINTHS. Nematodes

Not determined, encysted larvae around the digestive tract.

Phylometridae: not determined, adult in the body cavity (Fig. 14)

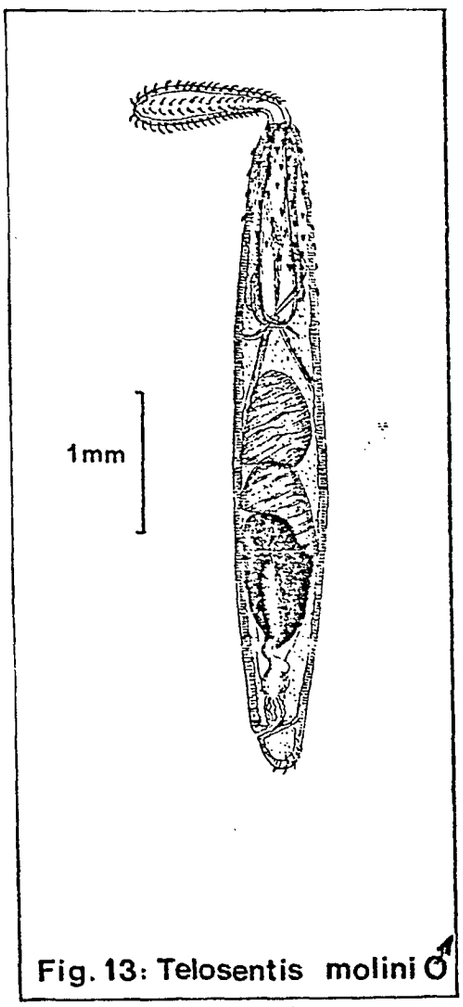

Fig. 13: Telosentis molini ♂

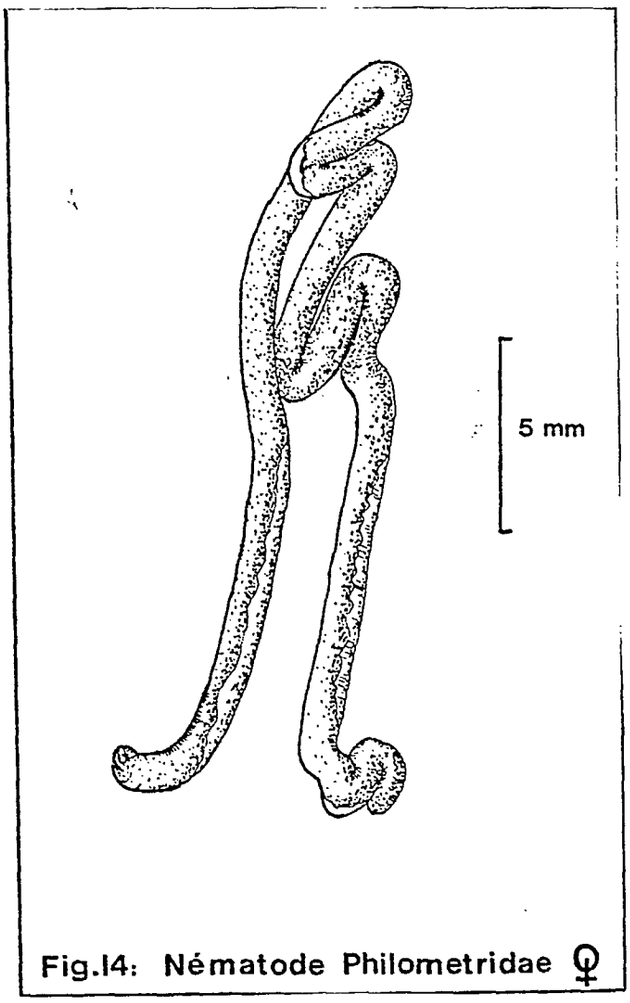

Fig.14: Nématode Philometridae ♀

ARTHROPODS. Copepods

Caligus pageti Russel, 1925, chalimus stage and adult attached to the skin (Fig. 15 and Plate IV, photo II).

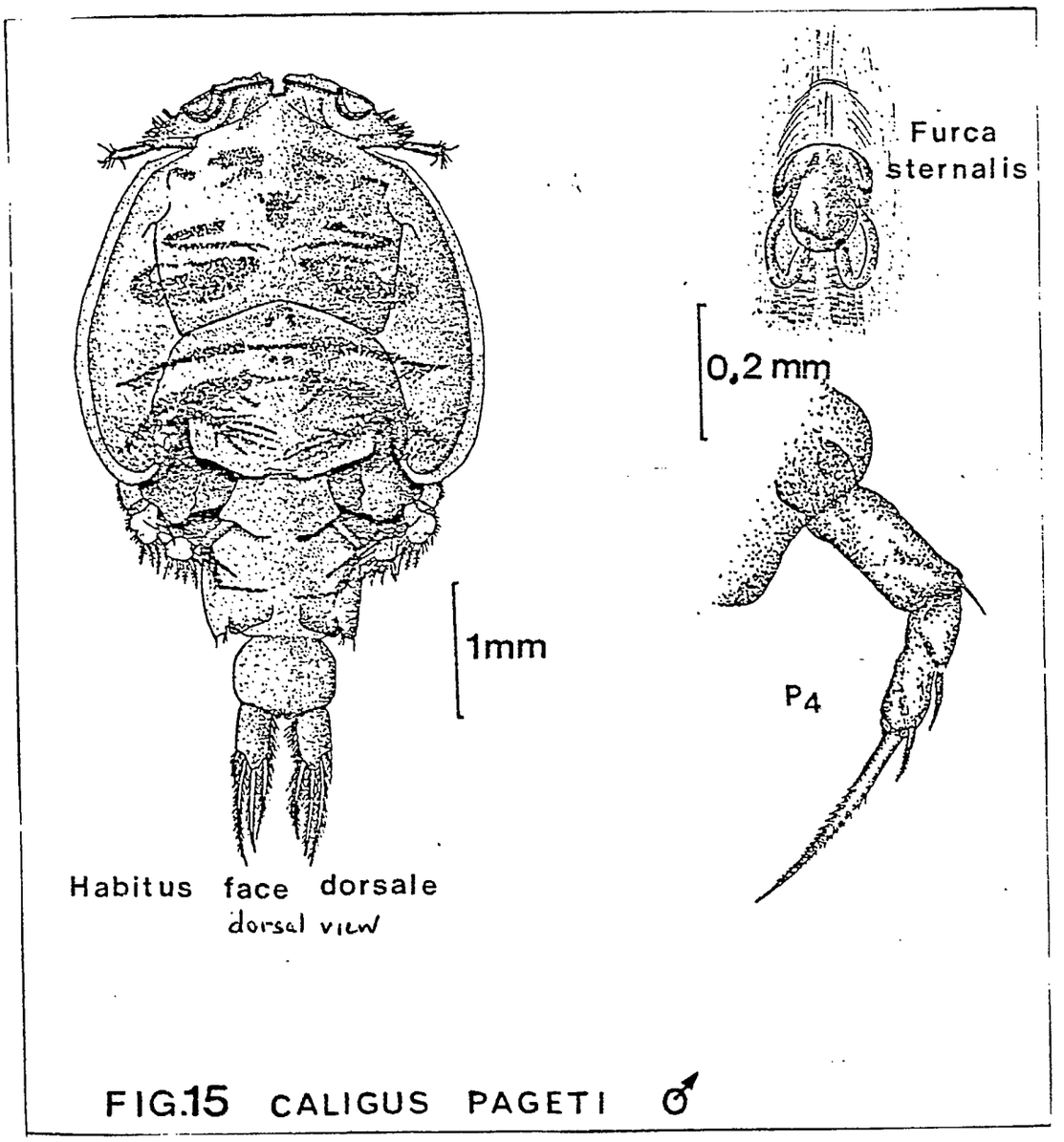

FIG.15 CALIGUS PAGETI ♂

Isopods

Motocya epimerica Coste, the male on the body or the tongue, the female in the gill cavity (Fig. 16).

The incidence of parasitism due to metazoans was determined for the various sites (Table 3).

	TREMATODES				CESTODES adults	ACANTHOCEPHALANS	NEMATODES		MYRIAPODS	ISOPODS
	metacercaria SKIN	MUSCLE	LIVER + BODY CAVITY	DIG. TUBE	STOMACH	DIG. TUBE	adults BODY CAVITY	larvae L3 BODY CAVITY	Chilopoda adults SKIN	GILLS SKIN
Etang de Canet	+	++	++++	+				R		
Etang de Bages	R	+	+++	+		++				
Bassin de Thau	+++	+	+++	+++		+	RR	++	RR	
Canal du Rhône à Sète Niveau La Peyrade	+++	+	+	+					+	
Etang de Vic	+++	+		++						
Etang de Houres	++	+	+	+						RR
Etang du Prévost	+++	+		+						RR
Etang du Grec	++	+	+	+						RR
Etang de Hauguio	+++	+	+	+	RR				++	
Canal du Rhône à Sète Niveau Carnon	++	+	+	+					+++	
Rhône mort	+++	+++	+++	++		+		++	R	RR
Vacarès (Etang)	+++	+		+		+++				
Etang de Sirre	+	+	+	+						
Etang d'Urbino		+		+		+++				+

Table 3. Incidence of Metazoan Parasites at the Various Sites

Of the 16 parasites:

- 5 have never been reported by other authors, i.e., the coccidium, microsporidian, myxosporidian, the member of the family Microphalidae, the encysted nematode and the cestode (subject to revision) and may constitute new species.

- 1 was previously observed by investigators from the Museum but was never the subject of an in-depth study, i.e., the giant nematode of the body cavity.

- 4 have been described in other hosts (the ciliate of the family Urceolariidae (subject to revision), Ichthyophturius, the copepod).

Face dorsale
DORSAL VIEW

Profil
PROFILE

Face ventrale
VENTRAL VIEW

1 mm

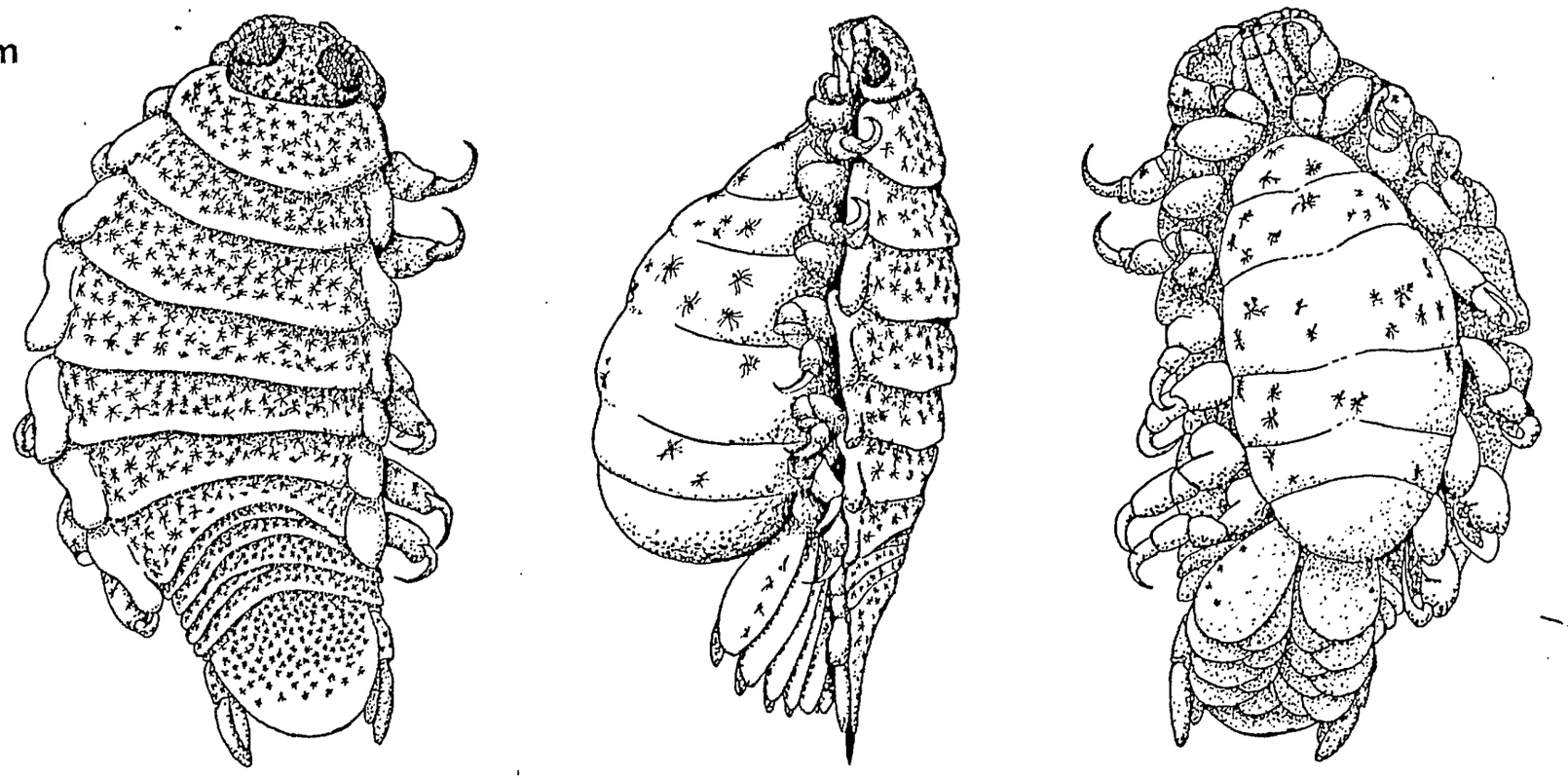

FIG-16: MOTHOCYA EPIMERICA (x15)

Individu en phase sexuelle femelle. La cavité incubatrice est pleine
INDIVIDUAL IN FEMALE SEXUAL PHASE. THE BROOD POUCH IS FULL

- 1 was found in the Languedoc-Provence area for the first time during the course of this study, i.e., Caligus pageti. Furthermore, it had never been observed before in an atherine.

- 6 only have already been reported in atherines.

C - Study of the Parasite

1/ Procedure

Three different approaches were employed in our study of the parasite, i.e.,

a) Dissection was done under a binocular lens. In some cases, the xenomas were examined under the light microscope, between the slide and coverslip.

b) Staining for light microscopy. Smears of interesting specimens were stained by the May-Grunwald-Giemsa method. Some specimens were also embedded in toto in hot paraffin. 5-µm thick serial sections were sliced with the microtome and stained with the following dyes:

- Heidenhain's Azan stain
- Masson stain } topographic stains
- Delamater's basic fuchsin - essentially for demonstrating nuclei
- histochemical stains will be discussed later.

These methods were adopted from Gabe (1968) and Martoja and Martoja-Pierson (1967).

c) Electron microscopy. The xenomas were also prepared for electron microscopic study. Preparation included the following steps:

- fixation in 2% osmic acid,buffered with Palade's fixative (pH 7.4) or with Millonig's phosphate buffer (pH 7.4). Prefixation with 2% or 4% glutaraldehyde in Millonig's buffer solution was optional.

- embedding in various resins (araldite, "spurr") following dehydration with ethyl alcohol and propylene oxide.

- sectioning with the ultramicrotome fitted with glass blades. Copper mesh plates were used. The specimens were impregnated with uranyl acetate and lead citrate (Reynolds) for greater contrast. Semi-fine test sections were directly stained on the slide with toluidine blue.

- Observation with the Zeiss EM 9 A electron microscope belonging to the General parasitology and ichthyology laboratory (Laboratoire d'Ichthyologie et de Parasitologie générale).

2/ Study of Parasite Implantation

a) Macroscopic Observations

. Observations without dissection. Implantation may follow one of two patterns. Either large aggregates of small xenomas of not more than 0.2 mm occur in the digestive tract (See Plate V, photo 16) or else large xenomas, which may attain 13 mm, become established in the fatty tissue of the body cavity, outside of any organ (Plate V, photo 15). Only the latter type of xenoma can be diagnosed in a live fish without resorting to dissection. In diameter, however, it must be close to the width of the fish for it to deform the side of the body cavity (Plate V, photos 13 and 14).

PLATE V

13 - (Top) healthy atherine and (bottom) specimen with a large xenoma in the body cavity near the rectum (X 1.7)

14 - Ventral view of the same subjects (X 1.8)

15 - Extreme case of parasitism of the body cavity: cysts (k), 0.5 to 6 mm, often vascularized (v) (X 3.3).

16 - Large numbers of cysts in the digestive tube. F = liver; I = intestine; K = cysts; R = rectum; TA = adipose tissue; VG = swim bladder (X 4.5).

17 - Live spores. VP = posterior vacuole (X 1,800).

18 - Young spores embedded in their sporogony vacuole (X 1,350).

PLANCHE V

PLATE V

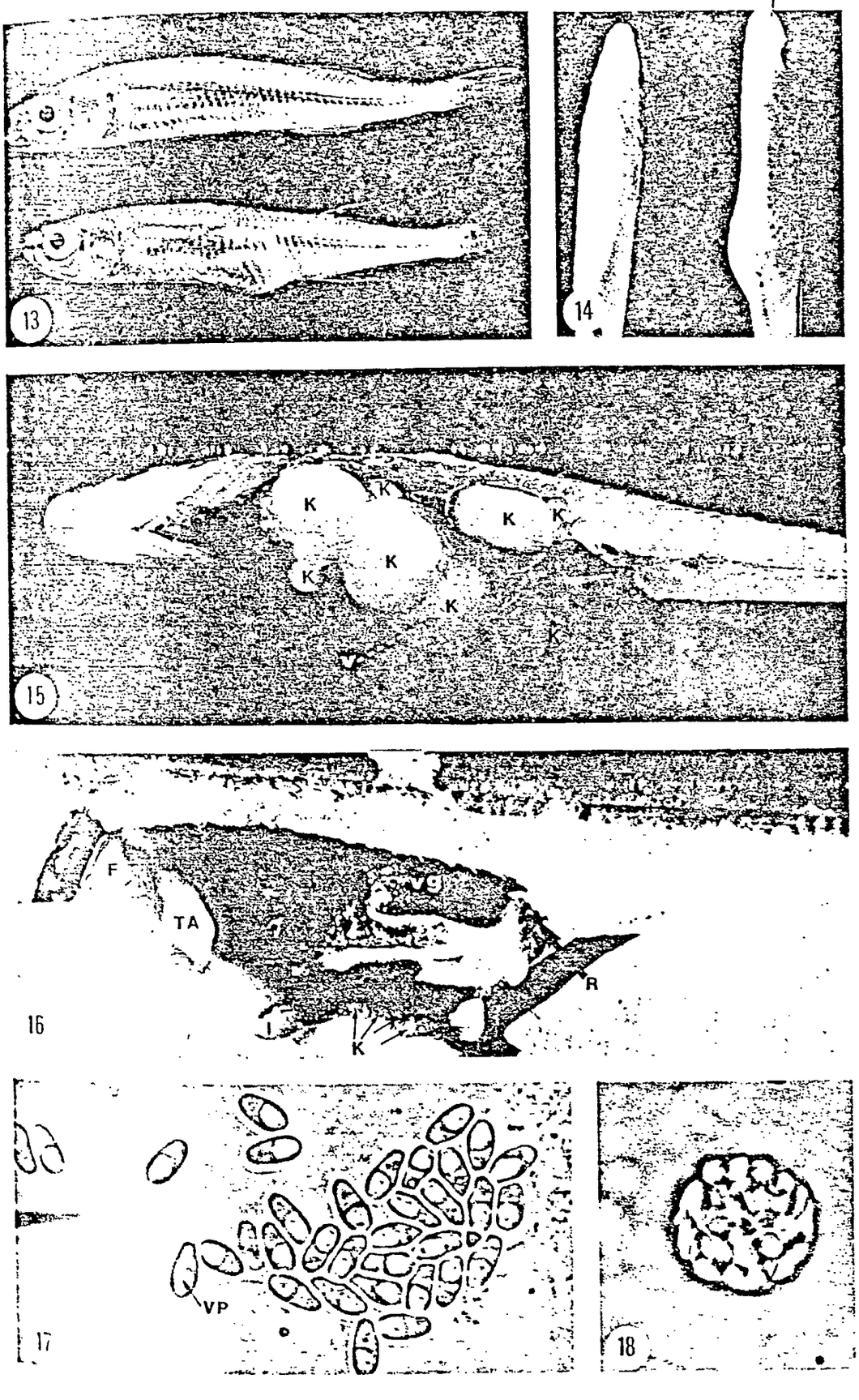

Roughly one-tenth of the fish with this type of xenoma can be recognized without dissection. Deformation, which may occur in the area of the liver and as far down as the rectum, is always symmetrical and never involves only one side. Glugea anomala (Moniez), a stickleback parasite, produces subcutaneous cysts. As a result, only one of the host's sides is dilated. Small spherical structures form and most of the cysts can be detected from the outside (Weissenberg, 1911; Debaisieux, 1920). The microsporidian infesting atherines can produce subcutaneous cysts, but only under experimental conditions that will be discussed later.

Observations following dissection. In most cases, it is necessary to dissect the atherine specimen. Dissection should be performed in fesh or frozen specimens. Insofar as possible, the lots of atherines should not be treated with formol or alcohol which causes opacification of the tissues, hindering identification of xenomas in the digestive tract. Regardless of the type of xenoma involved, it begins its existence the size of a single cell and cannot be seen under a binocular lens. It gradually grows. Once it reaches 50 µm, it becomes visible, but only upon very close scrutiny. The rate of recorded parasitism is consequently always below actual levels of infestation, but studying fresh fish that have not been treated chemically reduces the chances of error.

* Intestinal xenomas are small and rarely exceed 200 µm in diameter. They can be readily seen if over 50 µm in diameter and are present in large numbers. Characteristically, they are uniformly white, contrasting with the darkish brown colour of the digestive tract (Plate V, photo 16).

The xenomas in a particular area of the digestive tract are usually the same size. There may be several clusters in the same specimen with the diameters of the xenomas varying from cluster to cluster. This may be due to successive waves of implantation. At times, xenomas of different sizes co-exist in the same area, but correspond to 2 or 3 non-sequential size classes. Aggregates of equal-sized xenomas may be found throughout the digestive tract, or conversely, only within a very small area. There is considerable variation in the number of implantations. Occasionally, there is only one in the digestive tract, and at times, there are 4 or 5. Often, there are dozens. More rarely, there may be hundreds in only one segment of the digestive tube and close to a thousand in all.

In Table 4, the digestive tube has been more or less arbitrarily divided into 6 segments:

Segment No. 1 corresponds to the oesaphagus

Segment No. 2 corresponds to the stomach

Segment No. 3 corresponds to the anterior intestine as far as the first loop

Segment No. 4 corresponds to the intestine between the 2 loops

Segment No. 5 corresponds to the posterior intestine beginning at the second loop

Segment No. 6 corresponds to the rectum.

The table is based on 35 fish with infestation of the digestive tube that were caught between February 1976 and January 1977 at the following sites:

1 fish from the Etang du Grec

2 fish from the Canal du Rhône à Sète at Carnon

5 fish from the Etang de Mauguio

27 fish in the Rhône Mort, in Petite Camargue.

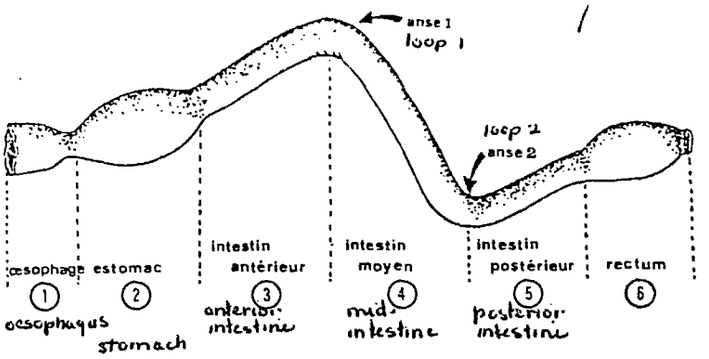

Segment number		1	2	3	4	5	6
Number of specimens with infestation of corresponding segments		0	14	16	17	22	17
Avg. number of cysts per segment		0	8.5	4.9	4.1	8	5.8
fish < 60 mm (between 0 and 1 year old)	Number of infested individuals	0	8	10	11	14	13
	Number of cysts per segment	0	7.4	3.1	5.2	7.7	6.2
fish > 60 mm (over 1 year old)	Number of infested individuals	0	6	6	6	8	4
	Number of cysts per segment	0	10	9.2	10.5	8.6	4.7

Table 4. Distribution of the Xenomas in the Digestive Tube

It was found that the posterior portion of the intestine (segment No. 5) constituted the preferred site of implantation in the greatest number of infested fish. There were progressively fewer fish with involvement of the other segments. When the specimens were divided into two size classes, i.e., over and under 60 mm, the same pattern was observed. On the basis of the number of xenomas per segment, the stomach was as heavily infested as segment

No. 5.

In brief, the posterior intestine (segment No. 5) is more frequently parasitized than the stomach (segment No. 2) but the degree of infestation is essentially the same for both (Legault and Delisle, 1967). Furthermore, the oesophagus is never involved, perhaps due to the absence of the digestive juices needed for the extrusion of the polar filament (Delisle, 1972).

In order to explain these results, two types of factors warrant consideration, i.e.,

1) one segment may prove more congenial for extrusion of the spore and implantation of a xenoma. This may be due to the presence in the chyle of substances favourable to development of the spore, or to the limited defenses of the host against the parasite, whereby development of the xenoma is promoted.

2) the longer time needed for spore-infested food to make its way through the segment may provide more parasites with the opportunity of penetrating the fish.

Actually, both of these factors probably come into play.

In the oesophagus, where there are never any xenomas, the environment is poor in chemical substances and the food passes through quickly.

In the stomach, where there is marked infestation (an average of 8.5 cysts), the reverse holds true. There is considerable secretion and the food passes through slowly.

There is unequal involvement of the intestine. In the first

two segments, i.e., segments Nos. 3 and 4, there is little infestation, whereas in the posterior third, it becomes more pronounced (an average of 8 cysts in segment No. 5). It is in this segment that the food and, consequently, the spores are concentrated for subsequent expulsion from the body.

The waste material is rapidly evacuated from the rectum which has little in the way of secretions. This explains why the rate of parasitism in this segment drops. Lastly, age, hence the size of the digestive tract (difference in the amount of food and consequently in the number of spores in the intestine) and diet may account for the difference in parasite numbers in fish over and under 60 mm in length. In the larger fish, essentially the same number of xenomas is found in the various segments of the intestine.

* Body cavity xenomas may reach 13 mm in diameter and are truly an impressive sight when they grow out of all proportion to the size of the host. A 5-cm-long fish, for instance, may harbour a 1-cm cyst. These cysts are spherical in shape. Kabata (1959) reported that cysts produced by Pleistophora hippoglossoideos Bosanquet, 1910, a muscle parasite, were elongate, reaching 2.5 x 10 mm in size.

In small, hence undoubtedly young, xenomas, the walls may be gelatinous and transparent. Only the center portion is white, but the wall very rapidly becomes opaque and white with a dense and well-defined system of vascularization (Plate V, photo 16). A xenoma embedded in adipose tissue behind the liver was found to receive its blood supply from a large vessel originating in the liver, which is a clearcut case of the host incorporating the cyst within its own system.

The cysts may become implanted in areas other than the body cavity proper, but this is far less common. Table 5 gives the distribution of 184 cysts examined.

Body cavity (adipose tissue, connective tissue)	85.5%
Swim bladder (interior or wall)	6.1%
Peritoneum	5.0%
Other sites (testicles, liver)	3.5%

Table 5. Distribution of Xenomas in the Body Cavity

The large xenomas differ in size, depending on their location, as may be seen from Table 6.

	Max. diameter	Avg. diameter
Adipose tissue, connective tissue (155 xenomas)	13 mm	3.9 mm
Swim bladder	6 mm	2.9 mm
Peritoneum	6 mm	3.5 mm

Table 6. Average Diameter of Xenomas in the Body Cavity

It should be pointed out that xenomas adhering to the peritoneum have a great deal of space at their disposal. Vascularization of these cysts may be compared, quantitatively and qualitatively, to that of xenomas occurring in adipose tissue. Cysts in the swim bladder, on the other hand, are smaller and vascularization

is less well developed.

With the exception of size, the appearance of the xenomas is essentially the same, irrespective of the site of implantation:

The xenomas may be spherical with generally good vascularization provided by one or two vessels that subdivide a number of times (Plate V, photo 15). This type of cyst is usually white with an average diameter of 4.5 mm. It is referred to in this text as a milky xenoma.

The cysts may be somewhat deformed without any signs of vascularization. They often have black spots and may occasionally be completely black. The average diameter is 2.9 mm. These white or cream-coloured chalky cysts are hard since their contents are compact. We have referred to them as chalky xenomas. They may develop highly irregular shapes and mold themselves to the shape of adjacent organs. Their contents become very hard and non-friable. Stunkard and Lux (1965) observed an identical progression to chalky, rigid and hard cysts in Clugea stephani.

There is actually an entire range of intermediate types, suggesting a progression from one type to the other. This hypothesis will be discussed in the section on the development of parasitism over time.

One of the remarkable features of the phenomenon is the virtual absence of any connection (other than through vascularization) between the xenoma wall and the host. The cysts can therefore be very easily detached without damaging them. They leave behind a well-defined spherical cavity.

In order to pinpoint the position of the xenomas in the body

of the fish, we divided the body cavity into three parts, i.e.,

- the anterior portion extending from the oesophagus to the posterior tip of the liver;

- the posterior portion, extending from the anus to the anterior portion of the quiescent gonad;

- the midportion, between the other two zones, comprising the two intestinal loops.

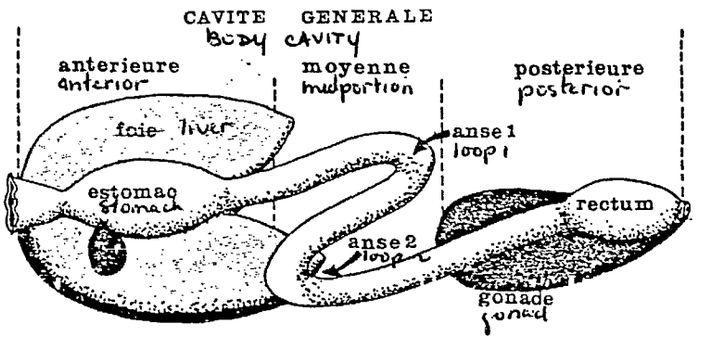

Areas involved	Body cavity Ant.	Mid	Post.	Swim bladder	Body cavity wall
Number of infested individuals	13	22	10	5	1
Percentage of infested areas	25%	43%	20%	10%	2%

Table 7. Distribution of Xenomas in the Adipose Tissue of the Body Cavity

The mid-region is obviously the most often parasitized. 43% of the specimens had cysts in the mid-region as opposed to 25% in the anterior portion and 20% in the posterior zone. This may be due to the fact that the xenoma is very loosely joined to the host. A cyst developing in the anterior portion will, as it grows, be pushed back by the liver to the mid-portion which does not contain

any bulky organs. The same phenomenon may occur in the posterior region of the body cavity. The end result is a predominance of cysts in the mid-portion.

. Observation of living spores. Under the optical microscope, living spores assume an elongate, ovoid shape (Plate V, 17). A transparent posterior area, traditionally referred to as the posterior vacuole, occupies roughly half of the spore. At times, young spores may be seen in smears within the sporogony vacuole (Plate V, 18). Ninety-two spores were measured. Fig. 17 respresents a histogram of frequency of the length and width of spores from a milky xenoma . The figures are given in Table 8.

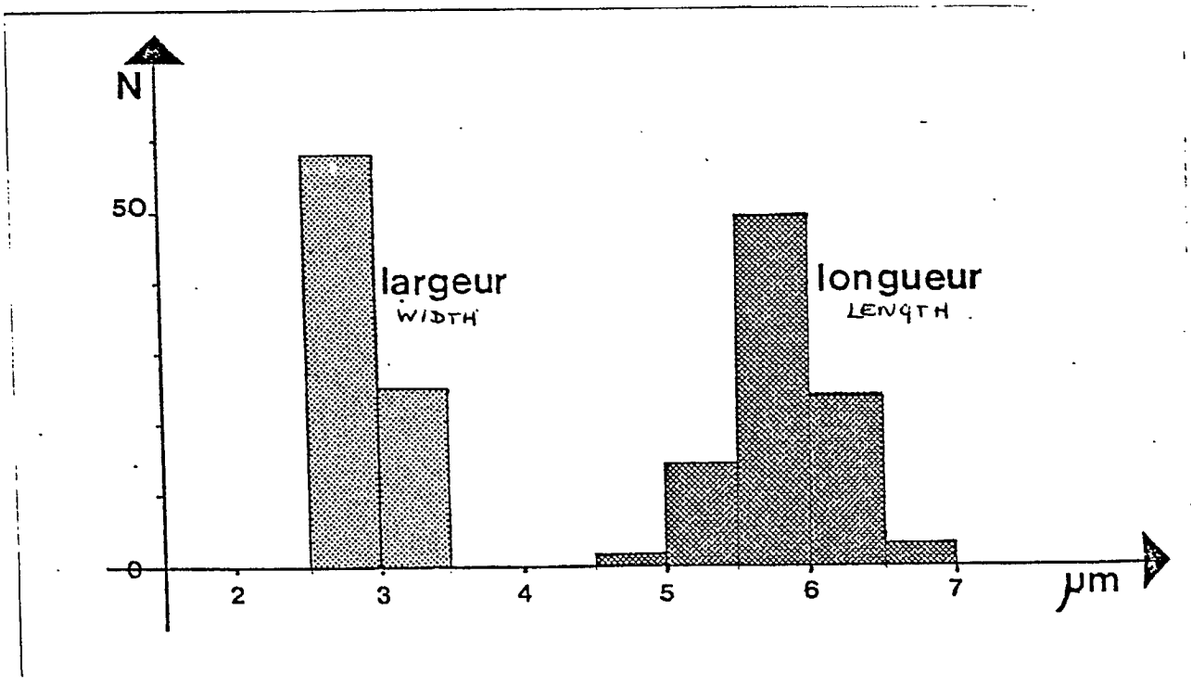

Fig. 17. Histogram of frequency of width and length of spores from a milky xenoma in a specimen from the Etang de Mauguio.

	Min. (µm)	Max. (µm)	Avg. (µm)	σ (µm)	n
Spore length	4.5	6.5	5.76	0.35	92
Spore width	2.6	3.3	2.98	0.08	83
Diameter of posterior vacuole	2.3	3.3	2.85	-	91
Filament length	-	-	135	-	1

Table 8. Measurement of Spores from a Milky Xenoma in a Specimen from the Etang de Mauguio

In conclusion, the atherine-infesting microsporidian is an average of 5.8 x 3.0 µm in size.

b) Microscopic Observations

. The xenoma. All the xenomas are built on the same model. The different concentric zones undergo changes during maturation. For a description, it is essential to determine the state of maturity, if not the age, of the cysts. Only an evaluation of the proportion of mature spores in relation to the other stages of development is decisive. Cyst size does not give an accurate picture. Toward the end of developmemt, the cysts may range from 10 to 13,000 µm in diameter, depending on where they are established. Mature spores have not been detected in very young cysts, probably because this stage is too small. After infesting young sticklebacks experimentally, Weissenberg (1921) was able to observe these stages in serial histological sections. The first spores therefore appear very rapidly. According to estimates that will be discussed in the section on experimental infestations, the spores first appear 15 to 30 days after implantation. After that, spore formation may last several months in the case of the largest xenomas. The zone containing the mature spores continues to expand at the periphery. Toward

the end of its development, the cyst is nothing more than a sackful of spores, all the other zones (which will be described later) having disappeared. The relative size of the spore zone in relation to the total cyst is consequently the only means of assessing cyst maturity. Wile this working hypothesis should be applied with caution, it will serve as a basis for this section. The description of the different concentric zones is based on observations of slide preparations of histological sections and preparations for electron microscopic examination.

The different zones of the xenoma (Plate VI)

PLATE VI

19 - Structure of the xenoma in the area of the wall, seen on a histological section (X 1,000).

20 - Ultrastructural appearance of the external side of the wall (P) infiltrating the area between the fibrocytes (arrows). NF represents a fibrocyte nucleus (X 3,600).

21 - Internal side of the wall (P) in contact with the microtubule-containing zone (ZT) and the zone with mitochondria and microtubules (ZMT) (X 14,500).

22 - Jellylike wall in a very young xenoma (X 5,000).

23 - Aggregate of pigment granules (X 31,500).

24 - Zone with giant host nuclei (NH) and merogonic stages (M) in the host cytoplasm (X 2,700).

25 - Detail of host nuclei still joined by a very fine isthmus (X 3,000).

26 - Zone with alveoli (A, B and C) still containing strips of host cytoplasm with merogonic stages (M). The alveoli or sporogony vacuoles are at different stages of development. A = sporont formation; B = separate sporonts; C = sporoblasts developing into spores (X 2,250).

27 - Spore-containing zone (X 3,600).

28 - Detail of an isolated area of host cytoplasm (CH) in a spore-containing area. NH = host nucleus; A = alveoli surrounding the area (X 600).

PLANCHE VI
PLATE VI

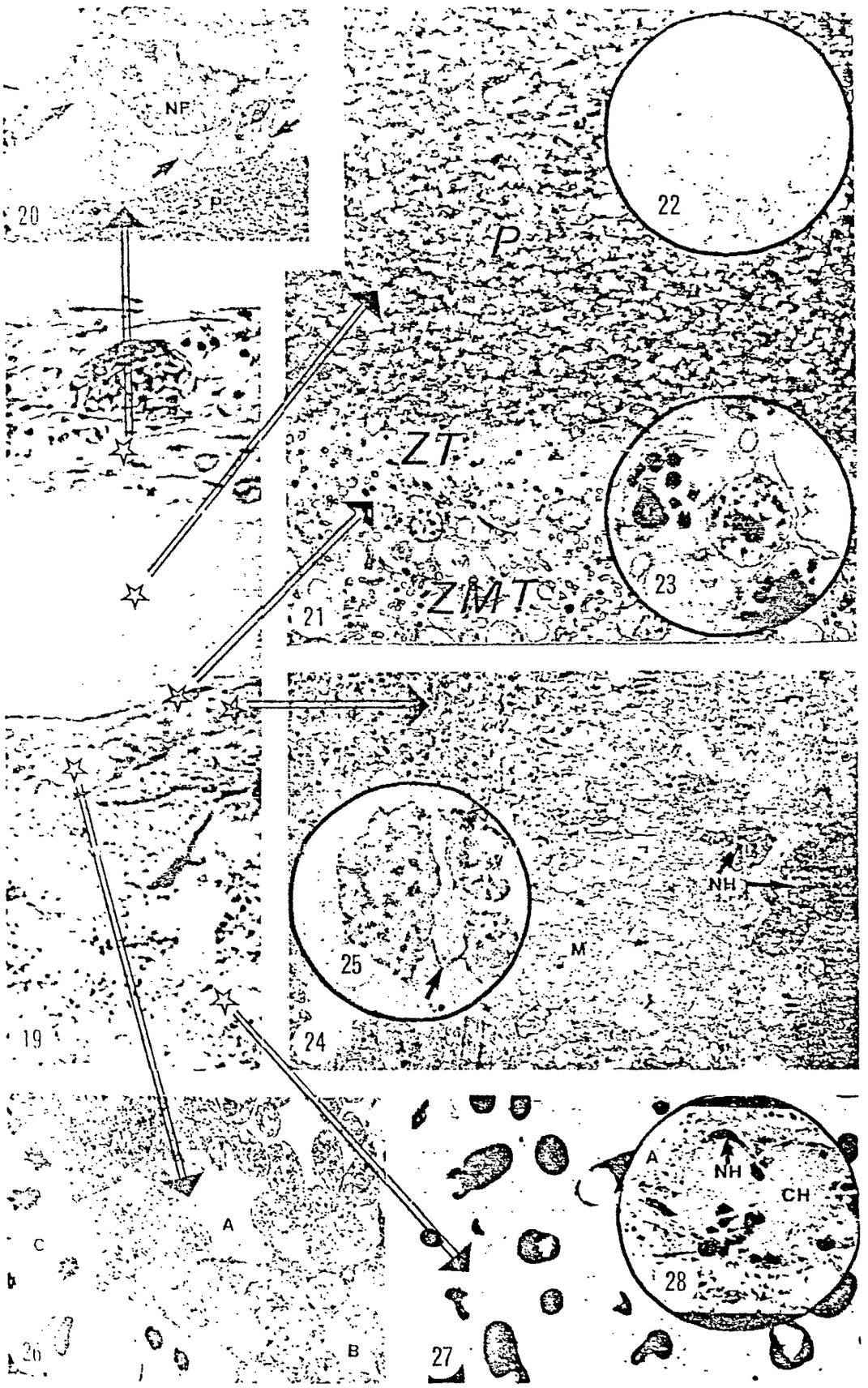

Starting from the periphery and working to the center, the following zones are observed:

1) The peripheral organization (Plate VI, photo 20) consists of structures that do not actually form part of the xenoma although they lie parallel to the wall and play a role in wall formation, cyst nutrition and support of the parasitic complex. While it may attain 80 µm in thickness, it is usually only 20 µm thick.

- Wall formation. Fibrocytes, 10 to 20 µm long, 3 to 5 µm thick, lying parallel to the cyst wall help to build the wall. A fibrous, connective-type substance works its way between the fibrocytes that secrete it, forming fine bands, 0.1 to 1 µm thick.

- Nutrition of the xenoma. The fibrous lattice-work described above also surrounds a number of blood vessels in the young cyst. This network consists of a few (2 or 3) large vessels that branch to such an extent that the fibers seem to be infiltrated with blood cells on the surface. Debaisieux (1920) recorded heavy vascularization and blood-filled lacunae around Glugea anomala xenomas. This vascularization undoubtedly serves to nourish the xenoma.

- Cyst support. A comparison of healthy tissues with tissues surrounding a xenoma shows that the natural connective network persists and supports the xeno-parasitic complex both in adipose tissue and in the digestive tract. The peripheral organization may exhibit varying degrees of pigmentation which is an extension of pigmentation of the mesentery or the swim bladder wall, depending on the location.

2) The cyst wall (Plate VI, 21) is an anhistic layer that fits around the xeno-parasitic complex in a perfect and continuous fashion. It consists of an accumulation of tangential connective

fibers produced by the fibrocytes in the peripheral organization. In histological sections as well as in electron microscopic micrographs, the appearance varies. It usually consists of parallel lines that become more compact towards the interior. The number of lines and the space in between depend essentially on xenoma age (Plate VI, 22). At times, the fibers are in disarray, forming a fine mesh network. The wall becomes homogeneous in appearance when old and only the external edge betrays its fibrous structure. Wall thickness may vary considerably, but it increases with xenoma age. It also depends on the site of implantation. The wall of a cyst in the digestive tube, for instance, will never exceed 5 µm, whereas in a body cavity xenoma, it often exceeds 30 µm and may attain 70 µm.

3) The host cytoplasm layer has been referred to as endoplasm by Woodcock (1904) and as protoplasm by Debaisieux (1920). It is seen as a single layer under the optical microscope but can actually be subdivided into 4 zones, one gradually giving rise to the next.

a) The zone with microtubules contains very few distinct elements. There are large numbers of microtubules (Plate VI, 21), 0.05 to 0.1 µm in diameter, but never exceeding 3 µm in length. In very young xenomas, these microtubules may be replaced with vacuoles of less than 3 µm in diameter. This zone is in contact with the wall and it has an irregular outer contour. The structure and location of this zone suggest a transit area for the exchange of substances between the host and parasite. It is rarely over 5 µm thick and may be altogether absent.

b) The zone with mitochondria and microtubules (Plate VI, 21) merges into the zone described above. It is rich in

mitochondria that range in diameter from 0.2 to 1 µm. This zone is often laden with granules, 0.05 µm to 0.2 µm, contained in vacuoles, 0.4 to 0.8 µm in diameter (Plate VI, 23). In histological sections, these granules appear as very fine black spots, irrespective of the stain used. These spots are actually pigment, but of an entirely different origin from the pigment in the peripheral organization. When a black xenoma is dissected, the first membrane may be highly pigmented (this is the peripheral organization). Underneath, the wall, which is either transparent or faintly white, reveals a second, very discreet layer of pigmentation in the mitochondrion and microtubule-containing zone.

c) The zone with giant nuclei (Plate VI, 24) is characterized by the large numbers of nuclei it contains. All the authors agree as to the origin of these nuclei. Weissenberg (1921) showed that the giant nuclei in Glugea anomala xenomas were derived from the host. His conclusions were based on observations of the initial stages of an experimental spore infection in stickleback alevins. In 1968, the author defined the xenoma as being characterized by the amitotic reproduction of a number of nuclei from a single hypertrophied nucleus. The phenomenon is thought to be peculiar to the genus Glugea.

It is exceptional in the history of animal parasitism. The parasite induces nuclear division by simple fragmentation without mitosis. This action on nuclear material is suggestive of viral activity. The nuclei assume a variety of angular, irregular shapes after division. At times, they are joined by 0.2 µm-wide bands (Plate VI, 25). They are generally oval and range in length from 3 to 12 µm and in width from 2 to 7 µm. Aggregates of chromatin

give it a characteristic spotted appearance. Another distinctive feature of this zone is the presence of dense ergastoplasm, ribosomes and mitochondria which, however, exist in fewer numbers than in the other abovementioned zones. Parasitic stages appear in the cytoplasm. The endoplasmic reticulum from the host forms a tight network around these stages, which is revealing of their dependence on the host cytoplasm. The thickness of the zone with hypertrophied nuclei is related to cyst maturity. In very young xenomas, it may take up all the available space. In mature xenomas, it is 10 to 100um thick. Toward the end of development, it disappears, just like the peripheral zones.

d) In the zone with alveoli (Plate VI, 26), the stages become more mature as they approach the center of the xenoma. The alveoli emerge when sporulation follows merogony. They correspond to elimination of the host's cytoplasm by the parasite which no longer requires the enzymatic activity of the host's mitochondria and endoplasmic reticulum. The sporogonic stages remain for a long time in the alveoli which constitute sporogony vacuoles. The alveoli become increasingly numerous in the center of the cyst. They join without breaking, forming large areas in which the host cytoplasm is reduced to narrow intervacuolar triangles. The first mature spores appear. They are released from their envelopes and become independent, forming the last zone.

4) The spore-containing zone (Plate VI, 27) does not exist at first, but it quickly develops to become the most important zone in terms of size. It produces the milky white liquid that escapes from a pierced xenoma. This is the infective fluid used for experimental infestation. There are isolated islets of host

cytoplasm in the spore mass (Plate VI, 28). They produce young stages at the periphery and the zones with hypertrophied nuclei, alveoli and spores. Debaisieux (1920) reported the presence of "disseminated islands of protoplasm" in Glugea anomala xenomas.

In the chalky xenomas, this zone constitutes the hard, somewhat friable portion, following resorption of intersporal fluid.

Examples of xenomas (Table 9).

From Table 9, which gives the relative sizes of the different layers, the following conclusions may de drawn:

- There is no relationship between the state of maturity and overall cyst diameter. Xenomas in the final stage of development may be of any size. Size, in fact, depends on location as well as age, but the organ involved does not determine a specific xenoma caliber. The past and current physiological condition of the fish and the characteristics of the infected organ, which may not be the same throughout, are also determining factors.

- Very young xenomas do not have a spore zone, but a mixed zone with young stages and some scattered alveoli, some of which, although not necessarily those in the center, may contain mature spores.

- Chalky xenomas, representing the final stage of development, lose most of their peripheral layers. A new chromophil layer appears.

- The digestive tube xenoma with a spore zone comprising 78% of the cyst volume was one of the rare cases in which young stages were found, suggesting that this type of xenoma develops very rapidly and that the mature stage remains for a long time unchanged in the digestive tube.

Type of xenoma	Milky	Milky	Milky	Chalky	With young stages	Without young stages
Location	subcutan. (experimental infest.)	body cavity (experimental infest.)	body cavity	swim bladder	dig. tube	dig. tube
Total diameter (µm)	350	800	3,000	1,600	100	100
Avg. thickness of peripheral organization (µm)	not measured	not measured	10	0-30	9	0
Avg. thickness of wall (µm)	20 (11.5%)	2 (0.5%)	12 (0.8%)	6 (0.75%)	2 (4%)	3 (6%)
Avg. thickness of zone with microtubules (µm)	6 (3.5%)	6 (1.5%)	3 (0.2%)	complete breakdown of zones; replaced with chromophil area.	2 (4%)	disappearance of zones
Avg. thickness of zone with microtubules and mitochondria (µm)	6 (3.5%)	14 (3.5%)				
Avg. thickness of zone with host nuclei (µm)	65 (37%)	80 (20%)	3 (0.2%)	15 (1.9%)	7 (14%)	
Avg. thickness of alveolar zone (µm)	zone with young stages and spores	zone with young stages. Spores very rare	12 (0.8%)			
Avg. radius of spore mass (µm)	75 (43%)	300 (75%)	1,500 (97%)	780 (98%)	39 (78%)	47 (94%)
Assessment of maturity	++	+	++++	end of development	++++	end of development

Table No. 9. Relative Thickness of the Different Zones in Six Examples of Xenomas

. Implantation. There are two major sites of implantation, i.e., the digestive tube and the body cavity (adipose tissues or organs). The two types of implantation are completely independent. Subcutaneous xenomas may also occur but only under experimental conditions when spore levels in the water are unusually high.

I - Implantation in the digestive tube (Plate VII). Digestive tube xenomas do not exceed 200 µm in diameter even when the cysts are mature and at the final stage of development. Fig. 18 shows three sites of implantation as well as the structure of the healthy organ.

PLATE VII

29 - Micrograph of a cyst (K) in the digestive tube surrounded by two layers. E = intestinal epithelium; M= muscle layers. The xenoma is clearly embedded in the connective corium (c) (X 200).

30 - The wall (P) of a digestive tube xenoma is lined on the inside by the spore zone (S) and on the outside by the intestinal muscle layer (M) (X 2,000).

31 - A digestive tube xenoma embedded in the connective tissue (c) between two muscle layers (M) and the epithelium (E). It contains only spores (S) (X 650).

32 - Fine structure of a digestive tube xenoma. C = connective corium bands; F = fibrocyte; P = wall; ZMT = zone with mitochondria and microtubules (X 5,000).

33 - Fine structure of one of the few digestive tube xenomas still containing young merogonic stages (SJ) in contact with the mitochondrion and microtubule-containing zone (ZMT). Fibrocytic cells (F) are caught between connective bands (c) accompanied by connective corium cells (CCC) and the xenoma wall (P) (X 5,500).

PLANCHE VII

PLATE VII

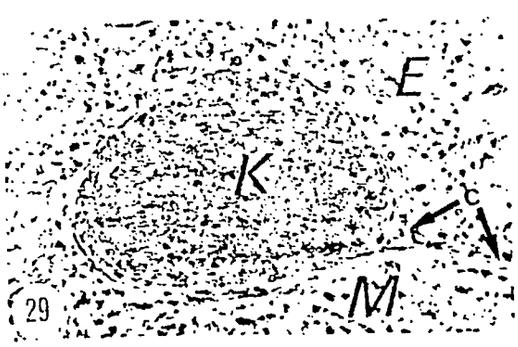

29

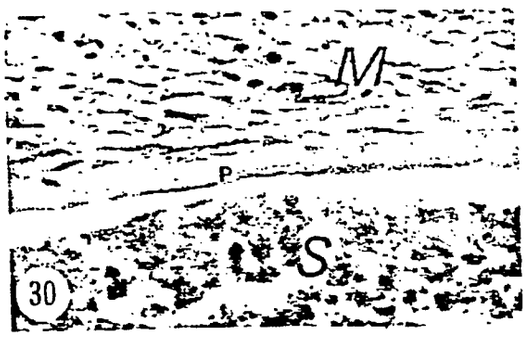

30

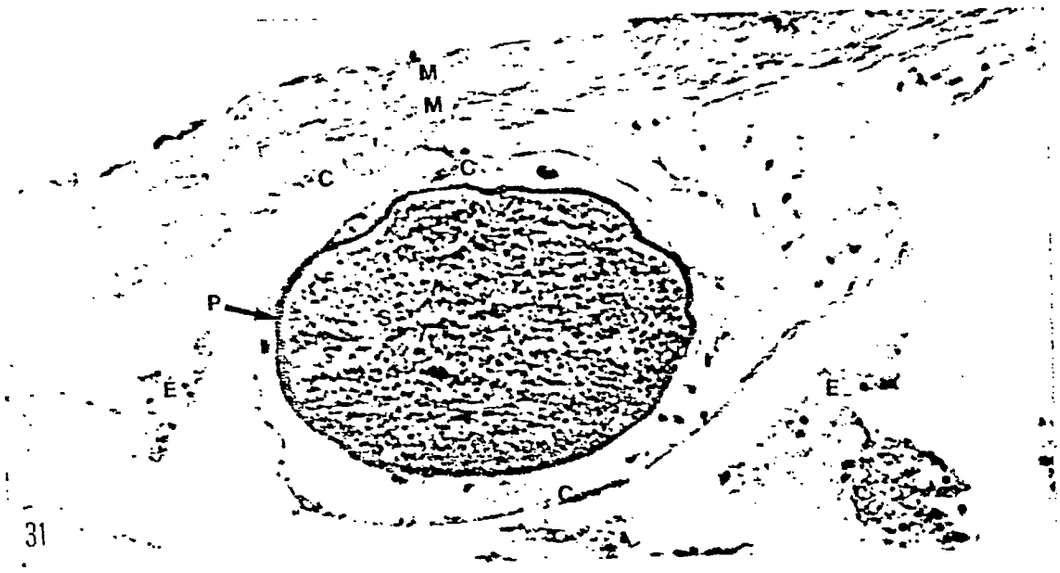

31

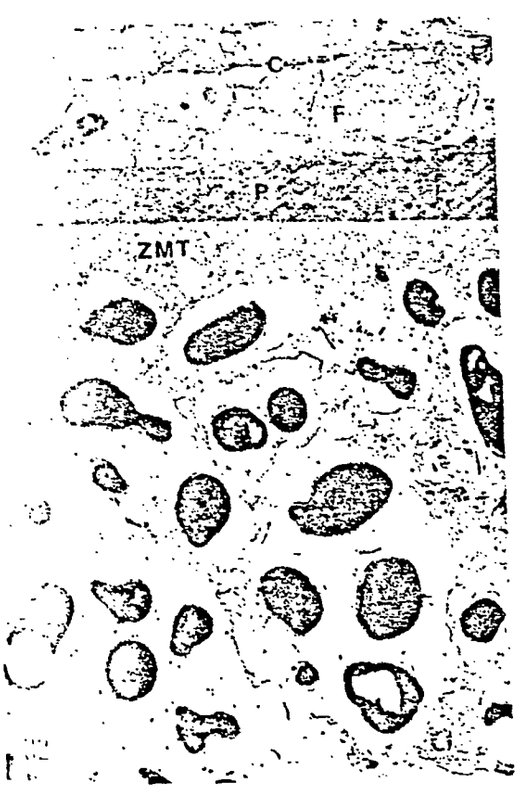

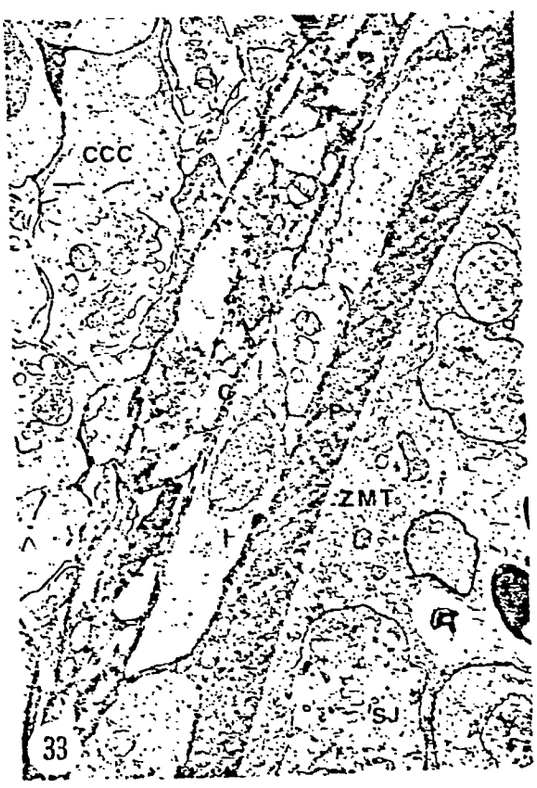

33

a) In the stomach, the stomach wall consists of four concentric layers. Working from the outside in, there are smooth muscles, outer longitudinal muscles and inner circular muscles. Finally, there is the connective corium which joins these muscle layers with the mucosal epithelium lining the lumen of the stomach. This connective tissue follows the fingerlike projections of the mucosa in the lumen. Implantation occurs exclusively in this connective tissue. It is an area that is both highly vascularized and extremely resistant.

b) In the intestine, the histological structure is the same although there is a greater abundance of villi. Any changes over the length of the intestines is minor, involving solely the diameter of the tube and the number and length of the villi. Here, too, xenomas occur only in the connective tissue, but since the diameter of the intestines is smaller than that of the stomach, they occasionally produce bulges which, if the infection is severe, undoubtedly interfere with the passage of material through the gut.

c) In the rectum, the muscle layers are thicker and the villi, far shorter. The connective tissue, which follows the contours of the villi, extends more deeply into the lumen. The parasite seems to have a preference for this portion of the corium. In Fig. 18d, the xenoma seems to occupy the center of the rectum. The mechanical effect is definitely more pronounced in this area. Various authors have reported this preference for the connective tissue in the digestive tube:

Fig. 18. cc = connective corium; eu = unstratified epithelium; l = digestive tube lumen; mcl = inner circular smooth muscles; mcs = outer circular striated muscles; mll = outer longitudinal smooth muscles; mls = inner longitudinal striated muscles.

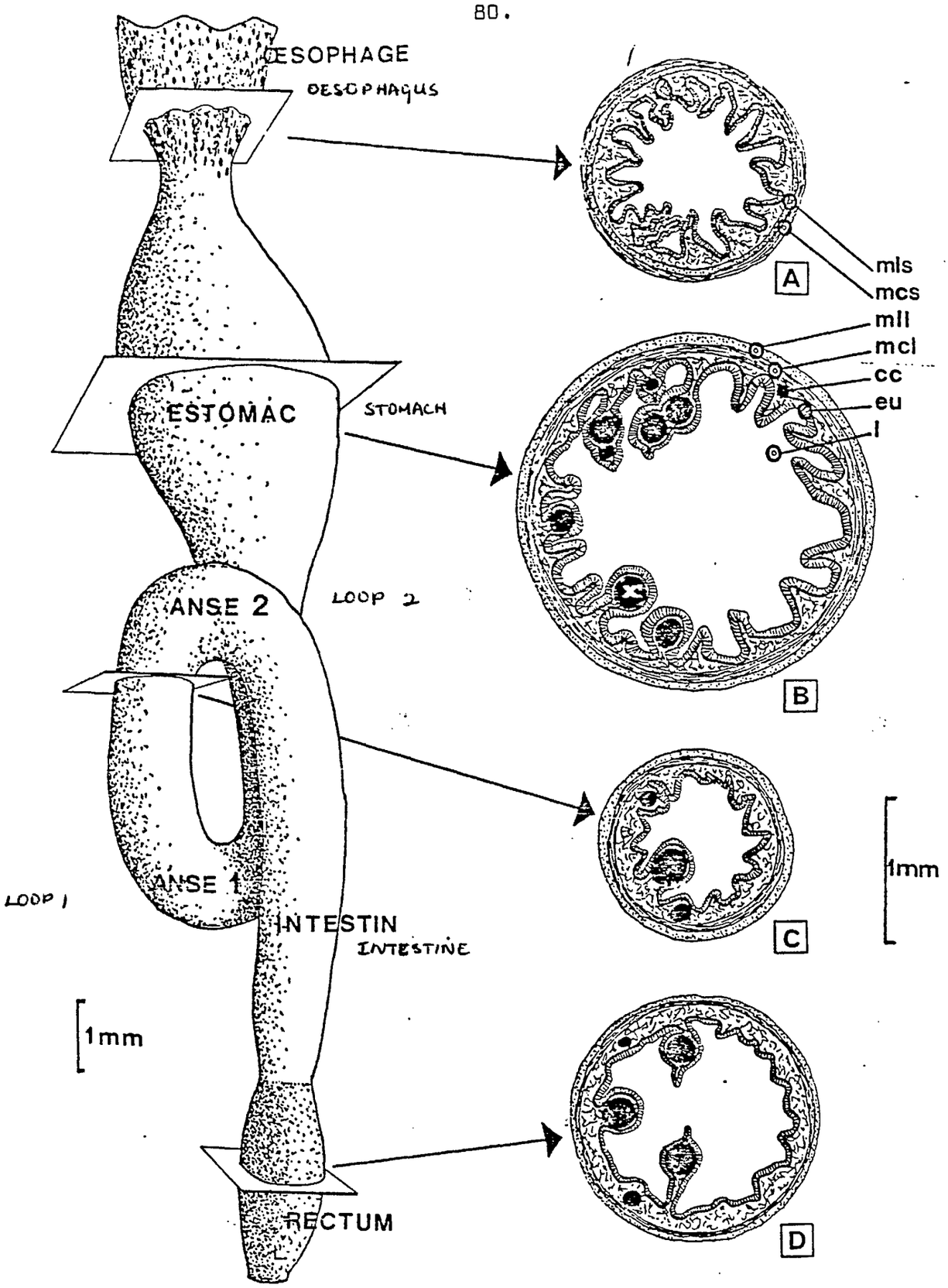

FIG.18: MODE D'IMPLANTATION DES XENOMES DU T.D.

Site of Xenoma Implantation within the Digestive Tube

- Glugea stephani invades the connective tissue of the digestive tube and various other organs in Pseudopleuronectes americanus (Stunkard-Lux, 1966).

- Glugea hertwigii cysts have been found in the connective tissue of the intestinal wall, liver, pancreas and in the mesentery of the smelt, Osmerus eperlanus (Wellings et al., 1969).

- Nosema tisae infests the intestinal submucosa in Silurus glanis (Lom and Weiser, 1969).

- Glugea branchiale parasitizes the connective tissue of the gills in Melanogrammus aeglefinus (Lom-Marshall, 1976).

2 - Implantation in the body cavity. Xenomas located outside the digestive tube can grow very large since 1-cm cysts have been found in fish 5-cm long. The most common site of infestation is the adipose tissue in the body cavity. The cysts may also be found near the different membranes lining the body cavity walls. The various possible sites of implantation are shown in Fig. 19.

Fig. 19. Anatomy of the atherine. 1 = epithelium and scales; 2 = outer musculature of the trunk; 3 = inner musculature; 4 = spinal cord; 5 = kidney; 6 = vertebra; 7 = swim bladder; 8 = swim bladder wall; 9 = adipose tissue; 10 = liver; 11 = pigmented peritoneum; 12 = digestive tube lumen; 13 = intestinal epithelium; 14 = connective corium; 15 = inner circular striated musculature of the gut; 16 = outer longitudinal striated musculature of the gut; 17 = gonad.

Sites of xenoma implantation. a = subcutaneous; b = swim bladder; c = attached to the swim bladder wall; d = adipose tissue; e = gonad; f = attached to the peritoneum; g = in the basal portion of the connective corium; h = in the distal portion.

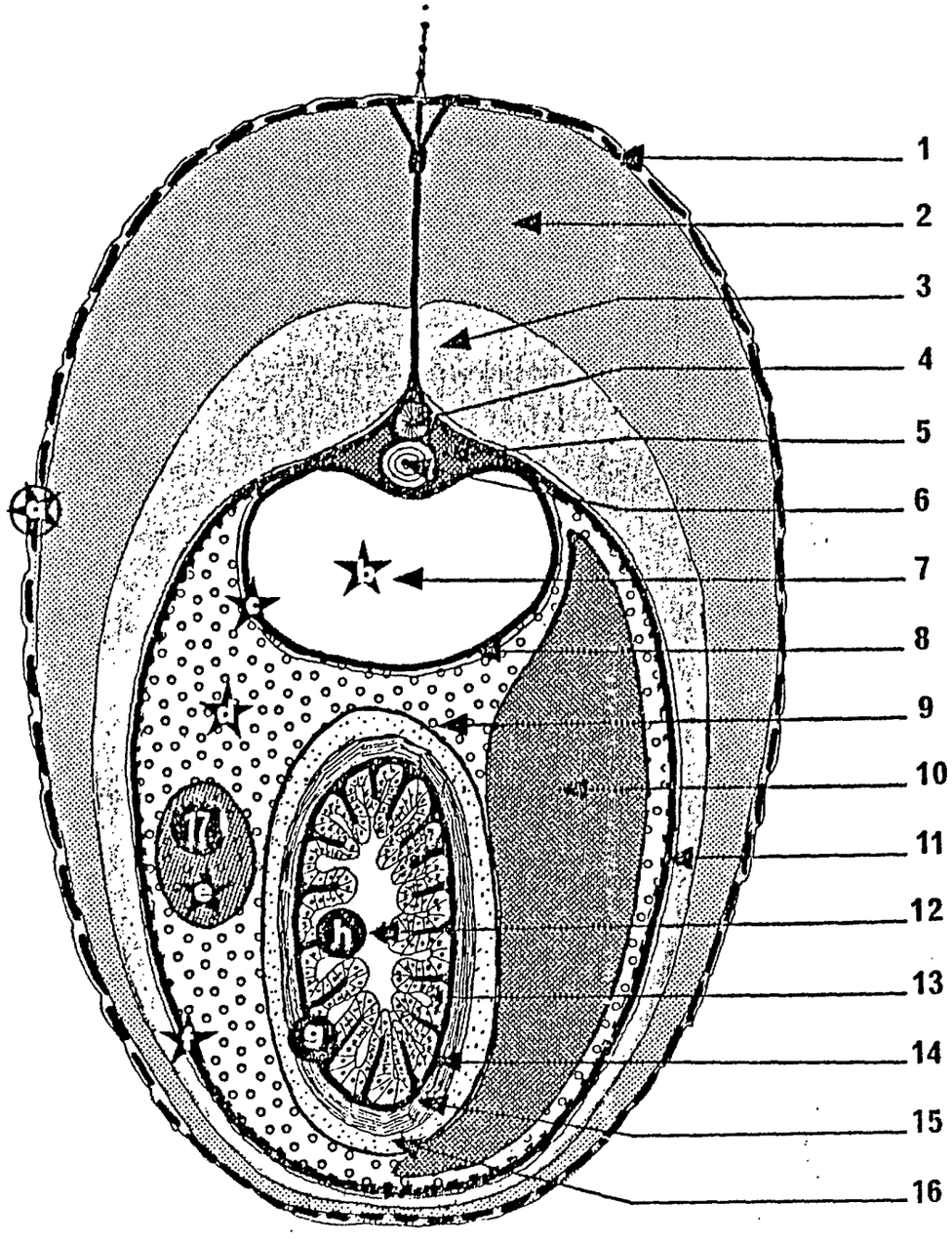

xénomes sous cutanés
subcutaneous xenomas

xénomes de la cavité générale (au sens large)
xenomas of the body cavity (considered in its broadest sense)

xénomes du tube digestif
digestive tube xenomas

FIG-19

EMPLACEMENTS DES DIFFERENTS KYSTES DANS L'ORGANISME HOTE.

LOCATION OF DIFFERENT CYSTS IN THE HOST ORGANISM.

In the body cavity, the cysts are embedded in adipose tissue. It is difficult to determine, however, which tissue actually acted as the initial support. Adipose tissue is crisscrossed with blood vessels and numerous capillaries. There are also connective fibers that form a latticework among aggregates of fat and around the vessels. We will propose several hypotheses to explain this phenomenon when discussing the subject of inoculation and circulation of the infective organism in the host.

Three particular sites of implantation in the body cavity and appendices were studied in detail.

a) In fat tissue (Fig. 20). A milky cyst, 5.5 mm in diameter, was found in the anterior portion of the body cavity, near the digestive tube and the liver. Like the digestive tube, this relatively young xenoma was surrounded by adipose tissue which was very dense along the intestinal tract. A connective framework gave support to the digestive tube, the xenoma and a rich system of vascularization which, while normal in this area, was diverted by the xeno-parasitic complex. The peripheral organization consisted of elongate cells neighbouring blood vessels and areas where there seemed no limit to the blood supply, much like the blood lacunae reported in Glugea anomala (Debaisieux, 1920). Beneath this system, there was a thick zone of widely-spaced fibers prefiguring the cyst wall, which typically was definitely fibrous, as in all young xenomas.

Figs. 20, 21 and 22. - elp = local thickening of the peritoneum; epp = extension of peritoneum pigmentation; mcp = pigmented connective membrane; mt = musculature of the trunk; opx = peripheral organization of the xenoma; p = pigmented peritoneum; pvg = swim bladder wall; px = xenoma wall; ta = adipose tissue; td = digestive tube; vg = swim bladder; vs = major blood vessels.

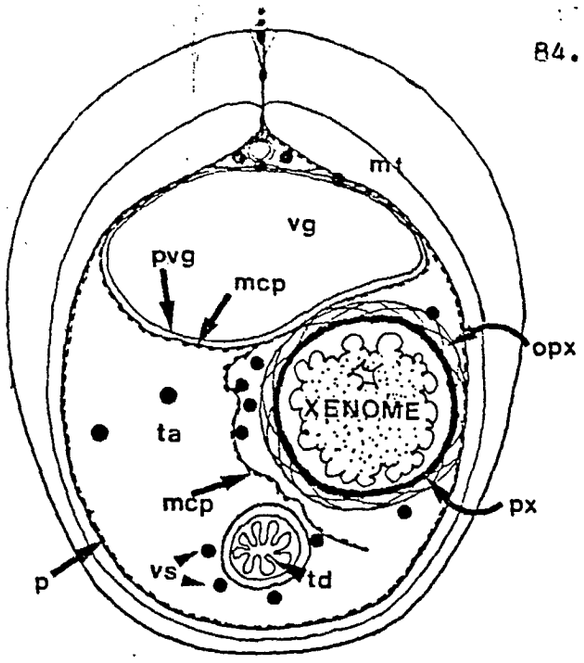

FIG.20: Exemple d'implan-
-plantation dans le tissu adipeux

EXAMPLE OF IMPLANTATION IN ADIPOSE TISSUE

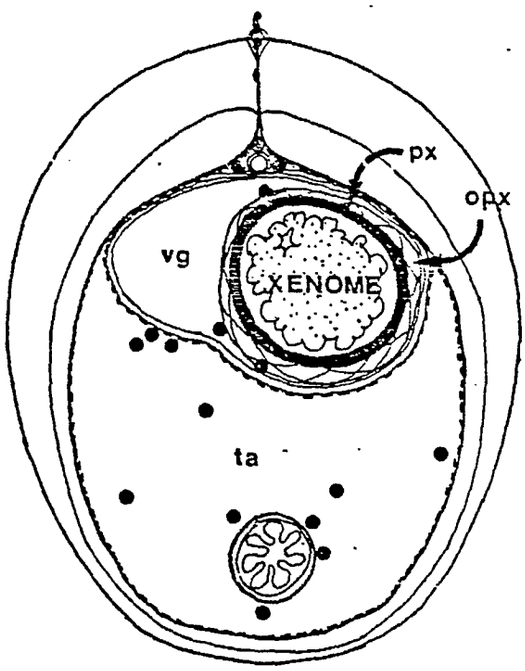

FIG.21: Implantation dans la vessie gazeuse

EXAMPLE OF IMPLANTATION IN THE SWIM BLADDER

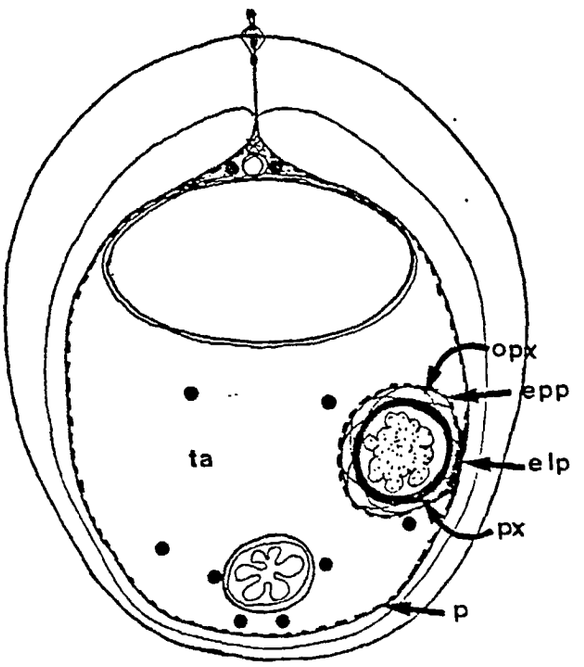

FIG.22: Implantation sur le péritoine

EXAMPLE OF IMPLANTATION ON THE PERITONEUM

b) In the swim bladder (Fig. 21). A milky xenoma, 2.5 mm in diameter, was found in the anterior portion of the swim bladder. The bladder is normally a pouchlike structure with a thin transparent wall that expands under the influence of a complex gas. It is bordered dorsally by the kidneys and the spinal column, laterally by a pigmented peritoneum and ventrally by a visceral mass buried in fat tissue. In addition, the swim bladder is surrounded by connective tissue. None of these structures are influenced by the xenoma in their midst. The bladder cavity contains only gas. When a xenoma becomes established in the bladder, it is always attended by a peripheral organization which attains a thickness of up to 30 µm and contains numerous cells, blood vessels and connective fibers. Further research is necessary to explain the implantation tissue derived from the parasite as well as the origin of the tissues surrounding it.

c) In the peritoneum (Fig. 22). A chalky cyst was observed attached to the body cavity wall. Histological sections revealed a typical chalky xenoma. The peripheral organization formed a narrow layer except on the side of the wall where it was 50 µm thick. At this site, fibrocytes came in contact with a thickening in the peritoneum, producing a solid attachment between the cyst and host tissues. Black pigment surrounded the peripheral organization, prolonging the usual pigmentation of the peritoneum and thereby revealing the close interaction between the two tissues. This was one of the rare cases in which the xenoma was securely attached to the host.

c) Historical Background and Bibliography

Chatton (1920) was the first to use the term "xeno-parasitic complex."

Weiser (1976) defined two main types of xenomas:

- a syncytial xenoma in which the infected cells come together to form a common plasmatic mass following disintegration of the cytoplasmic membranes. There is no increase in the initial number of nuclei.

- a neoplastic xenoma in which the number of cells and consequently of nuclei increases under the influence of the parasite. This type of xenoma may be further subdivided into two types:

+ Pleistophora debaisieuxi-type xenomas. The cells undergo active division and each parasitic stage occurs in a typical cell or xenocyte. The resulting cells show a 10 to 30-fold increase in number.

+ Glugea-type xenomas. Nuclear fragmentation considerably augments the number of nuclei. Cytoplasmic division has never been observed.

Lom and Marshall (1974) distinguished four types of xenomas, i.e.,

1)- xenomas, 2 mm and over, with numerous host nuclei (e.g., Glugea anomala, G. hertiwigii, Nosema fennica).

2)- small xenomas (a few mm) with single hypertrophied host nuclei (e.g., Glugea branchiale, G. acerinae, G. tisae).

3)- xenomas with brushlike edges, floating in vacuole fluid (e.g., Glugea cotti).

4)- hypertrophied ganglion cells following a particular kind of development (e.g., Glugea lophii).

The xeno-parasitic complex encountered in the atherine corresponds to Weiser's Glugea-type neoplastic xenoma and to Lom and Marshall's number-one type of xenoma and is comparable to the complex

produced by a few other species.

In Glugea anomala-induced cysts, the peripheral organization contains blood lacunae and the wall consists of concentric connective sheaths. Beneath the wall, the protoplasm extends into the cyst, with large nuclei. The sporogony vacuoles exhibit different stages of sporulation. The spores are in the center of the xenoma with fragments of protoplasm scattered between the spores (Debaisieux, 1920).

In the case of infection due to Nosema fennica, the cysts are attached to the gills of Silurus glanis and include a 30-µm-thick wall, a layer of damaged host nuclei, a plasmatic layer with vegetative stages and mature spores in the center (Lom and Weiser, 1969).

In cysts produced by Glugea stephani, a parasite of Pseudopleuronectes americanus, the tunic is diffuse in young xenomas but compact in older stages. Beneath the tunic lies a 50-nm plasmatic membrane with numerous folds. The wall acts as a filter since it contains many highly charged ions which facilitate the transfer of charged molecules and the evacuation of toxins. The layer consisting of host cytoplasm is 50 to 100 µm thick in xenomas 1 to 4 mm in diameter. It includes an endoplasmic reticulum, a Golgi apparatus and mitochondria. It is here that schizogony stages begin. In the center, sporogony is attended by elimination of host cytoplasm (Weidner, 1976).

3/ Ultrastructural Study of the Parasitic Cycle

The Atherina boyeri-infesting microsporidian has a typical cycle. The study of this cycle was based on articles devoted to the genus Glugea THELOHAN 1891 and especially on the work of Sprague and Vernick (1968) on a related species, Glugea weissenbergi Sprague and Vernick 1968, an Apeltes quadracus parasite. By means of histological and ultrastructural techniques, it was possible to study the entire cycle successfully with the exception of a few stages which were not observed.

a) The Beginning of the Cycle:

According to Weissenberg (1968), the Glugea anomala xenoma begins with a single cell. The author drew his conclusions from work in stickleback alevins which were experimentally infested. Serial sections of the infected host seven days after infestation revealed amebula stages in mesenchymal migratory cells. These amoebic stages have never been observed outside host cells. The germ in its cell seems to be embedded in a vacuole and, at this stage already, deforms the nucleus. The amoebic stage of Glugea hertwigii is 1.5 µm in diameter and of Nosema pimephales Fantham et al., 1941, 2 µm in diameter and is uni- or binucleate (Fantham et al., 1941). According to Sprague and Vernick (1968), primordial cells known as gemmules arise from host nuclei.

b) The First Phase of Merogony

Merogony begins when the sporoplasm divides in the host cell. At a more advanced stage, the phase develops in the peripheral area with large nuclei, completely within the host cytoplasm. Not all parasitic cells are at the same stage of development at the same time. Merogony may continue at the periphery while the center is

packed with mature spores. The various merogonic elements have a number of points in common. They are surrounded by the following organelles:

. Endoplasmic reticulum. Endoplasmic reticulum cavities are separated from parasitic elements by less than 50 nm. The reticulum generally contains ribosomes, but only in the area opposite the parasite (Plate VIII, 34, R). There may be a break between two saccules but the resulting empty space is never large. These cavities vary in thickness but are usually 30 to 60 nm thick. Locally, there may be considerable narrowing or widening (Plate VIII, 35). These extreme cases may be due to fixation-related swelling or tangential sections. In the vast majority of cases, a single vesicle surrounds the parasite (Plate VIII, 36) but at times, there may be two or three, probably due to branching (Plate VIII, 35, E).

. Mitochondria are concentrated near the parasitic elements (Plate VIII, 34, 35, 36, M). They range from 0.6 to 1.3 um, are spherical in shape with a typical lamellar structure and are often surrounded by ergastoplasm.

PLATE VIII

C = parasite cytoplasm; E = ergastoplasm; M = mitochondria; N = Nuclei; R = ribosomes.

34 - Meront stage (X 35,500)

35 - Meront stage (X 21,600)

36 - Sporogonic stage (X 19,800).

PLANCHE VIII

PLATE VIII

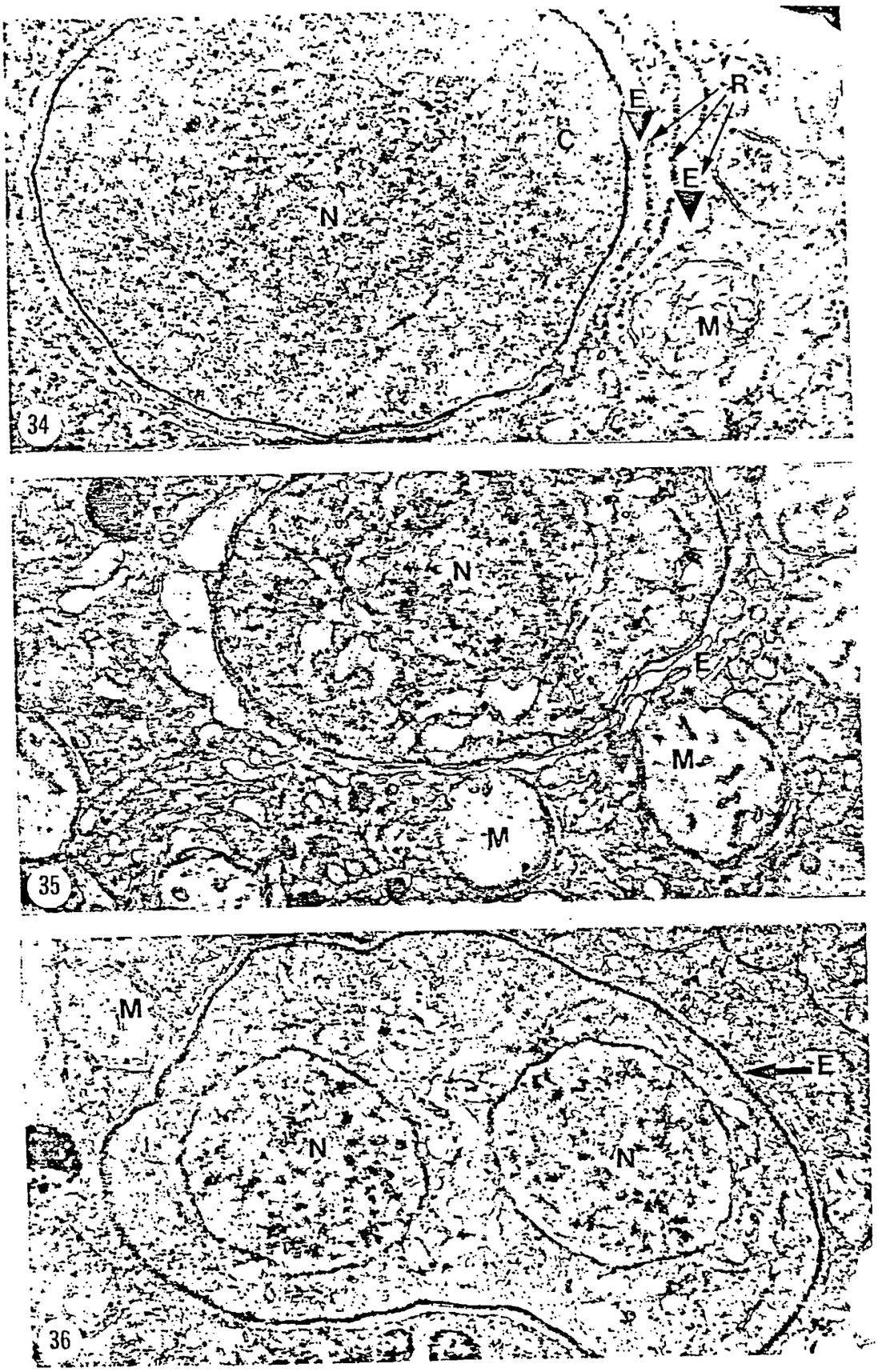

. Ribosomes exist in large numbers and may either be free in the cytoplasm or else, in contact with the reticulum. None have been found between the ergastoplasm and parasite wall (Plate VIII, 34, R).

. Vacuoles of every size and type are scattered throughout the cytoplasm. They may be spherical or tube-shaped.

During merogony, the parasite appears in various forms, i.e., as meronts or cylindrical vegetative plasmodia.

- The meront is a uninucleate, oval or ciruclar element, that at most, is 2.5 times as long as it is wide (Plate VIII, 34-35). It is surrounded by a simple membrane. The cytoplasm is endowed with a substantial perinuclear endoplasmic reticulum (1 to 5 saccules) (Plate XI, 45) and is rich in granular material of various types, e.g., ribosomes, and in tubules. The nucleus is fairly large and may attain 2.3 µm in diameter. It is transparent with clearly visible chromatin (Plate VIII, 36, N).

- The cylindrical vegetative plasmodium is plurinucleate. It varies in size. Under a light microscope, large elements, over 20 µm in length and roughly 3 µm in width, may be seen in a smear preparation stained with May-Grünwald-Giemsa stain. Under the electron microscope, measurements on a micrograph showed that the parasite may reach 25 µm. The plasmodium is consequently elongate with a length up to six times the width, hence, the name "cylindrical plasmodium" (Plate X, 42-43). These stages are characterized by large numbers of spherical nuclei containing discrete aggregates of chromatin. These nuclei are rarely observed undergoing mitosis. They are usually found in pairs and may be the result of recent mitosis (Plate X, 42-43, double arrows). Up to 8 have been detected under the electron microscope (due to the angle of the section) and up to 16 under the light microscope in a stained

smear preparation. They are smaller in diameter (up to 1.9 um). These plasmodia correspond to the stages with 16 or 32 nuclei described by Sprague and Vernick (1968) in Glugea weissenbergi. In the parasite, the endoplasmic retidulum is very loosely structured. The plasmodia divide by constriction (Plate X, 44). Occasionally, the isolated element contains two nuclei (Plate XI, 46) and at times, division is initiated in the center of the cylinder, splitting it in two. While fragmentation apparently results in uninucleate elements, it seems to be a random process. There are no basic differences between the meronts and plasmodia.

Two aspects involving the onset of merogony warrant discussion:

- Microtubules are often observed. Each tubule consists of a plasma membrane, approximately 50 nm in diameter and variable in length (over 0.5 um). These microtubules are formed by the parasite (Plate IX, 37 and 40), and arise from the plasma membrane in groups of 5 to 12, in parallel formation on the same plane (Plate IX, 39). They may assume hairpin shapes while retaining their parallel order. At the edge of the parasite wall, the ergastoplasm may be discontinuous or skirt around the microtubule (Plate IX, 39 - 40, E). Microscopic sections show a string of

---

PLATE IX

CH = host cytoplasm; CM = meront cytoplasm; E = ergastoplasm; m = mitochondria; N = nuclei.

37 - Meront releasing tubules (arrow) (27,500).
38 - Rows of tubules, always lined with ergastoplasm (arrows) (X 31,000).
39 - Rows of tubules released by a meront (arrow) (X 81,700).
40 - The tubules are tightly lined with ergastoplasm (X 87,700).
41 - Non-cylindrical second-type plasmodium (X 14,800).

PLANCHE IX
PLATE IX

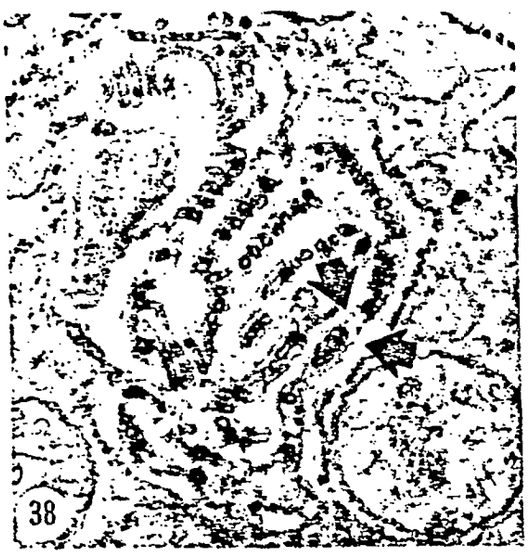

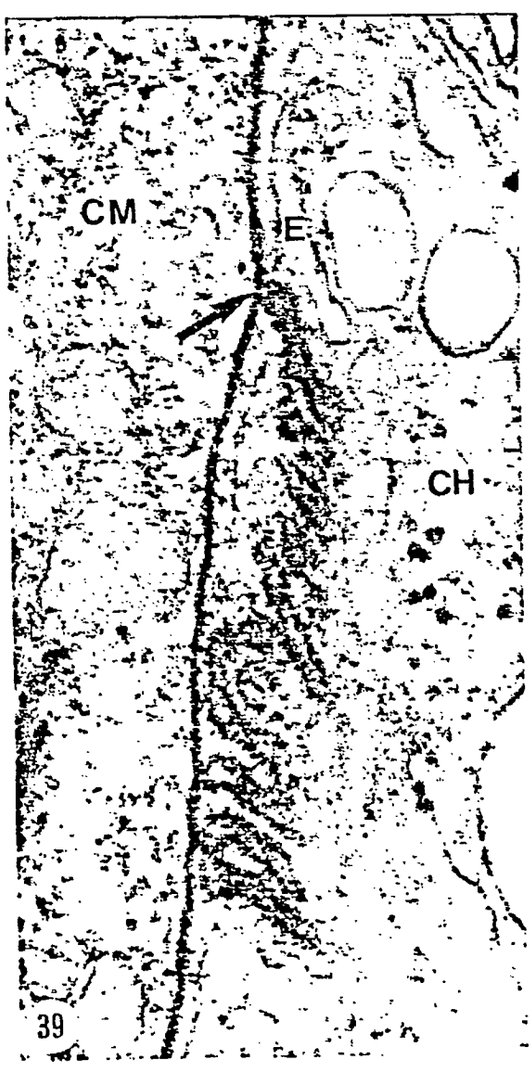

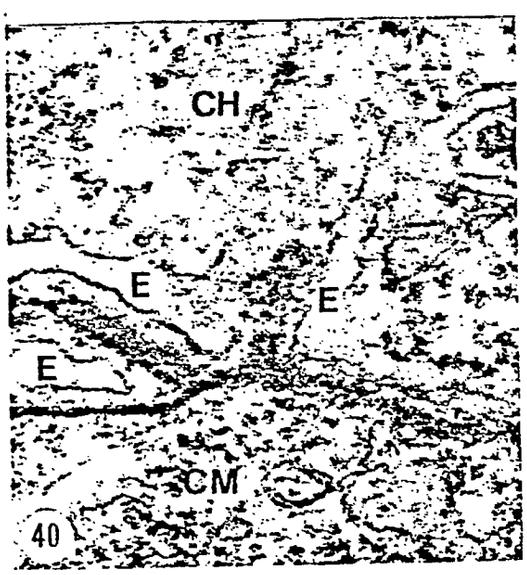

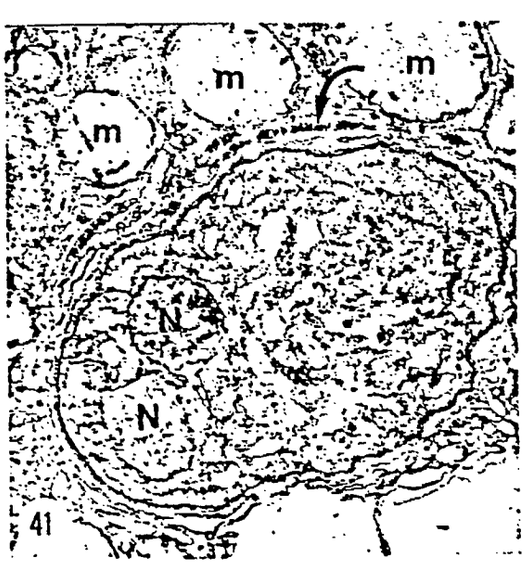

small circles lined with two ergastoplasmic saccules (Plate IX, 41). These small circles may cluster, forming a characteristic figure with up to one hundred microtubules (Plate IX, 38). Sprague and Vernick (1968) suggested that these elements, which they referred to as "annulate lamellae", were actually prolongations of the hypertrophied host nucleus but this hypothesis has since been discarded.

- Kinetic centers and nuclear division. Nuclear division begins with the emergence of kinetic centers. A flat-bottomed depression containing two superimposed disks, 3 nm thick and 200 nm in diameter, forms at the surface of the nuclear envelope. The latter is either interrupted at this point or else its structure is severely disrupted (Plate XIX, 79).

In Glugea habrodesmi Loubès et al, 1976, there are three disks, but no break in the nuclear membrane is observed (Loubès et al, 1976). Three or four small spheres known as polarized vesicles, with an average diameter of 80 nm, lie above the depression. A number of chromosome spindle fibers form the junction between the nuclear envelope at the site of the depression and aggregates of chromatin, generally found midway between the two spindle plates at opposite ends of the nucleus. Spindle fibers sometimes

---

PLATE X

CH = host cytoplasm; E = ergastoplasm; I = interrruption in the ergastoplasm; m = mitochondrion; N = nucleus

42 - Cylindrical vegetative plasmodium. The nuclei are often in pairs (arrows). The ergastoplasm may be discontinuous (I) (X 8,900).

43 - Cylindrical vegetative plasmodium (X 9,900).

44 - Division of the cylindrical plasmodium by constriction (black triangles). Tubule formation (curved arrows). There is only one ergastoplasm vesicle (straight arrow) (X 22,300).

PLANCHE X

PLATE X

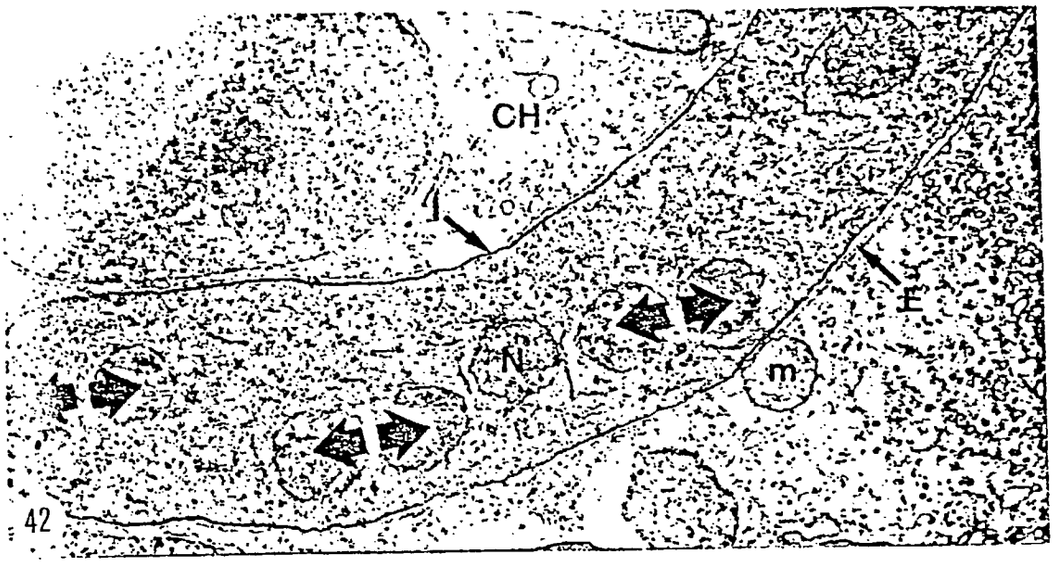

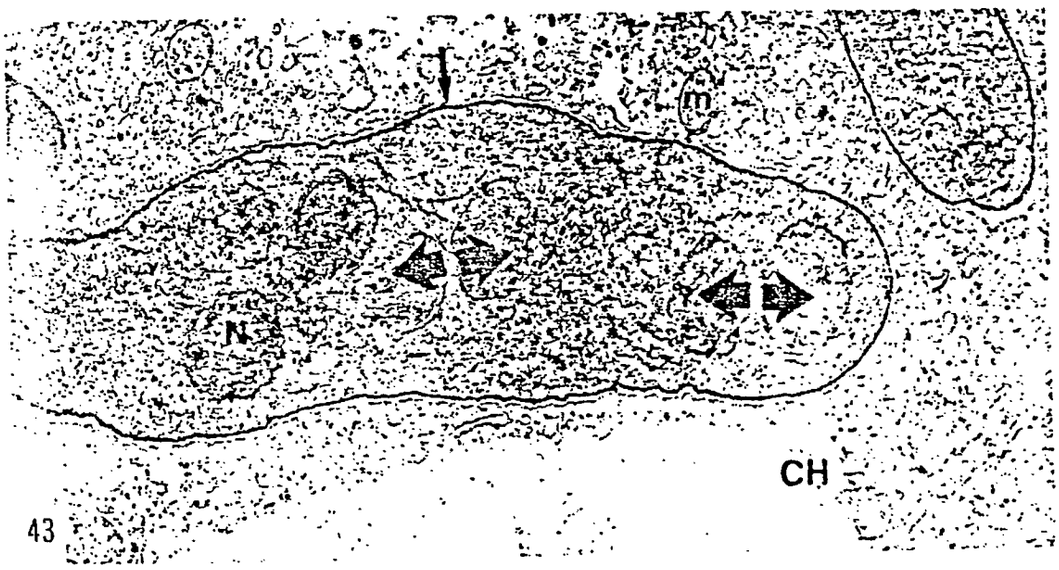

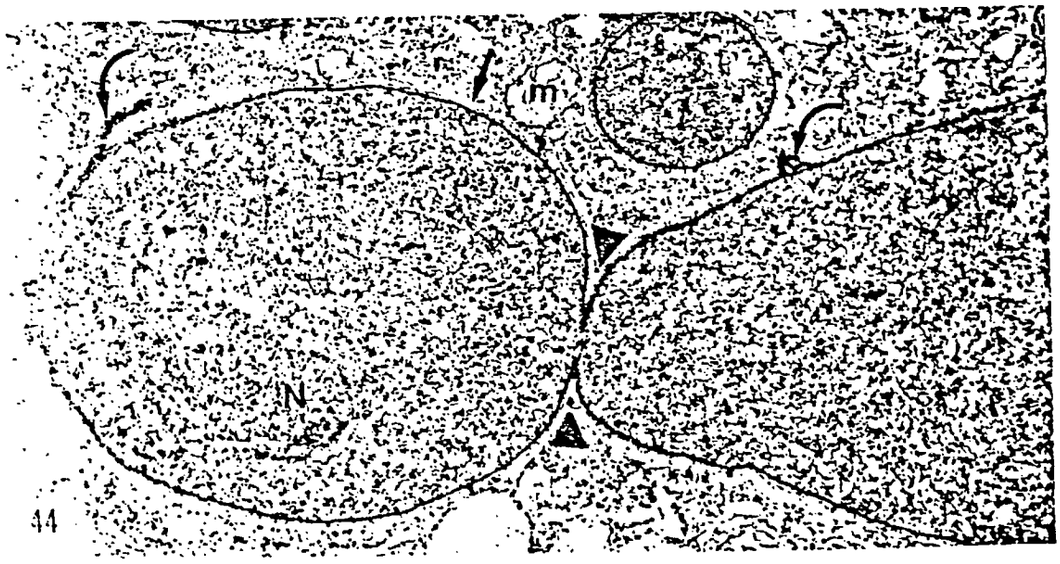

cross in the center of the nucleus. The subsequent events could not be correctly observed. At times two daughter nuclei were seen connected by a long narrow nuclear bridge which undoubtedly contains continuous spindle fibers (Plate XIX, 81). This very likely marks the end of mitosis. At times, a second division begins before the first one has finished. The nucleus consequently may have four depressions. At other times, the nucleus is in the final stages of division (with the nuclear bridge) and one of the daughter nuclei already has two spindle plates (Plate XIX, 81), suggestive of a lengthy process. Fig. 23 contains diagrammatical drawings of these different situations.

During merogony, the parasitic stages may evolve in one of two directions, i.e., either the meront-plasmodium cycle is perpetuated or sporulation becomes the final outcome. In the latter case, the host cytoplasm is eliminated or at least pushed aside. There is a substantial transformation involving some degree of independence from organelles such as the ergastoplasm and mitochondria. This occurs through vacuolation of the space between the host reticulum and the parasite wall (Plate XI, 47, arrows). The phe-

---

PLATE XI

E = ergastoplasm; N = nucleus; R = parasite endoplasmic reticulum

45 - Vegetative plasmodium laden with ergastoplasm (R) (X 13,000).

46 - Division of plasmodium by constriction (black triangles) isolating plurinuclear fractions (X 11,700).

47 - Beginning of isolation of parasitic stages. Vacuolation (black triangles) of the space between the parasite and host ergastoplasm (E) (X 27,000).

48 - Non-cylindrical plasmodium with numerous nuclei at an advanced stage of isolation (triangle) (X 11,600).

49 - Partial formation of sporont walls. The arrows point to characteristic deposits of material which will serve to thicken the envelope (X 21,600).

PLANCHE XI

PLATE XI

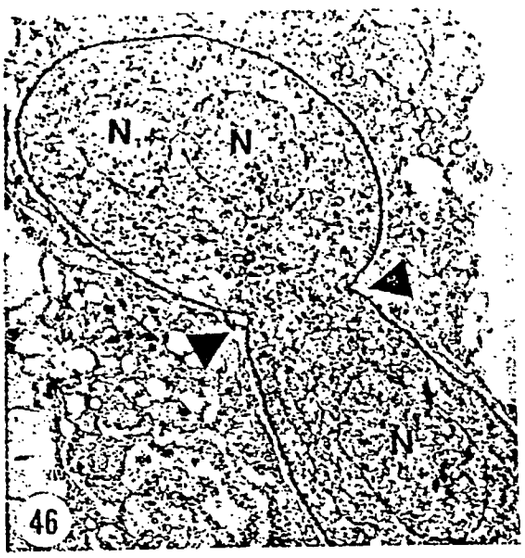

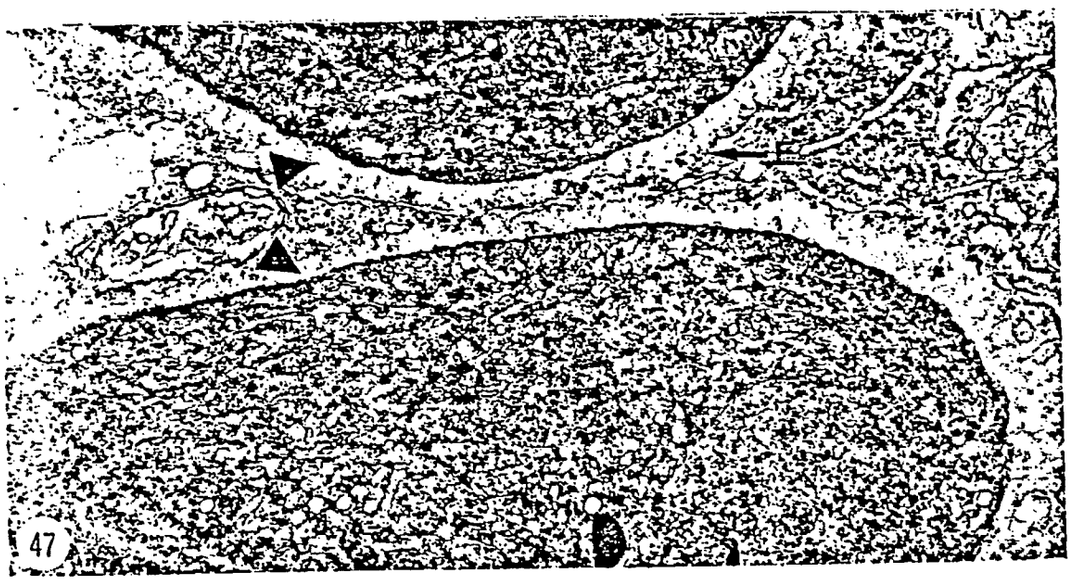

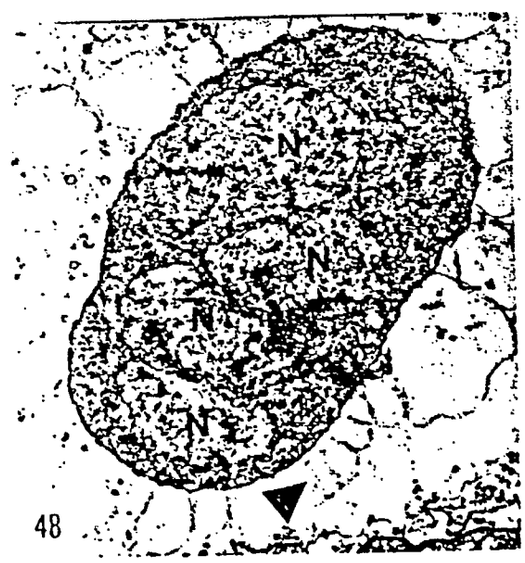

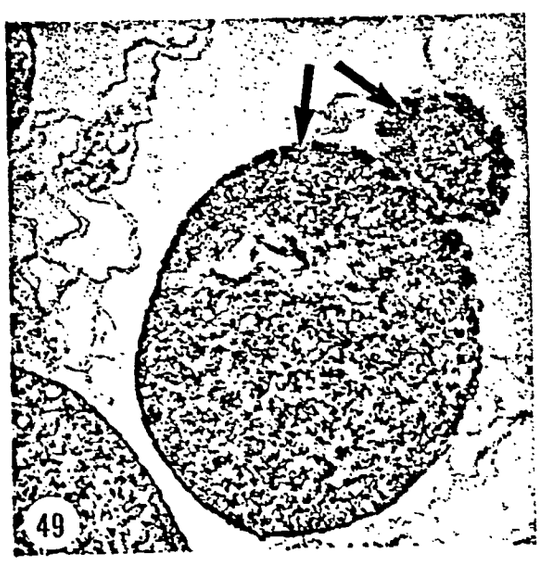

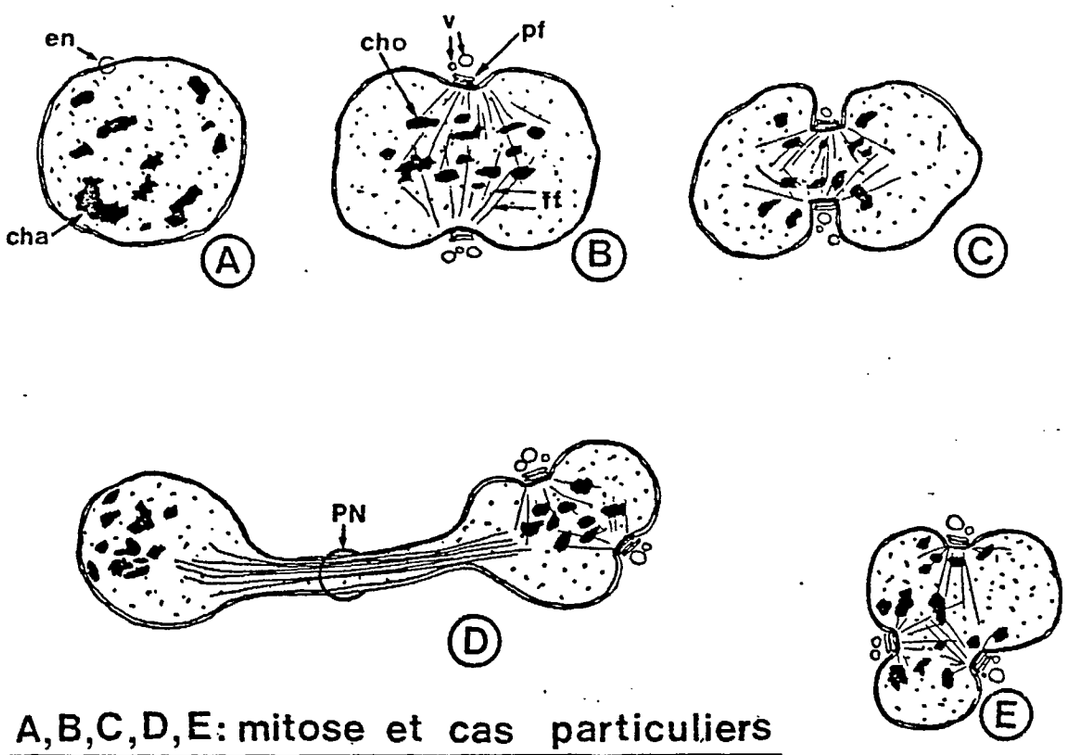

A,B,C,D,E: mitose et cas particuliers

Different types of mitotic division

F: détails des centres cinetiques

Details of kinetic centres

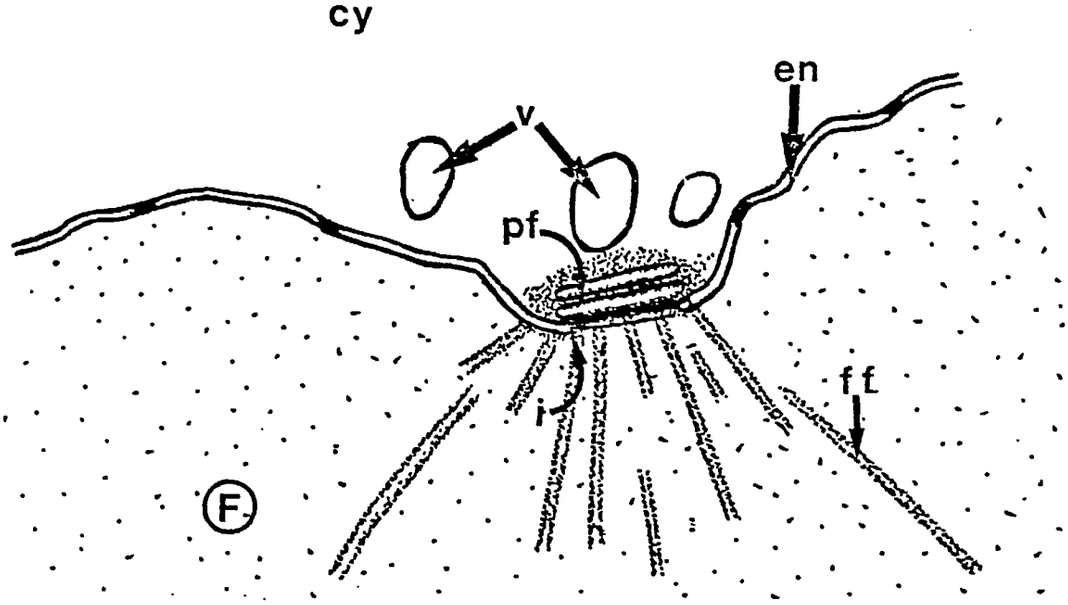

Figure 23 : *La division nucléaire* Nuclear Division

cha = chromatine ; cho = chromosome ; cy = cytoplasme du parasite ; en = enveloppe nucléaire ; ff = fibre fusoriale ; i = interruption de l'enveloppe nucléaire ; pf = plaque fusoriale ; pn = pont nucléaire ; v = vésicule polarisée.

cha = chromatin; cho = chromosome; cy = parasite cytoplasm; en = nuclear membrane; ff = spindle fiber; i = break in the nuclear membrane; pf = spindle plate; pn = nuclear bridge; v = polarized vesicle.

nomenon may occur in parasitic stages with a variable number of nuclei. They no longer have the cylindrical appearance of the plasmodia we have already described (Plate IX, 41; Plate XI, 48). This bipolarity during merogony has already been observed in other species.

In Glugea anomala, elongate plasmodia with 2 to 30 nuclei have been encountered. Some of them, globular in shape, become isolated and produce uninucleate sporonts (Debaisieux, 1920). In Nosema fennica Lom and Weiser, 1969, the plasmodia are round, 11 µm in diameter and contain 9 nuclei. They are derived from the first schizogonic division. There are also banded stages (3 x 13 µm) with five nuclei which comprise the second schizogonic stage (Lom and Weiser, 1969). In Glugea berglax Lom and Laird, 1976, two types of merogonic division have been described. One yields elongate schizonts or plasmodia that break off in sections to produce a chain of schizonts. The other yields circular multinucleate schizonts which give rise to sporonts. The tiny vacuoles between the host and the parasite (Plate XI, 48) proliferate. This marks the formation of the sporogony vacuole which continues to grow in size until it isolates the parasite from the host cell. It corresponds to the alveoli observed in histological sections of the xenoma. A comparable phenomenon was recorded by Loubès et al (1976) in Glugea habrodesmi. The plasmodium was embedded in a thick complex wall. The sporogony vacuole formed by pushing back the plasma membrane of the plasmodium with the aid of the fingerlike projections on the internal side of the envelope.

In conclusion, the following zones correspond to each other:

zone with giant nuclei and first merogony;

zone with alveoli and second merogony and sporulation;

zone with spores and end of sporulation.

c) The Second Phase of Merogony

This phase begins when the plasmodium becomes isolated from the host cytoplasm and results in the formation of sporonts after cytoplasmic division. In the resulting vacuole, two main processes occur simultaneously, i.e., cytoplasmic division and structural transformation into sporonts (mainly involving thickening of the wall).

- Cytoplasmic division. The non-cylindrical plasmodium divides by constriction (Plate XII, 50, arrows) and often results in the formation of star-shaped elements (Plate XIII, 54-55). These structures were measured. Under the electron microscope, up to 6 arms were recorded, whereas in stained smear preparations, up to 12 arms were observed. Often, several "stars" exist in the same vacuole, in which case, there may be as many as 20 arms. This suggests that there may be two successive divisions

---

PLATE XII

CC = kinetic centers; CP = parasite cytoplasm; e = thickening of the envelope; m = thin portion of the envelope; N = nucleus; P = sporont wall undergoing changes; R - endoplasmic reticulum; V = sporogony vacuole.

50 - Division of the plasmodium into sporonts (arrows) with simultaneous thickening of the wall (X 18,000).

51 - Same phenomenon with constriction (arrows) and a developed endoplasmic reticulum around the nucleus (X 15,750).

52 - Sporont envelope during thickening process (X 49,500).

53 - Completed envelope (X 49,500).

PLANCHE XII
PLATE XII

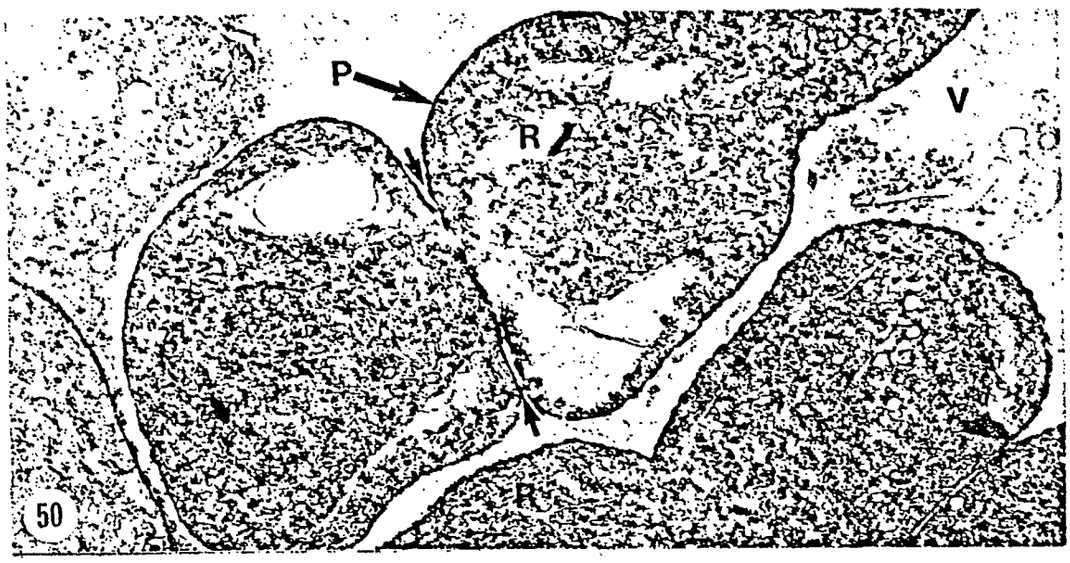

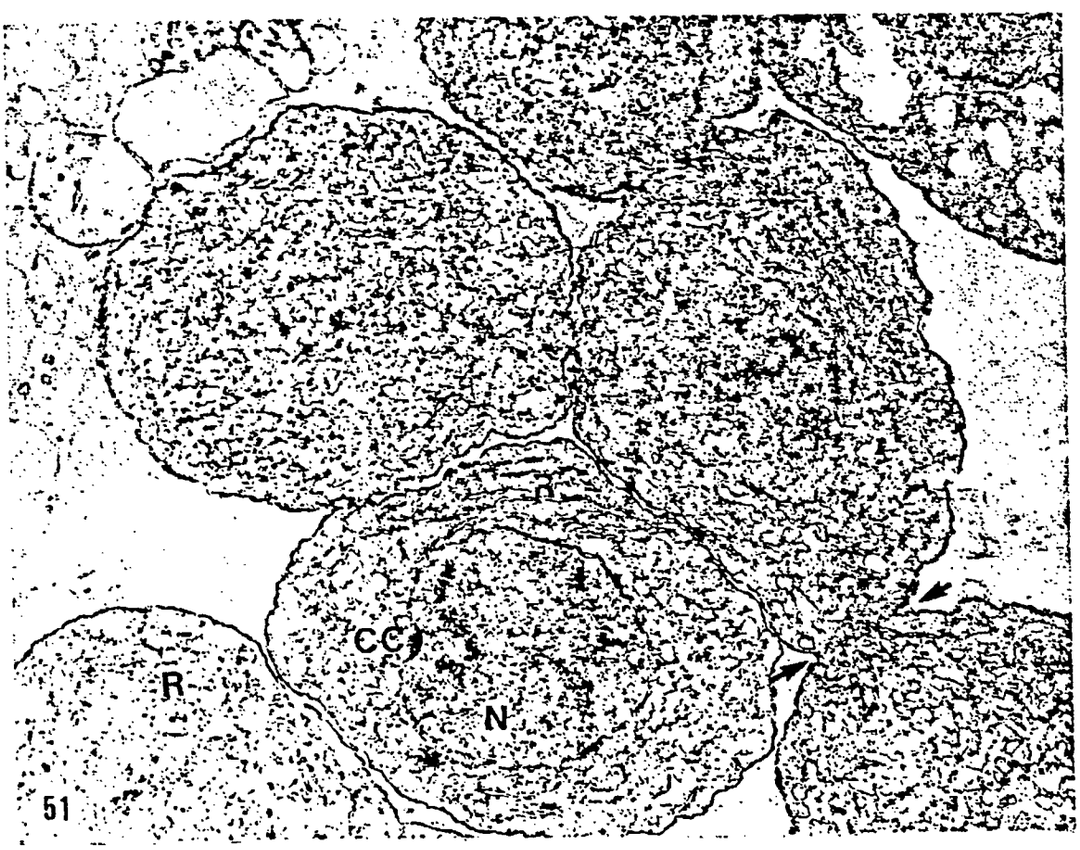

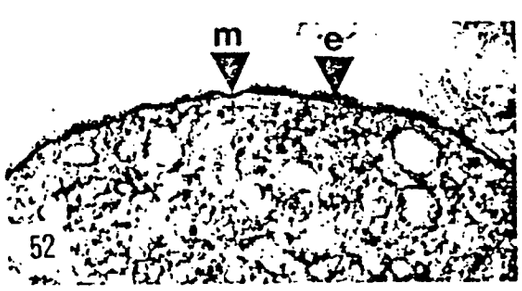

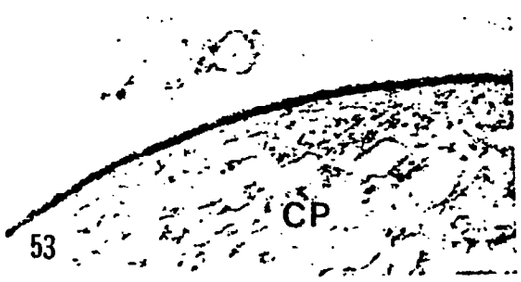

(Plate XIII, 54-56). The process ends with the formation of numerous sporonts (Plate XIII, 56, V2).

- Structural changes. At the onset of division, the plasmodium wall is mixed, i.e., made up of a plasma membrane (roughly 10 nm) in which certain layers undergo considerable thickening (up to 30 nm) (Plate XII, 52). These thickened areas undoubtedly result from a secretory phenomenon in the parasite. They grow in size until they join, at which time the entire wall presents a thickened appearance (Plate XII, 53). Thickening of the wall ceases before division comes to an end. At that stage, the vacuole is approximately 13 µm in diameter. The nucleus is faint in outline but can be detected because of clumps of chromatin at the periphery. The average diameter of the nucleus is 1.75 µm. The cytoplasm contains a substantial reticulum. There may be up to 8 vesicles around the nucleus (Plate XIII, 55).

PLATE XIII

M = meront; PV = sporogony vacuole wall; R = endoplasmic reticulum; V = sporogony vacuole.

54 - Vacuole containing three star-shaped structures resulting from cytoplasmic division. The vacuole walls (arrows) is still vacuolated (X 7,200).

55 - End of sporont formation (X 21,600).

56 - Several sporogony vacuoles at different stages. V1 = fractionation into sporonts. V2 = separate sporonts (X 4,950).

PLANCHE XIII
PLATE XIII

54

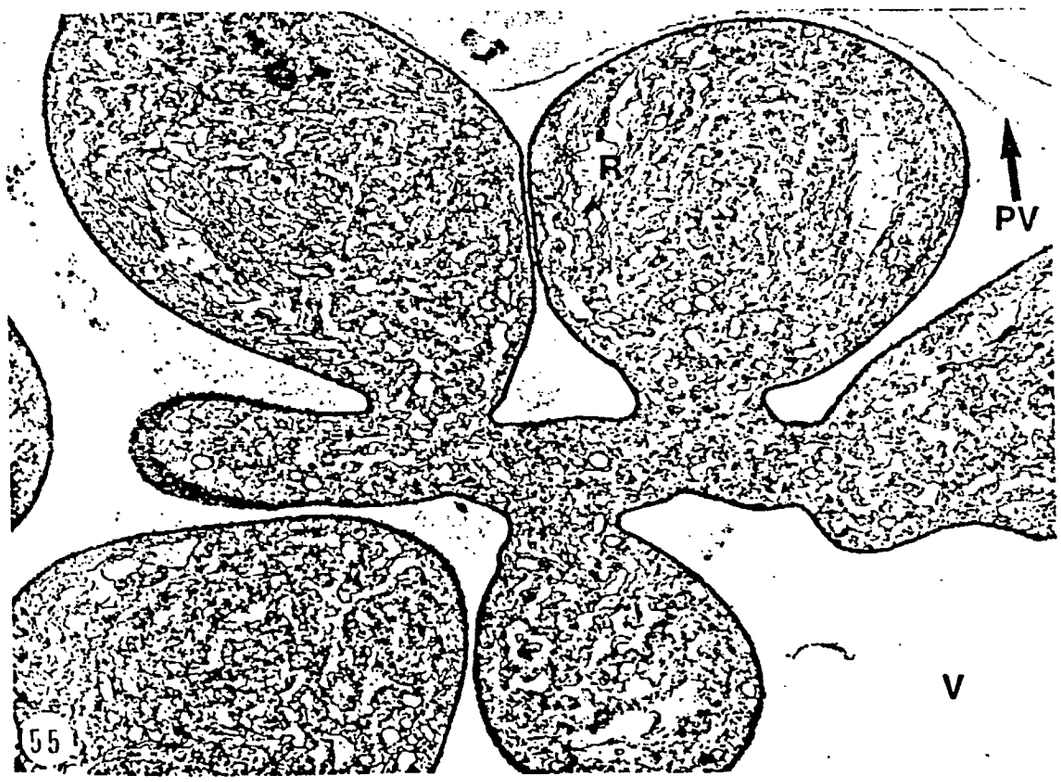

55

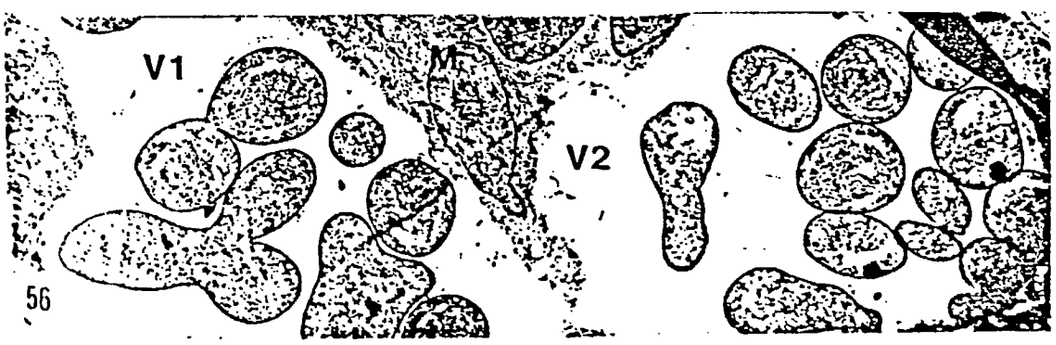

56

d) The Sporonts

The sporonts represent the end result of star-like division of the plasmodium. There may be over 12 sporonts in the same sporogony vacuole (Plate XIII, 56, V2). They are characterized by a regular outline, a nucleus with chromatin and a substantial endoplasmic reticulum (Plate XIV, 58).

e) The Sporoblasts

In photos showing fine structures, 11 to 19 sporblasts may be counted in the same sporogony vacuole (Plate XIV, 59). Under the light microscope, groups of 33 elements were observed in stained smears but they may have represented the elements from two neighbouring vacuoles. Theoretically, they arise from sporonts that have split in two (Sprague and Vernick, 1968; Lom, 1976). This phase was not observed. Sporoblasts are circular to oval in shape with contours that are often distorted by the release of tubules (Plate XIV, 57, 59, 60). They are generally once to twice as long as they are wide, but at times may be remarkable for their elongated shape (Plate XIV, 59, SA). The average envelope is 29 nm thick and does not seem to have undergone any changes since the sporont phase. Loubès et al (1976) stated that sporoblast nuclei were

---

PLATE XIV

C = chromatin; G = Golgi apparatus; N = nucleus; R = endoplasmic reticulum; SA = elongated sporoblast; ST = tubule sections; T = tubule; V = sporogony vacuole.

57 - Sporoblast (X 21,600).

58 - Sporont (X 20,000)

59 - Sporogony vacuole containing a large number of sporoblasts (X 5,400).

60 - Stages producing tubules which are initially large in diameter (X 13,900).

61 - Sporoblasts may contain Golgi bodies. Tubule tips are very fine (X 33,000).

PLANCHE XIV

PLATE XIV

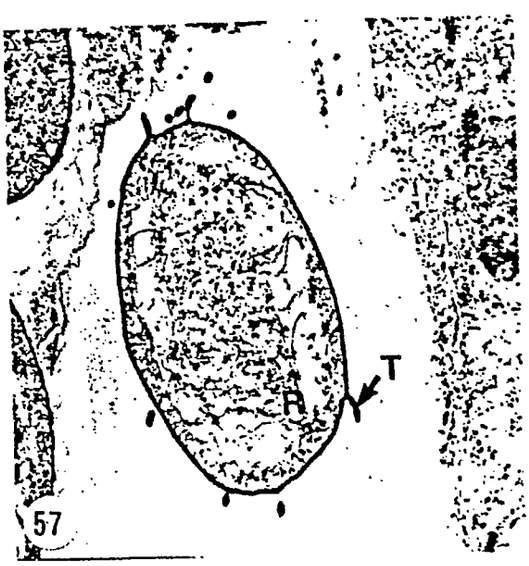

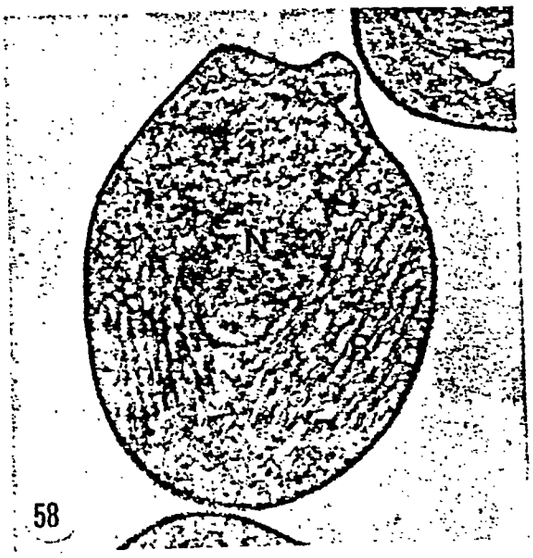

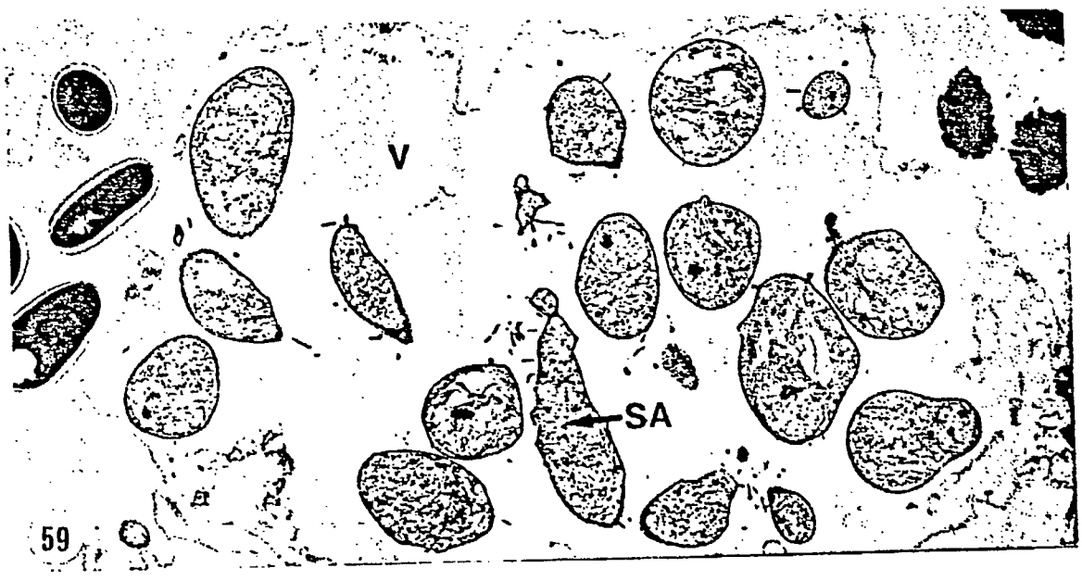

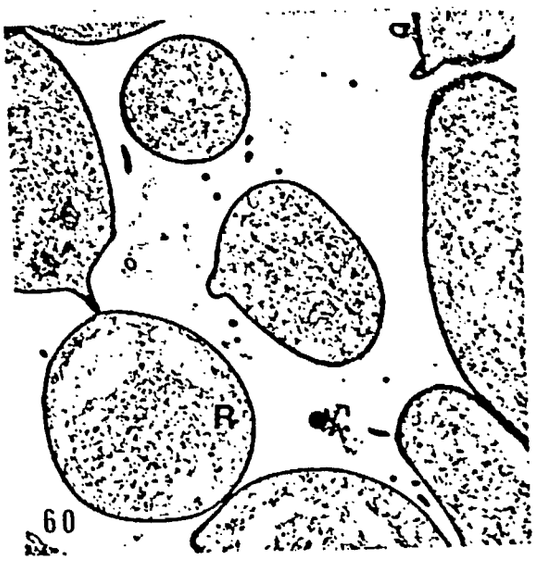

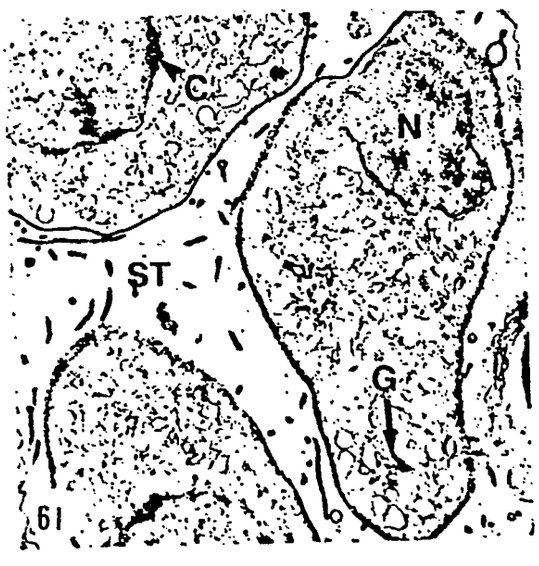

less active than sporont nuclei. In the present case, the nucleus did not seem to have lost any of its activity (Plate XIV, 61). In the cytoplasm, there are Golgi vesicles made up of aggregates of tiny vacuoles, roughly 50 nm in size, surrounded by larger vacuoles (20 nm) (Plate XIV, 61, G).

The main statistical measurements taken in stages ranging from the plasmodium to the sporoblast are shown in Table 10. The figures in parentheses represent the number of measurements taken, the others represent averages.

	Dividing plasmodium. Mixed wall	Dividing plasmodium. Thick wall = sporonts	Sporoblasts
Width of elements	2.9 µm (39)	2.4 µm (26)	2.35 (7)
Diameter of nucleus	1.75 µm (18)	1.45 µm (8)	1.5 µm (7)
Wall segment that has not undergone thickening	10 nm (8)	-	-
Thick portion of mixed wall	30 nm (8)	-	-
Thick wall	-	29 nm (11)	29 nm (12)
Diameter of vacuole	11 µm (5)	13.5 µm (5)	15.35 µm (9)

Table No. 10. Measurements in Plasmodium to Sporoblast Stages.

From Table 10, it may be seen that:

- this part of the cycle does not correspond to an increase in parasite number;

- the nucleus seems to remain unaltered;

- the plasma membrane becomes thicker at the onset of plasmodium division but does not develop further in the sporoblast stage;

- statistically speaking, there is very little change in the sporogony vacuole.

f) Sporogenesis

This corresponds to the progressive transformation of the sporoblast into a spore. The phenomenon will be described in three of its aspects, i.e.:

- formation of the polar filament and polar sac
- formation of the spore case
- development of the nucleus and cytoplasm.

Formation of the polar filament. For greater ease in understanding, it is necessary at this stage to describe the structure of the filament in the mature spore. When mature, the filament is roughly 150 nm in diameter (Plate XVII, 76) and is divided into three parts which we will proceed to describe.

The axial portion has a radius of 40 to 50 nm and includes:

A: a grey axis with a radius of 13 nm

B: a transparent layer, 15 nm thick

C: a very fine dark layer (roughly 2.5 nm)

D: a transparent layer, 10 nm

E: a dark layer, roughly 5 nm.

The intermediate portion includes only a single Zone:

F: a thick transparent layer (16 nm).

The peripheral portion varies in thickness from 15 to 20 nm and includes:

G: a dark layer, 5 nm

H: a transparent layer, also 5 nm

I: a very dark lining layer, ranging in thickness from 5 to 10 nm and sometimes more.

Lom and Corliss (1967) also counted three main zones in Pleistophora hypessorbryconis but failed to describe them in detail. These zones included a dense outer layer with fibrils, a transparent layer and the center containing a dense coiled substance.

On the basis of photographs taken by Schubert (1969) of Pleistophora hyphessobryconis, Vavra (1976) described two additional layers in the peripheral portion, thereby bringing the number of layers up to 11. In order to facilitate comparison, the various stages of sporoblast development will be defined by the number of spirals in the coiled filament.

Zero stage no longer corresponds to the sporoblast proper. The filament consists of 4 to 8 sections in a common vacuole (Plate XV, 62, VC). At this point the filament is only a dark unorganized axis. It seems to emerge from the vacuole since sections may be seen embedded in the cytoplasm (Plate XV, 62, arrows). Typical filament structure suggests that all the sections of the axis at zero stage belong to the same element. There is some question about the shape of the common vacuole, but a crescent (or half ring) shape was observed (Plate XV, 63, v).

The axis begins to lengthen after it has perforated the vacuole wall. In a few rare instances, it exhibits a concentric structure (Plate XV, 62, double arrows). In this particular case, the total radius was 30 or 35 nm and included:

- a dense axis with a radius of 9 nm
- a transparent layer, 11 nm
- a dark thin layer, roughly 2 nm
- a transparent layer, 7 nm
- a dark lining layer, 5 nm.

These layers correspond to layers A,B,C,D and E in the mature filament. As a result, these five layers were considered part of the axial portion.

PLATE XV

A = geometric structure reminiscent of a Golgi apparatus; f = developing filament; N = nucleus; v and VC = common filament vacuole.

62 - Zero stage in filament formation. Sections of the amorphous filament axis are embedded in a common thick-walled vacuole. Sections occur free in the cytoplasm (single arrow) near the geometric structure. In exceptional cases, the axis may be structured (double arrows) (X 63,000).

63 - Same stage showing the crescent or half-ring structure of the common vacuole (X 27,900).

64 - Another example of an axis in the common vacuole (X 77,500).

65 - The common vacuole contains only two axes which will later separate (X 101,700).

66 - Stage one in which one filament coil seems to have developed (X 25,000).

PLANCHE XV

PLATE XV

62

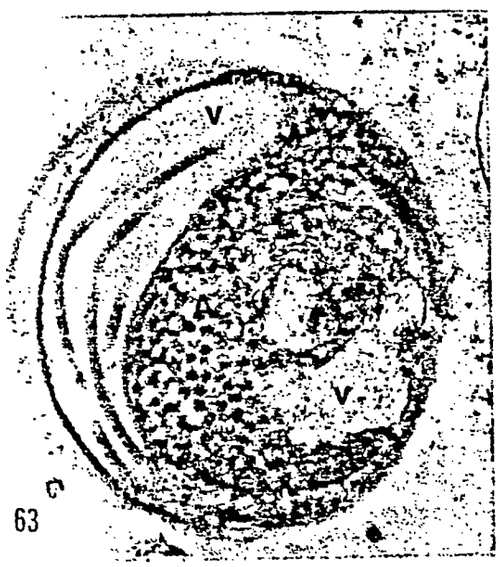

63

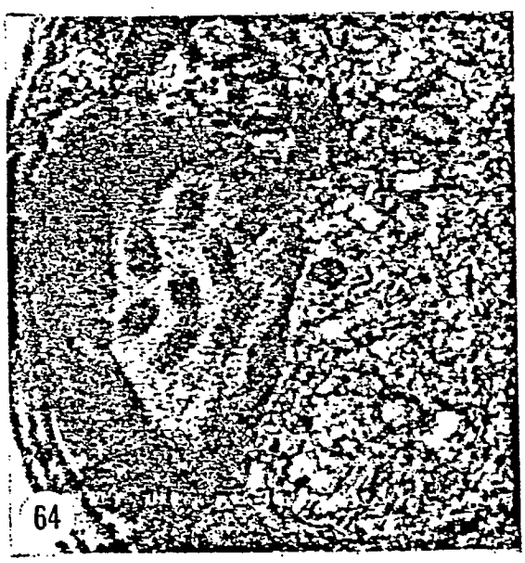

64

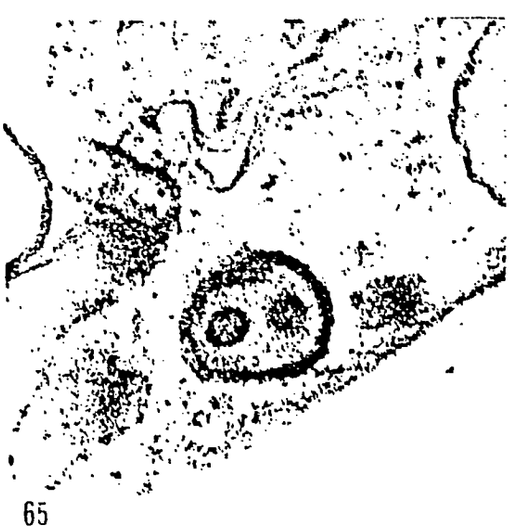

65

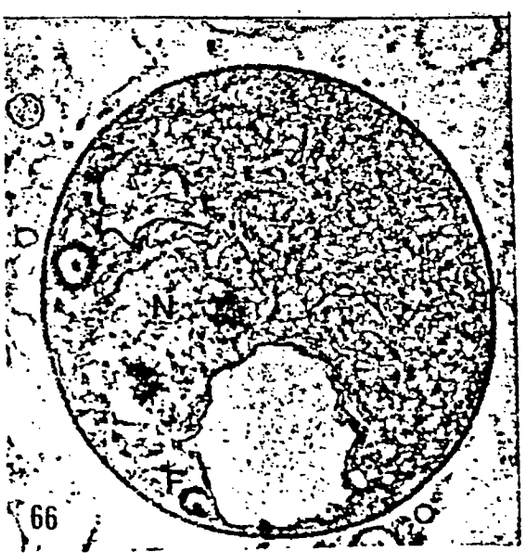

66

Actually, however, the filament axis is usually a dense mass without any obvious layers. Molecular material is already present but there is generally no structural organization until stages 9 or 10 and often later.

For completion of the filament, the intermediate transparent portion and the peripheral portion must become organized around the axis. This additional build-up originates in a granular structure which is also encountered in Icythyosporidium sp. Schwartz, 1963 (Sprague and Vernick, 1974) and Nosemoides vivieri (Vinckier, Devauchelle and Prensier, 1970) Vinckier, 1975.

This structure consists of granules, roughly 50 nm in diameter and almost 100 nm apart. They are joined by diffuse bands, forming geometric patterns (Plate XVI, 67) representing perfect squares (Plate XVI, 69) or occasionally hexagons (Plate XVI, 71).

PLATE XVI

A = geometric Golgi apparatus; AG = accumulation of granules; F = filament; G = typical Golgi apparatus; L = release of an axis; M = filament section; N = nucleus; R = endoplasmic reticulum; V = common vacuole.

67 = Stage 0 (X 27,000).

68 = Stage 10. The last coils of the developing filament are represented solely by their axes (arrows) (X 21,600).

69 - Stage 9. Accumulation of granules connected to the peripheral portion of the developing filament (X 57,150).

70 - Stage 6. The formation of the first filament coils is thought to occur as a result of the release of the axis contained in the common vacuole. The axis takes with it part of the vacuole wall (X 27,000).

71 - Geometric structure with an hexagonal configuration (black triangle) (X 44,500).

72 - Stage 6 or 7. Abundant endoplasmic reticulum (X 40,000).

PLANCHE XVI
PLATE XVI

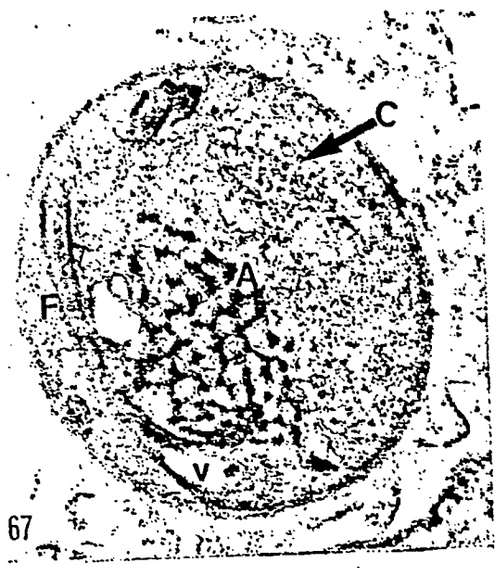

67

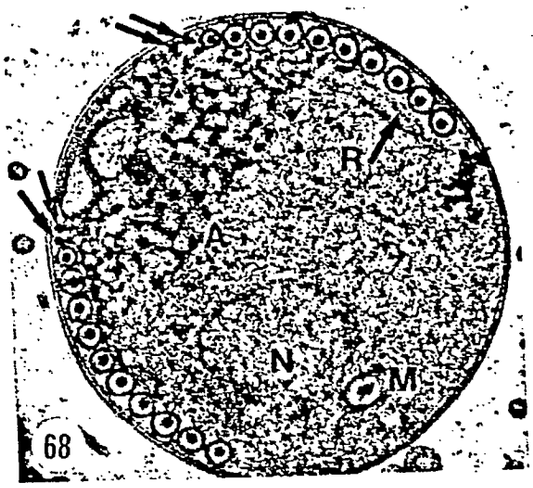

68

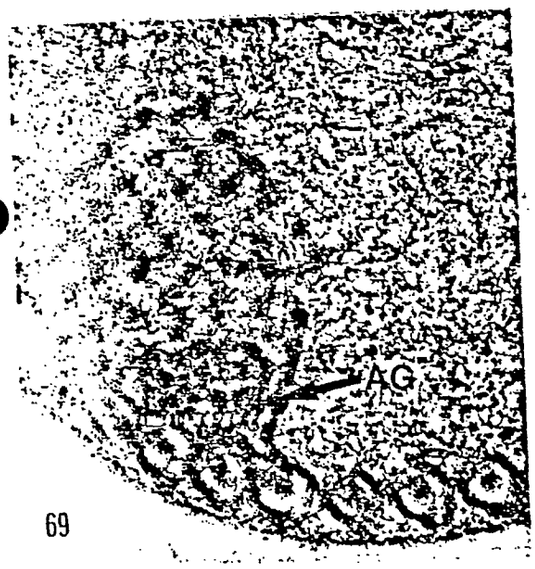

69

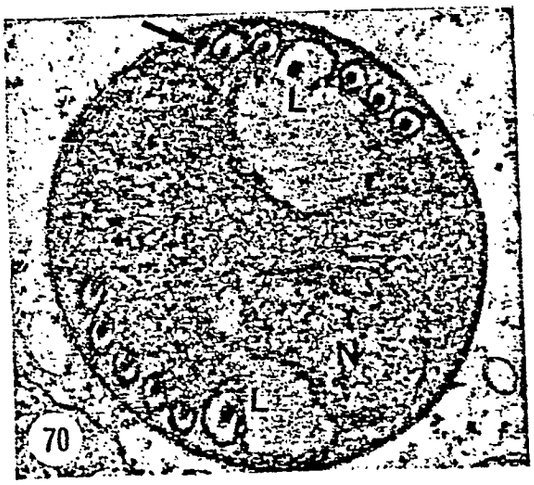

70

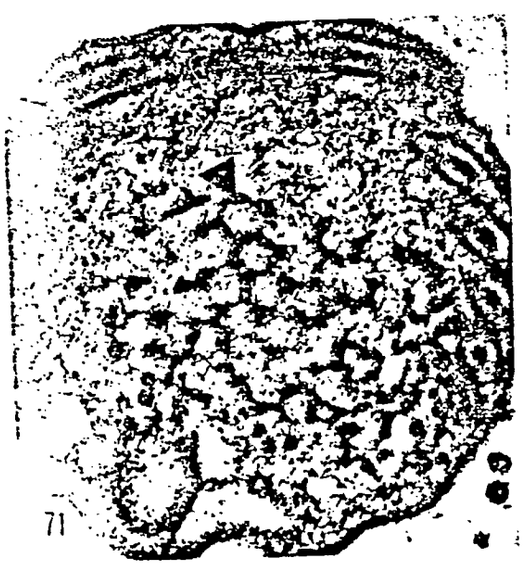

71

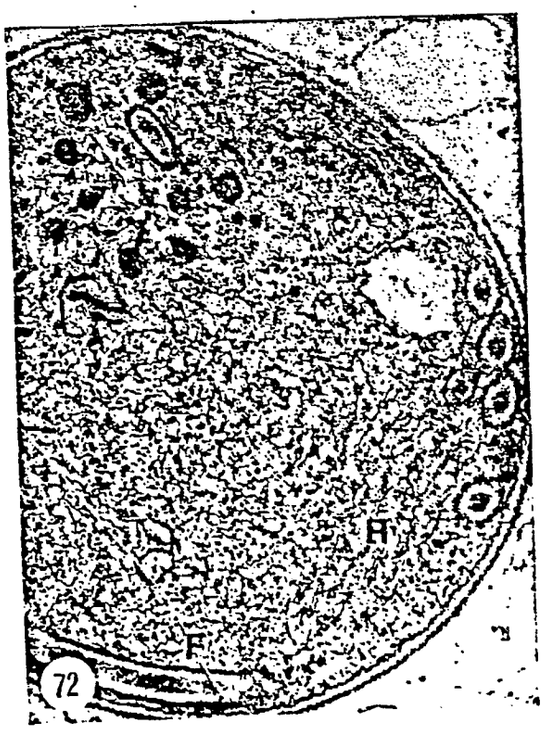

72

Usually, it is not possible to distinguish the geometric patterns because of a certain amount of disarray (Plate XVI, 68).

Near the filament, a transfer of material takes place in the exact prolongation of the developing peripheral portion (Plate XVI, 69, AG).

The central zone which is framed by the geometric figures is also structured. A fine (2 to 4 nm) membrane can be seen parallel to the perimeter. The central residual zone is 20 to 50 nm in diameter (Plate XVI, 67 - 71, arrow).

Fig. 24 gives the measurements for the granular structure with the corresponding figures for the future unsubdivided 3-zone filament which is described below.

It is as though the filament, with the axis besides, were a condensed version of the geometric patterns. The granular structure, which can be likened to the Golgi apparatus, gradually deposits molecular material that, as a result of the geometric structure, is already partially arranged. Elongation of the axis must be a comparable phenomenon although it was not observed. Just how the axes in the common vacuole (Plate XV, 62, 63 and 64) succeed in emerging from the vacuole has not yet been determined. The vacuole is shaped like a crescent or ring (Plate XV, 63). If the latter hypothesis is correct, the filament is already coiled within. There is evidence (Plate XVI, 70, L) that the filament emerges from the vacuole coil by coil, taking with it part of the vacuole wall which forms the external portion of the filament. This is not in contradiction with observations on the formation of this portion

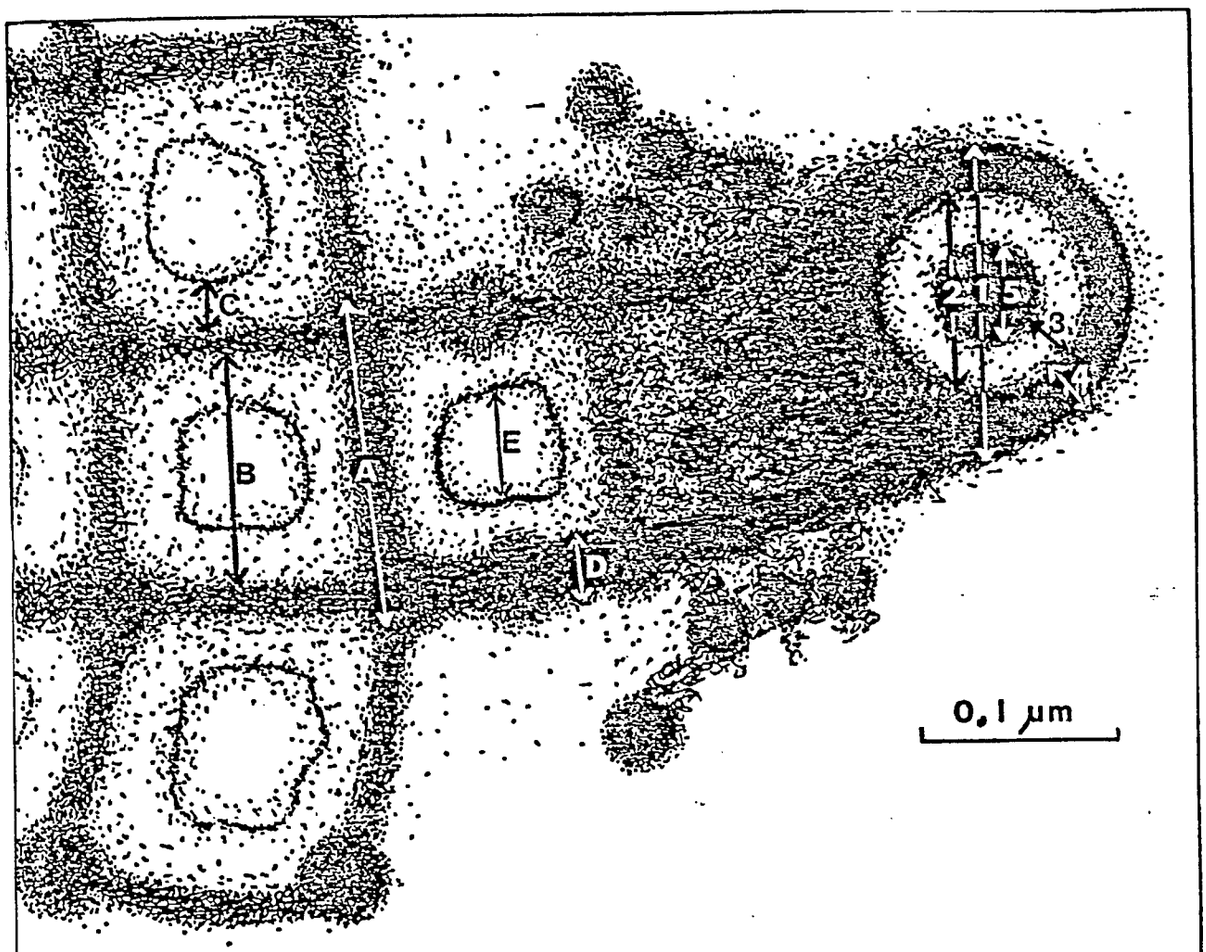

DIMENSIONS COMPAREES : COMPARATIVE DIMENSIONS

(A)	140 à 220 nm	125 à 200 nm	(1)
(B)	70 à 100 nm	100 nm	(2)
(C)	10 à 20 nm	20 à 30 nm	(3)
(D)	25 à 30 nm	20 à 35 nm	(4)
(E)	20 à 50 nm	50 à 70 nm	(5)

Fig. 24 : ELABORATION DU FILAMENT POLAIRE

Development of the Polar Filament

since the vacuole wall, which is 25 to 35 nm thick, also seems to have been produced by the geometric granules (Plate XV, 63). Rare instances in which two axes are enveloped by the same external portion provide evidence of the vacuolar origin of this part (Plate XV, 65). In histological sections, the filament displays a permanent structure after stage 10. Before that, three layers may be seen (Plate XVI, 72):

- the dense axial portion with a radius of 25 to 35 nm. There are no signs of subdivision;
- the transparent intermediate portion, 20 to 30 nm;
- the peripheral portion with no signs of subdivision, 20 to 35 nm. The overall diameter decreases as the filament develops;
  - . stages land 2, simple structure; average diameter: 195 nm
  - . stages 3 to 12, simple structure; 160 nm
  - . stages 10 to 17 (= spore), complex structure; 115 nm.

The process is illustrated diagrammatically in Fig. 25.

Formation of the polaroplast. The polaroplast does not begin to form until stages 8 or 9. Thereafter, two structures begin to differentiate:

+ a structure speckled with vesicles and containing interlacing bands occasionally arranged in hexagonal patterns (Plate XVII, 74, PV). This is the future vesicular polaroplast.

+ a structure over 350 nm thick which is clearly lamellar in structure and which is undoubtedly made up of a series of simple membranes (Plate XVII, 73, PL). This is the future lamellar polaroplast. The polar filament which is locally straight and ends at the anterior portion in a polar cap passes through these two structures.

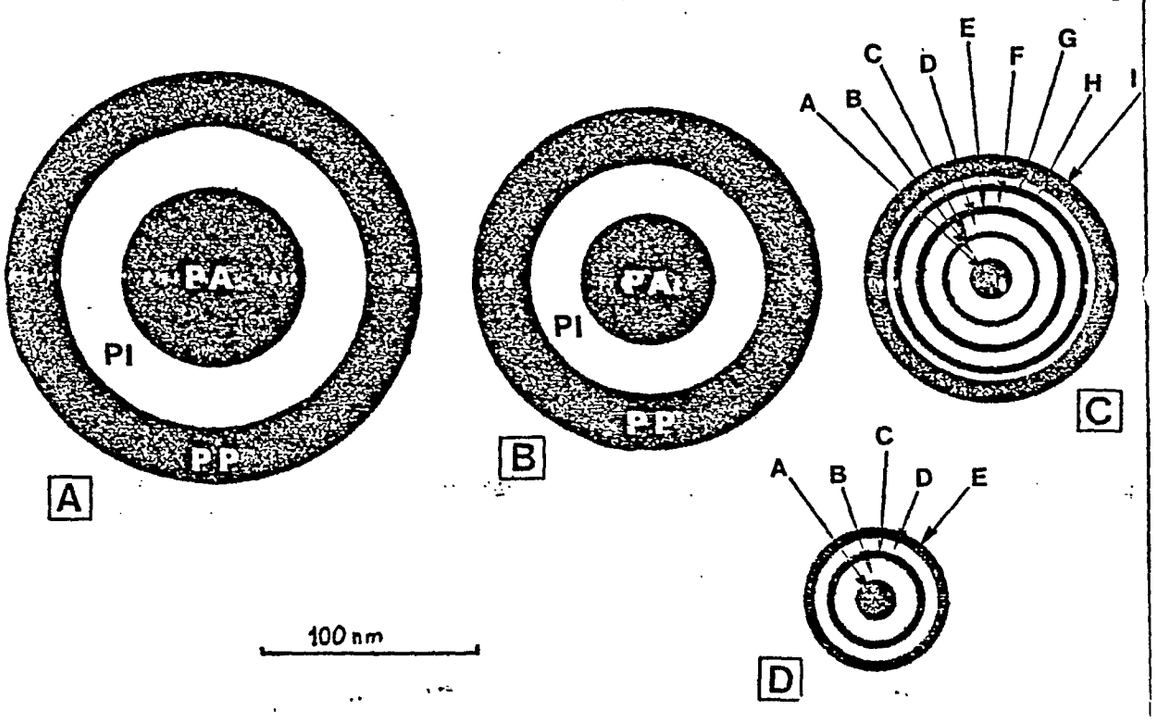

Figure 25 : Evolution du filament Developmental changes in the filament

A : stade 3 stage 3

B : stade 11 stage 11

C : spore mûre (stade 16) mature spore (stage 16)

D : axe isolé dans le cytoplasme, stade 0. axis isolated in the cytoplasm, 0 stage

PA = Partie axiale ; PI = Partie intermédiaire ; PP = Partie périphérique.

PA = axial portion; PI = midportion; PP = peripheral portion.

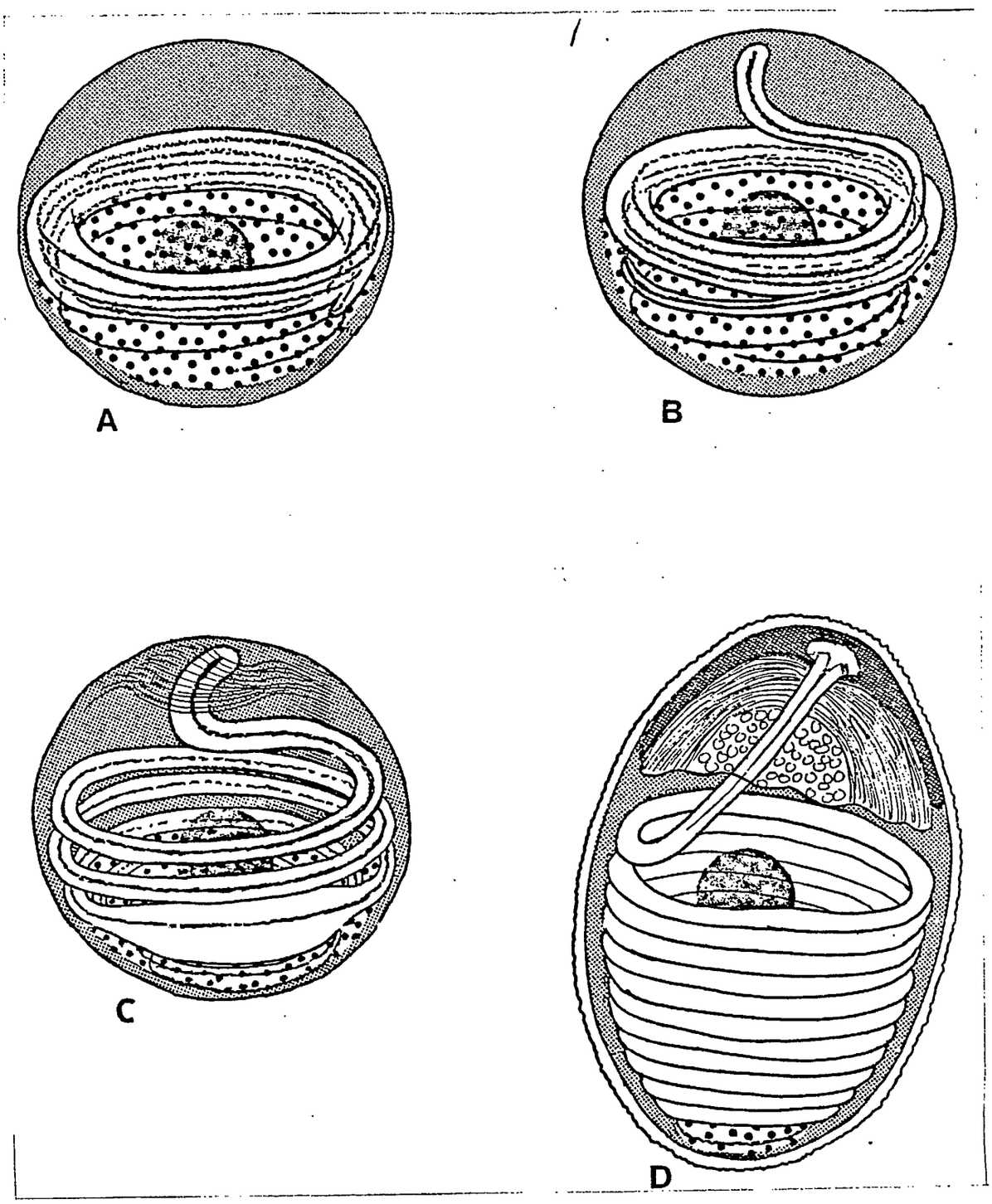

Fig. 26. Hypothesis Related to Filament Formation

A: D stage. Most of the filament axis is contained in the common vacuole. It emerges into the cytoplasm where granules are organized in a geometric pattern (Plate XV, 62-63).

B: Stage 1. A coil emerges from the vacuole while the bare axis elongates (Plate XVI, 67).

C: Stage 4 or 5. The vacuole releases the last coils (Plate XVI, 70).

D: Stage 12. The filament develops from the posterior end only (Plate XVII, 73).

Formation of the spore case. The double structure of sporont and sporoblast walls was not recorded here and is not observed until the polar filament begins to form. The case consists of a wavy plasma membrane, a transparent middle layer which becomes the endospore and a dark peripheral layer, irregular in thickness, which develops into the exospore. Table 11 provides a summary of measurements taken of these layers. Averages are followed by the number of measurements in parentheses.

	Sporoblast	Stages 0 to 8	Stages 8 to 11	Spore
total thickness of covering	29 nm (12)	34 nm (16)	98 nm (7)	155 nm (8
thickness of plasma membrane	not observed	10 nm (6)	10 nm (7)	9 nm (4
thickness of endospore	not observed	11.5 nm (6)	63 nm (11)	90 nm (8
thickness of exospore	not observed	12 nm (6)	20 nm (11)	65 nm (8

Table No. 11. Measurements of Different Parasitic Coverings

Development of the nucleus and cytoplasm, During the course of development, the nucleus tends to shrink (from an average diameter of 1.3 μm at the beginning of the process to 0.7 μm at the end). It becomes more opaque to electrons and finally is lost in the cytoplasmic mass (Plate XVII, 75). The endoplasmic reticulum is generally located between the nucleus and filament coils, forming a buffer-like structure between these organelles. The Golgi apparatus lies outside the geometric granular structure and may occasionally be seen (Plate XVI, 67). The entire cytoplasm becomes more opaque assuming the characteristic dark appearance of spores (Plate XVII, 75).

g) The Spore

The abovementioned transformation culminates in the formation of the spore whose highly characteristic structure corresponds to three distinct functions:

- protection (provided by the spore case)
- active penetration of the host (the filament with all its anterior structures, the polaroplast and posterior vacuole)
- reproduction (sporoplasm).

Protective structures. The spore case consists of a plasma membrane which adheres to the inside surface of the case as well as of an endospore and exospore (Plate XVII, 73; Plate XVIII). There is a sinuous border between these two layers. The endospore does not have the same thickness throughout and may range from 60 to 120 nm thick in the same spore. Slightly to the side of the spore apex, these two zones lose two-thirds of their thickness and combined measure only 50 nm. This more vulnerable area plays a key role in the extrusion process.

PLATE XVII

end = endospore; ex = exospore; PL = lamellar polaroplast; PV = vesicular polaroplast; V = structure perhaps corresponding to the posterior vacuole.

73 - Stage 11. The covering and polaroplast are already developed but the filament is still being formed although it is already structured (X 40,500).

74 - Tangential section of a vesicular polaroplast showing an hexagonal structure (X 39,100).

75 - Stage 10 or 11. At this stage, the spore has already acquired its elongated shape. (21,600).

76 - Stage 13. Complex structure of the filament which seems to be surrounded by a membrane fragment (black triangle) (X 110,000).

PLANCHE XVII

PLATE XVII

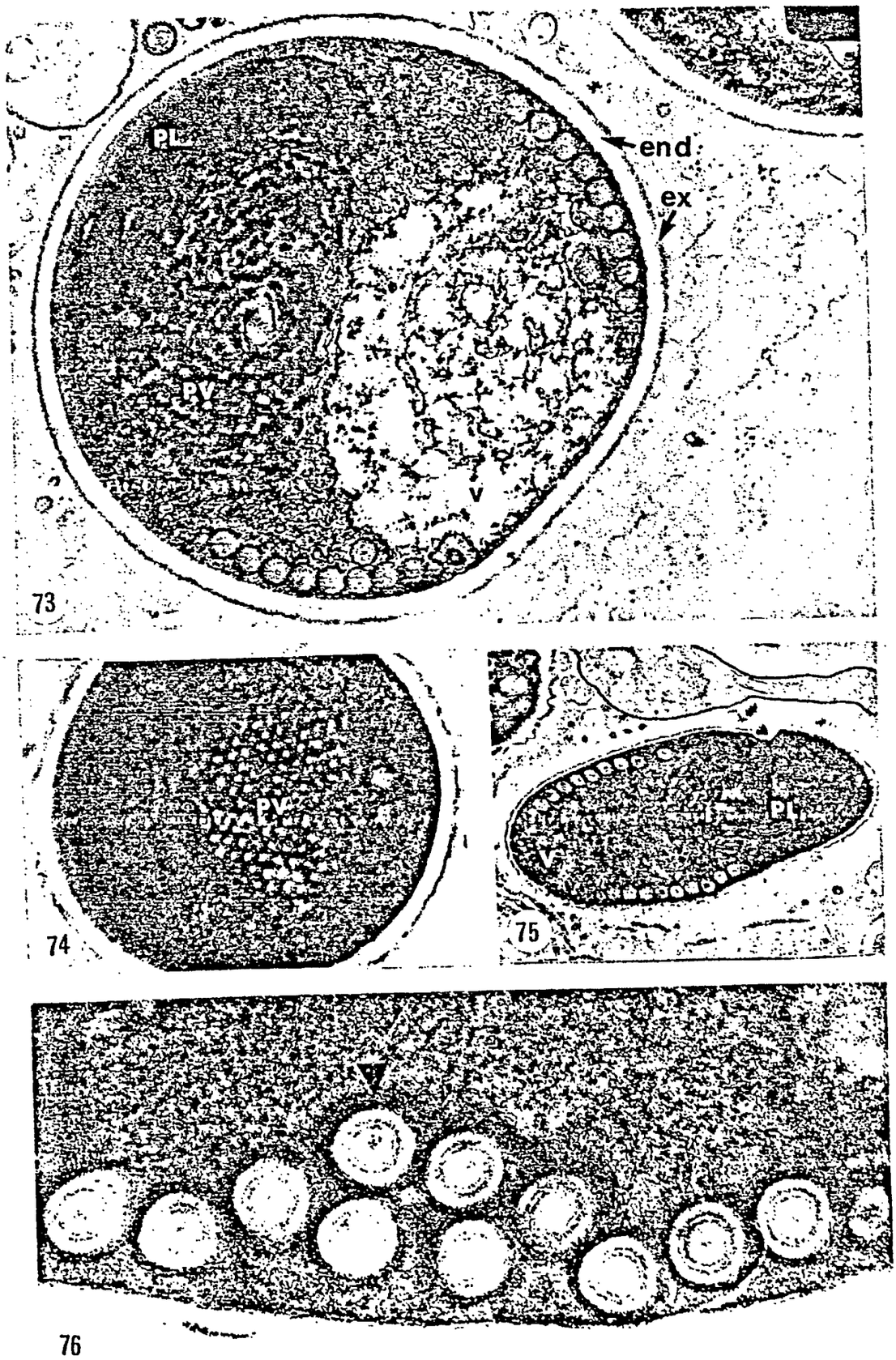

Extrusion structures. The polar filament consists of two parts. The posterior portion has already been described and is coiled in the posterior half of the spore with roughly 17 spirals. The anterior portion emerges from the coil to become straight. Measurements taken in this area indicate that the order of the concentric layers has not changed. Only the diameter of the central grey axis increases from 25 nm to 80 nm, suggesting that the tubular structure becomes larger at this particular site. In Pleistophora hyphessobryconis, an electron-dense substance fills the center of the filament (Lom and Corliss, 1967). According to Weidner (1972), the interior of the filament contains a water-repellent glycoprotein which is released from the protective sheath during extrusion in Spraguea lophii (Doflein, 1898) Weissenberg, 1976.

The polar cap contains numerous complex structures (Fig. 27). The filament enlarges anteriorly in what looks like the head of a nail. Filament layers G and H are capped by an obliquely stratified band (Plate XVIII, 77, A) which is comparable to a band observed in Caudospora simulii Weiser, 1946, and referred to as a "hinge" by Vavra (1976) on account of its role during extrusion. It may correspond to the polar band described by Vivarès et al (1977) in Ormieresia carcini Vivarès, Bouix, Manier, 1977. The dark outermost layer (layer I) detaches from the filament to form the polar sac.

The polaroplast lies beneath the polar cap and fills the space between the filament and the wall. It may be further broken down into two parts, i.e.:

.. the lamellar polaroplast, roughly half a micron thick in the area of the filament. It consists of thirty lamellae adjoining the anterior polar filament. The lamellae are slightly

wavy with a total thickness of 120 nm. They are separated from one another by a fine dark layer. Each lamella consists of two transparent layers on either side of a dark middle layer.

.. the vesicular polaroplast runs alongside the filament (Plate XVIII, 78, PV) for a distance of over 1 μm until it encounters the lamellar polaroplast. It is made up of large tubules and vesicles in alignment. The posterior edge coincides with the beginning of the filament spiral.

While the posterior vacuole has often been reported, it was never observed in this species under the electron microscope. Vacuoles were seen in a posterior position in the developing spore (Plate XVII. 73 - 75, V), but they disappeared once the spore attained maturity. Under the light microscope, a transparent area generally referred to as the posterior vacuole was observed posteriorly in all the living spores (Plate V, 17, VP). A comparison with micrographs clearly showed that the polaroplast produced an opaque area anteriorly and the filament spirals, a transparent area posteriorly.

Fig. 27. C = "hinge" in a stratified band arrangement; CP = polar cap; END = endospore; EX = exospore; f = straight portion of filament; PL = lamellar polaroplast; PV = vesicular polaroplast; r = endoplasmic reticulum; T = substance filling hollow tube; ZC = transparent zone in light microscopic examination of living spores; ZD = dense zone.

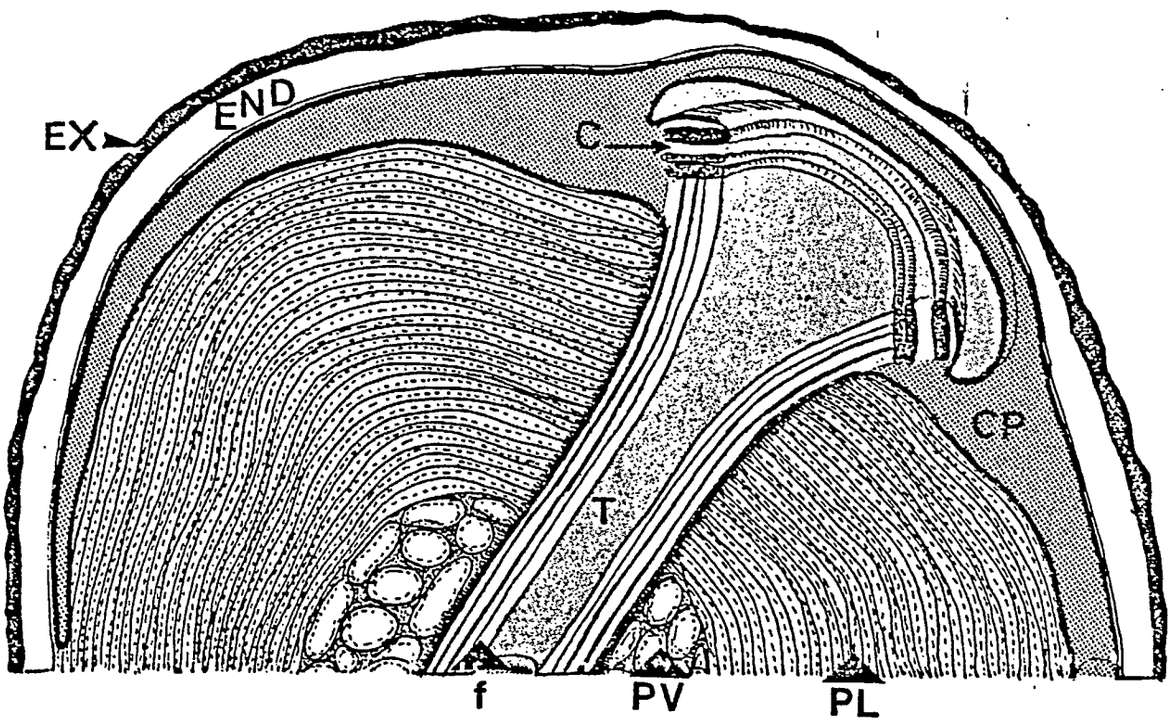

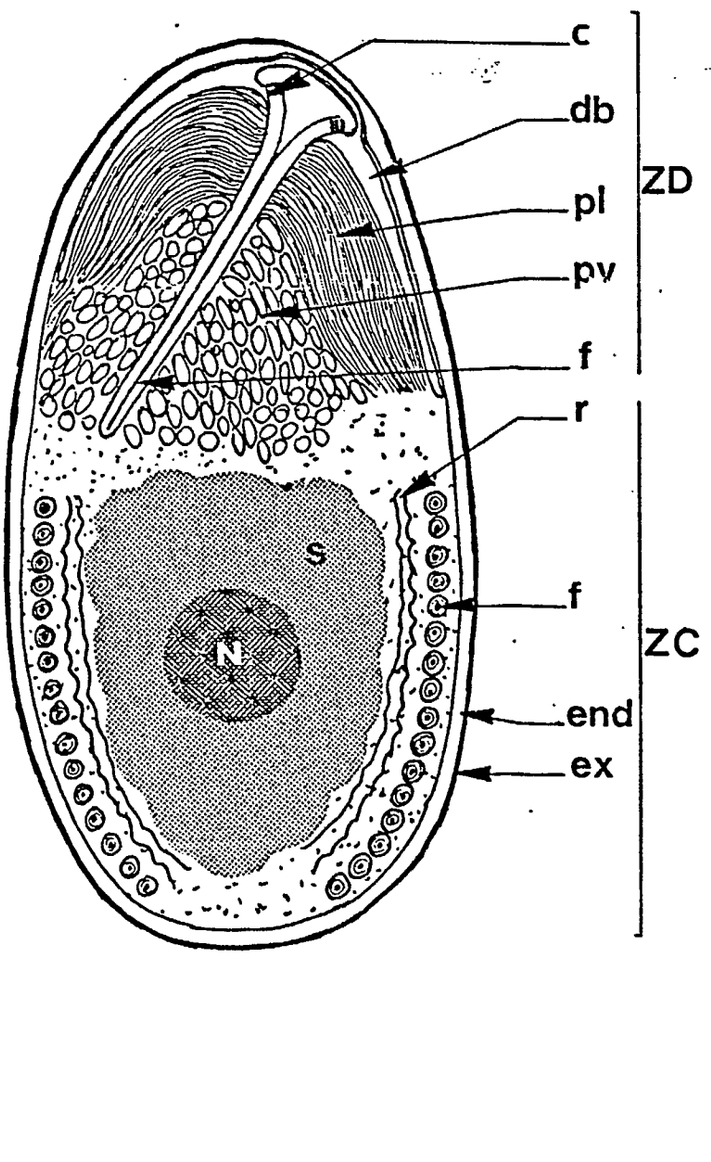

FIG. 27:
DETAILS DE LA SPORE

Detailed Structure of the Spore

The nucleus is very small (0.7 µm in diameter). Usually it can not be discerned in the reduced opaque cytoplasm surrounding it.

The cytoplasm is extensively pitted and contains ergastoplasm around the nucleus and alongside the filament spirals. It is often striated with a highly regular alignment of the ribosomes.

h) Extrusion of the Spore

In living specimens, the entire spore spins as the filament is extruded. The latter is 20 times longer than the spore itself and when it is violently ejected, it knocks aside all the other spores in its path. The empty spore is then seen with a very large central vacuole (Plate XXI, 95, V). Micrographs of the extrusion process make it possible to establish the course of events (Plate XX). As the filament unwinds, the coils gradually become more widely spaced (84 - 85) and lose their parallel configuration (86 - 87). The cytoplasm becomes less opaque (85 - 87) while intense vacuolation occurs (83 - 85 - 87). Fig. 28 gives a diagrammatic representation of events at the spore opening.

Once the filament has been extruded, the central vacuole continues to grow (88 to 91) with numerous folds in the wall (90 -

---

PLATE XVIII

A = band; EN = endospore; EX = exospore; F = filament; M = filament; MC = cytoplasm membrane; PL = lamellar polaroplast; PV = vesicular polaroplast; S = polar sac.

77 - Structure of the polar cap in the mature spore (X 114,750).

78 - Structure of the polaroplast in the mature spore (X 81,900).

PLANCHE XVIII

PLATE XVIII

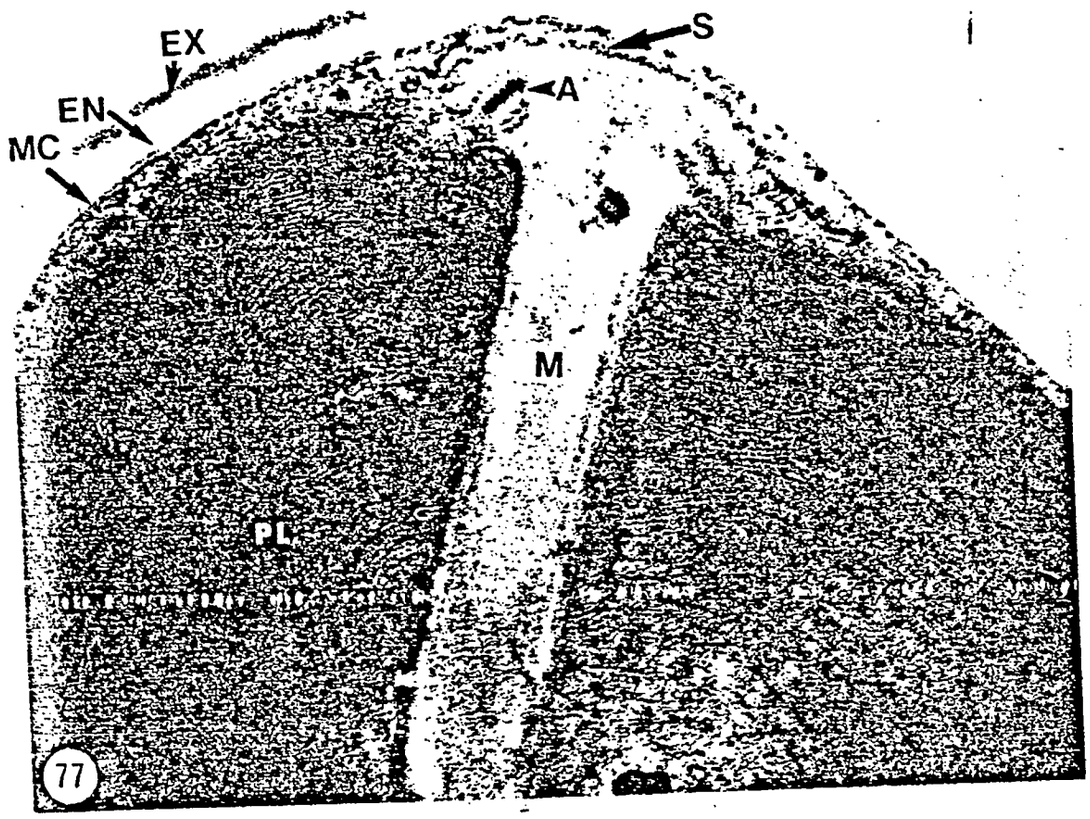

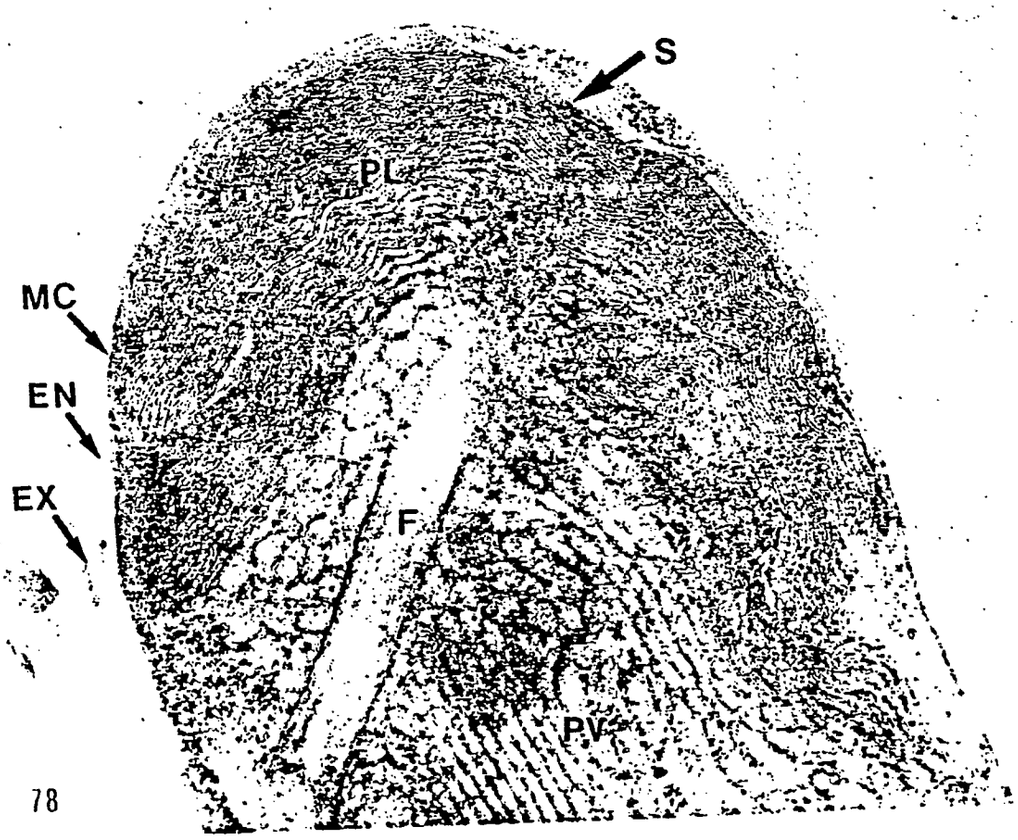

92). A saclike structure is attached to the opening in the spore case (88 - 90 - 91, arrows) and the polaroplast seems to undergo a structural change, although it is often invisible.

These findings enabled us to evolve the following hypothesis which is illustrated by Fig. 28.:

. An unknown chemical or physical signal modifies the spore case at the anterior portion where it is thinnest.

. The spore is osmotically hyperconcentrated (This is perhaps related to its electron density). Even a slight injury to the spore case produces a massive inflow of water due to osmosis (a). Weidner (1972) attributed this osmotic role entirely to the polaroplast.

. Water penetrates the basal disk via the upper membrane and spreads throughout the disk. It can then pass into the lamellar polaroplast without any difficulty.

. The polaroplast begins to swell as the lamellae spread apart. The internal pressure is very high (b). According to Lom and Corliss (1967), the spore must be activiated. The polaroplasm fills with water and internal pressure produces extrusion.

. The anterior structures, i.e., thin spore case and polar cap, are ripped asunder and the filament is forcibly ejected by

---

PLATE XIX

C = parasite cytoplasm; CH = chromatin; FF = spindle fibers; MN = nuclear membranes; PN = nuclear bridge; S = saccules or spindle plates; V = polarized vesicles.

79 - Active spindle plates (X 70,000).

80 - Depression in the nuclear envelope seen in a tangential section (X 21,600).

81 - End of nuclear division (with nuclear bridge) and onset of future mitosis (black triangle) (X 21,600).

82 - Spindle plates at opposite ends of the nucleus (X 32,000).

PLANCHE XIX
PLATE XIX

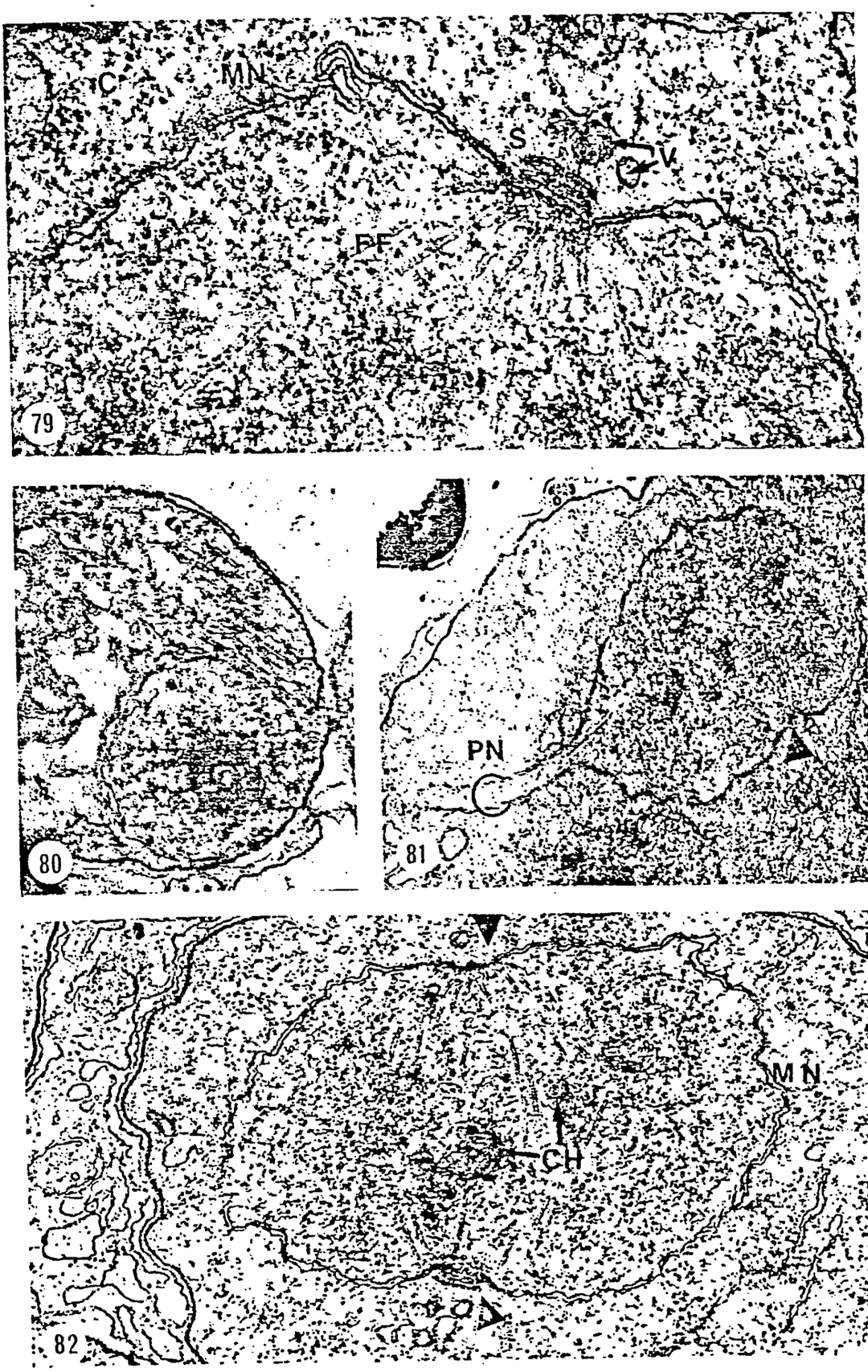

by eversion (c). Ishihara (1967) described the extruded filament as inside out. The filament contents then act as a protective sheath.

. The filament is rapidly extruded. The coils unwind, throwing the organization of the spore into disarray.

. The filament tip is sealed (by a vacuole?). Once the whole filament is completely extruded, the sporoplasm squeezes through the filament tube into the terminal pouch (d). According to Dissanaike-Canning (1957), West (1960), Sprague and Vernick (1968), the sporoplasm is attached to the filament which extracts it from the spore as it everts. For Lom and Vavra (1963), the sporoplasm passes through the filament. Erickson et al (1968) observed that the filament ended in a saclike structure constituting the germ. Lom (1971) added that the lamellar neck served as an anchoring device. In the spore, the posterior vacuole swells until it fills all the space available. According to Weidner (1972), the filament contents act as a protective sheath following extrusion by eversion. The sporoplasm passes through the filament into a terminal pouch. The nucleus is without a membrane but does not mix with the cytoplasm. The polar sac is the only organ damaged.

PLATE XX

83 to 92 - Sequence of events leading to extrusion of the filament. The filament unwinds losing its parallel configuration. A central vacuole (v) enlarges until it fills all the space available. Arrows point to a structure that may contain the infective germ and which is thought to pass through the filament (X 21,600).

93 - Detail of anterior tip (X 75,600).

94 - The filament passes through the tear in the wall and polar sac (X 64,800).

PLANCHE XX

PLATE XX

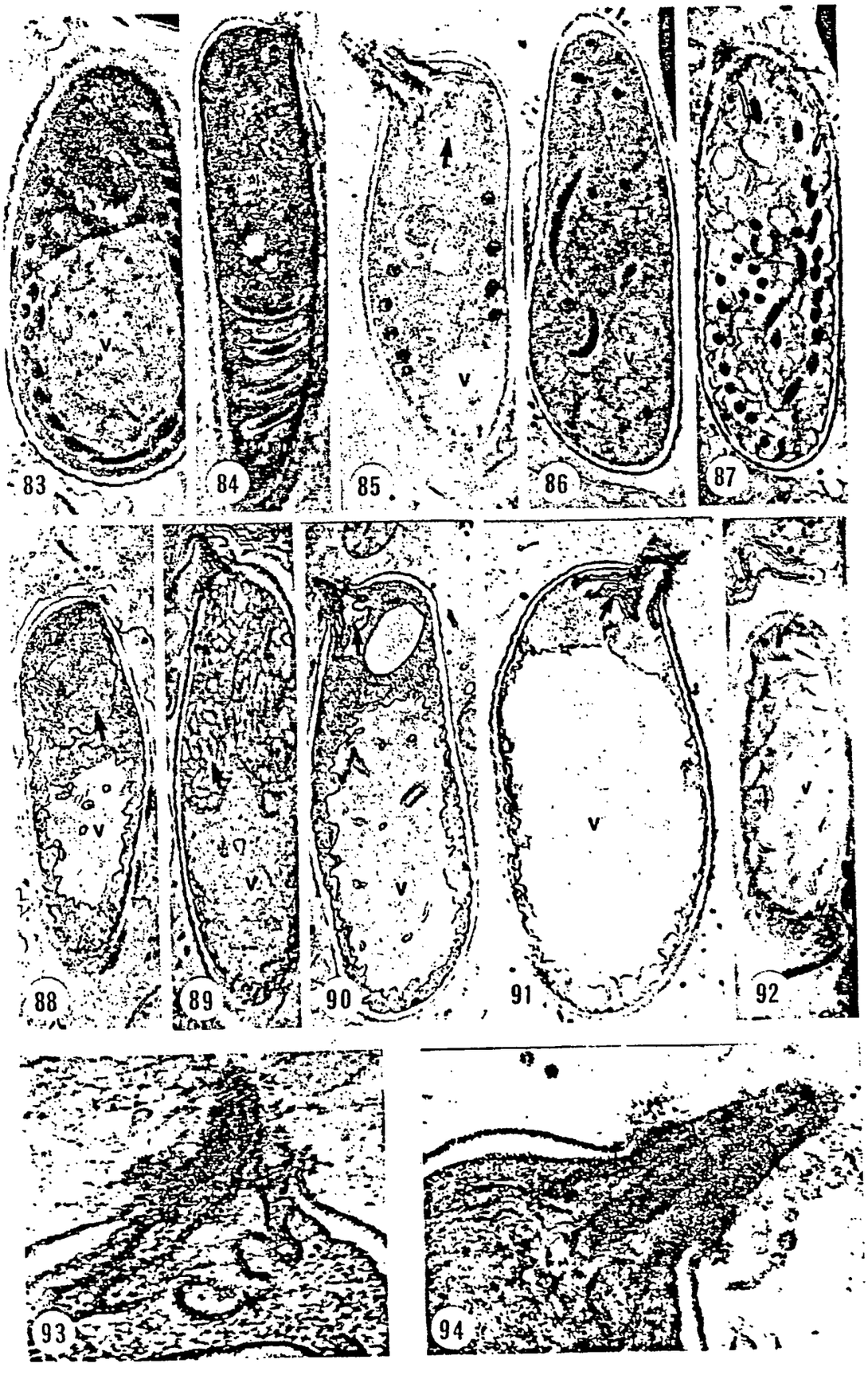

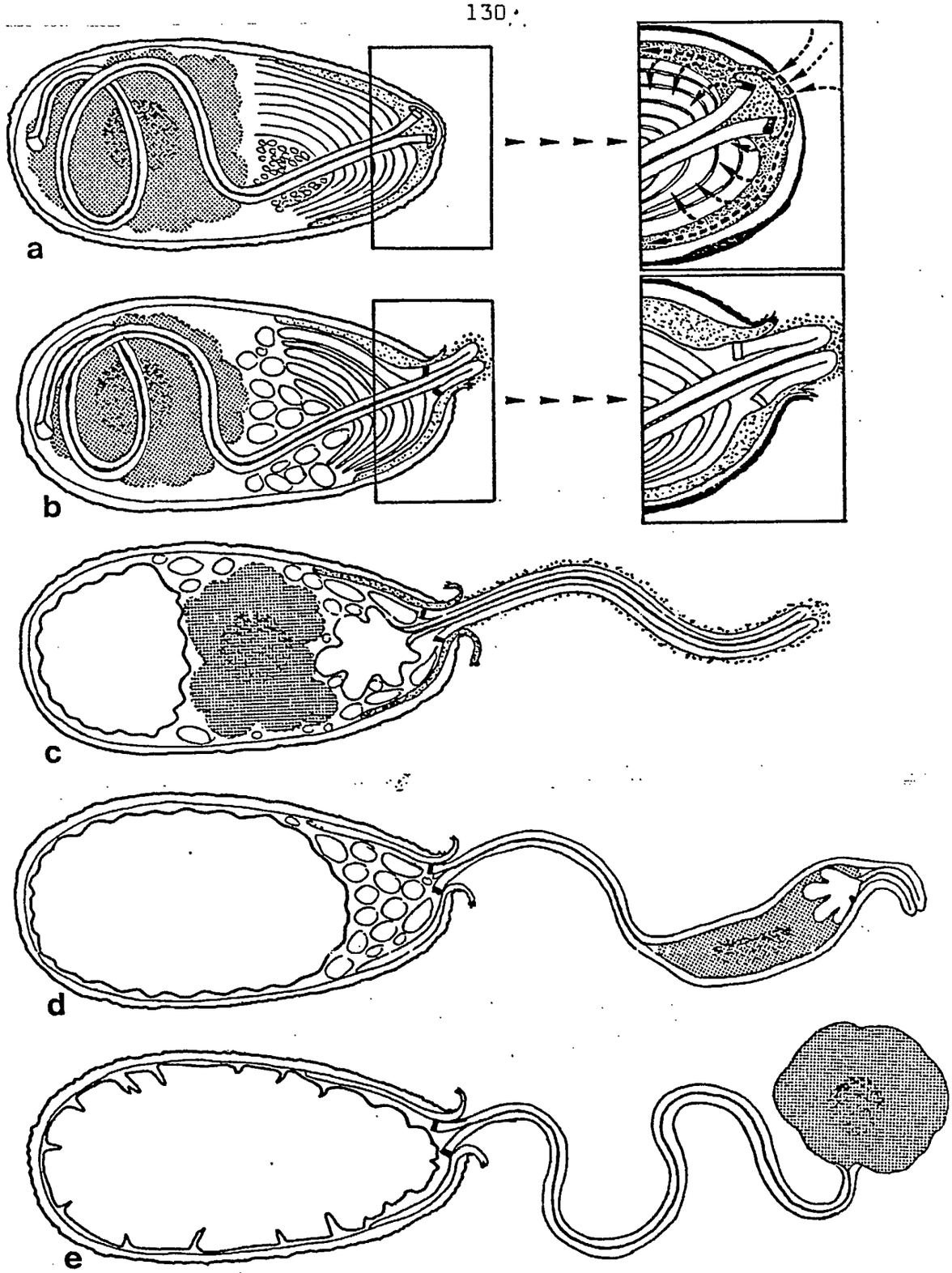

Fig. 28. Theory Relating to Extrusion of the Filament

a - Weakening of the apex results in massive penetration with water.
b - The polaroplasts swell and increase internal pressure. The wall rips.
c - The filament is rapidly extruded by eversion.
d - The sporoplasm passes through the filament. A vacuole enlarges in the spore.
e - The sporoplasm makes its way to a pouch at the end of the filament.

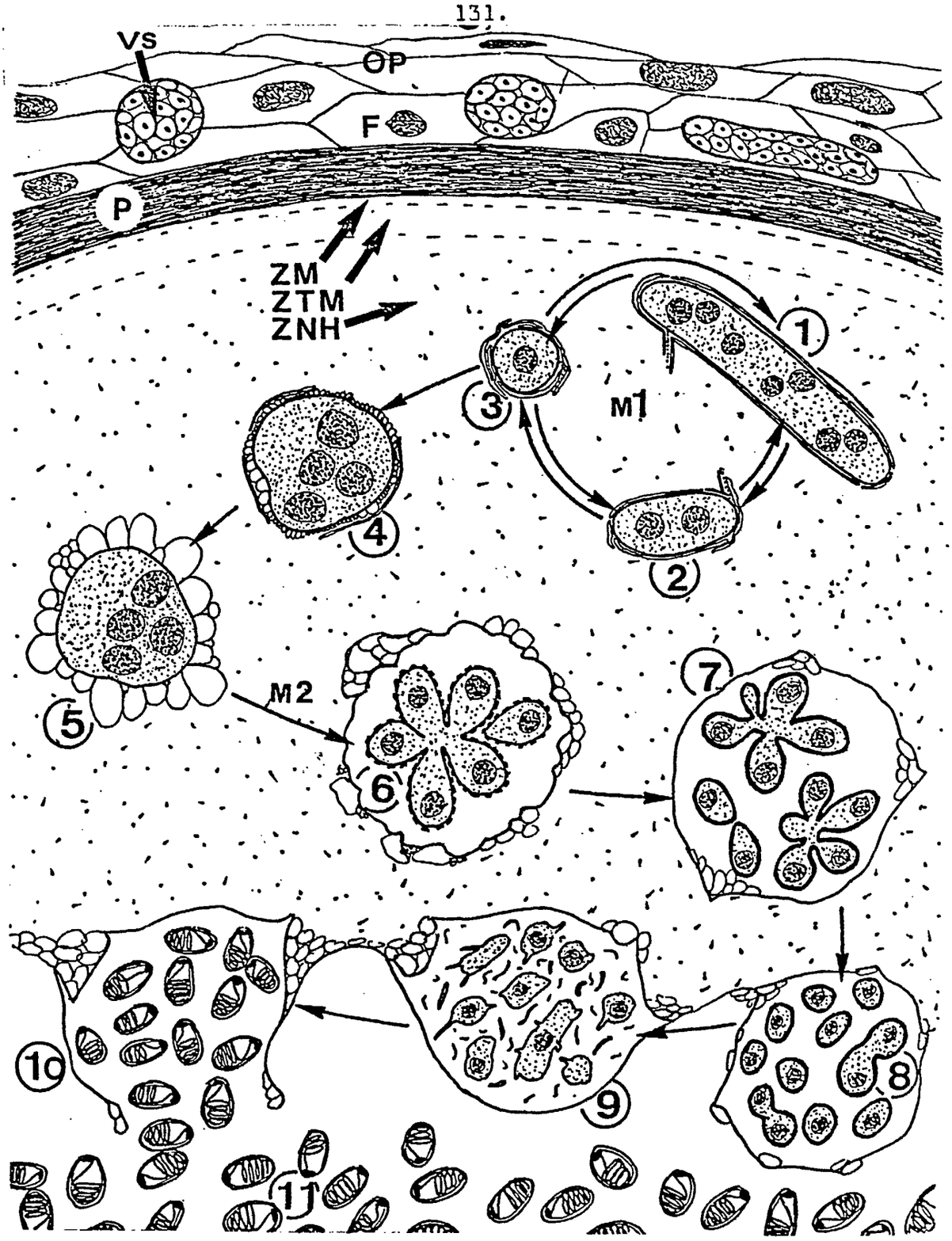

Fig. 29. Life Cycle of Glugea atherini

1. Cylindrical vegetative plasmodium. 2. Intermediate stage. 3. Uninucleate meront. 4. Non-cylindrical plasmodium in the early stages of isolation. 5. Isolation is almost completed. 6. Plasmodium division. Onset of envelope thickening. 7. Thickened envelope. 8. Sporonts. 9. Sporoblasts. 10. Spores. 11. Spores released from the vacuole in the center of the xenoma.

F = fibrocyte. M1 = first-type merogony. M2 = second-type merogony. OP = peripheral organization. P = xenoma wall. VS = host blood vessel. ZM = zone with microtubules. ZNH = zone with host nuclei. ZTM = zone with microtubules and mitochondria.

4/ Histochemistry

a) Introduction and Background

Certain staining techniques made it possible to study tissue carbohydrates, proteins and lipids.

Authors delving into microsporidian histochemistry have concentrated on the chemical changes occurring in the different parasitic stages at the time of structural changes. The following genera have been studied in this context: Thelohania, Pleistophora, Stempellia, Nosema and Glugea. Whereas these studies have dealt with various parasitic stages, we decided to look into the chemical make-up of the different areas comprising Glugea-induced cysts. It should be mentioned that it is only recently that research has been conducted on the histochemical nature of parasitic stages. The chitinous make-up of the spore case, however, was demonstrated by Dissanaike and Canning in 1957 and Vavra (1959) provided evidence of a positive PAS granule in the anterior spore. He referred to it as the polar cap. This structure was later considered the same as the basal disk. Recent studies have shown the chemical characteristics of pre-spore stages (Maurand and Bouix, 1969; Maurand and Loubès, 1973; Bouix, Maurand and Loubès, 1974; Vivarès, Loubès and Bouix, 1976). These authors reached the following conclusions:

- There are mucosubstances in and around developing sporoblasts. In the case of Thelohania maenadis, these substances differ, depending on whether they occur inside or outside the sporoblast. Intrasporoblast glucides are essentially acid and related to sulfomucins, whereas granules and other matter outside the sporoblast do not contain sulfur (Vivarès, Loubès and Bouix, 1976).

- The protein matter which the spore case acquires in the course of sporogenesis is no longer detected once the spore attains

maturity. It may well be that is masked by chitin toward the end of development as a result of molecular combination (Vavra, 1967).

- Carbohydrate and lipid reserves were not detected during sporogenesis.

b) Study of the Atherine-Infesting Microsporidian

1) Host-derived components. We considered that the numerous complex areas which were described in our section on milky xenomas of the body cavity warranted histochemical analysis. Of the wide range of methods available, we selected the following:

- general topographic stain: Heidenhain's azan stain
- standard stains for carbohydrates: PAS, alcian blue, metachromatic reaction
- standard stains for proteins: Schiff's alloxan stain, the reactions of Danielli, Barnett-Seligman, Martig-Zacharias and Chevremont-Frederic.

General appearance. Heidenhain's azan stain coloured the cyst wall dark blue, demonstrating its carbohydrate origin. Fibers, stained the same colour, extended from the wall among the fibrocytes in the peripheral organization. Tiny blue granules were also observed in the underlying host cytoplasm which embraces the zone with tubules, the zone with mitochondria and tubules and the zone containing giant nuclei. These three areas were hard to distinguish under the optical microscope.

Merogonic stages occasionally stained orange-yellow like typical cytoplasm.

Small pockets of host cytoplasm among the spores displayed

the same characteristics in the middle. These pockets consist of carbohydrate-rich host cytoplasm. Giant nuclei were clearly visible and were of two types which, however, could not be distinguished under the electron microscope. Some of these nuclei stained purplish blue, whereas others were bright red, more compact and almost spherical in shape. The periphery of the pockets gave the same dye reaction as the alveolar zone. In these areas, the host cytoplasm stained differently. It appeared more purplish, demonstrating either the presence of numerous temporary parasitic stages -- generally stained orange or red -- or the presence of various secretions.

In the alveoli, sporulation stages stained light blue to orange in the case of sporoblasts and red, in the case of spores.

Results. Stains for demonstrating carbohydrates generally produced positive results in the host-derived components of the xenoma. Staining for proteins, on the other hand, generally yielded negative results, although Danielli's tetra-azoreaction was positive. Brown granules were seen in the host cytoplasm near the wall and in the cytoplasmic pockets in the center. Proteins were more concentrated in the area next to the cyst wall, which undoubtedly corresponds to the zones with tubules and mitochondria.

Our findings in the host-derived components of the xenoma are summarized in the following table.

		Paroi du xénome xenoma wall	Cytoplasme hôte host cytoplasm	Cytoplasme des îlots cytoplasmic pockets
Glucides Carbohydrates	APS	+++	++	++
	Bleu Alcian pH 2,1 alcian blue	+++	++	++
	Métachromasie pH ',2 metachromasia	-	-	-
Protides Proteins	Alloxane Schiff	-	-	-
	Danielli	-	+	+
	Barnett-Seligman	-	-	-
	Martig-Zacharias	-	-	-
	Chevremont-Frederic	-	-	-
Azan de H. H's azan		Bleu blue	ponctuations bleues blue specks	ponctuations bleues blue specks

Interpretation. These findings indicate that the parasitic stages are surrounded by carbohydrate substances in the host cytoplasm and especially in the xenoma wall which sends fibers into the peripheral organization. The presence of collagen-like carbohydrates (positive PAS reaction, negative metachromatic reaction) in these two structures indicates that they are closely related. The relationship may be trophic, with substances passing from one zone to the other, or else, structural due to the development of these two areas. At this stage, it is not possible to say which of these hypotheses is the more likely. It was interesting to note that the composition of the host cytoplasm was essentially the same in the central pockets. Cytoplasmic carbohydrates undoubtedly play a role in the development of the parasite, at least during merogony. The pockets also contained aggregates that gave a positive PAS reaction but stained little or not at all with alcian blue. These substances were not visible in the peripheral host cytoplasm or at least, did not occur in concentrated form. They were thought to be strongly acid sulfur-containing mucosubstances (which Vivarès et al., 1976 described within the sporoblast). There was very little protein matter in the host component of the xenoma. No real explanation can be offered for the high concentration of proteins with a positive reaction to Danielli's tetra-azoreaction along the edge of the xenoma wall. It may be that protein matter concentrates in that area before it is dispersed in the cytoplasm. Also, tubules, which were observed in large numbers under the electron microscope, may be responsible for the phenomenon since this type of structure is generally thought to play a role in trophic exchange. Since intestinal xenomas were generally in the last stage of development, only the walls could be studied. They were found to be

in all respects like the walls of body cavity xenomas.

2) Parasite components.

General appearance: Heidenhain's azan stain demonstrated changes in the parasite cytoplasm during the course of its development.

Only in merogonic stages did the cytoplasm display a typical yellow colour. Early sporulation stages in the alveoli often appeared light blue which may be indicative of acid mucopolysaccharides. As the spore reached maturity, it turned orange, then red, revealing a predominance of protein matter. It should be mentioned that these advanced stages did not have any carbohydrate reserves. The same findings were recorded by Vivarès et al; (1976) who, in addition, did not find any stores of lipid material.

Results. Our findings are comparable to those recorded by the abovementioned authors who mainly studied the various stages of sporogenesis. The following table summarizes our staining results in the parasite component of the xenoma.

	Mérogonie Merogony	Sporontes Sporoblastes sporonts sporobasts	Spores jeunes young spores	Spores mûres mature spores
Azan de H H's azan	jaune yellow	bleu clair light blue	orange	rouge red
A.P.S.	-	-	+	+
Bleu alcian alcian blue	-	-	++	-
Métachromasie metachromasia	-	-	++	-
Alloxane Schiff	-	-	+	+
Danielli	-	±	+	+
Barnet-Seligman	-	±	±	-
Martig-Zacharias	-	-	-	-
Chevremont-Frederic	-	-	-	-

. In cylindrical and non-cylindrical merogonic stages, the cytoplasm stained yellow with Heidenhain's azan. This was the only instance in which a typical cytoplasm reaction was recorded. None of the other tests seemed positive.

. Star-shaped stages occurred in the sporogony vacuole and probably corresponded to individual sporont formation and emergence of the sporoblasts. These stages stained blue with azan, indicative of the presence of acid mucopolysaccharides. None of the structures in sporont or sporoblast stages reacted positively to the PAS test or alcian blue. There is no explanation for the lack of response of these stages to most of the histochemical tests.

. Interesting results were recorded in spores. They turned from orange to red with the azan stain during maturation. In young stages, an abundant positive PAS reaction was recorded in the periphery and occasionally in certain scattered areas, whereas in the mature spore, this reaction was observed in the polar cap.

A round posterior area, undoubtedly related to filament coils, was stained with alcian blue. The transformation of young spores into adult forms was not observed.

In young spores, one or more aggregates turned red as a result of metachromasia, whereas no reaction was observed in adult forms.

Schiff's alloxan stain demonstrated scattered granules in young spores. These granules clumped together into a single mass which often appeared posteriorly in adult spores. All the spores reacted positively to Danielli's stain which diffused throughout the cytoplasm from a central position.

The staining methods of Barnet-Seligman, Martig-Zacharias, Chevremont-Frederic never yielded positive results, undoubtedly for methodological reasons.

Interpretation. Heidenhain's azan stain showed that, in general, sporogenesis was attended by a shift from carbohydrate to protein matter in the spore cytoplasm. Concentrations of polysaccharides without any acid groups were found in the polar cap with the PAS test, whereas only scattered polysaccharides occurred in young spores. The alcian blue test showed that acid polysaccharides rich in electronegative groups remained at the periphery of the spore in the area with filament coils. Metachromasia demonstrated the disappearance or, at least, the transformation of carbohydrates with basophilic groups during maturation of the spore. Proteins with primary amino groups, which could be detected with Schiff's alloxan method, became concentrated and more abundant in the central-posterior area when the spore matured. Danielli's tetra-azoreaction revealed that, in general, there was abundant protein material in the spore cytoplasm.

Our conclusions are comparable to those reported by the authors we have already mentioned. The spore seems designed for resistance once it has reached the end of development. No lipid or carbohydrate reserves were observed but the abundant protein material encountered is undoubtedly structural in nature and takes part in forming the various organelles needed for extrusion and penetration of the host.

5/ Taxonomic Position

Analogies between the atherine-infesting microsporidian and one of the best studied Glugea species (Sprague and Vernick, 1968) plus the following points favour the inclusion of the microsporidian in the genus Glugea:

+ typical encystment referred to as Glugea xenoma
+ no diplokaryon
+ no pansporoblast but the presence of a sporogony vacuole
+ each sporont seems to produce two sporoblasts.

It is necessary at this stage to compare this microsporidian with the other Glugea species infesting fish. So far over 25 species have been described but for the most part the criteria for determination have been poorly defined.

a) Seven species are virtually undescribed and there are practically no means of distinguishing them, i.e.:

Species	Authors	Typical Host
Glugea caulleryi	Van den Berghe, 1940	Amnodytes lanceolatus
G. sp.	Bogdanova, 1961	Abramis ballerus
G. pseudotumefaciens	Pflugfelder, 1952	Brachydanio rerio
G. gasterostei	Voronin, 1974	Gasterosteus aculeatus
G. sp.	Pfeiffer, 1895	Leuciscus phoxinus
G. sp.	Sano, 1970	Plecoglossus altiverius
G. tisae	(Lom and Weiser, 1959)	Silurus glanis

b) Eight species have definitely smaller spores ($< 4\ \mu m$ long), i.e.:

G. acerinae	Jirovec, 1930	Acerina cernua
G. bychowskyi	Gasimagomedov-Issi, 1970	Alosa kessleri
G. cordis	Thelohan, 1895	Alosa sardina
G. destruens	Thelohan, 1891	Callionymus lyra
G. luciopercae	Dogiel-Bychowsky, 1939	Lucioperca lucioperca
G. machari	(Jirovec, 1934)	Dentrex vulgaris
G. anomala	(Moniez, 1887)	Gasterosteus aculeatus
G. shulmani	Gasimagomedov-Issi, 1970	Neogobius caspius

c) In one species, the spores are just as long, but much narrower:

G. depressa	Thelohan, 1895	Julis vulgaris

d) In two species, the spores are definitely larger, i.e.:

G. cotti	(Chatton-Courrier, 1923)	Cottus bubalis
F. fennica	(Lom-Weiser, 1959)	Silurus glanis

e) Although five species have been inadequately described, they have certain characteristics that distinguish them from the atherine-infesting microsporidian, i.e.:

G. puctifera	Theolohan, 1895	Gadus pollachius
G. acuta	Thelohan, 1895	Syngnathus acus
G. branchiale	(Nemeczek, 1911)	Gadus aeglefinus
G. dogieli	Gasimagomedov-Issi, 1970	Lucioperca lucioperca
G. intestinalis	Chen, 1956	Mylopharyngodon piceus

In G. punctifera, the spore is slightly smaller and only infests the eyes of the host. G. acuta parasitizes only the muscles, whereas G. branchiale is found in gill filaments. The sporonts of this species form chains and the xenomas are always under 1 mm. G. dogieli spores are slightly smaller and the cysts are always under

250 µm. G. intestinalis occurs in the intestinal mucosa.

f) Four species have been carefully described but differ from the atherine-infesting microsporidian.

G. weissenbergi	Sprague and Vernick 1968	Apeltes quadracus
G. stephani	(Hagenmüller, 1899)	Pleuronectes plastessa
G. berglax	Lom and Laird, 1976)	Macrourus berglax
G. hertwigii	Weissenberg, 1911	Osmerus eperlanus

Glugea weissenbergi Sprague and Vernick, 1968, has characteristics that have never been observed in the atherine-infesting Glugea, i.e., a stage with a double nucleus, foreshadowing sexual reproduction, and a sporont producing two sporoblasts that remain joined during formation of the two spores. Lastly, this species has been described only in the United States (Maryland). From its cycle, as observed under the electron microscope, however, it is clear that it is a related species. G. stephani (Hagenmüller, 1899) has been described a number of times. The spores are often smaller, occasionally like those of the atherine-infesting Glugea. It is found specifically in flat fish. G. berglax Lom and Laird, 1976, infests the digestive tract muscle, behaviour which was never observed with the species under study. G. hertwigii Weissenberg, 1911, infects primarily the digestive tube. It may spread to other organs, but these are solely secondary sites. It causes or contributes to a very high rate of mortality. Its cycle has been only partially described.

In conclusion, there are three types of criteria in classifying fish-infesting microsporidian species, i.e., parasitic behaviour, spore structure and life cycle. These three areas are rarely exa-

mined, with the result that most species are characterized by one or two inconclusive criteria. The host infested is often considered an adequate criterion despite the lack of any reasearch into specificity.

In view of the situation and because of the specific distinctions described above, the atherine-infesting microsporidian should be considered a separate species. It will be referred to as Glugea atherini n. sp. and will be described in detail in a later study.

CHAPTER THREE

GEOGRAPHIC DISTRIBUTION

III - GEOGRAPHIC DISTRIBUTION

A - Range of Microsporidiosis

Figures 1, 2 and 4 show the different sites where fish specimens were collected. These sites are located along the French Mediterranean coast (Roussillon , Languedoc and Provence), on the Atlantic seaboard (Arcachon basin), on the eastern coast of Corsica, and lastly, in northern Tunisia.

Three atherine species were studied, but only Atherina boyeri harboured the microsporidian.

Atherina hepsetus was caught in the Thau basin and the Etang d'Urbino in Corsica.

Atherina presbyter was collected in the Arcachon basin and near Port-Vendres in Roussillon.

Close to 80 lots of Atherina boyeri were collected in France, Corsica included, and Tunisia. The percentage of infestation depended on the site and time of year. A study of seasonal changes in infestation in the Etang de Mauguio will be discussed later.

Date of catch	Catch number	Site	Number of fish dissected	% infestation
19/11/1976	26	Etang de Bages	90	0
9/11/1976	22	Thau basin	7	0
9/12/1976	33	Etang de Moures	100	3
26/11/1976	31	Etang de Mauguio	80	7.5
26/11/1976	30	Rhône de Saint-Roman	100	16

Table No. 12. Percentage of Infestation in a Few Sites in November and December 1976.

Table 12 gives the rate of infestation at a given time of year, i.e., November and December 1976, in a few areas along the French coast. The Mauguio region seems to be the focus of microsporidian infestation. It gradually decreases to the west until it disappears altogether west of the Thau basin. The Etang de Moures may be considered an intermediate region.

Having described the situation in broad outline, we shall now assign each lagoon to one of the following groups on the basis of mean rate of infestation:

Group 1 = 0% infestation

Group 2 = 0% to 5% infestation

Group 3 = 5% to 10% infestation

Group 4 = over 10% infestation.

Etang de Canet: 1976; October = 0% (100 specimens)
group 1

Etang de Bages: 1976; November = 0% (90 specimens)
group 1

Thau basin: 1976; October = 0% (147 specimens); November = 0% (7 specimens)

1977; January = 0% (41 specimens)
group 1

Canal du Rhône à Sète, opposite Frontignan-La Peyrade: 1976; October = 0% (100 specimens)
1977; January = 0% (19 specimens); September = 0% 42 specimens
group 1

Etang de Vic: 1977; January = 2% (54 specimens)
group 2

Etang de Moures: 1976; October = 0% (19 specimens); December = 3% (100 specimens)
1977; March = 2% (50 specimens)
average rate of infestation = 2.5%
group 2

Etang du Prévost: 1976; December = 1.5% (79 specimens)
group 2

Etang du Grec: 1976; October = 13.5% (15 specimens)
1977; March = 4.5% (43 specimens)
Average rate of infestation = 7%
group 3

Etang de Mauguio: 1976; September = 12.25% (29 specimens); October = 7.25% (138 specimens); November = 7.5% (80 specimens); December = 5% (80 specimens)
1977; January = 10.5% (95 specimens); February = 9% (100 specimens); March = 7.5% (82 specimens); April = 5% (100 specimens); June = 0% (81 specimens); August = 2% (200 specimens); September = 3.5% (200 specimens); October = 3.5% (200 specimens); November = 2% (100 specimens); December = 2.25% (90 specimens).
1978; January = 5% (100 specimens); February = 10% (100 specimens); March = 5.5% (18 specimens).
Average rate of infestation = 5.1%
In view of maximum levels of infestation, the Etang de Mauguio was assigned to group 3.

Channel joining the Etang de Mauguio to the Mediterranean, opposite Carnon: 1976; September = 7.5% (77 specimens); November = 6% (16 specimens)
1977; September = 2% (53 specimens); October = 7.5% (40 specimens)
Average rate of infestation = 6%
group 3

Canal du Rhône à Sète, opposite the Etang de Mauguio: 1976; September = 7.7% (104 specimens)
1977; February = 2.5% (88 specimens)
Average rate of infestation = 5.2%
group 3

Rhône de Saint Roman (or Rhône Mort): 1976; November = 13% (200 specimens); December = 0% (17 specimens)
1977; January = 7% (100 specimens); September = 16.5% (6 specimens); November = 16.5% (55 specimens)
group 4

Etang du Vaccarès: 1977; January = 0% (69 specimens)
group 1

Etang de Berre: 1977; May = 2% (100 specimens)
group 2

Etang de l'Olivier: 1977; May = 21% (100 specimens)
group 4

Etang d'Urbino: 1977; July = 0% (13 specimens)
group 1

Etang de Tunis: 1977; December = 0% (100 specimens)
group 1

These various bodies of water are diagrammatically represented in Fig. 30 which also indicates the gradual decrease in infestation on either side of the Etang de Mauguio, culminating in the total absence of microsporiosis in the Thau basin.

Two areas were not completely explored, i.e., the lagoons in the Petite Camargue (between the Grande Roubine and the Petit Rhône) and the Camargue lagoons in the Rhône delta.

There were certain exceptions to the general pattern, i.e, there were no signs of infestation in the Etang du Vaccarès, whereas the

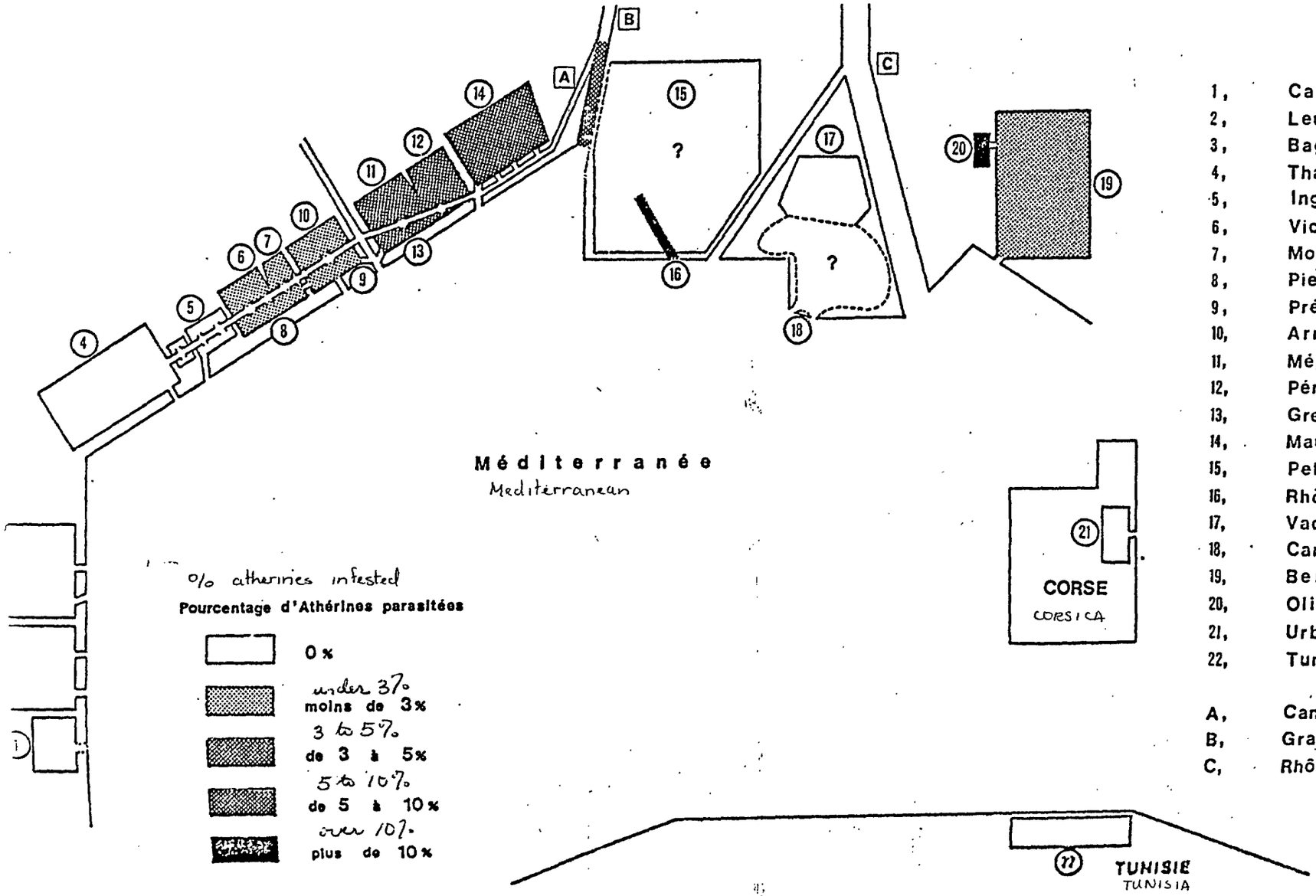

1, Canet
2, Leucate
3, Bages
4, Thau
5, Ingril
6, Vic
7, Moures
8, Pierre Blanche
9, Prévost
10, Arnel
11, Méjean
12, Pérols
13, Grec
14, Mauguio
15, Petite Camargue
16, Rhône Mort
17, Vaccarès
18, Camargue
19, Berre
20, Olivier
21, Urbino
22, Tunis

A, Canal du Rhône à Sète
B, Grande Roubine
C, Rhône

FIG.30 Répartition géographique et intensité de la microsporidiose

Range and Intensity of Microsporidian Infestation

rate of infestation was very high in the Rhône de Saint-Roman and the Etang de l'Olivier. Substantial variations in the rate of infestation occurred over the year, especially in the Etang de Mauguio, the most closely followed of the various sites, which was examined over a period of almost two years.

These peculiarities along with some very general ideas have enabled us to develop various hypotheses to explain the current state of microsporidiosis in atherines.

B - Explanations for the Geographic Range

Hypothesis One: The geographic range is due to the existence of physiological differences between two populations. If this should prove the case, the differences may be immunological (the natural defense mechanisms may be more or less effective, depending on the population) or else, physiological (the presence or absence of certain enzymes, higher or lower levels of one of the components of the blood, etc...). These factors may promote or inhibit parasite development.

In order to test our hypothesis, we selected two experimental approaches, i.e. 1) an electrophoretic study of certain enzymes was conducted to determine whether physiological differences existed between areas with and without microsporidian disease and 2) fish from disease-free areas were infested experimentally.

a) Enzymology of Atherina boyeri

Description of the enzymes studied. Eleven classes of enzymes were analyzed following electrophoretic separation in a starch gel in accordance with the method of Moretti et al (1957).

With electrophoretic techniques, enzyme and non-enzyme proteins can be separated on the basis of their electrical charge. A protein's rate of migration is determined primarily by its amino acid composition. Since every polypeptide chain is coded by a gene in the DNA molecule, some mutations may result in one amino acid being replaced by another with a different electrical charge. The new protein consequently displays different electrophoretic mobility. This means that whenever a change in the rate of migration is recorded, the gene coding for that protein has undergone some kind of mutation. On the basis of electrophoretic analysis, it is therefore possible to compare the genetic structure of populations and to determine whether the structure varies with environmental conditions. Following electrophoresis, the enzymes are identified by histochemical techniques. The methods used were described by Davidian-Britton (1978). Enzymes revealed by the same staining procedure are termed isoenzymes, i.e., proteins with the same enzyme structure but different mobility. Some of the isoenzymes are coded by different genes, others by alleles of the same gene. In the latter instance, the term allozyme is used.

A partial enzyme chart was established for Atherina boyeri following analysis of liver, caudal muscle, kidney and ovary extracts. The best results were obtained with liver and muscle extracts. The kidneys proved too small for a satisfactory demonstration of enzyme content. Most of the systems we studied could not be identified in the ovary outside of periods of reproduction, probably due to slackened activity.

Enzymology of the liver.

(a) Esterases. Five fractions were identified and are very likely coded by different genes (Plate XXII, 105).

- Esterase zero (ES-0) was the fastest moving fraction. It is inhibited by eserine and is consequently a cholinesterase compound. This enzyme is only faintly active and seemed identical in all the specimens examined. The gene coding it is therefore monomorphic.

- Esterase 1 (ES-1L) was also found in all the specimens we examined. In one case, two spots, i.e., ES-1F^{100} and ES-1F^{80}, were recorded. In all of the other specimens, only ES11F^{100}, the faster moving of the two, was found. This pattern is typical of genes with two codominant alleles.

- Esterase 2 (ES-2) produces 4 spots which are undoubtedly coded by the alleles of a single gene. (There were never more than two spots per fish). In some fish (homozygotes for the alleles coding this allozyme), only one spot was recorded, whereas in others (heterozygotes), there were two.

-Esterase 4 (ES-4) occurred in some individuals in the form of a spot with the same mobility. It was completely absent in others, probably due to the existence of an allele coding an enzyme that was no longer active, at least under experimental conditions.

- Esterase 5 (ES-5) was the slowest moving fraction encountered. It was very difficult to identify and as a result, could not be studied in detail.

(b) Glutamic-oxalacetic transaminases (GOTs). In most animals there are two GOT-coding genes: one codes an enzyme that is present only in the cytoplasm; the other, an enzyme in the mitochondria. Atherina boyeri constitutes a very special case in that it has 4 systems coded by 4 different genes. At least two of them are polymorphic for two alleles, i.e., GOT-1, the fastest moving with GOT-1^{100}, GOT-1^{110} and GOT-1^{120}. (These are dimeric enzymes; heterozygotes have 3 bands and homozygotes only 1) and GOT-3 with alleles GOT-3^{100} and GOT-3^{127}. GOT-2 also seems polymorphic, but it was difficult to study it in detail because the spot was close to the edge of the gel. GOT-4 exhibited a pattern of negative migration which was identical in all the samples studied.

The highly specific structure of the GOT compounds in atherines may find its origin in gene duplication which is a very common occurrence in fish.

(c) 6-phosphogluconate dehydrogenase (6-PGD) is also coded by a gene which is probably polymorphic. It could not be properly studied since only 10 samples were analyzed.

(d) Sorbitol dehydrogenase (SDH) was only faintly active but two spots were detected: one migrated positively, whereas the other, very slow, showed negative mobility.

(e) α-glycerophosphate dehydrogenase (αGPD) produced only a single spot which was remarkably constant in all the samples.

(f) malate dehydrogenase compounds (MDH). Eucaryotes typically contain two MDH-coding genes: one codes a cytoplasmic enzyme and the other, a mitochondrial enzyme. In A. boyeri, however, only a single enzyme was detected in every case.

(g) Isocitrate dehydrogenase (IDH). A single enzyme (IDH-IL) was identified. It was present in all the fish analyzed and exhibited the same electrophoretic mobility (monomorphic gene).

(h) Lactic dehydrogenases (LDH_s) are tetrameric molecules that in vertebrates are coded by two genes. One produces type A polypeptide chains, whereas the other produces type B chains. In general, the chains combine at random which may produce electrophoretic patterns with 5 bands (AAAA, AAAB, AABB, ABBB and BBBB). In certain cases asymmetrical molecules (AAAB and ABBB) are not viable (this is the case in certain reptiles -- Guillaume et al., 1976). In A. boyeri only two spots appeared. In this case, it may be that the pure AAAA and BBBB molecules are active. Both LDH-A and LDH-B genes are monomorphic.

Enzymology of the caudal muscle

Some of the enzymes encountered in the liver were also detected in the caudal muscle, i.e., GOT's, ADH, 6-PGD, MDH's and LDH's. Some, on the other hand, were different.

(a) Esterases. Two systems were detected: ES-1M with more rapid migration than ES-0 and ES-2M, which seems to be the same as ES-2 in the liver.

(b) SDH. There was only one fraction which was identical to the faster of the two fractions found in the liver.

(c) IDH. There was only one system . and it was identical in all the fish. It was definitely less mobile than the liver enzyme. Animals have two IDH fractions -- one in the cytoplasm, the other in the mitochondria and their activity differs with the organ in which they occur. In the kidney, both enzymes exhibit the same degree of activity. Elsewhere, in the muscle, for instance, one of them is virtually without activity, whereas in the liver, the other is inactive. Muscle IDH is therefore coded by a different gene (IDH-2M) from liver IDH (IDH-1).

In conclusion, of the 17 genes studied, 9 proved polymorphic, i.e., ES-1L, ES-2, ES-5, GOT-1, GOT-2, GOT-3, 6-PGD, SDH, LDH) and 8, monomorphic, i.e., ES-0, ES-4, GOT-4, α-GPD, MDH, IDH-1L, IDH-1M, IDH-2M).

Fish caught at three different sites were analyzed. The first site was on the Canal du Rhône à Sète near the Thau basin, opposite La Peyrade. No atherines with microsporidiosis have ever been caught in this area which we shall refer to as zone A. The second site was the Etang de Mauguio which is characterized by sudden variations in the rate of infestation due to the open configuration of the lagoon which promotes shifts in population. This area, which is open to parasitic infestation, was labelled zone B and the Rhône de Saint-Roman, zone C. The latter is characterized by its isolation from the sea and other lagoons, resulting in a very high rate of infestation. Findings from these three sites indicated first of all that the sampling from zone C was too small for a valid comparison. Consequently, only the first two areas will be

compared.

Differences were recorded between the two sites. None of the specimens collected in zone A had any of the following alleles: ES-1^{80}, GOT-1^{100}, ADH^{100}. Specimens from zone B, on the other hand, generally more richly endowed with these alleles, lacked ES-5^{80}. These findings undoubtedly have some basis in reality, but our sampling was too small to conclude that these alleles were totally absent. It is certain they are uncommon.

A comparison of the number of times different spots were recorded in samples from fish caught in the two sites proved of interest. The frequency of four enzymes was calculated.

Enzyme étudiée Enzyme studied	Phénotypes	Zone A	Zone B	Zone C	Totaux Total
Estérase 2	AA	2	2	0	4
	BB	0	1	0	1
	CC	0	0	0	0
	DD	0	3	1	4
	AB	0	0	0	0
	AC	0	5	0	5
	AD	3	2	0	5
	BC	1	0	0	1
	BD	4	1	1	6
	CD	0	2	0	2
Estérase 4	actif active	6	11	0	
	absent absent	5	5	3	
G.O.T.-1	AA = 120	0	0	0	
	BB = 100	8	12	1	
	AB = 120-100	0	4	2	
G.O.T.-3	AA = 127	0	2	0	
	BB = 100	8	11	1	
	AB = 127-100	0	3	2	

Table No. 13. Frequency of Phenotypes of Four Enzymes Studied in Three Areas.

1. Esterase 2 has four bands which, in order of rate of migration, have been labelled A, B, C and D. Theoretically, the 28 specimens analyzed could have produced a maximum of 56 spots (1 or 2 per specimen) corresponding to the two parental half chromosomes. A single spot represented a homozygote with twice the same allele. The frequency of each of these alleles was calculated.

Allele A = 18/56 = 0.32 = a
Allele B = 9/56 = 0.16 = b
Allele C = 8/56 = 0.14 = c
Allele D = 21/56 = 0.37 = d.

the total is equal to 0.99

Our first problem was to determine if the alleles were coded by the same gene. Hardy-Weinberg's law states that when a single gene has several alleles, such as A and B, with a frequency of a and b, the theoretical frequency of phenotype AA is equal to a^2, of AB equal to 2 ab and of BB, equal to b^2. When applied to our example, the law yielded the following results.

For AA (single spot, allele A), the theoretical frequency was equal to a^2, i.e., 0.32^2. Since 28 fish were analyzed, the product of the theoretical frequency times 28 yielded the theoretical number of fish, if the alleles under consideration were coded by the same gene. On the basis of these calculations, we obtained the following results:

Phénotype	Fréquence théorique = F Theoretical frequency = F	nombre théorique de poissons (F x 28) Theoretical number of fish (F × 28)	nombre réel de poissons Actual number of fish
AA	0,102	2,87	4
BB	0,026	0,72	1
CC	0,020	0,55	0
DD	0,137	3,83	4
AB	0,102	2,87	0
AC	0,090	2,51	5
AD	0,237	6,63	5
BC	0,045	1,25	1
BD	0,118	3,35	6
CD	0,104	2,90	2

With the exception of phenotypes AB and AC which presented anomalous behaviour undoubtedly because of the small sampling, it could be concluded that we were dealing with a single polymorphic gene with four alleles. Once this was established, the frequency of the four alleles in sites A and B could be compared. Table 13 shows the frequency of the various phenotypes. Phenotype AA corresponded to two A alleles, phenotype AB to allele A plus allele B. On this basis, the incidence of the various alleles could be established as follows:

Alleles	Zone A (a)	Zone B (b)	Total (t)
A(1)	7	11	18
B(2)	5	3	8
C(3)	1	7	8
D(4)	7	11	18
Total (n)	20	32	52 (N)

With the χ test, it is possible to determine whether the differences between the two sites are significant. The most practical equation is the following:

$$\chi^2 = N \left[\frac{1}{t1} \sum \frac{ai}{ni} + \frac{1}{t2} \sum \frac{bi}{ni} + \ldots \right]$$ (after Maxwell, 1961)

with, by way of example: $\frac{1}{t1} \sum \frac{ai}{ni} = \frac{1}{18} \left(\frac{7}{20} + \frac{11}{32} \right) = 0.0385$

Since the number of degrees of freedom is equal to 3 (number of sites minus 1, multiplied by the number of alleles minus 1), χ^2 must be greater than 7.82. Since our calculations yielded 7.977,

the test was considered significant at the 95% probability lavel.

2. Esterase 4. As the chromosomal significance of the presence or absence of this esterase was not known, we deemed it preferable to consider the phenotypes. The X^2 test was applied, using the following equation:

$$\chi^2 = \frac{N\left[|ad-bc| - 0.5\,N\right]^2}{(a+b)(c+d)(a+c)(b+d)}$$ (after Maxwell, 1961)

3. GOT-1. The incidence of alleles 100 and 120 was tested. It was found that the differences were not significant.

4. GOT-3. When the incidence of alleles 100 and 127 was tested, it was found, once again, that the differences were not significant.

All of these results, in particular those recorded with esterase-2, indicated distinct differences between the two sites in the relative proportion of alleles of the same gene. This suggests partial genetic isolation of different atherine populations, which agrees with the observations of Kiener and Spillmann who recorded an average of 23.8 gill rakers per fish in specimens from the Etang de Mauguio as opposed to 34.8 gill rakers per fish in atherines from the Thau basin. Individuals from the Etang de Mauguio had 43 to 45 vertebrae (average: 44.8), whereas in the Thau basin, the number ranged from 45 to 47 (average: 45.7).

These findings support our hypothesis that certain atherine populations became genetically,isolated, but is it adequate to explain why one of them never developed microsporidian-induced disease?

In order to find an answer to this question, specimens were infested experimentally.

b) Experimental Infestation

Experimental infestation was successful in three cases. The chief difficulty encountered consisted of maintaining the atherines under artificial conditions for a sufficient period of time. Details of our experiments will be described in the section on contamination of the host. From Table 15, it may be seen that spores from infested fish from the Etang de Mauguio were capable of producing xenomas in the body cavities of fish collected in the parasite-free site. Since this clearly demolished the hypothesis that physiological incompatibility prevented infestation of one of the populations, we had to look elsewhere for an explanation.

Hypothesis Two: The spores are present in all the lagoons, but in certain areas cannot undergo normal development because of the physicochemical conditions of the environment. Since it was possible to induce infestation by preserving the saline and temperature levels encountered at the time the specimens were collected, it was clear that the conditions existing locally were favourable to the emergence of microsporidiosis at that site. It may be then assumed that the general regime of the water in that area was incompatible with development of the parasite. As there is evidence to suggest that the free phase of the cycle is the most susceptible to outside influences, the spores may become less virulent after they have been in the water. It may also be hypothesized that an intermediate host considerably favours contamination of the atherine population and that in parasite-free zones, the intermediary is absent or displays different behaviour. Infestation was achieved without any intermediary, simply by injecting the spores orally,

Site	Incidence of isopod	Rate of microsporidian infestation
Canet-Bages	+	0%
Thau and environs	+++	0%
Vic-Moures-Prévost	exceptional	1.5 to 2.5%
Grec-Mauguio	exceptional	5 to 7%
Rhône de St-Roman	exceptional	11%
Vaccarès	0%	0%
Berre-Olivier	0%	2 to 21%
Urbino	+	0%

Table No. 14. Comparison of the Incidence of the Isopod and Microsporidian.

but it must be admitted, the success rate was very low. It was also interesting to compare sites harbouring Mothocya epimerica with those infested with Glugea atherini.

With the exception of the Etang du Vaccarès which was not thoroughly explored, isopods were generally present when the microsporidian was not and vice versa, undoubtedly because of the divergent needs of these two parasites. Both species seem highly susceptible to ecological conditions which have still to be defined.

Hypothesis Three: The spores are incapable of moving from one site to the next. If that is indeed the case, infested fish entering a microsporidian-free area could theoretically spread the disease. In order to explain this hypothesis, it is necessary to understand exactly how migration takes place. While migration between the sea and lagoons is well documented, it is not known whether the fish migrate between the various lagoons. Only by marking fish

populations will it be possible to obtain such information. There is evidence, however, that populations tend to be loyal to their native lagoons. Kiener and Spillmann (1969) showed, among other things, that the average number of gill rakers varied considerably from lagoon to lagoon. They recorded 22.9 for the Etang de Canet and 34.8 for the Thau basin. The number of gill rakers is characteristic for each lagoon and depends on environmental conditions. If this adaptation is essential for the survival of the fish, a population will obviously return to its native lagoon because a change would lead to reduced competitiveness, if not death.

If it is assumed that the fish rid themselves of their parasites at sea, they can return to any lagoon without spreading the parasite. The only path left for dissemination then is the Canal du Rhône à Sète but it is discontinuous and consequently a poor axis for migration.

Hypothesis Four: We are dealing with a recently evolved species or else a species with a new host specificity resulting from spontaneous genetic mutation. The atherine-infesting microsporidian may arise from another species (or variety) that is specific to another host. The focus (Mauguio-Rhône Mort) would then be the starting point from which the new species is currently spreading. It would be interesting to study the geographic range of this microsporidian in 5 or 10 years' time to check our hypothesis, which is supported by certain arguments, i.e., the cycle resembles that of Glugea anomala Moniez 1887, a Gasterosteus aculeatus parasite. Sticklebacks are known to be frequent inhabitants of the Etang de Mauguio after heavy rainfalls. Delisle (1969) described the light-

ning quick development of Glugea hertwigii-induced microsporidiosis in American smelts. The rate of infestation soared from 5.5% in the summer of 1965 to 47.8% in the summer of 1967 to reach 93.2% in September 1967. The parasite is clearly undergoing a change of some kind.

There is one argument, however, that pleads against this hypothesis. As we shall seen in the section on the pathogenic action of the parasite on the host, infected atherines do not seem to suffer unduly from the presence of the microsporidian. This seems to indicate that the parasite is extremely well adapted to its host since during the course of its cycle it does not seem to have any adverse effect, despite the production of up to 20 billion spores in a single xenoma. This behaviour is suggestive of a long-standing (in geological terms) adaptation between host and parasite. This argument should be used with a certain amount of discretion.

Several of the above hypotheses may be considered simultaneously. A study of population movements will no doubt provide an answer to our question. At certain times at least, microsporidiosis is potentially able to spread to any of the lagoons. Yet, there are problems involved in passing from one lagoon to the next because of the direction of migration and some areas are simply more favourable to completion of the cycle than others. In a closed environment, such as exists in the Rhône Mort, where migration is not possible, the rate of infestation rises. Likewise, in an environment with distinctly different saline levels from those found in neighbouring lagoons (e.g., the Etang de l'Olivier in which the water is virtually fresh and where there are very likely few shifts

CHAPTER FOUR

DEVELOPMENT OF MICROSPORIDIOSIS IN ATHERINES

in population), the rate of infestation is also very high. In an open environment, such as prevails in the Etang de Mauguio where saline levels are high and often close to those recorded in the Mediterranean, the rate of infestation fluctuates considerably throughout the year with shifts in population.

In conclusion, the behaviour of the host and requirements of the parasite seem to be predominant factors in the geographic distribution of Glugea atherini, but no completely satisfactory explanation has yet been found.

IV - DEVELOPMENT OF MICROSPORIDIOSIS IN ATHERINES

A - Contamination of the Host

1/ Means of Penetration

Experimental infestations have demonstrated that the parasite penetrates the host via the digestive tract. Stunkard and Lux (1966) noted that primary infection occurred in the digestive tract and concluded that this was the site of penetration of the spores. Wellings et al (1969) expressed the view that the spore penetrated directly via the mouth and that digestive juices caused extrusion of the filament, thereby halting further penetration by the parasite. The spores may pass through the intestines without becoming embedded. During experimental infestation, intact spores were found in the excreta. The spores may also empty by extrusion of the filament. Extrusion is undoubtedly triggered by definite but unknown laws. During our study, some acids (acetic and hydrochloric) and some bases (sodium, potassium, ammonium) were tested on spores produced by milky xenomas. The digestive juice from atherines was also tested, but none of these substances proved perfectly effective. Paradoxically, distilled water produced the most promising results. Extrusion was observed after a few minutes in a small number of spores placed in distilled water between slides and coverslips. Unlike spores from milky xenomas which only occasionally underwent extrusion on contact with distilled water, spores from chalky xenomas responded to distilled water by an immediate large-scale extrusion of filaments. Apparently, these spores, which are packed in a practically dry state in cysts where they form a chalky, friable and occasionally hard substance, open up with considerably greater ease. The spores mature imperceptibly as the xenoma progresses from the milky to the chalky state (no differences were detected under

the electron microscope) and become more sensitive to outside influences.

2/ Experimental Infestation

In order to take a closer look at penetration and internal development, seven trials were conducted in which atherines were experimentally infested. Three of these trials proved successful. Table 15 summarizes the procedures used. It is difficult to rear atherines, at least when a large number of fish must be maintained in a small volume of water. During non-experimental period, the water in the tanks (Plate XXII, 104) was continually filtered by means of a pump. Under these conditions, a lot of 50 atherines could be preserved for at least three months. During the course of infestation, following buccal injections or the use of spore suspensions, filtering operations were interrupted for fear of removing the parasite. This is when the risk of epidemics became greatest. Several diseases may ravage an entire lot in the course of a single day, i.e.,

- - Fin rot. In a very short space of time, the fish loses its fins which are eaten away at the tips. The rot is caused by bacteria that destroy the tissues and even the tail muscles resulting in hemorrhaging and secondary infections that kill the fish.

- Internal Scepticemia. Internal scepticemia may spread throughout the fish without there being any visible signs of external lesions. The diseased fish has trouble swimming and rolls as it moves. Examination of the blood reveals lysis of the red blood cells by very large numbers of bacteria. Nuclei from destroyed red blood cells may be seen in the serum (Plate IV, 12).

- Once Ichthyophtyrius multifiliis was observed in large numbers under the caudal epidermis. Although this ciliate is not dangerous, it helps to weaken the host.

Table No. 15. Experimental Intestation of Atherina boyeri

Experiment number	Rearing period (months)	Temp	g/l Cl^-	Type of inoculation	Type of spores	Source of fish	Fish dissected between 0 & 30 days		between 30 & 60 days		after 60 days	
							T*	I**	T	I	T	I
1	9-10-11 1976	19°-21°	0.8	direct oral injection. suspension in water	from a milky xenoma, Mauguio	Canal du Rhône à Sète, opposite Carnon	1	0	3	1	0	-
2	2-3-4 1977	18°	4	direct oral injection and suspension in water	from a milky xenoma, Mauguio	Canal du Rhône à Sète, opposite Frontignan-La Peyrade	5	0	5	2	0	-
3	2-3-4-5 1977	18°	4	"	"	"	12	0	0	-	0	-
4	2-3-4 1977	18°	4	gammarids placed 3 days earlier in contact with spores and suspension in water	"	"	8	0	0	-	0	-
8	9-10-11 1977	18°	20.5	oral injection + suspension in water	"	"	2	0	8	0	0	-
9	11-12 1977 1-2-3 1978	16°	9.0	oral injection + suspension in water	from a chalky xenoma preserved for 2 mos., 3-4°C	"	0	-	1	0	4	0
10	11-12 1977 1-2 1978	17-20°	11	suspension in water	milky xenoma, Mauguio	Rhône de St-Roman	1	1	-	-	-	-

* = total; ** = infected

Infestation trials were conducted in atherines from a site where microsporidiosis had never been observed. With each lot collected for experimental purposes, a group of roughly 100 fish was dissected to confirm the absence of the microsporidian. The site selected was the Canal du Rhône à Sète, opposite Frontignan-La Peyrade, near the Thau basin. In this particular section of the canal, saline levels vary considerably depending on the direction of the current and the different sources of water supply. As a result, infestation trials were conducted using the different saline levels to which the specimens had been previously exposed. Chlorine levels ranged from 4 to 20.5 g Cl^- per liter of water. In a few rare instances, experiments were carried out on fish from microsporidian-infested areas. Initially, these specimens were not reared for purposes of infestation, but after two or three months, we considered that a xenoma of over 3 months could be easily distinguished from a 1-month-old xenoma. The parasite was inoculated by one of three methods:

- Buccal injections. A spore suspension was prepared and introduced into a syringe without a needle. The tip of the syringe was placed in the mouth of the fish and roughly 0.5 cm^3 was injected. A white fluid exuded from the gills, but a large number of spores entered the digestive tract.

- Spore suspension in water. A crushed xenoma was mixed with the water in the tank. The fish absorbed the spores as they fed and breathed.

- Via gammarids (Gammarus locusta). The amphipods were previously placed in spore-contaminated water. Dissection of the digestive tracts of these crustaceans revealed the presence of numerous non-extruded spores. The gammarids were then placed in the tanks with fasting atherines and were all consumed in a few minutes.

Spore penetration consequently occurred via neutral hosts which could be considered the vectors.

Of the 53 fish dissected after the first 15 days of the experiment, 4 were infested:

Infestation No. 1. Forty-eight hours after an oral injection and contact with large numbers of spores in suspension, one individual developed three subcutaneous xenomas, roughly 300 µm in diameter, in the interstices of gill cover and socket bone. The xenomas were young with thick gelatinous coverings and, on electron microscopic examination, very few spores.

Infestation No. 2. Forty-two days after an oral injection, two xenomas, 1 mm and 1.5 mm, were found in the body cavity of one specimen, one against the liver and the other against the swim bladder. Only a few spores were detected. The xenomas were obviously in the early stages of development. In another specimen, a xenoma, 1.5 mm, was detected near the liver after the same latency period. In experiment No. 2, consequently, two of the five fish dissected between the 30th and 60th days were infested.

Infestation No. 10. Eighteen days after exposure of the fish to a spore suspension in water, a very young subcutaneous xenoma, 0.5 mm, was detected on the gill arch. The spores occupied only a very small area in the center of the xenoma.

On the basis of these four cases of experimental microsporidian infestation, it was possible to draw the following conclusions and elaborate the attendant hypotheses.

a) Infective spores are produced by milky xenomas. It is therefore unnecessary to wait until the milky xenoma develops into

a chalky cyst.

b) Infestation can be induced with chlorine ion levels ranging from 0.8 to 20.5 g Cl^- per liter at temperatures of 18^0 to 21^0C. The water in the Etang de Mauguio reached 19^0 in June, 26^0 in August and 23^0 in September when specimens were collected. Natural infestation is thought to occur at that time of the year.

c) Using the crustaceans as intermediate hosts failed to yield any results but it should be noted that in this particular experiment, it was not possible to keep the fish alive for more than 20 days.

d) While subcutaneous xenomas were obtained under experimental conditions, i.e., by exposing the fish to high numbers of spores in a water suspension, they were never observed in nature.

e) Young xenomas have transparent gelatinous walls, but pigmentation may develop at this stage.

f) Average growth is variable and depends on the site of implantation, i.e., 1/3 mm in 45 days in a subcutaneous cephalic location, but 1.5 mm for the same period of time in the body cavity. Since the number of parasitic stages undoubtedly increases exponentially as a result of merogony, it may be assumed that growth of the xenoma continually accelerates providing that no limiting factor intervenes.

If a xenoma can grow to 1.5 mm in a month and a half, then an adult xenoma can measure 5 to 13 mm in less than six months.

g) Since implantation in the corium of the intestine was not achieved with the experimental procedures used, infection of the body cavity must have occurred directly. Implantation occurs completely independently in these two sites, raising the question of how the infective organism penetrates to the center of

the fish from the intestines. It should be pointed out that Delisle (1972) considered the digestive tube the primary site of implantation by Glugea hertwigii with the peritoneum, liver, gonads, swim bladder, adipose tissue and lastly, the kidneys, as the secondary sites.

Some authors have succeeded in infesting specimens experimentally but for the most part, such attempts have failed. Stunkard and Lux (1965) tried to infest pleuronectids with Glugea stephani but with negative results. Weissenberg (1968) succeeded in contaminating sticklebacks with Glugea anomala but supplied few details on the experimental procedure. Lom (1969) used Pleistophora hyphessorbryconis, a parasite found in the muscle, connective tistue and body cavity of some aquarium fish. The microsporidian was transmitted orally to laboratory bred and wild Carassus auratus specimens. The infected tissues were crushed and injected into the muscles of specimens from a few species, ie., Carassus auratus, Cyprinus carpio, Tinca tinca. In every case, microsporidiosis was observed. Delisle (1972) obtained negative results when trying to infest fish by means of spore suspensions. During the great Glugea hertwigii epidemics, however, fish from the affected areas which appeared healthy when caught, developed 100 µm cysts after three days, undoubtedly as a result of natural contamination. Olson (1976) described some remarkable experiments which were conducted on a pleuronectid, Parophrys vetulus. Experimental infestation with Glugea stephani succeeded on various occasions, enabling the author to draw the following conclusions: infestation occurs at temperatures above 15°C. Contamination is more effective with crustaceans used as vectors but can still be achieved perorally or by means of a spore suspension in water. Glugea

stephani is a pleuronectid-specific microsporidian. Trials with fish from different taxonomic categories proved disappointing.

3/ Host Specificity of the Parasite

Specificity may hinge on two points: 1) extrusion of the filament may require conditions that are only available in a suitable host and 2) the injected sporoplasm may survive only in an appropriate host; otherwise, it will de destroyed by defense systems or unfavourable physicochemical conditions.

Irrespective of the mechanism involved, it is set in motion at the time of contamination.

In order to obtain a clearer picture of host specificity, we conducted a series of infestation trials with different fish species (Table 16).

While none of the trials produced positive results, it is advisable to avoid drawing any conclusions since we were working with a small sampling and encountered procedural problems.

The absence of the microsporidian in many species dissected, including the two other atherine species, argues in favour of a high degree of specificity on the part of the parasite.

4/ Factors Influencing the Rate of Infestation

While it is possible to identify the factors involved, just how they act remains unclear. They may act on contamination by promoting or preventing penetration of the spore. They may also act on the implantation process, i.e., once the spore has entered

No.	Species	Rearing period (mos.)	Temp.	Cl^- levels	Type of inoculation	Type of spores (source)	Time of dissection
5	Gambusia sp	1/1977 to 1/1978	20^o - 22^o	0 g/l	ingestion of bits of infected digestive tube	intestinal cysts	after 9, 15, 20, 59 and 190 days total: 5 fish
6	Solea solea	8-9/1977	22^o	22 g/l	buccal injection + suspension	milky xenoma	after 12, 13 and 17 days total: 4 fish
7	Crenilabrus sp.	8-9/1977	22^o	22 g/l	buccal injection + suspension	milky xenoma	after 25 days total: 6 fish
12	Gasterosteus aculeatus	1-2/1978	17^o - 20^o	?	spore suspension	milky xenoma	after 39 days total: 1 fish
13	Gasterosteus aculeatus	1-2/1978	17^o - 20^o	0 g/l	spore suspension	fresh and old chalky and milky xenomas	after 21 and 27 days total: 6 fish.

Table No. 16. Host Specificity of the Parasite and Experimental Infestation.

the organism, they abet or hinder its development. Since these two sets of factors cannot be dissociated, they will be discussed together.

a) Influence of the host's size and sex. 1,545 fish collected in the same lagoon (Mauguio) over a period of one year and a half, from October 1976 to March 1978, were divided into 18 lots consisting mostly of 100 specimens per lot and were dissected to determine the effect of size and sex on infestation. Results are summarized in Figs. 31 and 32.

The fish were separated according to sex and assigned to different classes, each class representing a 5-mm increment in length (Fig. 31). The rate of infestation was calculated for males and females in each class (Fig. 32).

It will be noted that there was not an even distribution of size. A large percentage of the specimens fell in the 55 to 70 mm category with numbers falling off at either end of this peak. This may be due to three phenomena, i.e., an increase in the mortality rate among the larger fishes, accelerated growth during the first year of life and the selectivity of fish nets which let the smaller individuals escape. As a result, the rate of infestation cannot always be considered significant. It is generally accepted that 30 individuals are needed for a proper sampling of the actual population. In males, the rate of infestation was only significant in individuals 40 to 80 mm long, whereas in females, it was significant in specimens 45 to 85 mm in length. (Irrespective of the type of curve used, there was always a 5 to 10 mm discrepancy in favour of the females, providing further evidence of sexual dimorphism).

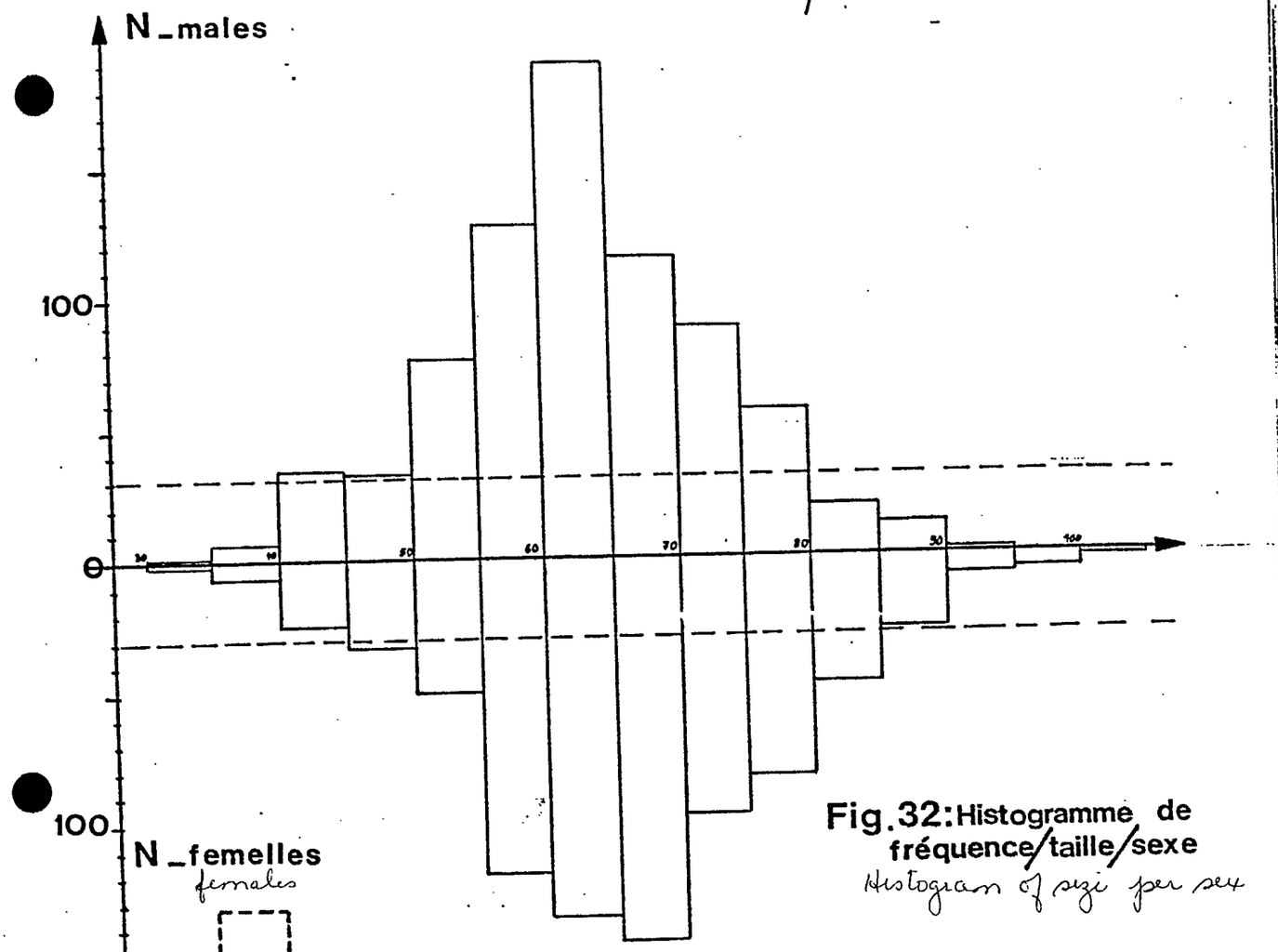

Fig.32: Histogramme de fréquence/taille/sexe
Histogram of size per sex

Rate of Infestation (%) per size for each sex

Fig. 32: pourcentage de parasitisme/taille/sexe

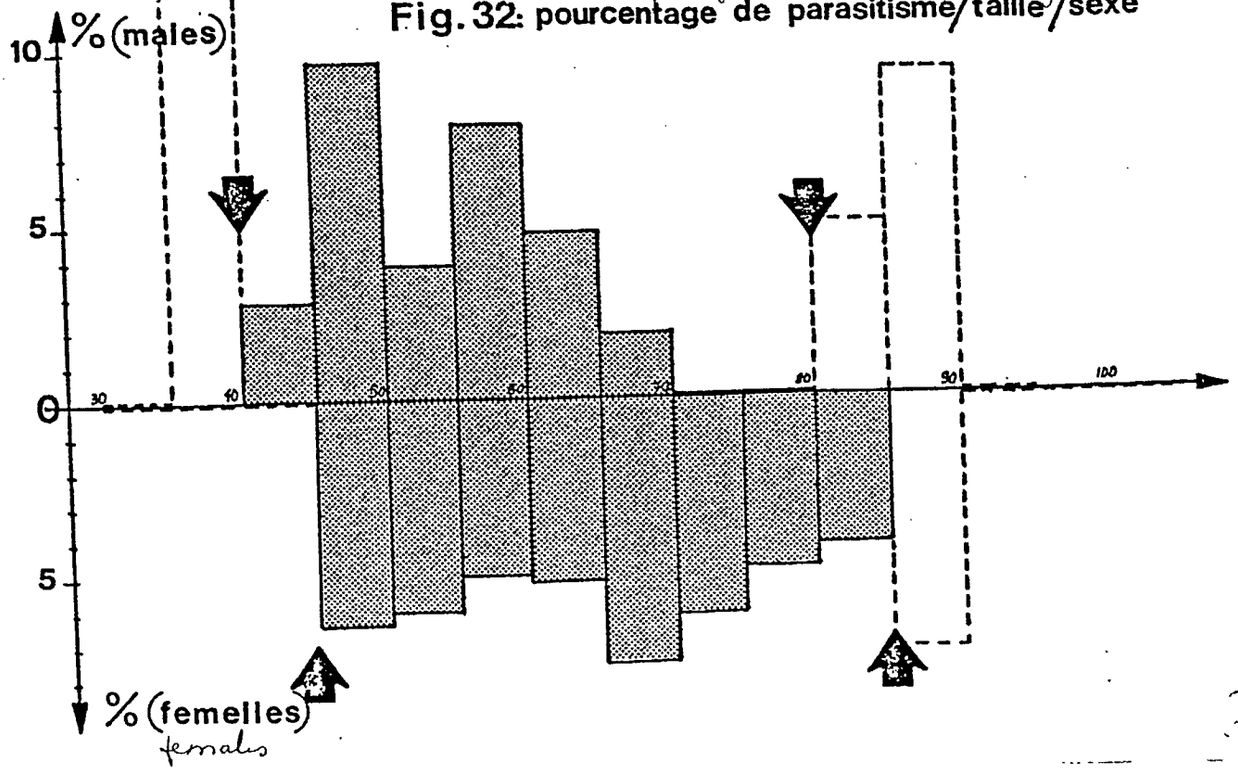

20

From Fig. 32, it may be concluded that in females, the rate of infestation (5 to 6%) does not seem to be associated with size, whereas in males, the maximum rate of infestation is noted in specimens 45 to 60 mm long with a decline in the rate at either end of the peak. No infestation was observed in fish over 70 mm long. This phenomenon cannot be explained and was undoubtedly the cause of differences between males and females in the total rate of infestation (Table 17).

Lagoon ETANG	Sex-ratio	Number of samples nombre de prélèvements	Total number N. total	Total rate of infestation Parasitisme global	Number of males N. mâles	Rate of infestation in males Parasitisme chez les mâles	Number of females N. femelles	Rate of infestation in females Parasitisme chez les femelles
Vic Moures	0,70	3	204	2,20 %	84	0,6 %	120	3,33 %
Prévost	0,75	1	79	1,25 %	34	3 %	45	0 %
Grec	1	2	58	6,9 %	29	3,45 %	29	10,33 %
Mauguio	0,96	19	1664	4,5 %	815	3,9 %	849	5,0 %
Rhône Mort	0,76	4	306	11,1 %	132	12,1 %	174	10,33 %
Berre	0,89	1	100	2 %	47	0 %	53	3,8 %
Olivier	1,70	1	100	21 %	63	19 %	37	24,5 %
Global	0,92	31	2511	5,6 %	1204	5,15 %	1307	6,03 %

Table No. 17. Influence of Sex on the Rate of Infestation

In males, consequently, size influenced the rate of infestation with the greatest contamination occurring in atherines under 60 mm in length. Beyond a total length of 70 mm, the rate plummeted to 0%. The overall rate of parasitism in fish over and under 70 mm was as follows:

males under 70 mm = 5.01%

males over 70 mm = 1.12%

females under 70 mm = 5.64%

females over 70 mm = 5.09%.

The rate was consequently 5% to 6% in females and young males. Older males exhibited little microsporidiosis, i.e., 1% or one-fifth the rate recorded in younger specimens .

b) Influence of abiotic parameters. Fig. 33 represents seasonal changes in the rate of infestation in the Etang de Mauguio with corresponding modifications in abiotic parameters such as temperature, pH, dissolved oxygen and saline levels. In general, due to the complexity of these phenomena, it was not possible to find a direct relationship between one or more parameters and the rate of infestation. If such a relationship exists, it would be masked by mixes and shifts in population. Modifications in the rate of infestation must be considered in a larger framework in which each parameter constitutes one of many facets of an overall change represented by the seasonal cycle.

The data plotted in Fig. 33 refer to specific instances and should be taken only as indications in the general description of the seasonal cycle. By and large, the rate of infestation is highest in winter and lowest in summer. The curve is not strictly reproduc-

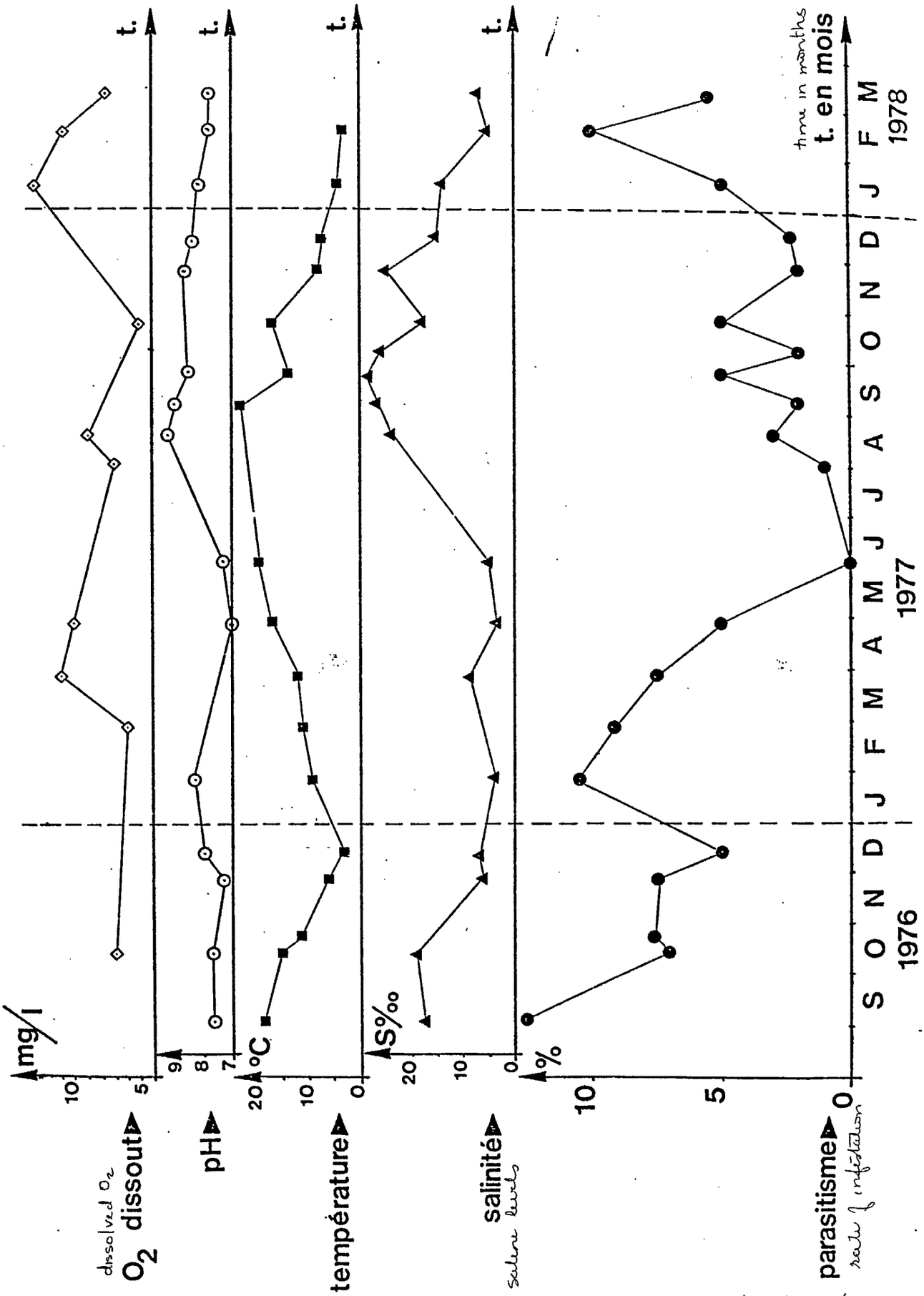

Rate of Infestation and Abiotic Parameters Etang de Mauguio

Fig.33 Parasitisme et paramètres abiotiques - Etang de MAUGUIO

ible from one year to the next, indicating the parasite's susceptibility to these parameters. It may be said that the rate of infestation is inversely proportional to the temperature but roughly proportional to saline levels, but there is not a truly direct relationship between these two parameters and infestation.

B - Internal Phase

1/ Penetration of the Tissues and Migration

The parasite can become implanted in the digestive tube or various other parts of the fish organism. At first sight, initial implantation in the digestive tube may be considered the necessary springboard for implantation in the body cavity. As mentioned earlier, Delisle (1969) advanced the view that the digestive tract was the primary site of implantation, potentially giving rise to secondary sites in the peritoneum, liver, oesophagus, gonads, etc.

This does not hold true for the atherine-infesting microsporidian. During infestation experiments, xenomas developed in the body cavity but not in the digestive tract. This suggests that the injected sporoplasm migrates to a certain part of the body and takes hold.

Just how does this migration occur? Weissenberg (1968) noted that macrophage-like migratory cells from stickleback mesenchyma, penetrated the connective tissue and phagocytized Glugea anomala germ cells. Development is consequently intracellular. Weidner (1972) observed in Nosema lophii (Doflein, 1898) that the sporoplasm was in a sac at the end of the filament. If the sporoplasm is not inside a cell, it breaks down within a few minutes. It may be phagocytized by macrophages, but in the phagocytic vacuole, it is in an extracellular environment and cannot survive. Macrophages are not vehicles for migration.

In spite of these contradictory views, the following may be put forward: if the spore is in a hollow between mucosal villi at

the time of extrusion, the 100 to 150 µm length of filament is capable of penetrating the tissues. There is reason to believe that the sporoplasm reaches as far as the corium, if not the outer muscle layer. As a result, a digestive tube xenoma arises in all likelihood from sporoplasm that successfully penetrated a cell in the corium. In all probability, the spores reach the rest of the body via the circulatory system. The sporoplasm penetrates a blood cell or else, is phagocytized by a specialized cell, such as a macrophage, which circulates in the blood or lymphatic system.

2/ Establishment and Growth

Very little is known about what brings migration in the body to an end. It may well be that the hypertrophying xeno-parasitic complex is blocked in a small-sized capillary. Once arrested in its course, the xenoma develops. In the digestive tract, there is an exclusive preference for connective tissue, but this is less clearcut elsewhere in the body.

Host tissues respond by a defense reaction. This is generally the interpretation given to the peripheral organization, made up of blood vessels and fibrocytes, and the xenoma wall. This response is diverted by the parasite for its own benefit. The collagen sclerosing the fibrocytes is transformed into a structure providing isolation and protection while the blood vessel in the host tissue serve to provide nourishment for the cyst.

In a few rare instances, ultrastructural examination of mature digestive tube xenomas revealed the presence of numerous everted spores. The filaments had extruded through the xenoma wall (Plate XXI, 97) to occur in large numbers in the connective corium (Plate XXI,

96). There are two possible hypotheses:

- Extrusion is caused only by the fixation process (glutaraldehyde, and osmic acid) in which case, the interest resides solely in a study of the extrusion process.

- Extrusion is a normal process occurring under natural conditions. It is a very interesting instance of microsporidian expansion within a host from a primary site of implantation. This could explain why cysts are often concentrated in large numbers in a small area of the intestine. They may be the result of intracystic extrusion. Once the xenoma becomes established, it grows in size, its overall volume depending on the site of implantation (maximum diameter = 0.2 mm in the digestive tube, but 13 mm in the fat tissue of the body cavity). It then shrinks in size as the liquid component is eliminated. When the cyst consists only of spores and fluid, it has a paste-like and even firm consistency. Some xenomas are hard, friable and break easily. Electron microscopy has revealed that most spores remain intact, although those in the periphery may be damaged (Plate XXI, 98-99, SD).

This is the final stage in the development of the microsporidian in the host. The xenoma then enters a latency period.

PLATE XXI

95 - Spores with extruded filaments (FD) and central vacuole-like area (V), larger than the posterior vacuole in intact spores (see inset) (X 30,000).

96 - Section of extruded filaments in the peripheral organization (OP) with connective fibers (c) (X 21,500).

97 - Intracystic extrusion: spores inside the intestinal cyst (IK) with filaments (FD) extruding through the wall (PK) (X 21,500).

98 - Detail of degenerate spores (SD) at the edge of chalky body cavity xenomas (21, 500).

99 - Edge of the same xenoma with indistinct wall boundaries (PK), degenerate peripheral spores (SD) and live spores in the center (SV) (X 5,000).

PLANCHE XXI

PLATE XXI

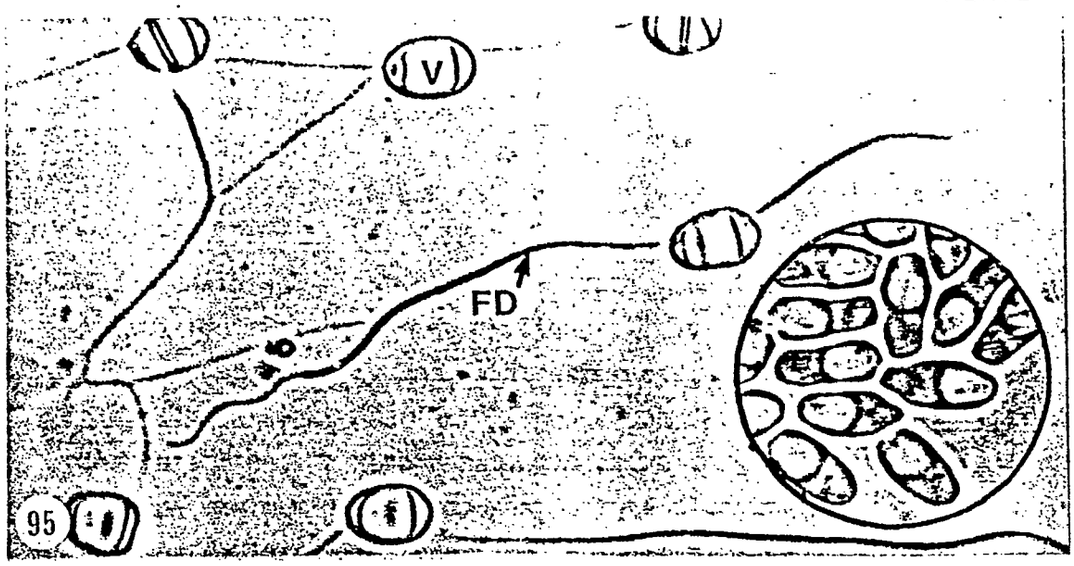

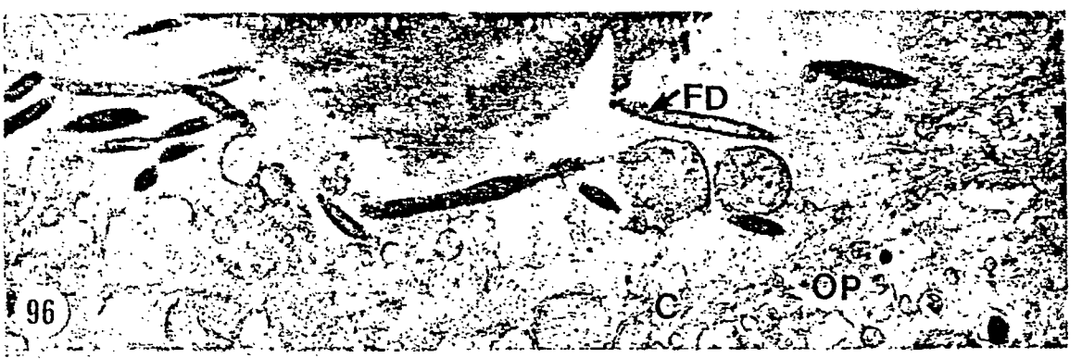

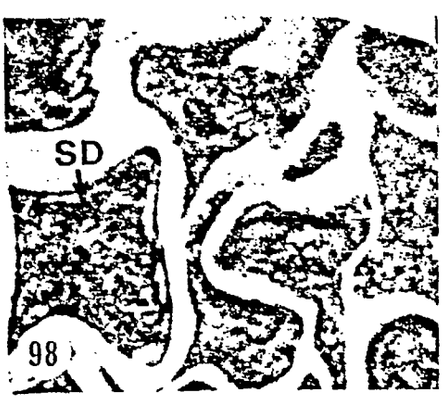

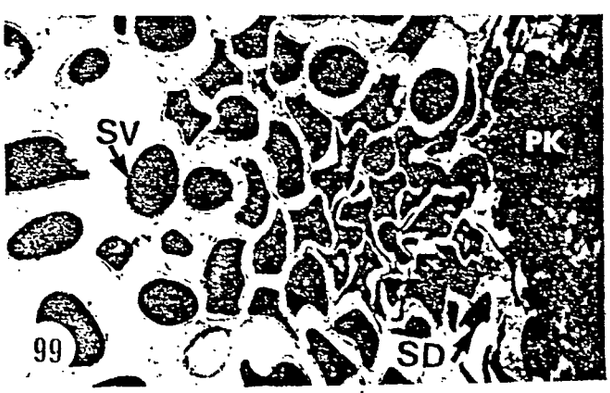

3/ Pathogenic Action

Several tests were conducted to determine potential parasitic action on the host during the internal phase. The presence of 1-cm xenomas in 5-cm-long fish indicates that this action is not immediately harmful to the animal.

In order to detect a direct action on the blood, serum from healthy specimens and atherines with large xenomas in the body cavity was subjected to electrophoretic analysis and variations in the protein composition of the blood were recorded. Tests were also carried out to determine the action of intestinal xenomas on digestive enzymes. This was followed by gel diffusion trials to detect the presence of antigen-antibody reactions between parasite proteins and fish serum.

Lastly, we induced a bacterial epidemic to establish whether the parasite had an effect on the host's general defense system.

(a) Influence of the Parasite on Blood Proteins. Only large xenomas, which because of their size might have an influence on the protein composition of the blood, were considered. This influence may be due to various causes.

Technique.

Electrophoresis was conducted with a TRIS-boric acid Na_2EDTA buffer at pH 8.35. Acrylamide gels were used. Gel from tubes is prepared shortly before use and contains approximately 7.5% acrylamide with a pore size of 5 nm. Sheet gel is commercially available with a 'Gradipore' gradient in which the concentration increases

from 0% to 35%. Amidoblack is used for staining and 7% acetic acid for differentiation.

On a tube acrylamide gel (Plate XXII, 100), this type of electrophoresis known as disc electrophoresis, separates the protein fractions on the basis of their electrical charges. Since the latter are roughly proportional to the length of the protein chains, the protein is actually identified by its mass. Up to 17 bands are obtained by this method (Fig. 34).

The use of gradient gels (Plate XXII, 101) produces more refined results since the proteins are progressively filtered through increasingly finer gel pores. Up to 30 bands are obtained (Fig. 34).

Results were quantified by means of an integrator which plotted the optical density curve of the gel and measured the area (proportional to the amount of protein) of each curve (Plate XXII, 100, 102, 103). A relative figure, assigned to each fraction, was then converted into a percentage value.

PLATE XXII

100 - Tube acrylamide gel with integration curve (serum) (X 0.9).

101 - Sheet acrylamide gel with gradient. 7 electrophoretic analyses with, from left to right, 1 female, 1 male, 2 females, 1 male, 1 female and 1 male. The clearcut influence of sexual differences is observed only during the period of reproduction (from March to July) (X 1).

102 - Integration curve above a negative of electrophoretic analysis of blood serum from a male atherine. In males, the area between A and B is poor in proteins (X 1).

103 - Same representation for a female specimen. The area AB is very rich in proteins (X 1).

104 - Installation with tanks for experimental infestation.

105 - (French text, illegible) (translator)

PLANCHE XXII
PLATE XXII

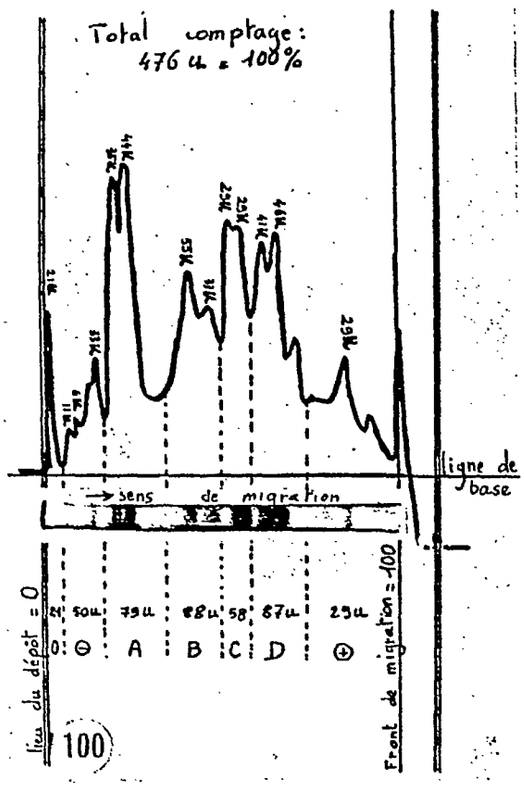

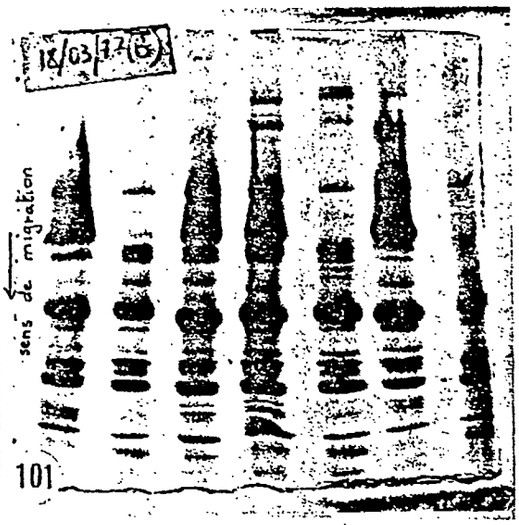

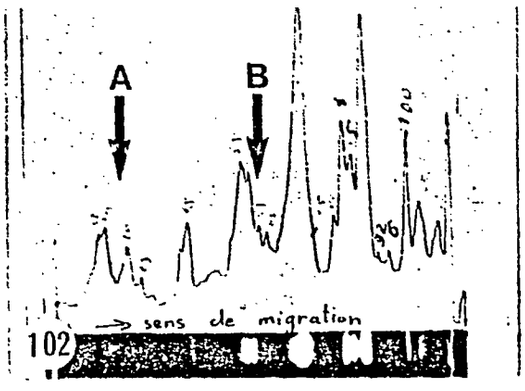

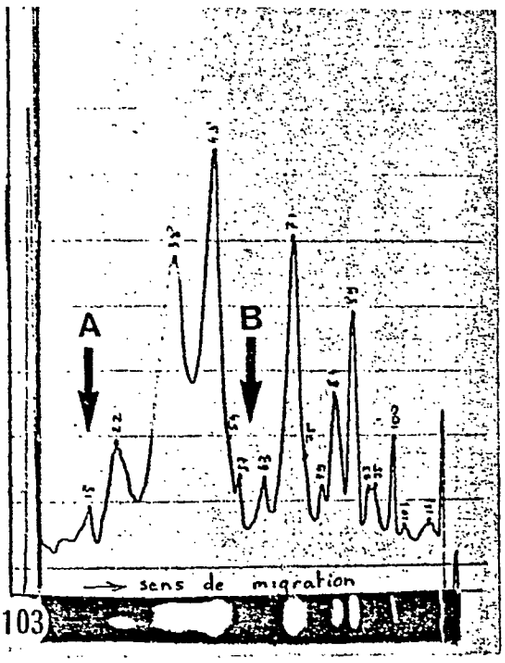

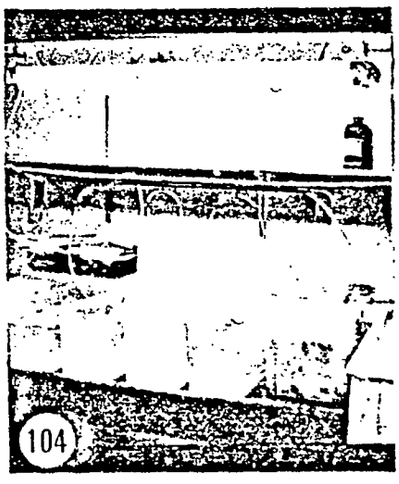

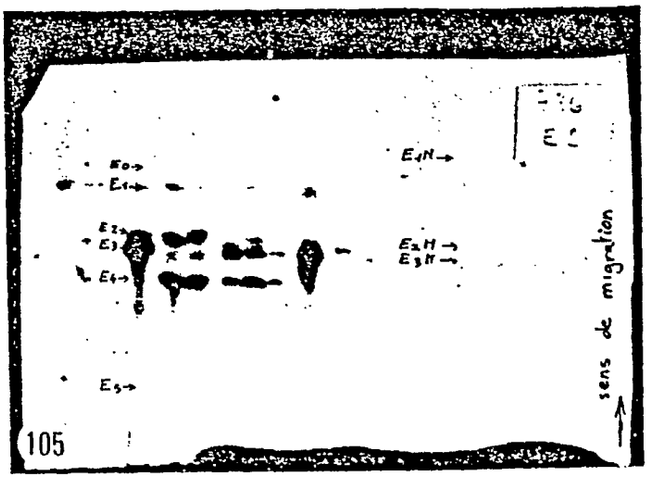

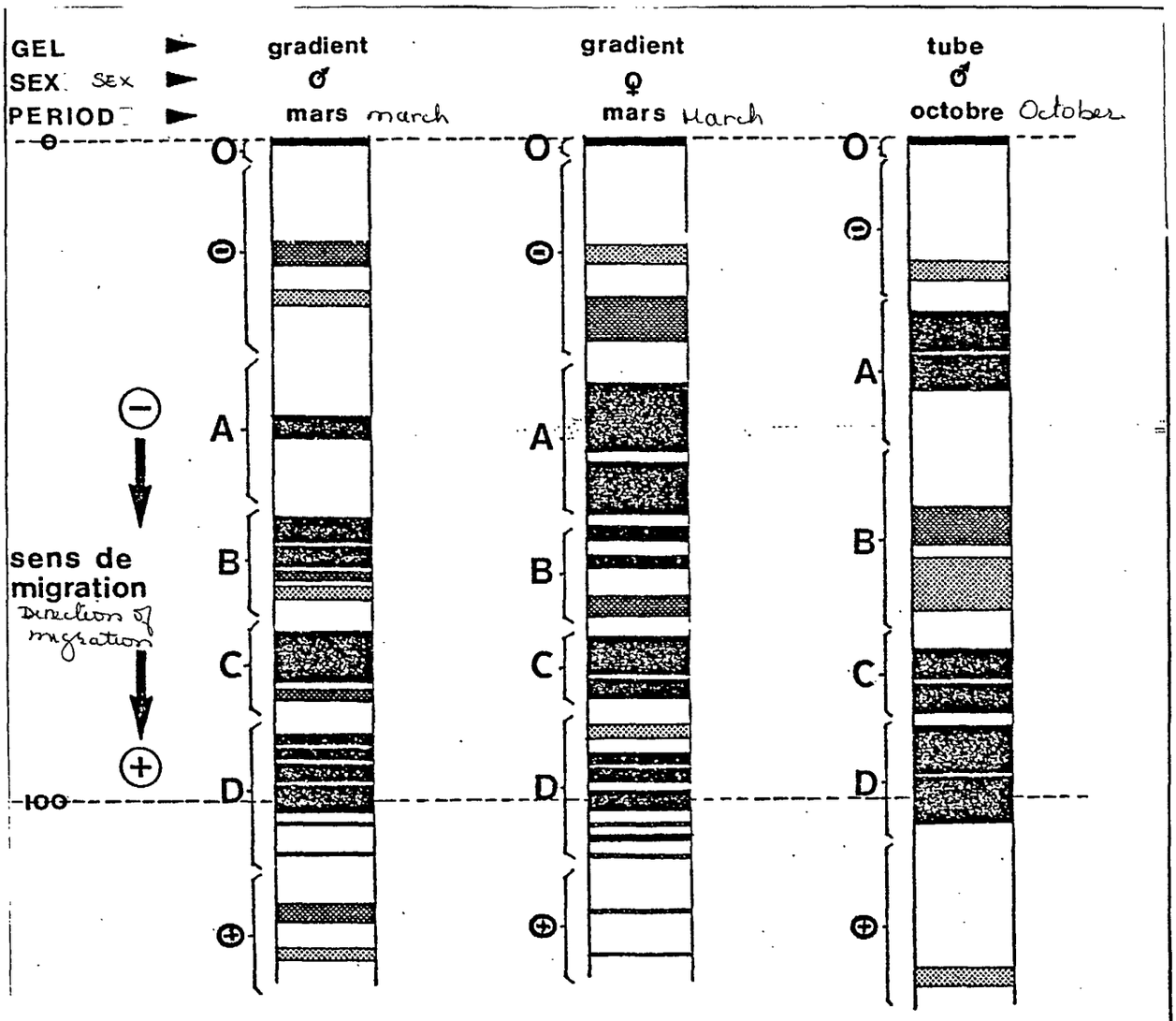

Three Simplified Examples of Electrophoretograms.

FIG.34 : TROIS EXEMPLES SIMPLIFIES D'ELECTROPHOREGRAMMES

Results

For an initial approach, the gradient gel method proved too refined. The tube gel method was also too refined (17 bands) and would have required lengthy calculations. The prteins were therefore grouped into 7 series corresponding to groups occurring on the gel.

Series 0 consisted of 1 band ranging from 0 to 3 in relation to fraction D
" - " " 3 bands " " 3 " 33 " " " " "
" A " " 3 " " " 33 " 55 " " " " "
" B " " 3 " " " 55 " 73 " " " " "
" C " " 2 " " " 73 " 88 " " " " "
" D " " 2 " " " 88 " 111 " " " "
" + " " 3 " " " above 111 " " " " "

Percent averages were calculated for each series, comparisons being made in groups of fish divided according to sex, size, month of catch, sampling site, presence of other parasites (only isopods), exposure or non-exposure to rearing in the laboratory and lastly, presence or absence of the microporidian.

In each series and paired lot, averages were compared by means of Student's 't' test using the following equation:

$$t = \frac{\bar{X}1 - \bar{X}2}{S\sqrt{\frac{1}{n1} + \frac{1}{n2}}} \qquad \text{with } S = \sqrt{\frac{(n1-1)\,\sigma^2_1 + (n2-1)\,\sigma^2_2}{n_1 + n_2 - 2}}$$

Depending on the t value obtained, with t_{95} and t_{99} corresponding to a probability level of 95% and 99%, respectively, it was possible to determine whether averages for the paired lots represented significant (95%) or highly significant (99%) differences.

Our calculations revealed the following:

. Differences in sex were not significant outside periods of reproduction. Plate XXII, 101, 102 and 103 reveals noteworthy differences in series (-) in March. As a result, comparisons will be made only during periods of sexual quiescence.

. Differences in size. The fish were divided into five size groups: 41 to 50 mm, 51 to 60 mm, 61 to 70 mm, 71 to 80 mm and 81 to 90 mm. Pairing did not produce any significant differences. Size will consequently not be considered in our calculations.

. Differences in sampling sites. Two zones were compared, i.e., zones with and without microsporidiosis, corresponding to two geographic areas separated by the Etang d'Ingril.

In this instance, gross differences became apparent. Comparisons were based on the respective proportion (in %) of each series in the paired lot of fish. If a series is represented by a larger percentage value in a given lot of fish, this may mean that the protein is present in greater amounts or else that the overall protein level (not determined) has dropped, in which case, the series in question, which has not changed, becomes proportionately larger.

Series C (zone with parasites) $<$ series C (zone without parasites)
highly significant difference (99.9%)

Series D (zone with parasites) $>$ series D (zone without parasites)
significant difference (95%).

Certain parallels may be found with the differences in enzyme content recorded in fish populations from the two zones (cf the section on geographic distribution).

As a result of the above, comparisons will be made only among fish from one zone, i.e., the microsporidian-infested area.

. Differences in catch times. October was compared with January with the following results:

series (-) October $>$ series (-) January (highly significant difference)
series A October $<$ series A January (significant difference)
series C October $<$ series C January (highly significant difference)
series (+) October $>$ series (+) January (highly significant difference).

The time of year when specimens are collected is clearly a very important factor. The physiology of the fish changes considerably with their biological rhythm which is dependent on climatic factors. Consequently, only individuals collected in the same month will be used for purposes of comparison.

. Fish with and without isopod parasites.

series A without disopods $>$ series A with isopods (significant dif.)
series C without isopods $>$ series C with isopods (significant dif.)

These findings serve only as an indication of the isopod's influence on the atherine since the isopod and microsporidian never share the same range (cf Table 14).

. Differences between wild and laboratory-reared lots. In this instance, the sampling size was too small for a valid comparison. Despite the absence of results, we considered it advisable to make comparisons only within each group and not between the wild and laboratory-reared fish.

Once all the restrictions concerning sex, collection sites, catch times and rearing practices were taken into account, a comparison was made between healthy and infected fish. The latter were all collected in the microsporidian-infested zone in October and November (period of sexual quiescence) and none were reared in laboratory tanks. No significant differences were observed between the two groups, suggesting either that the parasite has no influence on blood proteins or that the influence is too slight to be detected by the method used.

(b) Digestive Enzyme Tests. In order to determine the action of digestive tube xenomas on digestion, enzyme tests were performed on the intestines of healthy and highly parasitized fish (Fig. 35).

Techniques

The technique used has the advantage of producing immediate results and not requiring purified extracts. All that is needed for this APIZYM system is crushed tissue for analysis and four buffer solutions, pH 5.4, 7.1, 7.5 and 8.5. On the basis of the staining reaction obtained, it was possible to detect the presence of 19 different enzymes and quantify their activities. The enzymes included 3 phosphatases, 2 esterases, 1 lipase, 5 proteinases and 8 carbohydrases (Fig. 35).

Results

Averages calculated for samples obtained from healthy fish indicated marked alkaline phosphatase, leucine aminopeptidase, acid phosphatase, phosphoamidase, β-glucosaminidase activity.

The standard deviation between alkaline phosphatase and leucine aminopeptidase

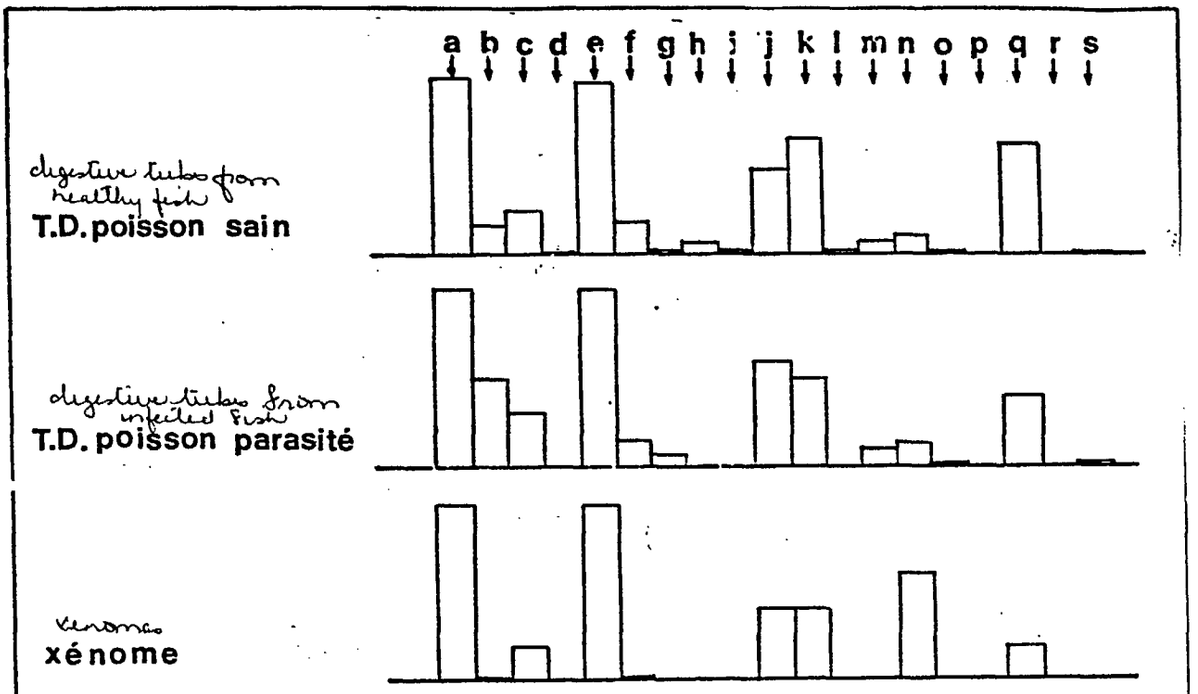

a Phosphatase alcaline (alkaline phosphatase)
b Estérase (C 4)
c Estérase Lipase (C 8)
d Lipase (C 14)
e Leucine aminopeptidase
f Valine aminopeptidase
g Cystine aminopeptidase
h Trypsin
i Chymotrypsin
j Phosphatase acide (acid phosphatase)
k Phosphoamidase
l α galactosidase
m β galactosidase
n β glucuronidase
o α glucosidase
p β glucosidase
q β glucosaminidase
r α mannosidase
s α fucosidase

111

was very small, whereas it was very high between the three other enzymes, suggesting considerable digestion-related variability in secretion (a Circadian factor was ruled out since all the samples were taken at the same time of day). Esterase (C4) proved just as variable albeit far less active.

Esterase lipase, valine aminopeptidase, and β-glucoronidase exhibited moderate, stable activity.

When the tests were applied to highly infected individuals, essentially the same results were recorded. Only esterase (C4) proved more active but because of its variability, reflected in a very high standard deviation, the Student 't' test did not demonstrate any significant difference in activity.

The explanation for our findings resides in the site of infection. All of the xenomas were located in the connective corium; none were found in the mucosa which consequently was not impaired in its function.

(c) Gel diffusion. This is a very simple, but also very limited technique whereby antibody-antigen reactions between the host and parasite can be detected.

Technique

The principle is very simple. Particles assumed to be antigenic are placed in the presence of immunoglobulin-containing serum from the host. If the blood protein "recognizes" the microsporidian antigen, the two molecules agglutinate with the antigen neutralizing

the antibody. The procedure is carried out on an agar-coated slide. Crushed, centrifuged samples are placed in small wells in the agar. Migration takes place over a 24-to-48-hour period. The molecules migrate toward one another. If a reaction occurs, migration ceases and an opaque, arch-like deposit forms in the agar.

Four tests were carried out using an extract from a body cavity xenoma which was crushed by an ultrasound technique in which all the cells were smashed but the spores were left intact. The preparation was then centrifuged. The fish serum was also previously centrifuged.

Results

In four separate experiments, the xenoma extract was placed in contact with a) fish serum from an xenoma-bearing atherine; b) serum from a healthy specimen from the same site (Etang de Mauguio); c) serum from an atherine collected in a microsporidian-free site; or d) mixture of serums from 5 healthy fish from the same site.

After over 48 hours of migration, none of the four experiments yielded positive results. The lack of reaction may be explained as follows:

1) procedural errors. Perhaps the samples had not been adequately crushed, the agar was either under or over concentrated, there were impurities in the extract, interfering with migration, or else, the reagents were not concentrated enough (The method is sensitive to levels of 5 µg/ml). This explanation is unconvincing since the experiment was repeated.

2) lack of humoral reaction. This is a fairly frequent occurrence in fish, even in the presence of more harmful parasites.

3) The parasite may never be in contact with the blood. Some authors, such as Weidner (1973) are of the opinion that the sporoplasm must be injected into a cell or else it will die. It survives only if it is immediately injected into a cell. In this cell the parasite is isolated from the blood and is thought to migrate in the fish's body and finally become established. In this case, no humoral reaction can take place. It should be noted that the reaction around the hypertrophying xenoma is strictly cellular.

(d) Experimental Bacterial Infection. Bacterial infection is the most common disease encountered when rearing atherines. Two main types of infection cause ravages, i.e, fin rot and generalized internal scepticemia (Plate IV, 12). Continual filtration is needed to prevent these epidemics from occurring. If filtration must be interrrupted for the purposes of the experiment, the fish must not be kept under crowded conditions and must be divided into several tanks.

In order to test the susceptibility of parasitized fish to bacteriosis, 50 atherines caught in the Rhône Mort were reared in a laboratory setting. The tank was large enough to avoid massive mortality.

Filtration was discontinued on December 1, 1977. On December 2, four deaths were recorded; on the 5th, five more; on the 6th, 1; on the 7th, two and on the 12th, four. The epidemic was eradicated but resumed with 18 deaths on February 6, 1978 and 4 (the last survivors) on February 7, 1978.

During the epidemic, the dead fish were removed from the tank

each day and dissected.

Fig. 36 shows the progression of the epidemic and indicates, for each date, the number of dead fish and the theoretical and actual number of infested individuals among the dead specimens.

In four instances, the actual number of parasitized fish was once, twice, and four times the theoretical figure, if the infestation rate observed in living fish was applied to the dead specimens.

This tends to show that infested individuals have a higher degree of susceptibility to bacterial disease. It was interesting to note that often the specimens were not highly infected , e.g., only a few intestinal xenomas, providing evidence that the phenomenon is highly complex. The host is not actually physically weakened, but the mere presence of the parasite rather than its numbers, affects its system of defense.

In view of the absence of a gel diffusion reaction, several explanations for this phenomenon may be advanced.

+ In the early stages of implantation, the parasite induces a pronounced humoral reaction in the host, which weakens it, increasing its vulnerability to bacteria. The reaction is highly attenuated when the xenoma is large and cannot be detected by gel diffusion methods.

+ The parasite secretes substances (metabolic residues, toxins) that have an influence on neither blood proteins nor defense substances, as a result of which they can not be detected with the type of tests we carried out. They may act directly on the production of essential molecules, such as vitamins. Loss of these mole-

Date de dissection Dissection date	2/12	5/12	6/12	7/12	12/12		6/2	7/2
Nombre de morts Number of dead fish	4	5	1	2	4		18	4
Nombre de morts parasités Number of dead fish with parasite	3	2	0	0	1		2	0
Nombre de poissons restants Number of remaining fish	39	34	33	31	27		4	0
% de morts parasités % of dead fish with parasite	75	40	0	0	25		11	0
% global de parasitisme de la veille Total theoretical rate of infestation in %	18,6	12,8	8,8	9,1	9,7		7,4	0

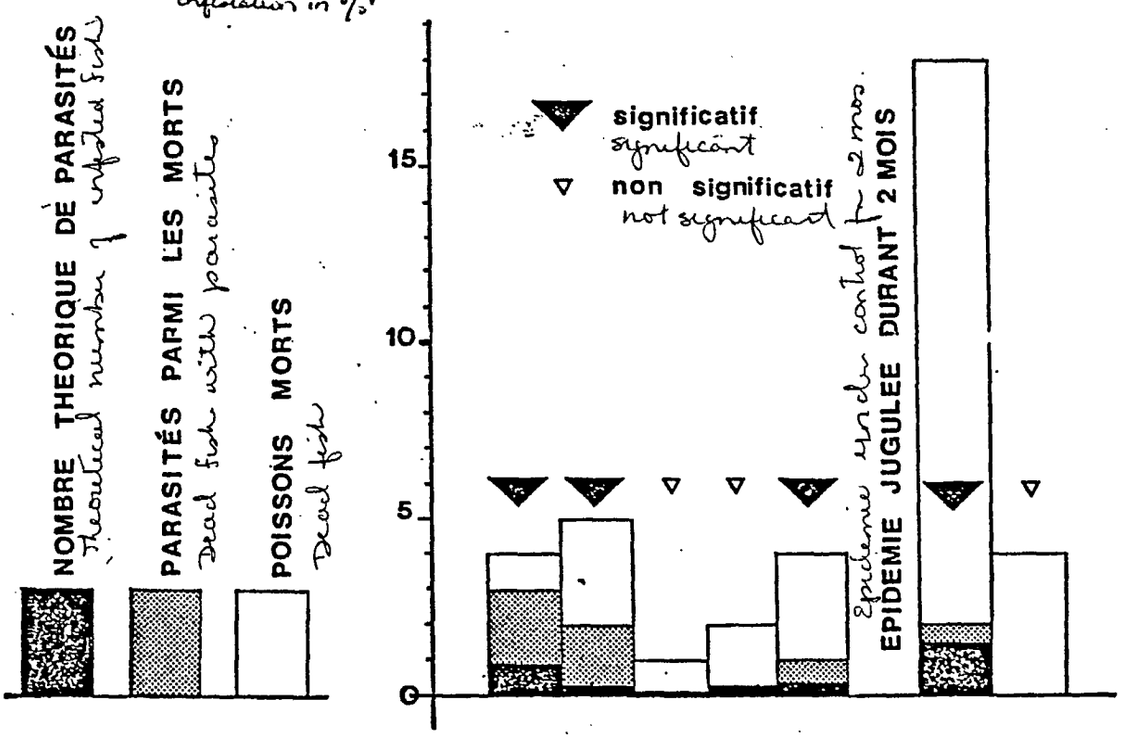

Fig.36: BACTERIOSE EXPERIMENTALE

Experimental bacterial infection

40

cules weakens the host or simply its system of defense.

4/ Enzymology of the Cyst

We touched only briefly on this aspect of the problem which would have required long and painstaking research. Because of the exceptional size of these xenomas, it is possible to contemplate a host of studies aimed at acquiring a better understanding of the mechanisms involved in the xenoparasitic complex.

In the course of our investigation, two very limited trials were carried out.

a) Enzyme test in a crushed xenoma preparation. By way of indication, a milky xenoma (undergoing development) was tested. Our findings are given in Fig. 35. While a comparison with digestive enzymes is meaningless, it should be noted that alkaline phosphatases, leucine aminopeptidase and β-glucuronidase exhibited marked actiity. Changes in the enzyme composition of the xenoma during development warrants closer scrutiny.

b) Enzyme electrophoresis on starch. Following migration and demonstration, the following findings were obtained in a developing (milky) xenoma, 5 mm in diameter:

- many enzymes failed to exhibit any activity, i.e., ADHs, α-GPD, SDH, IDH, 6-PGD.
- some displayed very limited activity, prossibly due to contamination from neighbouring tissues. MDH and GOT4 displayed positive mobility.
- lastly, only the LDHs were clearly visible although faint. Both A and B isoenzymes were present but exhibited slightly faster movement. This was particularly true of LDH A. The spots were only faintly visible as a result of the large proportion of ripe spores in the xenoma. Although these results are partial, they indicate

that the internal enzyme activity of the xenoma is noticeably different from that of the liver or muscle. Here, too, it would be interesting to follow changes in the enzyme composition of the xenoma as it develops. The transformation of LDH enzymes suggests that protein synthesis follows a different pattern in the xenoma. This is either because the LDHs demonstrated are produced by the parasite, enzyme levels in the host cytoplasm being too low to be visible or else, because they are produced by the host, in which case, the parasite affects the physiology of the host cell both qualitatively as well as quantitatively.

C - Free-Living Phase

The free-living spore in the water is in a resistant phase. Its complex ovoid capsule provides excellent protection for the internal structures needed to penetrate the host. The spores are released into the water when the host dies. A Glugea boyeri xenoma has never been observed opening and releasing its spores from a living fish. Weissenberg (1968) recorded this phenomenon in Glugea anomala, a stickleback parasite, but in this case, the xenomas were subcutaneous.

In the experiments conducted with infested gammarids, microscopic examination of the digestive tubes and excrements revealed that the spores were intact. We observed in the laboratory that in the vast number of cases, dead atherines sank to the bottom of the tank where they were devoured by crustaceans (gammarids, crabs, shrimps) and small fish (gobies, blennies). Many other small animals must do likewise. If the cadaver contains a xenoma, the spores enter the digestive tube of the necrophagous animals which then take over the job of dissemination. If a live fish is devoured, the spores

will also be found in the excreta of the predators. The spores obviously passively follow certain food chains and are ingested in turn by crustaceans, fish and even birds. Until otherwise proven, Atherina boyeri is the only species infected with Glugea atherini. Naturally, decomposition of the cadaver, which requires four to eight days (observations in the aquarium), results in the release of spores in the water and direct contamination of the host.

The loop is looped. Fig. 37 shows the cycle with the hypothetical transmission via various neutral hosts.

The atherine is infested by spores contained
- in the water
- in the excreta of small necrophagous animals
- in the digestive tube of its prey (small necrophagous crustaceans, neutral vectors)

L'Atherine s'infeste par les spores contenues:
- dans l'eau
- dans les excréments des petits nécrophages
- dans le T.D. de ses proie (petits crustacés nécrophages, hotes transporteurs neutres)

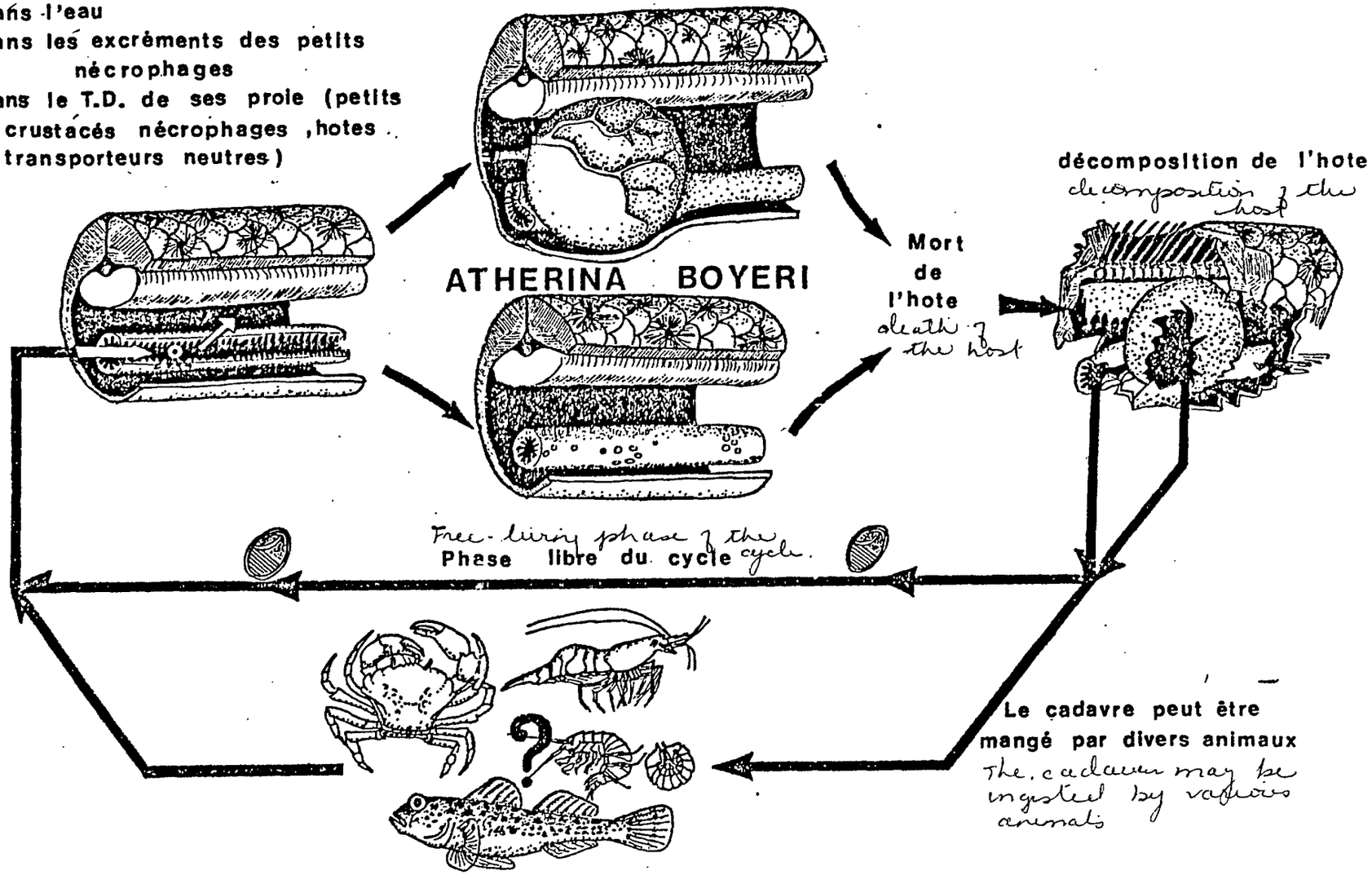

FIG. 37: Cycle biologique de GLUGEA ATHERINI

Biological cycle of glugea atherini

CHAPTER FIVE

DEVELOPMENT OF PARASITISM OVER TIME:

THE SEASONAL CYCLE

V - DEVELOPMENT OF PARASITISM OVER TIME: THE SEASONAL CYCLE

A study of the seasonal progression of microsporidiosis requires large numbers of specimens to be collected throughout the year. This is exactly how we proceeded in the Etang de Mauguio which is probably the focus of the disease.

Specimens were collected once or twice a month over a year-and-a-half period from October 1976 to March 1978.

Our findings should be regarded with caution, however, for the following reasons:

. The Etang de Mauguio does not have homogeneous populations. The lagoon is 11 km by 3.5 km. As a result, the marine or limnic influence is not the same at two distant points and the fish populations are exposed to different conditions depending on the zones they inhabit.

. There undoubtedly exists a native population that migrates little and spends the winter in the lagoon. It is a small population since winter catches are poor. The lagoon harbours primarily a migrant population which spends the summer in the lagoon and the winter in the Mediterranean. In fact, the phenomenon is even more complex since substantial changes in weather conditions are attended by small-scale migration between sea and lagoon and vice versa. It could well be that some populations migrate between the Mediterranean and the Etang de Mauguio several times in the year, which explains why there are many growth rings, but not one (representing the winter ring) is more noticeable than the others.

In view of the above, the fish caught in the nets left by the fishermen over a 24-hour period represent a random sampling of a population continually on the move. The result is an irregularly

shaped curve that should be viewed with caution (Fig. 33).

Infestation of the digestive tube is totally independent of involvement of the body cavity. The phenomenon is determined by external conditions. As a result, the two types of implantation will be studied separately.

1/ Digestive Tube Xenomas

The following table indicates how the phenomenon evolves in the course of the year.

Sampling Date	% infestation	Number	Sampling Date	% infestation	Number
Jan. 1976	0%	8	Jan. 1977	2.1%	95
Feb.	-	-	Feb.	1.0%	100
Mar.	-	-	Mar.	0	82
April	-	-	April	0	100
MAy	-	-	May	-	-
June	-	-	June	-	-
July	-	-	July	0	81
Aug.	-	-	Aug.	0.5%	200
Sept.	0	29	Sept.	0	200
Oct.	3.6%	138	Oct.	0	200
Nov.	0	80	Nov.	0	100
Dec.	1.25%	80	Dec.	0	90

Sampling Date	% infestation	Number
Jan. 1978	0	100
Feb.	1	100
Mar.	0	18

Table No. 18. Rate of Infestation with Digestive Tube Xenomas in Specimens from the Etang de Mauguio.

Except for a sudden rise in infestation in the fall and winter of 1976-1977, the rate of infestation with digestive tube xenomas was virtually nil. Digestive tube xenomas represented 13.5% of the total number of xenomas recorded. The phenomenon is far from being cyclic and does not necessarily recur each year in the same way, indicating the high degree of susceptibility of the parasite to external conditions.

The percentage also varies from site to site. In the Rhône Mort, we recorded 12% infestation with intestinal xenomas in November 1976, 7% in January 1977, 0% in September 1977 and 13% in November 1977. In this instance 93% of the xenomas detected were located in the intestines suggesting that the conditions to which the fish are exposed have a fundamental influence on the type of implantation.

2/ Body Cavity Xenomas

It was shown that on the basis of xenoma size and shape, the chalky cysts were histologically the natural outcome of milky xenoma development which may be described in morphological terms, e.g.:

. colour. 69% of milky xenomas are white; 12.5%, gray and 19%, black. 42% of chalky xenomas are white; 31%, gray and 27%, black. Chalky xenomas are clearly more pigmented.

. size. The average diameter of milky xenomas is 4.5 mm and of chalky xenomas, 2.9 mm.

These figures were based on 53 xenomas from fish obtained from various sites in the fall of 1976. Morphological change, consequently, results in reduced size, hardening of the contents and

	Catch Date Date de la pêche	No. of catch N° de la pêche	Number of Specimens N	Total infestation rate (%) % total de parasitisme	% milky xenomas % de xénomes "laiteux"	% chalky xenomas % de xénomes "crayeux"
Jan	Janvier 76	2	8	0	0	0
Sept	Septembre	10	29	10,25	10,25	0
Oct	Octobre	14 & 17	138	3,5	3,5	0
Nov.	Novembre	31	80	7,5	7,5	0
Dec.	Décembre	36	80	2,5	1,25	1,25
Jan.	Janvier 77	44	95	8,5	2,25	6,5
Feb	Février	49	100	8	2	6
Mar.	Mars	52	82	7,5	1,25	6
Ap.	Avril	54	100	5	3	2
June	Juin	58	81	0	0	0
aug.	Août	60 & 61	200	1,5	1	0,5
Sept	Septembre	63 & 65	200	3,5	2,5	1
Oct.	Octobre	68 & 70	200	3,5	3	0,5
Nov.	Novembre	73	100	2	1	1
Dec.	Décembre	75	90	2,25	1	1
Jan.	Janvier 78	76	100	5	3	2
Feb	Février	79	100	9	2	7
Mar.	Mars	80	18	5,5	0	5,5

Tableau n° 19 : Taux de parasitisme par xénomes de type "laiteux" et "crayeux" dans l'étang de Mauguio.

Table No. 19. Rate of Infestation with Milky and Chalky Xenomas in the Etang de Mauguio.

increased pigmentation.

It then remained to be determined whether the relative percentage of each type of xenoma underwent changes in the course of the year. It was first necessary to establish the total rate of infestation. Table 19 gives our findings on a monthly basis.

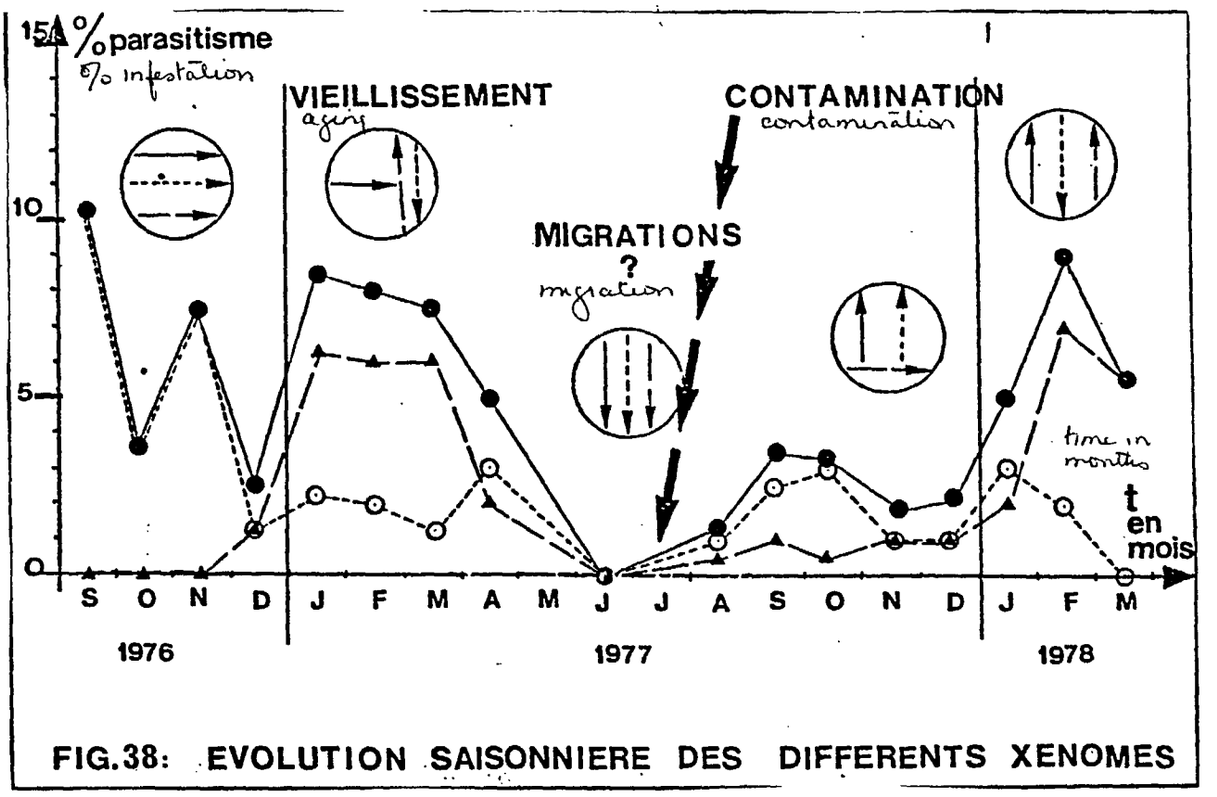

FIG.38: EVOLUTION SAISONNIERE DES DIFFERENTS XENOMES

Fig. 38. Seasonal Changes in the Rate of Infestation with Both Types of Xenomas.

Fig. 38 indicates total infestation (●——●) with the percentage of milky xenomas (⊖- - -⊖) and chalky xenomas (▲— —▲). The corresponding arrows indicate their development at three characteristic point in the seasonal cycle. (↓) represents a decrease, (↑), an increase and (→), more or less obvious stagnation in infestation. With the three arrows combined, the following conclusions could be drawn:

. From September to December (↑ ↑), infestation increases very slowly, indicating a period of contamination that starts in August-September and begins to be noticeable in the fall and winter. This is consequently a period of xenoma growth, just following contamination.

. From January to March (→ ↑ ↓), it may be assumed[1] that the effects of end-of-summer contamination peak toward the end of the winter, i.e., three months later,[2] that there is no contamination at the beginning of winter since the percentage of milky xenomas drops and[3] that milky xenomas are developing into chalky xenomas, which explains why there is a definite increase in this type of cyst. This is a period taken over by the aging process.

. From April to August (↓ ↓ ↓), there is a sharp decline in overall parasitism which must reflect either migration or death of the fish. The first hypothesis is the more likely of the two since in summer when the water becomes foul, virtually the entire atherine population returns to the sea. Catches at this time of year are very meager. Not a single lot could be obtained in July.

In conclusion, the seasonal cycle may be divided into four main periods:

- contamination at the end of the summer and beginning of the fall;

- increase in the percentage of milky xenomas in the fall and beginning of the winter;

- aging of the cysts toward the end of the winter and in the spring;

- mixing of populations and dispersal of infected individuals in summer.

There may be three explanations why a low rate of infestation was observed in fish returning from the sea in the summer:

1. The fish rids itself of the parasite or dies at sea;

2. The fish does not return to the same lagoon, diluting the rate of infestation;

3. Newly hatched individuals obviously to not bear cysts from the pervious year.

It must not be concluded that fish from the Etang de Mauguio migrate as far as the Thau basin since, if they did, the basin would contain traces of infestation (cf section on geographic distribution) In addition, Kiener and Spillman (1969) showed that each lagoon or group of lagoons corresponded to a certain type of fish as reflected by the number of scales,vertebrae, gill rakers, etc., which suggests minimal loyalty to a particular lagoon.

These phenomena are far from being perfectly understood and a thorough study of atherine migration will undoubtedly shed further light on the subject.

GENERAL CONCLUSIONS

This investigation was devoted to the study of microsporidiosis in atherines and was based on material on which relatively little work has been done. The microsporidian Glugea atherini is a new discovery, the parasitic fauna infesting Atherina boyeri being largely unexplored (of the 16 different parasites encountered, only 6 had been previously reported).

Following initial research, I was tempted to draw up a complete list of the protist parasites found in lagoonal or marine fish in the region, but decided instead that in the time allotted, a careful study of a single species, adopting a synecological approach, would prove more rewarding.

There are approximately 75 different microsporidian species infesting fish. Twenty-five of them belong to the genus Glugea. In general, particularly considering their potential economic impact, they have been little studied in fish. The cycle of some species has been observed under the electron microscope but in only a few rare instances is the epidemiology known. The physiology of fish-infesting microsporidians is a virtually uncharted field.

My research was divided into four major parts:

1) first, the new parasite was carefully identified;

2) second, we determined its geographic range and distribution within the host;

3) third, the mechanisms governing implantation and development of microsporidian xenomas was examined;

4) lastly, the host-parasite relationship and pathogenic action of the microsporidian were studied.

A number of different techniques were employed in our research. In addition to dissection, performed in close to 4,500 specimens, histology and electron microscopy served as the foundations of our investigation. A number of biochemical techniques, such as various types of electrophoresis, enzyme tests, gel diffusion and histochemistry were also used to acquire a better understanding of the physiology of the xenoparasitic complex. Lastly, aquarium experiments were considered essential to elucidate parasite transmission and pathogenic action.

Like most species belonging to the genus Glugea, the atherine-infesting microsporidian encysts in a highly specific fashion in a single host cell. The normal organization of the cell is completely disrupted. The nucleus divides into thousands of hypertrophied elements. A single cell may reach a record diameter of 13 mm and contain 20 billion spores.

This result is achieved by a now well-defined cycle which begins with a highly active phase known as first-type merogony. Parasitic stages continually increase and multiply. This is followed by second-type merogony which terminates in sporogony in which cell division contributes to increasing the number of final stages, i.e., the spores.

Despite all the spores released in the water after the death of an atherine, the parasite is apparently unable to colonize the Thau basin and lagoons lying west of it. The reasons for this limit in the range are not fully understood. It is thought that physicochemical conditions are not favourable to the cycle although

experimental infestation remains possible. In addition, the migratory behaviour of atherines, which is largely unknown, seems to play a major role.

Penetration and implantation of microsporidians are two widely debated points in the literature. While it is generally accepted that the polar filament everts, this has not been clearly demonstrated. This is also true of displacement of the sporoplasm. What we know about the mode of penetration is the result of logical deduction rather than direct observation. In the atherine-specific microsporidian, the sporoplasm may remain in the connective tissue layer of the digestive tube and form small rapidly developing xenomas. The sporoplasm may also migrate to most parts of the body with the exception of muscles and skin. The xenomas may become very large in the body cavity and the question of their pathogenic action arises.

The parasite does not seem to have a great deal of influence on the host. It does not modify the protein composition of the blood, does not seem to induce an antigen-antibody reaction and has no effect on digestive enzymes and intestinal tissues. There is only one point permitting a tentative hypothesis to be advanced. Microsporidiosis seems to reduce atherine resistance to bacterial action, suggesting weakening of the fish due to involvement of an unanalyzed component of the blood (carbohydrates, lipids) or of the body's defense system. It may be that the organism defends itself vigorously at the time of penetration but that these reactions cease as soon as the xenoma is isolated by a characteristic tissue reaction.

Regardless of the mechanism involved, a vast field of study

was explored. A number of questions were raised that merit answers in the interests of understanding microsporidians of lower vertebrates. The biological material is of exceptional interest. The xenomas are easily obtained since the rate of infestation is often 7% to 8% and may even reach 22% (the Etang de l'Olivier). Also, there is considerable material available. Microsporidians are extremely small single-celled organisms (6 µm long) but produce macroscopic xenomas, frequently 5 to 10 mm in diameter. As a result, most biochemical techniques could be applied after slight modification, which is exceptional in protistology.

Lastly, there are some topics which were barely touched upon in this thesis which warrant further attention, i.e.,

- With electrophoretic studies of the xenoma's enzyme composition, it would be possible to elucidate changes undergone by the infected cell. It could then be determined if, like some viruses, the microsporidian directly modifies the cell genome.

- Further experimental infestation studies would make it possible to define how penetration occurs and what the parasite's requirements are with respect to abiotic factors. Also, by trying to infest other atherine species and taxonomically less related fish, it would be possible to determine the host specificity of theparasite. Lastly, substances could be tested for their action on microsporidiosis since sooner or later, fish such as the atherine will be subject to artificial breeding techniques.

SUMMARY

BIOLOGY OF A MICROSPORIDIAN, *Glugea atherini* n. sp., A PARASITE OF THE ATHERINE, *Atherina boyeri* RISSO, 1810 (PISCES - TELEOST) OCCURRING IN FRENCH MEDITERRANEAN COASTAL LAGOONS.

Glugea atherini is a new species which specifically infests a small lagoonal fish, i.e., *Atherina boyeri*. The parasite forms either small xenomas in the digestive tube wall or large xenomas (up to 13 mm) in the host's body cavity.

An ultrastructural study of the xenoma and parasite's life cycle revealed that the parasite becomes embedded in the cytoplasm of a hypertrophied host cell. The complex is then encysted as a result of a tissue reaction. The parasite does not seem to have a significant pathogenic effect. It does not interfere with blood proteins or digestive enzymes. No antigen-antibody reactions were recorded. Infected fish, however, exhibit greater susceptibility to bacterial disease.

The parasite's range extends from the Etang de Vic to the Etang de Berre. It seems to be absent from Corsica and Tunisia. Several hypotheses are proposed to explain this distribution.

Experimental infestation proved successful.

Changes in the pattern of microsporidiosis over time was studied for close to a year and a half.

BIBLIOGRAPHY

BIBLIOGRAPHY

Aguesse, P., 1957: Classification of poikilohaline water systems: difficulties encountered in the Camargue and new attempts at classification.

Aleem, A.A., 1952: Ecological findings in two peridinian species inhabiting brackish water.

Audouin, J., 1962: Hydrology of the Etang de Thau.

Bebars, M.I., 1976: Biochemical study of the soluble proteins of the crystalline lens in mullets from the Languedoc-Roussillon region.

Berrebi, P. and Bouix, G, 1978: Initial observations of microsporidiosis in Atherina boyeri Risso, 1810 (Pisces - Teleost), the atherine species inhabiting the lagoons of Languedoc.

Bougis, P., 1959: Atlas of marine fish, Boubée et Cie, Paris, volume I, 1-201, volume II, 1-234.

Bouix, G., Loubès, C. and Maurand, J., 1974: Sporogony in microsporidians. Cytochemical findings in a few species.

BRAUN M., 1977 : Contribution à l'étude biologique des zones d'estuaire du littoral méditerranéen : Copépodes parasites de poissons. D.E.A., Univ. Sci. Techn. Languedoc, Montpellier, 1-39.

BREWER G.J. et SING C.F., 1970 : An introduction to isoenzyme technique Academic Press, New York and London, 1-186.

CANNING E.U., ELKAN E. et TRIGG P.I., 1964 : Plistophora myotrophica spec. nov. causing high mortality in the common toach Bufo bufo L. with notes on the maintenance of Bufo and Xenopus in the laboratory. J. Protozool. 11, 157-166.

CANNING E.U., 1976 : Microsporidia in Vertebrates : host parasite relations at the organismal level. in Comparative Pathobiology, vol. 1 : Biology of the Microsporidia, Plenum Press, New York, 137-161.

CASABIANCA M.L. et KIENER A., 1969 : Gobiides des étangs de Corse : Systématique, écologie, régime alimentaire, et position dans la chaine trophique. Vie et Milieu, Série A, 20, 611-634.

CASABIANCA M.L., KIENER A. et HUVE H., 1973 : Biotope et biocénose des étangs saumâtres corses : Biguglia, Diana, Urbino, Palo. Vie et Milieu, 23, 187-227.

CHATTON E., 1920 : Sur un complexe xéno-parasitaire morphologique et physiologique, Nereisheimeria catenata chez Fritillaria pellucida. C.R. Acad. Sci., 171, 55-57.

CHEN M. et POWER G., 1972 : Infection of American smelt in Lake Ontario and Lake Erie with microsporidian parasite Glugea hertwigii (Weissenberg). Can. J. Zool., 50, 1183-1188.

DAVIDIAN-BRITTON J., 1978 : Premières données sur la structure génétique du complexe d'espèces de Mus musculus L. dans le bassin méditerranéen. Thèse, Univ. Sci. Techn. Languedoc, Montpellier, 1-72.

BEBAISIEUX P., 1920 : Etudes sur les Microsporidies. IV. Glugea anomala Monz. Cellule, 30, 217-243.

DELISLE C.E., 1969 b : Bimonthly progress of a non-lethal infection by Glugea hertwigii in young-of-the-year smelt Osmerus eperlanus mordax. Can. J. Zool., 47, 871-876.

DELISLE C.E., 1972 : Variations mensuelles de Glugea hertwigi (Sporozoa Microsporida) chez différents tissus et organes de l'Eperlan adulte dulcicole et conséquences de cette infection sur une mortalité massive annuelle de ce Poisson. Can. J. Zool., 50, 1589-1600.

Braun, M., 1977: Contribution to the biological study of the estuary regions of the Mediterranean coast: fish-infesting copepods.

Casabianca, M.L. and Kiener, A., 1969: Gobiidae species in Corsican lagoons: taxonomy, ecology, diet, and position in the food chain.

Casabiance, M.L., Kiener, A. and Huve, H., 1973: Biotope and biocenosis of Corsican brackish lagoons: Bigulia, Diana, Urbino, Palo.

Chatton, E., 1920: On a morphological and physiological xenoparasitic complex produced by Neresheimeria catenata in Fritillaria pellucida.

Davidian-Britton, J., 1978: Initial findings on the genetic structure of the complex of Mus musculus L. species in the Mediterranean basin. Thesis.

Debaisieux, P., 1920: Studies on the Microsporidia. IV. Glugea anomala Morz.

Delisle, C. E., 1972: Monthly variations in Glugea hertwigii (Sporozoa Microsporida) in different tissues and organs in the adult freshwater smelt and impact of the infection on the yearly massive mortality rate recorded in the fish.

DELISLE C.E. et VEILLEUX C., 1969 : Répartition géographique de l'Eperlan arc-en-ciel Osmerus eperlanus mordax et de Glugea hertwigi (Sporozoa Microsporida) en eau douce, au Québec. Nat. Can., 92, 337-358.

DELPHY J., 1916 : Scoliose abdominale chez le Mugil auratus Risso et présence d'une Myxosporidie parasite de ce Poisson. C.R.Acad. Sci., 163, 71 à 73.

DISSANAIKE A.S. et CANNING E.U., 1957 : The mode of emergence of the sporoplasm in Microsporidian and its relation to the structure of the spore. Parasitology, 47, 92-99.

DOGIEL A.V., PETRUSHEVSKII G.K. et POLYANSKI Y.I., 1958 : Parasitology of Fishes. Transl. by Z. KABATA, Oliver and Boyd, Edinburgh and London, 1961, 1-384.

ERICKSON B.W. et VERNICK S.H., 1967 : Observations on spores of Glugea sp. using shadow Caosting and Electron Microscopy. Am. Zool. 7, 777-778 (Abstract 308).

ERICKSON B.W., VERNICK S.H. et SPRAGUE V., 1968 : Electron microscope study of the Everted Polar Filament of Glugea weissenbergi (Microsporida, Nosematidae). J. Protozool 15, 758-761.

FANTHAM H.B., PORTER A. et RICHARDSON L.R., 1941 : Some microsporidia found in certain fishes and insects in eastern Canada. Parasitology 33, 186-208.

GABE M., 1968 : Techniques histologiques. Masson et Cie Editeurs, Paris, 1-1113.

GASC C., LOUBES C., MAURAND J. et BOUIX G., 1976 : Sur une nouvelle espèce de Microsporidie parasite de Myriapodes Diplopodes du Sud-Dahomey. Acta Tropica, 33, 169-176.

GLUGE G., 1838 : Notice sur quelques points d'anatomie pathologique comparée suivie de quelques observations sur la structure des branchies des Epinoches. Bull. Ac. Roy. Belg. 5, 771-772.

GOLVAN Y.J., 1969 : Systématique des Acanthocéphales. Mémoires du Museum National d'Histoire Naturelle. Série A, Tome LVII, Ed. du Museum, Paris, 30-340.

GUELORGET O. et MICHEL P., 1976 : Recherches écologiques sur une lagune saumâtre méditerranéenne : l'étang du Prévost (Hérault). I : le milieu. Thèse, Univ. Sci. Techn. Languedoc, Montpellier, 1-95.

GURLEY R.R., 1893 : On the classification of Myxosporidia a group of Protozoan parasites infesting fishes. Bull. U.S. Fish Comm., 11, 407-420.

Delisle, C. E. and Veilleux, C., 1969: Range of the American smelt Osmerus eperlanus mordax and Glugea hertwigii (Sporozoa, Microsporida) in freshwater in Quebec.

Delphy, J., 1916: Abdominal scoliosis in Mugil auratus Risso and presence of a myxosporidian parasite.

Gabe, M., 1968: Histological techniques.

Gasc, C., Loubès, C., Maurand, J. and Bouix, G., 1976: On a new species of microsporidian parasite infesting myriapods-diplopods in southern Dahomey.

Gluge, G., 1838: Discussion on some points of comparative pathological anatomy followed by a few observations on the gill structure in sticklebacks.

Golvan, Y.J., 1969: Taxonomy of acanthocephalans. Transactions of the National natural history museum. Series A, Volume LVII.

Guelorget, O. and Michel, P., 1976: Ecological research on the Etang du Prévost (Hérault), a Mediterranean brackish lagoon. I. The environment. Thesis.

1954
HALEY A.J. : Microsporidian parasite, Glugea hertwigi, in American smelt from the Great Bay region, New Hampshire. Trans. Amer. Fish. Soc., 83, 84-90.

HASHIMOTO K. et TAKINAMI K., 1976 : Electron microscopic observations of the spore of Plistophora anguillarum, a Microsporidian Parasite of the Eel. Bull. Jap. Soc. Sci. Fish., 42, 411-419.

HENSEL E., 1973 : Dynamique de l'étang du Prévost (Languedoc) par la méthode de télédétection IR. D.E.A., Univ. Sci. Techn. Languedoc, Montpellier, 1-52.

HELLER R., 1968 : Manuel de statistique biologique. Gauthier-Villars Eds, Paris, 1-295.

HERVE P., 1978 : Ichthyofaunes comparées de 2 étangs littoraux du Roussillon : Canet-Saint Nazaire et Salses-Leucate. Ecologie générale et biologie de diverses espèces de Poissons. Thèse Univ. Pierre & Marie Curie, Paris VI, 1-253.

HILDEBRAND H. et VIVIER E., 1971 : Observations ultrastructurales sur les sporoblastes de Metchnikovella wohlfarthi n. sp. (Microsporidie) parasite de la Grégarine Lecudina tuzetae. Protistologica, 7, 131.

HOFFMAN G.L., 1967 : Parasites of North american freshwater fishes. Univ. of California press, Berkeley and Los Angeles, 65-68.

HOSHINA, 1951 : On a new microsporidian Plistophora anguillarum n. sp., from the muscle of the eel Anguilla japonica. J. Tokyo Univ. Fish. 38, 35-46.

ISHIHARA R., 1967 : Some observations on the fine structure of sporoplasm and polar filament of Nosema bombycis. J. Protozool. 14 (Suppl.) 29.

JENSEN H.M. et WELLINGS S.R., 1972 : Development of the polar-filament polaroplast complex in a microsporidian parasite. J. Protozool. 19, 297-305.

KABATA Z., 1959 : On two little-known microsporidia of marine fishes. Parasitology, 49, 309-315.

KIENER A. et SPILLMANN C.J., 1969 : Contributions à l'étude systématique et écologique des Athérines des Côtes françaises. Mém. Mus. Nat. Hist. Nat., A, 60, 33-74.

KIENER A. et SPILLMANN C.J., 1972 : Note complémentaire sur l'étude systématique et écologique de Atherina boyeri Risso 1810 (Poisson) dans sa zone de dispersion actuelle. Bull. Mus. Hist. Nat., 1, 60; 33-74.

Hensel, E., 1973: Dynamics of the Etang du Prévost (Languedoc) by the IR remote sensing method.

Heller, R., 1968: Manual of biological statistics.

Herve, P., 1978: Comparison of the ichthyofauna of two coastal lagoons of the Roussillon area, i.e., Canet-Saint-Nazaire and Salsæs-Leucate. General ecology and biology of various fish species. Thesis.

Hildebrand, H. and Vivier, E., 1971: Ultrastructural observations of the sporoblasts of Metchnikovella wohlfarthi n. sp. (Microsporidia), a parasite infesting the gregarine, Lecudina tuzetae.

Kiener, A. and Spillmann C.J., 1969: Contribution to the taxonomic and ecological study of atherines inhabiting French coastal regions.

Kiener, A. and Spillmann, C.J., 1972: Further contributions to the taxonomic and ecological study of Atherina boyeri Risso, 1810, (Pisces) in its current zone of dispersal.

KOHLER A., 1975 : Observations biologiques et biométriques sur Atherina boyeri Risso dans l'étang du Prévost à Palavas (Hérault). Vie et Milieu, 26, 157-174.

KUDO R., 1920 : Studies on Myxosporidia. A synopsis of genera and species of Myxosporidia. Univ. of Illinois, 1-265.

KUDO R., 1924 : A biologic and taxonomic study of the Microsporidia. Univ. of Illinois, 1-268.

LADIGES W. et VOGT D., 1965 : Die susswasserfische Europas. Edited by P. PAREY, Berlin, 1-250.

LAINSON R., GARNHAM P.C., KILLICK-KENDRICK R. et BIRD R.G., 1964. Nosematosis, a microsporidial infection of rodents and other animals, including man. Br. Med. J., 2, 470-472.

LAVENU F., 1972 : La télédétection des radiations infrarouges appliquée à l'étude hydrologique des étangs côtiers, et plus particulièrement à celle de l'étang de Thau (Languedoc). Thèse, Univ. Sci. Techn. Languedoc, Montpellier, 1-85.

LEGAULT R.O. et DELISLE C.E., 1967 : Acute infection by Glugea hertwigi Weissenberg in young-of-the-year rainbow smelt Osmerus eperlanus mordax (Mitchill). Can. J. Zool., 45, 1291-1292.

LOM J., 1969 : Experimental transmission of a microsporidian, Plistophora hyphessobryconis, by intramuscular transplantation. J. Protozool. 16, supp. 17.

LOM J., 1971 : Observation sur la structure du filament polaire du genre Nosema. J. Protozool. 18 (suppl.), 51-52.

LOM J., 1972 : On the structure of the extrued microsporidian polar filament. Z. Parasitenk. 38, 200-213.

LOM J. et CORLISS J.O., 1967 : Ultrastructural observations on the development of the microsporidian protozoon Plistophora hyphessobryconis Shaperclaus. J. Protozool. 14, 141-152.

LOM J. et LAIRD M., 1976 : Parasitic Protozoa from marine and euryhaline fish of Newfoundland and New Brunswick. II. Microsporida. Trans. Amer. Microsc. Soc. 95, 569-580.

LOM J. et VAVRA J., 1963 : Mucous envelopes of spores of the subphylum Cnidospora (Doflein, 1901). Vestn. Cesk. Spol. Zool., 27, 4-6.

LOM J. et WEISER J., 1969 : Note on two microsporidian species from Silurus glanis and the systematic status of the genus Glugea Thelohan. Folia paras. (Praha) 16 : 193-200.

LOUBES C., MAURAND J., GASC C. et BOUIX G., 1976 : Etude ultrastructurale de Glugea habrodesmi n. sp. (Microsporida Glugeidae), parasite des Myriapodes, Habrodesmus falx Cook et Oxydesmus granulosus Palisot de Beauvois (Myriapoda Polydesmidae). Protistologica 12, 435-450.

Kohler, A., 1975: Biological and biometric observations of Atherina boyeri Risso in the Etang du Prévost at Palavas (Hérault).

Lavenu, F., 1972: Remote sensing with infrared radiation applied to the hydrologic study of coastal lagoons, in particular, the Etang de Thau (Languedoc). Thesis.

Lom, J., 1971: On the structure of the polar filament in the genus Nosema.

Loubès, C., Maurand, J., Gasc, C. and Bouix, G., 1976: Ultrastructural study of Glugea habrodesmi n. sp. (Microsporida, Glugeidae), a parasite of the myriapods, Habrodesmus falx Cook and Oxydesmus granulosus Palisot de Beauvois (Myriapoda, Polydesmidae).

MAILLARD C., 1976 : Distematoses de Poissons en milieu lagunaire. Thèse, Univ. Sci. Techn. Languedoc, Montpellier, 1-383.

MARGILETH A.M., STRANO A.J., CHANDRA R., NEAFIE R., BLOM M., McCULLY R.M. 1973 : Disseminated nosematosis in an immunologically compromised infant. Arch. Pathol. 95, 145-150.

MARTOJA R. et MARTOJA-PIERSON M., 1967 : Initiation aux techniques de l'histologie animale. Masson et Cie Ed., Paris, 1-345.

MAURAND J. et BOUIX G., 1969 : Mise en évidence d'un phénomène sécrétoire dans le cycle de Thelohania fibrata (Strickland, 1913) Microsporidie parasite des larves de Simulium. C. R. Acad. Sci., 269, 2216-2218.

MAURAND J. et LOUBES C., 1973 : Recherches cytochimiques sur quelques Microsporidies. Bull. Soc. Zool. Fr. 98, 373-383.

MAURAND J., FIZE A., FENWICK R. et MICHEL R., 1971 : Etude au microscope électronique de Nosema infirmum Kudo 1921, Microsporidie parasite d'un Copépode cyclopoïde ; creation du genre nouveau Tuzetia à propos de cette espèce. Protistologica, 1971, 7, 221-225.

MAXWELL A.E. 1961 : Analysing qualitative data. Methaen et CO, L.T.D., London, 1-163.

MONIEZ R., 1887 : Observations pour la révision des Microsporidies. C.R. Acad. Sci., 104, 1312-1314.

MORETTI J., BROUSSIER G. et JAYLE M.F., 1957 : Réalisation technique et premières applications de l'électrophorèse sur gel d'amidon. Bull. Soc. Chim. Biol., 39, 593-605.

NARASIMHAMURTI C.C. et KALAVATI C., 1972 : Two new species of Microsporidian parasites from a marine fish Saurida tumbil. Proc. Ind. Ac. Sc., 76, 165-170.

NELSON J.B., 1962 : An intracellular parasite resembling a microsporidian associated with ascites in Swiss mice. Proc. Soc. Exp. Biol. Med., 109, 714-717.

NEPSZY S.J. et DECHTIAR A.O., 1972 : Occurrence of Glugea hertwigi in Lake Erié rainbow smelt (Osmerus mordax) and associated mortality of adult smelt. J. Fish. Res. Bd. Canada, 29, 1639-1641.

OLSON R.E., 1976 : Laboratory and field studies on Glugea stephani (Hagenmuller), a Microsporidian parasite of Pleuronectid flatfishes. J. Protozool., 23, 158-164.

Maillard, C., 1976: Distematosis in fish in a lagoonal environment. Thesis.

Martoja, R. and Martoja-Pierson, M., 1967: Initiation to animal histology techniques.

Maurand, J. and Bouix, G., 1969: Evidence of a secretory phenomenon in the cycle of Thelohania fibrata (Strickland, 1913), a microsporidian parasite of Simulium larvae.

Maurand, J. and Loubès, C., 1973: Cytochemical research on some microsporidians.

Maurand, J., Fize, A., Fenwick, R. and Michel, R., 1971: Electron microscopic study of Nosema infirmum Kudo, 1921, a microsporidian parasite of a cyclopoid copepod. Creation of a new genus, Tuzetia, with respect to this species.

Moniez, R., 1887: Observations for the revision of microsporidian classification.

Moretti, J., Broussier, G. and Jayle, M.F., 1957: Electrophoresis on starch gel: technical procedure and initial applications.

OLSON R.E. et PRATT I., 1973 : Parasites as indicators of English sole (Parophrys vetulus) nursery grounds. Trans. Am. Fish. Soc., 102, 405-411.

PETIT G., 1953 : Introduction à l'étude écologique des étangs méditerranéens. Vie et Milieu 4, 569-604.

PETRI M. et SCHIØDT T., 1966 : On the ultrastructure of Nosema cuniculi in the cells of the Yoshida rat ascites sarcoma. Acta. Pathol. Microbiol. Scand., 66 , 427-446.

PUTZ R.E., HOFFMAN G.L. et DUNBAR C.E., 1965 : Two new species of Plistophora (Microsporidea) from North american fish with a synopsis of Microsporidea of freshwater and euryhaline fishes. J. Protozool., 12, 228-236.

PUTZ R.E. et McLAUGHLIN, 1970 : Biology of Nosematidae (Microsporida) from freshwater and euryhaline fishes. Amer. Fish. Soc. U.S.A., Symposium on Diseases of Fishes and Shellfishes, F. Snieszko 124-132.

RAIBAUT A., 1967 : Recherches écologiques sur les Copépodes Harpacticoïdes des étangs côtiers et des eaux saumâtres temporaires du Languedoc et de Camargue. Thèse, Univ. Sci. Techn. Languedoc, Montpellier, 1-238.

ROMESTAND B., 1972 : Sur les protéïnes de l'hémolymphe des Cymothoadiens (Isopode parasite de Poissons) et leurs variations. Thèse, Univ. Sci. Techn. Languedoc, Montpellier, 1-79.

SCHRADER F., 1921 : A microsporidian occuring in the smelt. J. Parasit., 7, 151-153.

SHUBERT G., 1969 : Ultracytologische Untersuchungen an der Spore der Mikrosporiedenart Heterosporis finki, gen. n., sp.n. Zeitsch. Parasitenk., 32, 59-79.

SINDERMANN C.J., 1966 : Diseases of Marine fishes. Adv. mar. Biol., 4, 1-89.

SINDERMAN C.J., 1970 : Principal diseases of marine fish and shellfish. Academic Press, N.Y. & L., 1-369.

SPRAGUE V., 1966 : Ichthyosporidium sp. Schwartz, 1963, parasite of the fish Leiostomus xanthurus, is a Microsporidian. J. Protozool., 13, 356-358.

SPRAGUE V., 1969 : Microsporida and tumors, with particular reference to the lesion associated with Ichthyosporidium sp. Schwarz 1963. Nat. Cancer Inst. Mon. 31, 237-249.

SPRAGUE V., 1974 : Classification and phylogeny of the Microsporidia. Publ. Univ. of Maryland, 1-67.

Petit, G., 1953: Introduction to the ecological study of Mediterranean lagoons.

Raibaut, A., 1967: Ecological research on harpacticoid copepods of coastal lagoons and temporary brackish water in the Languedoc and Camargue regions. Thesis.

Romestand, B., 1972: On hemolymph proteins and variations in cymothoadians (fish-infesting isopod). Thesis.

SPRAGUE V., 1977 : Classification and phylogeny of the Micr
(in Comparative Pathobiology, vol. 2, Systematics of
poridia, Plenum Press, New York, 1-30).

SPRAGUE V. 1977 : Annoted list of species of Microsporidia (i
tive Pathobiology, vol. 2, Systemactis of the Micros
Plenum Press, New York, 31-334).

SPRAGUE V., 1977 : The zoological distribution of Microsporid
parative Pathobiology, vol. 2, Systematics of the Mi
Plenum Press, New York, 335-386.

SPRAGUE V. et VERNICK S.H., 1971 : The ultrastructure of Enc
cuniculi (Microsporidia Nosematidae) and its taxonomi
cance. J. Protozool. 18, 560-569.

SPRAGUE V. et VERNICK S.H., 1968 : Light and electron micros
of a new species of Glugea (Microsporidia Nosematidae
4.spined Stickleback Apeltes quadracus. J. Protozool.,
571.

SPRAGUE V. et VERNICK S.H., 1968 : Observations on the spores
tophora gigantea (Thelohan, 1895) Swellengrebel ,191
ridan parasite of the fish Crenilabrus melops. J. Pr
662-665.

SPRAGUE V. et VERNICK S.H., 1974 : Fine structure of the Cyst
sporulation stages of Ichthyosporidium (Microsporida).
zool., 21, 667-677.

STUNKARD H.W. et LUX F.E., 1965 : A microsporidium infection
gestive tract of the winter flounder, Pseudopleuronec
canus. Biol. Bull., 129, 371-387.

SUMMERFELT R.C., 1964 : A new microsporidian parasite from th
shiner, Notemigonus crysoleucas. Trans. Amer. Fish. S
6-10.

SUMMERFELT R.C. et WARNER, 1970 : Incidence and intensity of
of Plistophora ovariae Summerfelt , 1964, a microspo
site of the Golden shiner, Notemigonus crysoleucas.
Soc. USA, Symposium on Disease of Fishes and Shellfis
zko, 142-160.

THELOHAN P., 1892 : Observations sur les Myxosporidies et ess
fication de ces organismes. Bull. Soc. Phil., 4, 165-

THELOHAN P., 1895 : Recherches sur les Myxosporidies. Bull.
26, 100-394.

TRILLES J.P., 1969 : Recherches sur les Isopodes "Cymothoida
françaises. Apperçu général et comparatif sur la bi
sexualité de ces Crustacés. Bull. Soc. Zool. Fr., 94,

Thelohan, P., 1892: Observations on myxosporidians and attempts at classification.

Thelohan, P., 1895: Research on myxosporidians.

Trilles, J.P., 1969: Research on Cymothoidae isopods in French coastal regions. General and comparative surveyof bionomics and sexuality.

TUZET O., MAURAND J., FIZE A., MICHEL R., FENWICK R., 1971 : Position d'un nouveau cadre systématique pour les genres de Microsporidies. C. R. Acad. Sc. Paris, 272, 1268-1271.

VAVRA J., 1959 : Beitrag zur Cytologie einiger Mikrosporidien. Vestn. Cesk. Spol. Zool., 23, 347-350.

VAVRA J., 1976 : Structure of Microsporidia (in Comparative Pathobiology, vol. 1, Biology of the Microsporidia, Plenum Press, New York), 1-86.

VAVRA J., 1976 : Development of Microsporidia (in Comparative Pahtobiology, vol. 1, Biology of Microsporidia, Plenum Press, New York, 87-110).

VERNICK S.H., SPRAGUE V. et LLOYD B.J., 1969 : Further observations on the fine structure of the spores of Glugea weissenbergi (Microsporida, Nosematidae). J. Protozool. 16, 50-53.

VINCKIER D., 1975 : Nosemoides gen. n., N. vivieri (Vincker, Devauchelle, et Prensier, 1970) Comb. nov. (Microsporidie). Etude de la différenciation sporoblastique et genèse des différentes structures de la spore. J. Protozool. 22, 170-184.

VINCKIER D., DEVAUCHELLE G. et PRENSIER G., 1971 : Etude ultrastructurale du développement de la Microsporidie Nosema vivieri. Protistologica 7, 273-287.

VIVARES C.P., 1978 : Grégarinoses et Microsporidioses de Brachyoures (Crustacés, Décapodes) de la Méditerranée occidentale. Aspects cytologiques, biochimiques et physiologiques. Thèse, Univ. Sci. Techn. Languedoc, Montpellier, 1-227.

VIVARES C.P., LOUBES C. et BOUIX G., 1976 : Recherches cytochimiques approfondies sur les Microsporidies parasites du Crabe vert de la Méditerranée, Carcinus mediterraneus Czerniavsky, 1884. An. Parasitol. Paris, 51, 1-14.

VIVARES C.P., TRELLU J. et CECCALDI H.J., 1977 : Etude de l'influence d'une microsporidiose sur les électrophorégrammes (protéinogrammes et zymogrammes) des protéines de l'hémolymphe de Carcinus mediterraneus (Crustacé, Brachyoure). Experientia 33, 1311.

VIVARES C.P., BOUIX G. et MANIER J.F., 1977 : Ormieresia carcini gen. n. sp. n., Microsporidie du Crabe Méditerranéen, Carcinus mediterraneus Czerniavsky 1884 : cycle évolutif et étude ultrastructurale. J. Protozool. 23, 83-94.

VIVIER E., 1975 : The Microsporidia of the Protozoa. Protistologica 11, 345-361.

Tuzet, O., Maurand, J., Fize, A., Michel, R., Fenwick, R., 1971: Position of a new taxonomic framework for microsporidian genera.

Vinckier, D., 1975: Nosemoides gen. n., N. vivieri (Vincker, Devauchelle, and Prensier, 1970) Comb. nov. (Microsporidia). Study of sporoblast differentiation and genesis of different spore structures..

Vinckier, D., Devauchelle, G. and Prensier, G., 1971: Ultrastructural study of the development of the microsporidian Nosema vivieri.

Vivares, C.P., 1978: Infestation of brachyurans (crustaceans, decapods) of the western Mediterranean with gregarines and microsporidians. Cytological, biochemical and physiological aspects. Thesis.

Vivares, C.P., Loubès, C. and Bouix, G., 1976: Detailed cytochemical research on microsporidians infesting the Mediterranean green crab, Carcinus mediterraneus Czerniavsky, 1884.

Vivares, C.P., Trellu, J and Ceccaldi, H. J., 1977: Study of the influence of microsporidiosis on the electrophoretograms (proteinograms and zymograms) of hemolymph proteins found in Carcinus mediterraneus (Crustacea, Brachyura).

Vivares, C.P., Bouix, G. and Manier, J.F., 1977: Ormieresia carcini gen. n. sp. n., a microsporidian of the Mediterranean crab, Carcinus mediterraneus Czerniavsky, 1884: life cycle and ultrastructural study.

VIVIER E. et SCHREVEL J., 1973 : Etude en microscopie photonique et électronique de différents stades du cycle de Metchnikovella hovassei, et observations sur la position systématique des Metchnikovellidae. Protistologica 9, 95-118.

VORONIN V.N., 1976 : Characteristics of the Genus Glugea (Protozoa, Microsporida) on the example of the type species Glugea anomala (Moniez, 1887) Gurley 1893 and its varieties. Parazitologiya 10, 263-267.

WALKER M.H. et HINSCH G.W., 1972 : Ultrastructural observations of a Microsporidian protozoan parasite in Libinia dubia (Decapoda) I : Early spore development. Z. Parasitenk. 39, 17-26.

WEIDNER E., 1972 : Ultrastructural study of microsporidian invasion into cells. Z. Parasitenkd. 40, 227-242.

WEIDNER E., 1973 : Studies of microsporidian disease transmission in winter flounder and smelt. Biol. Bull., 145, 159.

WEIDNER E., 1976 : Ultrastructure of the peripheral zone of Glugea induced Xenoma. J. Protozool. 23, 234-238.

WEIDNER E., 1976 : Some aspects of microsporidian physiology (in Comparative Pathobiology, vol. 1, Biology of Microsporidia, Plenum Press, New York) 111-126.

WEISER J., 1976 : The Pleistophora debaisieuxi xenoma. Z. Parasitenk. 48, 263-270 (1976).

WEISSENBERG R., 1911 : Uber einige Microsporidien aus Fischen (Nosema lophii Doflein, Glugea anomala Moniez, Glugea hertwigii nov. spec.). Sitzungsberg. Ges. Naturf. Freunde Berlin, 8, 344-357.

WEISSENBERG R., 1913 : Beitrage zur Kenntnis des Zeugungskheises des Mikrosporidien Glugea anomala Moniez und hertiwigi Weissenberg. Arch. Mik. Anat. 82, 81-163.

WEISSENBERG R., 1921 : Zur Wirtsgewebslaeitung des Plasmakorpers der Glugea anomala . Cysten. Arch. Protistenkd 42, 400-421.

WEISSENBERG R., 1968 : Intracellular development of the Microsporidian Glugea anomala Moniez in hypertrophying migration cells of the fish Gasterosteus aculeatus L., an example of the formation of "xenoma" tumors. J. Protozool., 15, 44-57.

WEISSENBERG R., 1976 : Microsporidian interactions with host cells. (in Comparative Pathobiology, vol. 1, Biology of the Microsporidia, Plenum Press, New York, 203-237).

Vivier, E. and Schrevel, J., 1973: Light and electron microscopic study of different stages of the *Metchnikovella havassei* cycle and observations on the taxonomic position of the Metchnikovellidae.

WELLINGS S.R., ASHLEY L.E. et McARN G.E., 1969 : Microsporidial infection of English Sole Parophrys vetulus. J. Fish. Res. Bd. Canada, 26, 2215-2218.

WEST A.F., 1960 : The biology of a species of Nosema (Sporozoa : Microsporidia) parasitic in the flour beetle Tribolium confusum. J. Parasitol. 46, 747-754.

WOODCOCK H.M., 1904 : Note on a remarkable parasite of plaice and flounders. Rep. Lancashire Sea-Fish. Lab., 63-72.